Polyelectrolyte Microcapsules:
A versatile and sensitive tool for the detection of protein and nucleic-acid analytes

By

Sujit Kumar Verma

A Thesis submitted in partial fulfillment
of the requirements for the degree of

Doctor of Philosophy
in Biochemistry

Approved Dissertation Committee

Prof. Dr. Sebastian Springer
Jacobs University Bremen

Prof. Dr. Michael Köhler
Technische Universität Ilmenau

Prof. Dr. Mathias Winterhalter
Jacobs University Bremen

Prof. Dr. Werner M. Nau
Jacobs University Bremen

Date of Defense: 23rd May, 2017

Department of Life Sciences & Chemistry

Statutory Declaration

Family Name, Given/First Name	Verma, Sujit Kumar
Matriculation number	20330803
What kind of thesis are you submitting: Bachelor-, Master- or PhD-Thesis	PhD Thesis

English: Declaration of Authorship

I hereby declare that the thesis submitted was created and written solely by myself without any external support. Any sources, direct or indirect, are marked as such. I am aware of the fact that the contents of the thesis in digital form may be revised with regard to usage of unauthorized aid as well as whether the whole or parts of it may be identified as plagiarism. I do agree my work to be entered into a database for it to be compared with existing sources, where it will remain in order to enable further comparisons with future theses. This does not grant any rights of reproduction and usage, however.

This document was neither presented to any other examination board nor has it been published.

German: Erklärung der Autorenschaft (Urheberschaft)

Ich erkläre hiermit, dass die vorliegende Arbeit ohne fremde Hilfe ausschließlich von mir erstellt und geschrieben worden ist. Jedwede verwendeten Quellen, direkter oder indirekter Art, sind als solche kenntlich gemacht worden. Mir ist die Tatsache bewusst, dass der Inhalt der Thesis in digitaler Form geprüft werden kann im Hinblick darauf, ob es sich ganz oder in Teilen um ein Plagiat handelt. Ich bin damit einverstanden, dass meine Arbeit in einer Datenbank eingegeben werden kann, um mit bereits bestehenden Quellen verglichen zu werden und dort auch verbleibt, um mit zukünftigen Arbeiten verglichen werden zu können. Dies berechtigt jedoch nicht zur Verwendung oder Vervielfältigung.

Diese Arbeit wurde noch keiner anderen Prüfungsbehörde vorgelegt noch wurde sie bisher veröffentlicht.

…….

Date, Signature

01.09.2017,

Acknowledgements

I dreamt of being a PhD and it feels great when I stand on the verge of achieving my dream. I take this opportunity to thank all those who stood by my side and made me complete my research work. It was fun, challenging, exciting and at the same time a lot of learning. I had innumerable experiences and I came across many people who made my journey more memorable and the one which I will cherish throughout my life.

First, I would like to thank with sincere gratitude and whole heartedly to Prof. Sebastian Springer, my thesis supervisor, mentor, a great leader and a very nice person. He has been a constant support and I thank him for his guidance in shaping my research, for his valuable inputs, preparing for the scientific world and overall providing an excellent research environment. Your encouraging words, valuable suggestions and countless scientific discussions made my PhD stay easy through the various good and bad times. Thank You very much Sebastian.

I also take this opportunity to thank my committee members Prof. Dr. Michael Köhler, Prof. Dr. Mathias Winterhalter and Prof. Dr. Werner M Nau for evaluating my thesis and providing valuable suggestion through my research work.

I would also like to thank my project collaborators Prof. Dr. Gerd Klöck, Dr. Anja Karin Albrecht and Verena Siebecke from Hochschule Bremen for their continuous support and valuable suggestions.

A very special thanks to all the members of the Springer lab; Ankur, Britta, Cindy, Esam, Gayane, Linda, Monte, Natalia, Raghavendra, Sunil, Susi, Swapnil, Tatiana, Uschi, Venkat and Zeynep for being a continuous support and providing a cheerful and healthy working environment in the lab. A very special thanks to Uschi for being the life support system of the lab and to be ever ready for helping out whenever required. I would also like to thank all my students who worked in this project; Ulla, Amanda, Radhika, Leona and Brieuc. Your contributions were very significant in the progress of the project.

I would also like to thank BMBF for providing the financial support to carry out my research work and Jacobs University for providing the necessary infrastructure and a vibrant multicultural environment.

I would also like to express my gratitude and thanks to my family (mother, mother in law, brother, sister in law, and my two cute and loving nieces) back home in India whose constant love, prayers, blessings and support provided me the energy to continuously move forward and for their support and unshakable belief in me.

At last, and more importantly I would like to thank my wife Neha who has been a constant support for me and helping me out in time of despair. No words are enough to express my thankfulness but still I say thank you. You are the best companion, my better half and overall my best friend. Thank you once again for all your support and loving me unconditionally. Love you!

I also would like to thank my God Sai Baba and Lord Shiva for showering their blessings and showing me the path forward.

I would like to dedicate this thesis in the memory of my father Radhey Shyam Verma (1950-2005) who would be very much proud of my achievement. I hope I made you proud.

Table of Contents

Abbreviations

AF	Alexa fluor
BSA	Bovine serum albumin
$CaCO_3$	Calcium carbonate
CLSM	Confocal laser scanning microscope
-COOH	Carboxyl
EC50	Half maximal effective concentration
EDC	1-ethyl-3-(dimethylaminopropyl) carbodiimide
EDTA	Ethylenediaminetetraacetic acid
ELISA	Enzyme linked immunosorbent assay
Fab	Fragment antigen binding
FACS	Fluorescence-activated cell sorting
Fc	Fragment crystallizable
FCS	Fetal calf serum
FITC	Fluorescein isothiocyanate
fg	Femtogram
GαM-AF488	AF488-labeled goat anti-mouse antibody
GαR-AF488	AF488-labeled goat anti-rabbit antibody
$h\beta_2m$	Human beta-2 microglobulin
kDa	Kilodalton
LbL	Layer by layer
LoB	Limit of blank
LoD	Limit of detection
LoQ	Limit of quantification
mAb	Monoclonal antibody
MFI	Mean fluorescence intensity
MHC	Major histocompatibility complex
MES	4-morpholinoethanesulfonic acid
µg	Microgram
mL	Milliliter
µm	Micrometer
NaN_3	Sodium azide
ng	Nanogram
nL	Nanoliter
nM	Nanomolar
PAA	Poly acrylic acid
PAH	Poly(allyllamine) hydrochloride
PBS	Phosphate buffer saline
PEG	Polyethylene glycol
PEM	Polyelectrolyte microcapsules
pg	Picogram
PS	Polystyrene
PSS	Polystyrene sulfonate
Rαhβ2M	Polyclonal rabbit anti- hβ2m antibody
RPMI medium	Roswell Park Memorial Institute medium
RT	Room temperature

S.*aureus*	*Staphylococcus aureus*
SDS-PAGE	Sodium dodecyl sulfate polyacrylamide gel electrophoresis
SEM	Standard error of the mean
SNARF	Seminaphtharhodafluor
Sulfo-NHS	N-hydroxysulfosuccinimide
VSVG	Vesicular stomatitis virus glycoprotein

Abstract

Development of novel detection systems for the detection of biological intermediates and markers is a challenging and fascinating task in modern diagnostics. Detection of such analytes, particularly at low concentrations, is of prime importance, as it may lead to early detection of disease and eventually better treatment.

In my PhD work described in the thesis, I have developed a simple, sensitive, and selective sandwich assay using microcapsules produced by layer-by-layer assembly, capable of detecting proteins and nucleic acids, using flow cytometry as an optical readout. The microcapsule-based assay described here is a novel single-bead assay, and it can serve as a universal platform for detecting diverse biomarkers, as the surface chemistry of the microcapsules can be adjusted. This makes them suitable for a great variety of applications in biochemistry and cell biology. The microcapsules described here have carboxylate groups at their surface, are chemically crosslinked, and are further surface-functionalized with adaptor proteins such as protein A and streptavidin. Adaptor proteins ensure an optimized orientation of antibodies or biotinylated oligos, which is useful for the detection of analytes and in the development of a sensor.

First, the capability of the protein A-coated microcapsules for detecting the disease biomarker human beta-2 microglobulin ($h\beta_2m$) in the femtomolar concentration range in is demonstrated both in buffer and in serum. Second, the streptavidin-coated microcapsules are used to detect nucleic acids in nanomolar concentration range.

The microcapsule based assay showed a 450-fold higher sensitivity than commercially available polystyrene beads for the detection of $h\beta_2m$, while both the microcapsules and the PS beads exhibited similar efficiency for the detection of nucleic acids. The developed assay allows rapid quantitative analyte measurement while providing high sensitivity and selectivity at very small sample quantities. The detection of analytes through protein A- and streptavidin-modified microcapsules as a platform for a single bead assay is shown in this study.

Chapter 1: Introduction

1.1 Layer-by-layer assembly of polyelectrolyte microcapsules

The search for new diagnostic and drug delivery tools has led researchers to consider polyelectrolyte microcapsules (in the following also simply called microcapsules) [1,2], which are hollow particles with diameters ranging from hundreds of nanometers to tens of micrometers and are made of thin layers of synthetic (and possibly biodegradable) polyelectrolytes. They are reproducibly fabricated using layer-by-layer assembly [3,4], a step-by-step assembly of polymers driven by their complementary interactions (e.g., electrostatic [4], hydrogen bonding [5–7], or covalent interaction [8–10]) on the surface of spherical templates [11] (**Figure 1.1),** followed by chemical dissolution of the cores to yield hollow multilayered shells. To increase the mechanical stability of the microcapsules, the polymers are covalently linked using one of several methods. For example, if carboxylate and amino groups are present, one uses 1-ethyl-3-(3-dimethylaminopropyl) carbodiimide (EDC) [12]. This process is termed crosslinking, and it results in the formation of stable amide bonds [1,12,13].

Microcapsules are a promising platform for biomedical applications, since their surfaces can be broadly modified according to their intended use [14–16]. The physical adsorption of biomolecules onto microcapsules is mediated by weak non-covalent interactions [17] that are sensitive to changes in salt concentration, temperature, and pH [17]. An improvement in this method is the covalent attachment of biomolecules with N-hydroxysulfosuccinimide (sulfo-NHS) after EDC crosslinking [18]. This two-step reaction results in the formation of a more stable amine-reactive sulfo-NHS ester that can be replaced by the substrate of choice to form an amide bond at physiological pH.

1.2 Polyelectrolytes and colloidal templates used for microcapsules

The preparation of microcapsules consists of simple layer-by-layer assembly of oppositely charged polymers on a surface of spherical organic templates [such as polystyrene latex (PS) [3], melamine formaldehyde (MF) [3,4,19], or on spherical inorganic templates such as silicon dioxide (SiO_2) [20,21], [calcium carbonate ($CaCO_3$) [22], cadmium carbonate ($CdCO_3$) [23,24], or manganese carbonate ($MnCO_3$) [19]], followed by chemical dissolution of the cores in acidic or aqueous solvents, as appropriate. Layer-by-layer assembly of oppositely charged polymers was first reported in 1992 by Decher et al. onto a charged planar surface [2,25]. The charged polymers can either be biologically stable [for example polyallylamine hydrochloride (PAH), polystyrenesulfonate (PSS), polyacrylic acid (PAA), polydiallyldimethylammonium chloride (PDAMAC), polyethyleneimine (PEI), or polyvinyl sulfonate (PVS)], or biodegradable [for

example poly-L-lysine (PLL), poly-arginine (pArg), dextran sulfate (DexS), or hyaluronic acid (HA)], depending on the intended use.

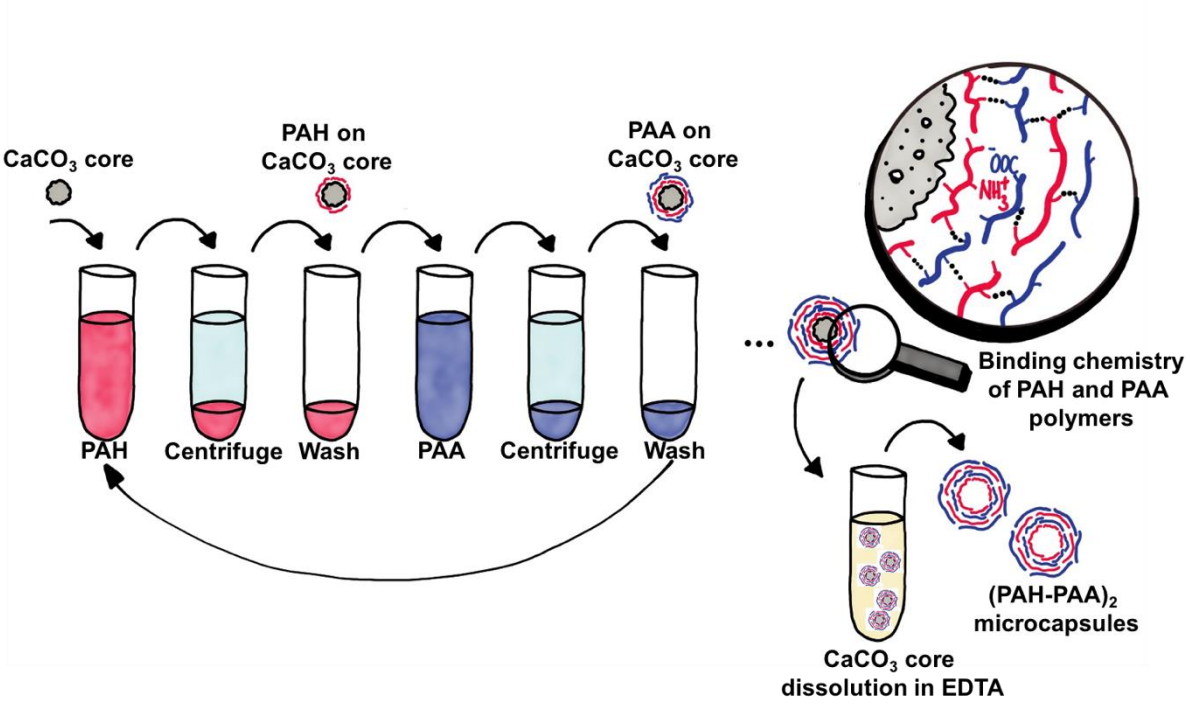

Figure 1.1: Schematic of microcapsule formation by alternative adsorption of oppositely charged polyelectrolyte layers on the surface of charged colloidal particles. Typical interactions between polymers are electrostatics, H-bonding, and covalent bonds. After a sufficient number of adsorption steps, the core particles are dissolved to yield hollow microcapsules. Figure not to scale. Figure courtesy Cindy Dirscherl.

1.3 General advantages of microcapsules for biotechnology applications

Since microcapsules were first described in 1998 [3,4], they have been used as systems for the controlled delivery of drugs [26], peptides [27], and plasmids [28], for intracellular sensing [29], and even for the retrieval of metabolites from cells [30]. Microcapsules have gained prevalence mainly due to their convenient physiochemical properties (biodegradability, size, charge density, colloidal stability, and permeability) [31–35]. Among the most significant advantages of microcapsules are the straightforward methods to adjust their properties according to their intended use [16,36]. Microcapsule functionality stems from the materials used for their fabrication, *e.g.*, the type of polyelectrolyte, the core material, or the presence of inorganic inclusions in the capsule shell.

Microcapsules contain a cavity that can be filled with cargo molecules such as fluorescent dyes [37], proteins [27], plasmids [28] or drugs [11,26,32,38]; this cargo can be delivered to cells or used for a detection process. Microcapsules can be made to bind to particular cell types with specific molecular recognition properties via functionalization with specific antibodies or

receptors [39]. The microcapsules can be easily detected in flow cytometry [40–42] and, due to their size (generally between 500 nm and 10 µm), they can be observed even with a simple microscope [29,37,43].

1.4 Sensing with beads – state of the field

Detection of ions, pH, plasmids, proteins, and nucleic acids has great relevance in the field of biological science, as it aids in understanding the effects of changes on the standard functioning of the cellular systems. The major challenge is to detect the analytes at lower concentrations than currently possible; this might help in the early diagnosis of the onset of disease and thus result in a more effective treatment, ultimately increasing the scope of biomedical sciences.

For proteins, the most common kind of analytes in biological systems, a number of currently very successful assay types exist. The most common assay type are plate assays, which are carried out in well plates, and where typically a capture antibody, or the analyte itself, are immobilized to the surface of the plate. The immobilized analyte is then typically detected with an antibody coupled to an enzyme (enzyme-linked immune-sorbent assay, ELISA), a fluorescent dye (fluorescence immunoassay, FIA, or fluorescence immuno-sorbent assay, FISA), or - now rarely - a radioisotope (radioimmunoassay, RIA) [44–47]. A special type of plate assay is the scintillation proximity assay, where the radiolabeled detection antibody elicits a scintillation signal if it is brought into the proximity of the solid plate when it engages the analyte [48–50]. Plate assays are the industry standard. They are usually easy to process and to read, since the washing steps can be easily automated, and they are the technical benchmark with which all novel systems must be compared in terms of specificity, reproducibility and robustness, assay time, cost, and sensitivity.

Other types of assay require no solid supports at all, and they are done entirely in solution. For example, the Lumigen SPARCL[1] assay uses two different antibodies to the same analyte, one of which is coupled to horseradish peroxidase and the other to a substrate, acridan. When both antibodies are brought into proximity through binding to the analyte, a chemiluminescence flash occurs that can be measured. There is also a solid support version of the same assay, but supportless proximity methods have the advantage that they are in principle very fast because the analyte does not have to diffuse to the solid support, but can react in homogeneous solution with the antibodies.

[1] http://www.lumigen.com/products/elisa/lumigen-sparcl 20.02.2017

Assays that use beads[2] can incorporate advantageous features of both support and support-less assays. Bead-based assays can either work on the principle that two different kinds of beads are brought into proximity through two different antibodies binding to the analyte (**see section 5.6.1.6**), or else beads may serve as solid support for a capture antibody, instead of the surface of the plate or test tube. A number of such bead-based assay systems are currently available in the market, and some are listed below.

1.4.1 Luminex xMAP technology (Thermo Fisher Scientific)[3]

This assay is based on the use of polystyrene or paramagnetic beads with specific dyes inside, and each dyed bead set is surface-functionalized with an antibody that is specific for an analyte of interest. Now, biotinylated antibody specific to the analyte is added to the wells of the microplate, which is then detected by adding streptavidin conjugated phycoerythrin (SA-PE), which then can be detected either in a flow cytometer or a plate reader. For multiplexing, each dyed bead is coated with antibodies specific for one analyte, and all beads are added together in a single well of the microplate. Luminex assays allow detection of up to 500 protein analytes with a detection limit of 10 - 100 pg/mL in cell culture supernatants, serum, saliva, urine, or plasma. The assay requires a small sample volume of 50 µL and is available in both magnetic and non-magnetic bead format.

1.4.2 Bio-Plex Cytokine Assay (BioRad)[4]

The Bio-Plex cytokine assay is a magnetic bead-based human cytokine assay allowing the detection of Interleukin (IL), Interferon (IFN-γ), and Tumor necrosis factor (TNF-α). The assay works on the principle of sandwich ELISA, where capture antibody bond to magnetic beads are specific for the analyte. To this antibody-analyte complex, biotinylated antibody against the analyte is added, which is finally detected by streptavidin-conjugated phycoerythrin. The assay uses 8 µm magnetic beads with simple washing steps (magnetic wash stations) with low variability and high precision measurements, and it is highly sensitive (detection limit of 10 pg/mL).

---

[2] The word 'bead' is here, and in the following, used to describe a nanometer- or micrometer-sized small particle that can be suspended. The polyelectrolyte microcapsules discussed in this thesis, as well as their precursors, the core-shell particles, fall under this definition of 'bead'.

[3] https://www.thermofisher.com/de/de/home/references/protein-analysis-guide/multiplex-assays-luminex-assays.html. 20.02.2017

[4] http://www.bio-rad.com/de-de/product/bio-plex-precision-pro-human-cytokine-assays. 20.02.2017

1.4.3 Live Cell Analysis with SmartFlare Probes (Millipore)[5]

SmartFlare uses nanoparticles as probes that are designed to emit fluorescence when they detect their RNA targets in live cells. SmartFlare, when incubated with live cells, enables sequence-specific RNA expression detection, and the cells can be then sorted depending on their individual expression level by flow cytometry. After the incubation, the probes exit the cells, and the cells can be used for further processes. SmartFlare RNA detection probes are meant to be used in stem cell and cancer cell research.

1.4.4 BeadStep Human GM-CSF Assay (Immunostep)[6]

This bead-based assay, marketed by the Spanish company Immunostep, uses the principle of sandwich ELISA to detect human granulocyte-macrophage colony-stimulating factor (GM-CSF), in serum, plasma, and cell culture supernatant samples. An analyte-specific antibody is conjugated to the bead to capture the analyte. To this, the biotinylated detection antibody specific for the analyte is added, forming a sandwich structure. The samples are finally detected in a flow cytometer by adding streptavidin-PE, which binds to the biotinylated antibody and fluorescence.

1.4.5 Bio-Plex Pro RBM Human Kidney Toxicity Kit (Bio-Rad)[7]

The assay is based on 6.5 µm magnetic beads for the detection and quantification of multiple proteins (IL-18, β_2M, albumin, MCP-1, calbindin, clusterin, cystatin C etc.) in human urine. The assay works on the principle of sandwich ELISA with the capture antibodies, which are specific to the analyte, bound onto the beads. After the capture antibody reacts with the analyte, the samples are incubated with the biotinylated detection antibody directed against the analyte, which creates a sandwich complex. The final detection complex is formed with the streptavidin conjugated phycoerythrin (SA-PE) that reacts with the biotinylated antibody. This assay is in microplate format, but potentially could be used in flow cytometry.

1.5 Microcapsules: A new tool for bio-sensing

Recently, interest has increased in the use of microcapsules as chemo-sensors and bio-sensors [37,40,51–53]. In principle, the wide possibilities for surface functionalization of microcapsules allow for the sensing of any analyte, either inside the cell or *in vitro*. Conjugation

[5] http://www.merckmillipore.com/DE/de/. 20.02.2017

[6] http://www.immunostep.com/-immuno-bead-assay/2766-beadstep-assay-human-gm-csf.html. 20.02.2017

[7] http://www.bio-rad.com/en-us/product/bio-plex-pro-rbm-human-kidney-toxicity-assays. 20.02.2017

of biomolecules to the microcapsule surface – for example, immobilization of an antibody on the surface – promises high specificity for the analyte, the most crucial step in the design of a biosensor assay [40].

The sensors, such as enzymes and dyes, can be located in the interior of the microcapsules and/or in their shell. For example, Kazakova *et al*. [37] have used microcapsules for the optical detection of oxygen, glucose, and lactate. They demonstrated that encapsulating enzymes such as lactate oxidase, peroxidase, and glucose oxidase within the microcapsule and incorporating fluorescent dyes into the microcapsule shell structure (by using electrostatic and hydrophobic interactions) enables optical monitoring of biologically important metabolites in individual microcapsules.

In other examples, the intracellular targeting of ion-sensitive substances as sensor compounds has enabled the real-time observation of intracellular environmental conditions [42]. Microcapsules make this possible, since the fluorophore is confined within the interior of microcapsules and not dispersed throughout the sample. Microcapsules not only protect the ion- or pH-sensitive dyes from the quenching effects of the surrounding environment [37], but may also help in their targeting and localization to a particular organelle or tissue.

Similarly, pH-sensitive microcapsules were prepared by encapsulating seminaphtharhodafluor (SNARF) dye, which changes color with pH (green in acidic, and red in alkaline conditions). These microcapsules were incubated with melanoma cells and observed under the microscope for fluorescence. Microcapsules far away from cells fluoresced red, and those taken up by cells emitted green fluorescence. This change in fluorescence is most likely due to the endocytic uptake of microcapsules from the alkaline cell culture medium into acidic endosomes or lysosomes [29].

Kast *et al*. have thus studied the acidification of endocytic vesicles in real time by monitoring SNARF-filled microcapsules. The emission of SNARF was recorded at 550-615 nm and 615-700 nm, and the ratio of both the emission wavelengths was plotted against time [42].

A more efficient way of measuring the pH of the capsule environment is to use two different dyes, one that is pH-sensitive and another that is pH-independent. Tracking the change in fluorescence intensity of both dyes at different time intervals and plotting the ratio of the fluorescence intensities of both dyes versus time gives a more reliable measurement. Microcapsules have also been used to detect protons, sodium and potassium ions [51], proteins [40], nucleic acids [40], urea [53], and glucose [52].

1.6 Surface modification of microcapsules

The efficient immobilization, on the surface of the microcapsules, of an antibody or another 'detector' molecule that binds to an analyte is the first step in preparing a biosensor from microcapsules. There are several ways described in the literature for immobilizing antibodies on solid surfaces. Classically, 'physical adsorption' (mediated by electrostatic interactions and van der Waals force and hence non-covalent) is the simplest method; however, it results in poor reproducibility [54], weak interaction between the surface and the antibody, and presumably random orientation, due to which the antigen binding site of the antibody may not remain free to bind the analyte. Physical adsorption is relatively weak and also sensitive to changes in pH, temperature, or salt concentration [55]. Thus, to achieve a more stable interaction, antibodies should be bound to the surface of the microcapsules with covalent bonds, or *via* an adaptor protein such as protein A (see 1.8).

1.7 Surface modification of microcapsules using EDC/sulfo-NHS chemistry

Covalent attachment gives better reproducibility than physical adsorption and results in a strong interaction between the surface and the antibody [56]; it is resistant to changes in pH, temperature, salt, and other conditions and allows immobilization of proteins on a microcapsule surface with or without a spacer arm with a higher sensitivity [57].

For covalent attachment, the amine groups in the lysine side chains of the antibody can be coupled with EDC [58] or glutaraldehyde [59,60]. The carboxylic acid groups on the terminating layer (outer surface) of microcapsules are activated via EDC, resulting in the highly active intermediate, O-acylisourea, which forms a stable conjugate by forming an amide bond[8]. EDC crosslinking is most efficient in acidic (pH 5-6) conditions and must be performed in buffers that have no carboxyl groups or amines, such as MES (4-morpholinoethanesulfonic acid). Better than EDC alone, the EDC/sulfo-NHS (N-hydroxysulfosuccinimide) [13,61] chemistry is the most efficient way of crosslinking. In a two-step reaction, sulfo-NHS is added to the active intermediate O-acylisourea, resulting in a dry-stable amine-reactive sulfo-NHS ester that is more stable than the O-acylisourea and eventually forms an amide bond between the carboxylic acid group and a primary amine at physiological pH (**Figure 1.2**)

[8] When not reacted quickly with a primary amine, the O-acylisourea becomes unstable in aqueous solution and undergoes hydrolysis, regenerating the carboxylic acid.

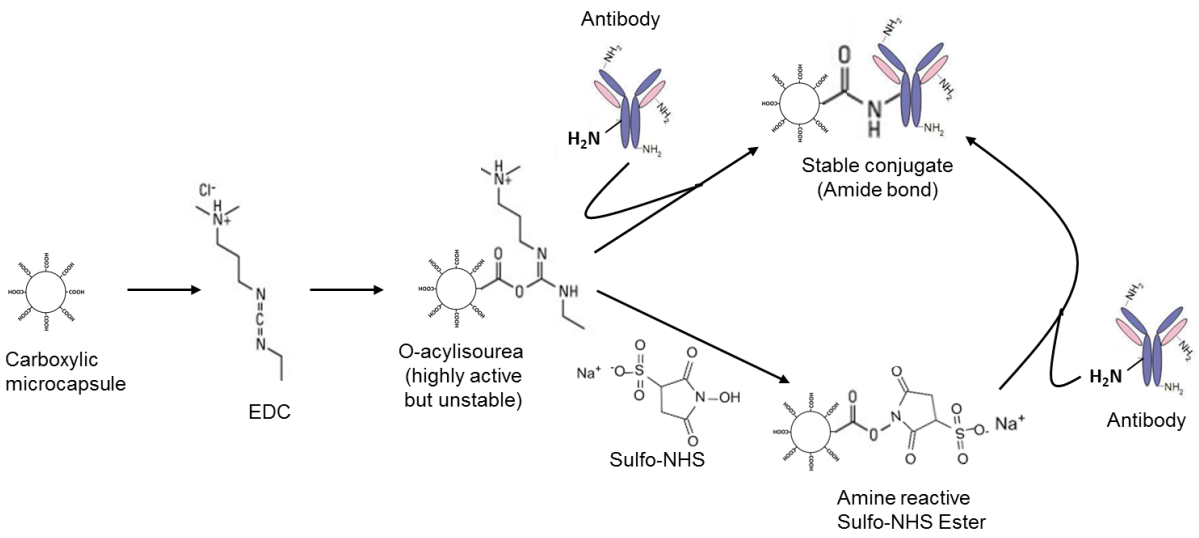

Figure 1.2: Surface modification of microcapsule using EDC/sulfo-NHS chemistry. Figure not to scale.

The procedure of protein immobilization onto the carboxyl surface of microcapsules via EDC/sulfo-NHS chemistry consists of several steps: first, the activation of carboxyl groups by adding a freshly prepared EDC/sulfo-NHS mixture[9]; then, the addition of the protein and coupling of primary amines of the protein to the NHS-activated surface; and finally, the deactivation (quenching) of unbound NHS groups either by ethanolamine [62] or Tris (in order to avoid nonspecific interactions).

The EDC and EDC/sulfo-NHS methods described here, while efficient, still lead to a random orientation of the antibody, potentially causing steric hindrance for the antibody [63] that might lead to the loss of binding capacity [64,65] and, as a result, lower efficiency of the sensor.

1.8 Surface modification of microcapsules using protein A

To attach more functional antibody molecules per microcapsule, oriented immobilization of antibodies on the surface is required, since this leads to more sensitive sensor [66,67]. This orients the Fab (Fragment antigen-binding) region of the antibody away from the surface of the microcapsule, into the solution, allowing it to bind the antigen. In optimized oriented immobilization, the antibody binds to the surfaces through the 'tail', the Fc (Fragment crystallizable) region. The best way to achieve optimized oriented attachment of antibodies

[9] While NHS is unstable in water, sulfo-NHS is water-soluble.

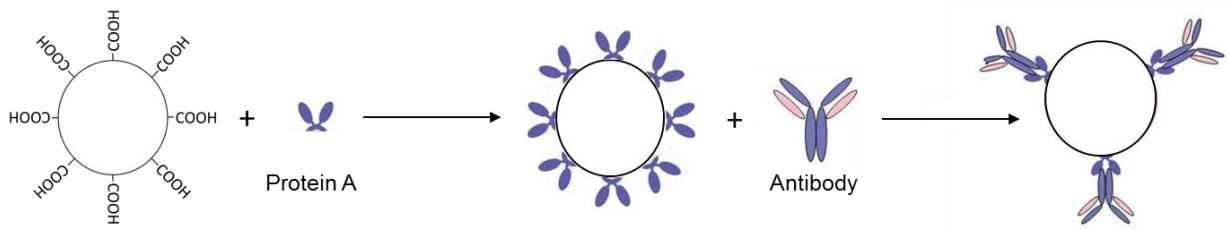

Figure 1.3: Schematic representation of surface modification of microcapsule with or without protein A-mediated through EDC/sulfo-NHS chemistry and subsequent immobilization of antibodies on the protein A microcapsule surface. Figure not to scale.

on surfaces is through the use of a first layer that consists of Fc-binding receptors or adaptor proteins (such as *Staphylococcus aureus* protein A). Such adaptor proteins bind the Fc region of the antibody and orient it on the microcapsule surface with the Fab region pointing towards the solution (**Figure 1.3**) [68,69].

Isotype	Human	Mouse	Rat	Goat
Total IgG	++	++	+	+
IgG1	++	–	+	+
IgG2	++	+	–	++
IgG3	+	++	–	
IgG4	++	++	++	
IgM	+	++		
IgD	–			
IgA	+			

Table 1.1: Binding of immunoglobulin (Ig) isotypes and subtypes to *S. aureus* protein A (++ strong binding, + weak binding, – no binding) [70–73].

Protein A is a cell wall protein of *Staphylococcus aureus* with a molecular weight of 42 kDa. It consists of a single polypeptide chain with little or no carbohydrate [74–77]. Protein A has a high affinity to the Fc region of IgG [78], positioning the Fab region outwards for the analyte to bind [70,79], and therefore, it is used in the preparation of biosensors and immunosensors [66,67]. Each molecule of Protein A can bind to two IgG molecules [76,77,80,81]. Optimal binding occurs at pH 8.2, although binding is also effective at neutral or physiological conditions. Protein A binds almost exclusively to the IgG isotype, but it binds with different affinity to different subtypes of IgG (**Table 1.1**). Based on the above chemistry, the best way to modify the surface of microcapsules is by using EDC/sulfo NHS chemistry for activation of

the surface carboxyl groups followed by coupling of protein A for the oriented immobilization of antibodies (**Figure 1.4**).

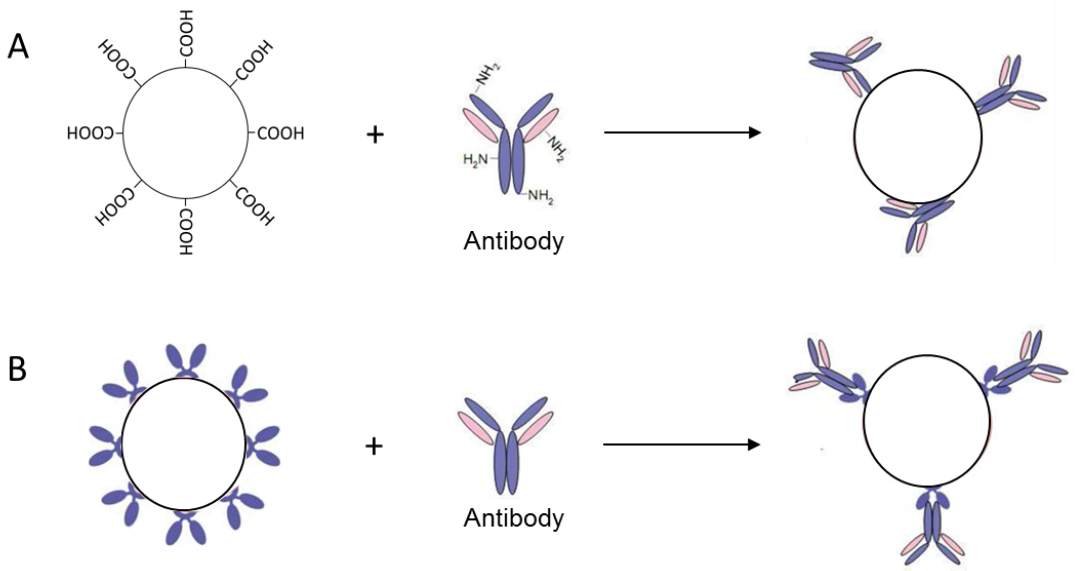

Figure 1.4: Schematic representation of random (**A**) and optimized (**B**) covalent immobilization of antibodies on the microcapsules' surface with (**B**) and without (**A**) Protein A attachment, mediated through EDC/sulfo-NHS chemistry. Figure not to scale.

1.9 Surface modification of microcapsules using streptavidin

Streptavidin is a tetrameric globular protein from the actinobacterium *Streptomyces avidinii* with a high binding affinity for biotin that is regarded the strongest known non-covalent biological interaction with a dissociation constant (K_d) of approximately 4×10^{-14} M [82]. It is commonly used as a linker to immobilize biotinylated molecules on surfaces[10]. The complex with biotin forms rapidly and is stable in wide ranges of pH and temperature [82]. The strong interaction has led to a large number of research, diagnostic, and biotechnological applications [83,84] for streptavidin-biotin technology. In most assays, streptavidin is coupled to a solid phase, such as a magnetic bead, a microtiter plate, or a biosensor chip, while biotin is coupled to the moiety of interest, often a nucleic acid, protein, or antibody. In my work, microcapsule surfaces modified with streptavidin have served as a universal platform, since they can be used to immobilize any biotinylated oligonucleotides (**Figure 1.5**).

[10] Streptavidin is more frequently used than the vertebrate protein avidin, mainly because of its availability in a number of engineered forms.

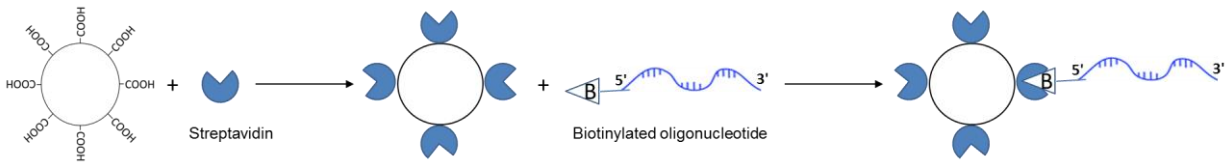

Figure 1.5: Schematic representation of of surface modification of microcapsules with streptavidin through EDC/sulfo-NHS chemistry and immobilization of biotinylated oligonucleotides on the microcapsule surface mediated through biotin-streptavidin interaction. Figure not to scale.

1.10 Aim of the project

The primary aim of the project described in this thesis was the development of an innovative and marker-free novel modular assay capable of detecting biological intermediates (nucleic acids, plasmids, transcripts, proteins, protein complexes, or small molecule metabolites) with high temporal and spatial resolution with the use of microcapsules and optical readout, preferentially based on proximity induction. To this end, techniques from the fields of material science and biophysics were employed and optimized for use in biological systems. Initial work focused on establishing a proof of principle for the assay in a single-bead configuration using two different approaches.

For the detection of proteins, the assay was developed in several steps. First, the binding efficiency of a monoclonal antibody on the surface of red surface-modified protein A microcapsules was detected by adding fluorophore-labelled secondary antibody. As the next step, two different microcapsules labelled with two different antibodies recognizing each other were used to obtain a biophysical proof of proximity. For the two-bead assay, two different microcapsules (red and green) were surface-modified with two different antibodies recognizing two different epitopes of the same antigen, thus bringing the microcapsules in close proximity.

For the detection of nucleic acids, microcapsules with oligonucleotides immobilized onto its surface and a fluorescently labelled oligonucleotide were used to detect a third oligonucleotide (analyte). We then tried detection of the third oligonucleotide with two microcapsules with oligonucleotides immobilized onto their surfaces. We also investigated the effects of microcapsule number and ratio, speed of acquisition, oligonucleotide length, reaction buffers, and blocking reagents on enhancing binding and specificity.

The rationale for using polyelectrolyte microcapsules to develop additional bead-based assays was as follows. In theory, the microcapsule-based assay offers several advantages over current bead-based assays: First, due to the porous nature of the wall of the microcapsules, they might be able to bind more proteins (e.g., capture antibodies) than beads with smooth

surfaces. Second, the microcapsules, due to the presence of $CaCO_3$ cores inside, should be easy to wash by centrifugation or filtration, whereas during the acquisition in flow cytometry the hollow microcapsules (after $CaCO_3$ cores have been dissolved in EDTA solution) can be read conveniently, in contrast to solid beads, which tend to settle at the bottom of the well or tube. This should make the microcapsules convenient for high throughput assays where acquisition with flow cytometry is carried out for longer duration. Moreover, due the porous nature of $CaCO_3$ cores, the microcapsules can be filled with different dyes for multiplexing assays, where microcapsules can be gated depending on the fluorescence in the flow cytometry.

1.11 References

[1] W. Tong, C. Gao, Stable microcapsules assembled stepwise from weak polyelectrolytes followed by thermal crosslinking, Polym. Adv. Technol. 16 (2005) 827–833. doi:10.1002/pat.659.

[2] J.. Decher, G., Hong, J.D., and Schmitt, Buildup of ultrathin multilayerfilms by a self-assembly process. 3.Consecutively alternating adsorptionof anionic and cationic polyelectrolytes on charged surfaces., Thin Solid Films. 210/211 (1992) 831–835.

[3] G.B. Sukhorukov, E. Donath, S. Davis, H. Lichtenfeld, F. Caruso, V.I. Popov, H. Möhwald, Stepwise polyelectrolyte assembly on particle surfaces: a novel approach to colloid design, Polym. Adv. Technol. 767 (1998) 759–767. doi:10.1002/(sici)1099-1581(1998100)9:10/11<759::aid-pat846>3.0.co;2-q.

[4] E. Donath, G.B. Sukhorukov, F. Caruso, S. a Davis, H. Möhwald, Novel Hollow Polymer Shells by Colloid Templated Assembly of Polyelectrolytes, Angew Chem Int Ed Engl. 37 (1998) 2201–2205. doi:10.1002/(SICI)1521-3773(19980904)37:16<2201::AID-ANIE2201>3.0.CO;2-E.

[5] J.H. Cheung, W.B. Stockton, M.F. Rubner, Molecular-Level Processing of Conjugated Polymers. 3. Layer-by-Layer Manipulation of Polyaniline via Electrostatic Interactions, Macromolecules. 30 (1997) 2712–2716. doi:10.1021/ma970047d.

[6] L. Wang, Z. Wang, X. Zhang, J. Shen, L. Chi, H. Fuchs, A new approach for the fabrication of an alternating multilayer film of poly(4-vinylpyridine) and poly(acrylic acid) based on hydrogen bonding, Macromol. Rapid Commun. 18 (1997) 509–514. doi:10.1002/marc.1997.030180609.

[7] G.K. Such, A.P.R. Johnston, F. Caruso, Engineered hydrogen-bonded polymer multilayers: from assembly to biomedical applications., Chem. Soc. Rev. 40 (2011) 19–29. doi:10.1039/c0cs00001a.

[8] Y. Liu, M. Bruening, Multilayer Dendrimer–Polyanhydride Composite Films on Glass, Silicon, and Gold Wafers, Angew. Chemie Int. Ed. 36 (1997) 2114–2116. doi:10.1002/anie.199721141.

[9] T. Serizawa, K. Nanameki, K. Yamamoto, M. Akashi, Thermoresponsive ultrathin hydrogels prepared by sequential chemical reactions, Macromolecules. 35 (2002) 2184–2189. doi:10.1021/ma011465s.

[10] T. Serizawa, D. Matsukuma, K. Nanameki, M. Uemura, F. Kurusu, M. Akashi, Stepwise preparation and characterization of ultrathin hydrogels composed of thermoresponsive polymers, Macromolecules. 37 (2004) 6531–6536. doi:10.1021/ma049154f.

[11] B.M. Wohl, J.F.J. Engbersen, Responsive layer-by-layer materials for drug delivery, J. Control. Release. 158 (2012) 2–14. doi:10.1016/j.jconrel.2011.08.035.

[12] P. Schuetz, F. Caruso, Copper-Assisted Weak Polyelectrolyte Multilayer Formation on Microspheres and Subsequent Film Crosslinking, Adv. Funct. Mater. 13 (2003) 929–937. doi:10.1002/adfm.200304483.

[13] Z. Grabarek, J. Gergely, Zero-length crosslinking procedure with the use of active esters, Anal. Biochem. 185 (1990) 131–135. doi:10.1016/0003-2697(90)90267-D.

[14] A.P.R. Johnston, C. Cortez, A.S. Angelatos, F. Caruso, Layer-by-layer engineered capsules and their applications, Curr. Opin. Colloid Interface Sci. 11 (2006) 203–209. doi:10.1016/j.cocis.2006.05.001.

[15] B.G. De Geest, A.G. Skirtach, G.B. Sukhorukov, J. Demeester, S.C. De Smedt, W.E. Hennink, Stimuli-responsive polyelectrolyte microcapsules for biomedical applications,

Am. Chem. Soc. Polym. Prepr. Div. Polym. Chem. 49 (2008) 1074–1075. doi:10.1039/b808262f.

[16] G.B. Sukhorukov, H. Möhwald, Multifunctional cargo systems for biotechnology, Trends Biotechnol. 25 (2007) 93–98. doi:10.1016/j.tibtech.2006.12.007.

[17] W. Bi, M. Tian, K.H. Row, Selective extraction and separation of oxymatrine from Sophora flavescens Ait. extract by silica-confined ionic liquid, J. Chromatogr. B Anal. Technol. Biomed. Life Sci. 880 (2012) 108–113. doi:10.1016/j.jchromb.2011.11.025.

[18] J. Wong, A. Chilkoti, V.T. Moy, Direct force measurements of the streptavidin – biotin interaction, Biomol. Eng. 16 (1999) 45–55.

[19] G.B. Sukhorukov, D.G. Shchukin, W.F. Dong, H. Möhwald, V. V. Lulevich, O.I. Vinogradova, Comparative analysis of hollow and filled polyelectrolyte microcapsules templated on melamine formaldehyde and carbonate cores, Macromol. Chem. Phys. 205 (2004) 530–535. doi:10.1002/macp.200300004.

[20] F. Caruso, Nanoengineering of Inorganic and Hybrid Hollow Spheres by Colloidal Templating, Science (80-.). 282 (1998) 1111–1114. doi:10.1126/science.282.5391.1111.

[21] C.S. Peyratout, L. Dähne, Tailor-made polyelectrolyte microcapsules: From multilayers to smart containers, Angew. Chemie - Int. Ed. 43 (2004) 3762–3783. doi:10.1002/anie.200300568.

[22] D. V. Volodkin, N.I. Larionova, G.B. Sukhorukov, Protein encapsulation via porous CaCO3 microparticles templating, Biomacromolecules. 5 (2004) 1962–1972. doi:10.1021/bm049669e.

[23] A.A. Antipov, G.B. Sukhorukov, S. Leporatti, I.L. Radtchenko, E. Donath, H. Möhwald, Polyelectrolyte multilayer capsule permeability control, Colloids Surfaces A Physicochem. Eng. Asp. 198–200 (2002) 535–541. doi:10.1016/S0927-7757(01)00956-6.

[24] D. Silvano, S. Krol, A. Diaspro, O. Cavalleri, A. Gliozzi, Confocal laser scanning microscopy to study formation and properties of polyelectrolyte nanocapsules derived from CdCO3 templates, Microsc. Res. Tech. 59 (2002) 536–541. doi:10.1002/jemt.10235.

[25] G. Decher, Fuzzy Nanoassemblies: Toward Layered Polymeric Multicomposites, Science (80-.). 277 (1997) 1232–1237. doi:10.1126/science.277.5330.1232.

[26] C.-L. Zhu, X. Song, W.-H. Zhou, H. Yang, Y. Wen, X.-R. Wang, An efficient cell-targeting and intracellular controlled-release drug delivery system based on MSN-PEM-aptamer conjugates, J. Mater. Chem. 19 (2009) 7765–7770. doi:10.1039/b907978e.

[27] R. Palankar, A.G. Skirtach, O. Kreft, M. Bédard, M. Garstka, K. Gould, H. Möhwald, G.B. Sukhorukov, M. Winterhalter, S. Springer, Controlled intracellular release of peptides from microcapsules enhances antigen presentation on MHC class I molecules, Small. 5 (2009) 2168–2176. doi:10.1002/smll.200900809.

[28] J.L. Santos, A. Nouri, T. Fernandes, J. Rodrigues, H. Tomás, Gene delivery using biodegradable polyelectrolyte microcapsules prepared through the layer-by-layer technique, Biotechnol. Prog. 28 (2012) 1088–1094. doi:10.1002/btpr.1576.

[29] O. Kreft, A.M. Javier, G.B. Sukhorukov, W.J. Parak, Polymer microcapsules as mobile local pH-sensors, J. Mater. Chem. 17 (2007) 4471. doi:10.1039/b705419j.

[30] D. Studer, R. Palankar, M. Bédard, M. Winterhalter, S. Springer, Retrieval of a metabolite from cells with polyelectrolyte microcapsules, Small. 6 (2010) 2412–2419. doi:10.1002/smll.200901997.

[31] C.J. Ochs, G.K. Such, B. Städler, F. Caruso, Low-fouling, biofunctionalized, and

biodegradable click capsules, Biomacromolecules. 9 (2008) 3389–3396. doi:10.1021/bm800794w.

[32] Y. Wang, V. Bansal, A.N. Zelikin, F. Caruso, Templated synthesis of single-component polymer capsules and their application in drug delivery, Nano Lett. 8 (2008) 1741–1745. doi:10.1021/nl080877c.

[33] L.L. del Mercato, P. Rivera-Gil, A.Z. Abbasi, M. Ochs, C. Ganas, I. Zins, C. Sönnichsen, W.J. Parak, LbL multilayer capsules: recent progress and future outlook for their use in life sciences., Nanoscale. 2 (2010) 458–467. doi:10.1039/b9nr00341j.

[34] D.G. Shchukin, T. Shutava, E. Shchukina, G.B. Sukhorukov, Y.M. Lvov, Modified polyelectrolyte microcapsules as smart defense systems, Chem. Mater. 16 (2004) 3446–3451. doi:10.1021/cm049506x.

[35] L. Krasemann, B. Tieke, Selective ion transport across self-assembled alternating multilayers of cationic and anionic polyelectrolytes, Langmuir. 16 (2000) 287–290. doi:10.1021/la991240z.

[36] P.R. Gil, L.L. del Mercato, P. del Pino, A. Mu??oz-Javier, W.J. Parak, Nanoparticle-modified polyelectrolyte capsules, Nano Today. 3 (2008) 12–21. doi:10.1016/S1748-0132(08)70040-9.

[37] L.I. Kazakova, L.I. Shabarchina, S. Anastasova, A.M. Pavlov, P. Vadgama, A.G. Skirtach, G.B. Sukhorukov, Chemosensors and biosensors based on polyelectrolyte microcapsules containing fluorescent dyes and enzymes, Anal. Bioanal. Chem. 405 (2013) 1559–1568. doi:10.1007/s00216-012-6381-0.

[38] M.S. Aw, M. Bariana, Y. Yu, J. Addai-Mensah, D. Losic, Surface-functionalized diatom microcapsules for drug delivery of water-insoluble drugs., J. Biomater. Appl. 28 (2013) 163–74. doi:10.1177/0885328212441846.

[39] Z.M. Qian, H. Li, H. Sun, K. Ho, Targeted Drug Delivery via the Transferrin Receptor-, 54 (2002) 561–587.

[40] S.K. Verma, A. Amoah, U. Schellhaas, M. Winterhalter, S. Springer, T.A. Kolesnikova, ???To Catch or Not to Catch???: Microcapsule-Based Sandwich Assay for Detection of Proteins and Nucleic Acids, Adv. Funct. Mater. 26 (2016) 6015–6024. doi:10.1002/adfm.201601328.

[41] A.N. Zelikin, K. Breheney, R. Robert, E. Tjipto, K. Wark, Cytotoxicity and internalization of polymer hydrogel capsules by mammalian cells, Biomacromolecules. 11 (2010) 2123–2129. doi:10.1021/bm100500v.

[42] L. Kastl, D. Sasse, V. Wulf, R. Hartmann, J. Mircheski, C. Ranke, A. Martı, R. Ferna, S. Carregal-romero, Multiple Internalization Pathways of Polyelectrolyte Multilayer Capsules into Mammalian Cells, (2013) 6605–6618.

[43] R. Zhang, K. Köhler, O. Kreft, A. Skirtach, H. Möhwald, G. Sukhorukov, Salt-induced fusion of microcapsules of polyelectrolytes, Soft Matter. 6 (2010) 4742. doi:10.1039/c0sm00218f.

[44] S.K. Vashist, E. Marion Schneider, E. Lam, S. Hrapovic, J.H.T. Luong, One-step antibody immobilization-based rapid and highly-sensitive sandwich ELISA procedure for potential in vitro diagnostics., Sci. Rep. 4 (2014) 4407. doi:10.1038/srep04407.

[45] S.W. Kim, I.H. Cho, J.N. Park, S.M. Seo, S.H. Paek, A high-performance fluorescence immunoassay based on the relaxation of quenching, exemplified by detection of cardiac troponin I, Sensors (Switzerland). 16 (2016). doi:10.3390/s16050669.

[46] W. Kim, L. Mineo, M.E. Koivunen, R.L. Krogsrud, R. Berg, S. Chapter, Principles of Immunochemical Techniques Used in Clinical Laboratories, Lab. Med. 37 (2006) 490–497. doi:10.1309/MV9RM1FDLWAUWQ3F.

[47] I.A. Darwish, Immunoassay Methods and their Applications in Pharmaceutical Analysis : Basic Methodology and Recent Advances, Int. J. Biomed. Sciense. 2 (2006) 217–235. http://www.pubmedcentral.nih.gov/articlerender.fcgi?artid=3614608&tool=pmcentrez&rendertype=abstract.

[48] N. Cook, A. Harris, A. Hopkins, K. Hughes, Scintillation Proximity Assay (SPA) Technology to Study Biomolecular Interactions, in: Curr. Protoc. Protein Sci., John Wiley & Sons, Inc., 2001. doi:10.1002/0471140864.ps1908s27.

[49] J. Berry, M. Price-Jones, Measurement of Radioligand Binding by Scintillation Proximity Assay, in: A.P. Davenport (Ed.), Recept. Bind. Tech., Humana Press, Totowa, NJ, 2005: pp. 121–138. doi:10.1385/1-59259-927-3:121.

[50] J.F. Glickman, A. Schmid, S. Ferrand, Scintillation proximity assays in high-throughput screening., Assay Drug Dev. Technol. 6 (2008) 433–455. doi:10.1089/adt.2008.135.

[51] L.L. Del Mercato, A.Z. Abbasi, M. Ochs, W.J. Parak, Multiplexed sensing of ions with barcoded polyelectrolyte capsules, ACS Nano. 5 (2011) 9668–9674. doi:10.1021/nn203344w.

[52] S. Chinnayelka, M.J. McShane, Microcapsule biosensors using competitive binding resonance energy transfer assays based on apoenzymes, Anal. Chem. 77 (2005) 5501–5511. doi:10.1021/ac050755u.

[53] L.I. Kazakova, L.I. Shabarchina, G.B. Sukhorukov, Co-encapsulation of enzyme and sensitive dye as a tool for fabrication of microcapsule based sensor for urea measuring, Phys. Chem. Chem. Phys. 13 (2011) 11110–11117. doi:Doi 10.1039/C1cp20354a.

[54] S. Ferretti, S. Paynter, D.A. Russell, K.E. Sapsford, D.J. Richardson, Self-assembled monolayers: A versatile tool for the formulation of bio- surfaces, TrAC - Trends Anal. Chem. 19 (2000) 530–540. doi:10.1016/S0165-9936(00)00032-7.

[55] A.K. Trilling, J. Beekwilder, H. Zuilhof, Antibody orientation on biosensor surfaces: a minireview., Analyst. 138 (2013) 1619–27. doi:10.1039/c2an36787d.

[56] J.L. ORTEGA-VINUESA, D. BASTOS-GONZÁLEZ, R. HIDALGO-ÁLVAREZ, Comparative Studies on Physically Adsorbed and Chemically Bound IgG to Carboxylated Latexes, II, J. Colloid Interface Sci. 176 (1995) 240–247. doi:10.1006/jcis.1995.0027.

[57] J.. A. Molina-Bolivar, F. Galisteo-Gonzalez, R. Hidalgo-Alvarez, Latex immunoassays: Comparative studies on covalent and physical immobilization of antibodies. II. IgG, J. Biomater. Sci. Polym. Ed. 9 (1998) 1103–1113. doi:10.1163/156856298X00352.

[58] P. Kocbek, N. Obermajer, M. Cegnar, J. Kos, J. Kristl, Targeting cancer cells using PLGA nanoparticles surface modified with monoclonal antibody, J. Control. Release. 120 (2007) 18–26. doi:10.1016/j.jconrel.2007.03.012.

[59] T.Q. Huy, N.T.H. Hanh, P. Van Chung, D.D. Anh, P.T. Nga, M.A. Tuan, Characterization of immobilization methods of antiviral antibodies in serum for electrochemical biosensors, Appl. Surf. Sci. 257 (2011) 7090–7095. doi:10.1016/j.apsusc.2011.03.051.

[60] Y. Yuan, M. Yin, J. Qian, C. Liu, B.D. Markway, O.J.T. Mccarty, U.M. Marzec, D.W. Courtman, S.R. Hanson, M.T. Hinds, S.T. Rashid, H.J. Salacinski, B.J. Fuller, G. Hamilton, A.M. Seifalian, J. Yand, D. Motlagh, A.R. Webb, G.A. Ameer, W.J. Zhang, W. Liu, L. Cui, Y.L. Cao, M. Yin, Y. Yuan, C.S. Liu, J. Wang, S. Meng, Z.J. Liu, L. Shen, Z. Guo, L.S.L. Chou, W. Zhong, Q.G. Du, J.B. Ge, E.P. McFadden, E. Stabile, E. Regar, E. Cheneau, A.T.L. Ong, T. Kinnaird, W.O. Suddath, N.J. Weissman, R. Torguson, K.M. Kent, A.D. Pichard, L.F. Satler, R. Waksman, P.W. Serruys, T. Suzuki, G. Kopia, S. Hayashi, L.R. Bailey, G. Llanos, R. Wilensky, B.D. Klugherz, G. Papandreou, P. Narayan, M.B. Leon, A.C. Yeung, F. Tio, P.S. Tsao, R. Falotico, A.J. Carter, N.A. Scott, T.C. Woods, A.R. Marks, M. Avci-Adali, A. Paul, G. Ziemer, H.P. Wendel, T.F. Luscher,

M. Barton, T. Shirota, H. Yasui, H. Shimokawa, T. Matsuda, R.H. Schmedlen, W.M. Elbjeirami, A.S. Gobin, J.L. West, B.H. Walpoth, G.L. Bowli, Q.K. Lin, X. Ding, F.Y. Qiu, X.X. Song, G.S. Fu, J. Ji, J. Lu, M.P. Rao, N.C. MacDonald, D. Khang, T.J. Webster, S. V. Pislaru, A. Harbuzariu, G. Agarwal, T. Witt, R. Gulati, N.P. Sandhu, C. Mueske, M. Kalra, G.S. Sandhu, R.D. Simari, J. Aoki, P.W. Serruys, H. van Beusekom, A.T.L. Ong, E.P. McFadden, G. Sianos, W.J. van der Giessen, E. Regar, P.J. de Feyter, H.R. Davis, S. Rowland, M.J.B. Kutryk, S. Silber, J.I. Rotmans, J.M. Heyligers, H.J. Verhagen, E. Velema, M.M. Nagtegaal, D.P. de Kleijn, E.S.G. Stroes, J. Middleton, L. Americh, R. Gayon, D. Julien, M. Mansat, P. Mansat, P. Anract, A. Cantagrel, P. Cattan, J.M. Reimund, L. Aguilar, F. Amalric, J.P.P. Girard, B.J. Nickoloff, J.M. Fowler, M.C. Stuart, D.K.Y. Wong, H. Wang, Y.L. Liu, Y.H. Yang, T. Deng, G.L. Shen, R.Q. Yu, A.A. Karyakin, G. V. Presnova, M.Y. Rubtsova, A.M. Egorov, M. Yin, Y. Yuan, C.S. Liu, J. Wang, J.C. Zhang, S.M. Li, C.L. Song, B. Liu, I. Vikholm, W.M. Albers, H. Xu, J.R. Lu, D.E. Williams, D.J. O'shannessy, E.J. Franco, H. Hofstetter, O. Hofstetter, Y. Iwasaki, Y. Omichi, R. Iwata, S. Kalachandar, L. Dongming, S. Offenbacher, Q.H. Guo, S.R. Guo, Z.M. Wang, Y. Yuan, C.S. Liu, M. Yin, Y. Zhang, M. Kardar, Y.W. Jung, J.Y. Jeong, B.H. Chung, I.H. Cho, E.H. Paek, H. Lee, J.Y. Kang, T.S. Kim, S.H. Paek, J.H. Kang, H.J. Choi, S.Y. Hwang, S.H. Han, J.Y. Jeon, E.K. Lee, C.L. Dai, Y. Yuan, C.S. Liu, J. Wei, C.C. Larsen, F. Kligman, C. Tang, K. Kottke-Marchant, R.E. Marchant, Site-directed immobilization of antibodies onto blood contacting grafts for enhanced endothelial cell adhesion and proliferation, Soft Matter. 7 (2011) 7207. doi:10.1039/c1sm05086a.

[61] J. V. Staros, R.W. Wright, D.M. Swingle, Enhancement by N-hydroxysulfosuccinimide of water-soluble carbodiimide-mediated coupling reactions, Anal. Biochem. 156 (1986) 220–222. doi:10.1016/0003-2697(86)90176-4.

[62] B. Johnsson, S. Löfås, G. Lindquist, Immobilization of proteins to a carboxymethyldextran-modified gold surface for biospecific interaction analysis in surface plasmon resonance sensors, Anal. Biochem. 198 (1991) 268–277. doi:10.1016/0003-2697(91)90424-R.

[63] D.Q. Tang, D.J. Zhang, D.Y. Tang, H. Ai, Amplification of the antigen-antibody interaction from quartz crystal microbalance immunosensors via back-filling immobilization of nanogold on biorecognition surface, J. Immunol. Methods. 316 (2006) 144–152. doi:10.1016/j.jim.2006.08.012.

[64] J.-Y. Jyoung, S. Hong, W. Lee, J.-W. Choi, Immunosensor for the detection of Vibrio cholerae O1 using surface plasmon resonance, Biosens. Bioelectron. 21 (2006) 2315–9. doi:10.1016/j.bios.2005.10.015.

[65] N. Patel, M.C. Davies, M. Hartshorne, R.J. Heaton, C.J. Roberts, S.J.B. Tendler, P.M. Williams, Immobilization of protein molecules onto homogeneous and mixed carboxylate-terminated self-assembled monolayers, Langmuir. 13 (1997) 6485–6490. doi:10.1021/la970933h.

[66] B. Feng, S. Huang, F. Ge, Y. Luo, D. Jia, Y. Dai, 3D antibody immobilization on a planar matrix surface, Biosens. Bioelectron. 28 (2011) 91–96. doi:10.1016/j.bios.2011.07.003.

[67] N. Tajima, M. Takai, K. Ishihara, Significance of antibody orientation unraveled: Well-oriented antibodies recorded high binding affinity, Anal. Chem. 83 (2011) 1969–1976. doi:10.1021/ac1026786.

[68] A.A. Karyakin, G. V. Presnova, M.Y. Rubtsova, A.M. Egorov, Oriented immobilization of antibodies onto the gold surfaces via their native thiol groups, Anal. Chem. 72 (2000) 3805–3811. doi:10.1021/ac9907890.

[69] H.Y. Song, X. Zhou, J. Hobley, X. Su, Comparative study of random and oriented antibody immobilization as measured by dual polarization interferometry and surface plasmon resonance spectroscopy, Langmuir. 28 (2012) 997–1004. doi:10.1021/la202734f.

[70] A. Forsgren, E. Alerts, Protein A from S . Aureus : I . Pseudo-Immune Reaction with Human γ -Globulin, (2017).

[71] A. Surolia, D. Pain, M. Islam Khan, Protein A: nature's universal anti-antibody, Trends Biochem. Sci. 7 (1982) 74–76. doi:10.1016/0968-0004(82)90082-2.

[72] H. HJELM, J. SJ??DAHL, J. SJ??QUIST, Immunologically Active and Structurally Similar Fragments of Protein A from Staphylococcus aureus, Eur. J. Biochem. 57 (1975) 395–403. doi:10.1111/j.1432-1033.1975.tb02313.x.

[73] T. Williams, W. Co, Copyright ~ 1969, 103 (1969) 828–833.

[74] M. Graille, E. a Stura, a L. Corper, B.J. Sutton, M.J. Taussig, J.B. Charbonnier, G.J. Silverman, Crystal structure of a Staphylococcus aureus protein A domain complexed with the Fab fragment of a human IgM antibody: structural basis for recognition of B-cell receptors and superantigen activity., Proc. Natl. Acad. Sci. U. S. A. 97 (2000) 5399–404. doi:10.1073/pnas.97.10.5399.

[75] I. Bj??rk, B. Petersson, J. Sj??quist, Some Physicochemical Properties of Protein A from Staphylococcus aureus, Eur. J. Biochem. 29 (1972) 579–584. doi:10.1111/j.1432-1033.1972.tb02024.x.

[76] J. Sj??quist, B. Meloun, H. Hjelm, Protein A Isolated from Staphylococcus aureus after Digestion with Lysostaphin, Eur. J. Biochem. 29 (1972) 572–578. doi:10.1111/j.1432-1033.1972.tb02023.x.

[77] T. MOKS, L. ABRAHMS??N, B. NILSSON, U. HELLMAN, J. SJ??QUIST, M. UHL??N, Staphylococcal protein A consists of five IgG???binding domains, Eur. J. Biochem. 156 (1986) 637–643. doi:10.1111/j.1432-1033.1986.tb09625.x.

[78] Z. Wang, G. Jin, Feasibility of protein A for the oriented immobilization of immunoglobulin on silicon surface for a biosensor with imaging ellipsometry, J. Biochem. Biophys. Methods. 57 (2003) 203–211. doi:10.1016/S0165-022X(03)00109-X.

[79] A.P. Le Brun, S.A. Holt, D.S.H. Shah, C.F. Majkrzak, J.H. Lakey, The structural orientation of antibody layers bound to engineered biosensor surfaces, Biomaterials. 32 (2011) 3303–3311. doi:10.1016/j.biomaterials.2011.01.026.

[80] R. Danczyk, B. Krieder, A. North, T. Webster, H. HogenEsch, A. Rundell, Comparison of antibody functionality using different immobilization methods, Biotechnol. Bioeng. 84 (2003) 215–223. doi:10.1002/bit.10760.

[81] A.T.B. JOHN J. LANGONE, MICHAEL D. P. BOYLE, STUDIES ON THE INTERACTION BETWEEN PROTEIN A AND IMMUNOGLOBULIN G I. Effect of Protein A on the Functional Activity of IgG, J. Immunol. 121 (1978) 327–332.

[82] N.M. Green, Avidin and streptavidin, Methods Enzymol. 184 (1990) 51–67. doi:10.1016/0076-6879(90)84259-J.

[83] M. Wilchek, E.A. Bayer, Introduction to avidin-biotin technology, Methods Enzymol. 184 (1990) 5–13. doi:10.1016/0076-6879(90)84256-G.

[84] O.H. Laitinen, H.R. Nordlund, V.P. Hytönen, M.S. Kulomaa, Brave new (strept)avidins in biotechnology, Trends Biotechnol. 25 (2007) 269–277. doi:10.1016/j.tibtech.2007.04.001.

2 Chapter 2: Results Summary

For my thesis work, I first investigated the binding of biomolecules (antibodies and oligonucleotides) to the microcapsule surface and its measurement by flow cytometry. Findings from these studies were then extended to using microcapsules as a detection tool for proteins and nucleic acids.

I used these microcapsules for the detection of biomarker human beta-2 microglobulin (hβ_2m, a protein found in blood and urine and used as biomarker for the detection of melanoma and renal failure) using protein A modified microcapsules. The microcapsules were able to detect the presence of hβ_2m in PBS and FCS with high specificity and selectivity. Such a sensitive tool for the detection of hβ_2m has been shown for the first time here.

I next used the microcapsules, surface-modified with streptavidin, for the detection of biotinylated MHC class I as well as oligonucleotides. The streptavidin-modified microcapsules were able to detect the presence of the analyte nucleic acid with sensitivity and high selectivity. As a next step, I compared the microcapsule assay sensitivity with that of commercially available PS beads, and I found that the microcapsules are more sensitive for the detection of protein, whereas for the detection of nucleic acid, both microcapsules and PS beads showed similar sensitivity.

I also tried the novel methodology of analyte-induced proximity between two microcapsules filled with red and green dye. However, these experiments showed high non-specific binding, with high background signals observed.

In this thesis, for better understanding and better illustration, these research findings are distributed to three major sections (**chapter 3 to 5**). The two major research findings of my thesis – that the microcapsules detect protein analyte with sensitivity and selectivity and that the microcapsules are a better tool to commercially available beads– are described in **chapter 3** and **chapter 4,** respectively. Within the chapters, each major section has been further simplified by dividing it to subsections. Below are the summaries of findings described in each of these sections. The analyte-induced proximity between two or more microcapsules has beed described in detail in **chapter 5.**

Chapter 3 is a published paper, and it explains the development of the microcapsules as a single bead assay for the detection of hβ_2m and nucleic acids. Microcapsules were able to detect the protein analyte hβ_2m with a limit of detection (LoD) value of 7.7 fg/mL in PBS and 212.5 pg/mL in fetal calf serum (FCS), whereas for the nucleic acid, the LoD values observed were 1.8 nM. In both the cases, the microcapsules were highly selective for the detection of the respective analytes.

Chapter 2: Results Summary

The publication details are: To Catch or not to Catch: Microcapsule-Based Sandwich Assay for Detection of Proteins and Nucleic Acids. S. K. Verma, A. Amoah, U. Schellhaas, M. Winterhalter, S. Springer, T.A. Kolesnikova, Adv. Funct. Mater, 2016, 26, 6015-6024.

Chapter 4 contains the follow-up work from the previous chapter and compares the sensitivity of the microcapsule-based assay with the commercially available beads. With respect for the detection of hβ_2m, the microcapsules showed a 450-fold better sensitivity, where both the microcapsules and the PS beads showed similar sensitivity for the detection of the nucleic acids. As an alternative application, microcapsules were able to detect the presence of the antibody in an hybridoma supernatant with high sensitivity as compared to the standard immunoassay plate systems. The presence of antibody in an hybridoma supernatant was detected at very low volume with LoD value of 3 nL/mL for microcapsule where for the standard immunoassay plate the detection limit was 152 nL/mL.

Chapter 5 discusses the novel idea of analyte induced proximity using microcapsules. For the experiments, microcapsules were filled with red (Atto-488 conjugated with BSA) and green (AF-647 conjugated with BSA) dyes. **Chapter 5.6.1** discusses induced proximity using antibodies in which as a biophysical proof of principle, first two antibodies recognizing each other were attached on the surface of protein A-functionalized microcapsules. After the proof of principle experiment, two antibodies recognizing two different epitopes of an antigen were attached to the microcapsule surface and were incubated together in the presence of analyte (specific signal) or in the absence of the analyte (background signal). However, a very high background signal was observed mainly due to the non-specific interactions between the microcapsules. To check if other assay conditions viz. buffer, charges, blocking, ratio of red and green microcapsules, concentration of microcapsules per reaction, speed of acquisition etc., different experiments were performed but the highest signal to background ratio observed was 3-4 fold.

In the second part, which is **chapter 5.6.2**, induced proximity between microcapsules using oligonucleotides is discussed. In a similar approach as discussed in 5.6.1, for a biophysical proof of principle, two complementary oligonucleotides were attached on the surface of streptavidin modified red and green microcapsules. In the next step, two or more microcapsules were brought together in the presence of the analyte oligo, which has half the sequence complementary to oligo attached on the red microcapsules and the other half complementary to the biotinylated oligo attached on the green microcapsule. The microcapsules with the oligonucleotides showed a very high background signal due to high

non-specific binding between the microcapsules. In the standardization experiments, 1% milk showed best blocking activity though future experiments needs to be performed.

All the experiments performed during the development process are described in detail with a future plan of experiments.

Statement of Authorship

The experimental work described in this thesis entirely belongs to me, unless specified otherwise for certain figures.

Chapter 3

In this chapter, I report on the surface functionalization of the microcapsules with protein A and streptavidin and the ability of the microcapsules to bind antibodies and biotinylated biomolecules (oligonucleotides and MHC class proteins). The protein A microcapsules are used for detecting the biomarker human beta-2 microglobulin (hβ_2m) in both PBS and FCS at femtomolar concentrations, and the streptavidin microcapsules are used for the detection of nucleic acids.

The work in this chapter is mostly described in a published paper that was mostly written by Tatiana Kolesnikova. This paper can be accessed at the following URL:
http://onlinelibrary.wiley.com/wol1/doi/10.1002/adfm.201601328/abstract.
Compared to the published paper, this chapter has some additional repeats of experiments, and some additional data. Some data are shown in different graphs, but for other data or models, the text of the chapter refers to figures of the paper. The different individual contributions to the paper by the authors are listed at the beginning of the appendix.

3 Chapter 3: Microcapsule-based immunoassay for the detection of proteins and nucleic acids

3.1 Introduction and aims of the work

The aim of the work reported in this chapter was to demonstrate the use of polyelectrolyte microcapsules in assays for the detection of soluble analytes with two proof-of-principle assay systems, one for a protein analyte and one for a nucleic acid.

First, the construction and functionalization of the capsules is described and characterized. Then, the assays are described; finally, the potential roles of these assays in biotechnology are discussed.

3.2 Quality control of the polyelectrolyte microcapsules

3.2.1 EDC crosslinking of microcapsules makes them resistant to extreme pH values

After layer-by-layer assembly, microcapsules[11] are only held together by electrostatic interactions between the polyelectrolytes. When at low pH values, the carboxylate groups become protonated or when at high pH values, the ammonium groups become deprotonated, one kind of polyelectrolytes lose their charge, and the microcapsules disintegrate because of the remaining uniform charge.

To prevent this, I tested crosslinking the polyelectrolytes with EDC (see 1.7). **Figure 3.1** shows that once crosslinked, capsules no longer disintegrated at pH 2 or pH 11, suggesting that their integrity now no longer depended on charge interactions. This experiment is also shown in Figure S1 of the paper. Thus, EDC crosslinking will allow the use of microcapsules at any pH value.

[11] The word 'microcapsules' in this chapter refers only to the polyelectrolyte microcapsules that were used in my work, not to any other technique or chemistry. Sometimes, 'microcapsules' also includes core-shell-particles, *i.e.*, microcapsules before the removal of the carbonate core, or it means just the polyelectrolyte layers of a core-shell particle, for example in this sentence.

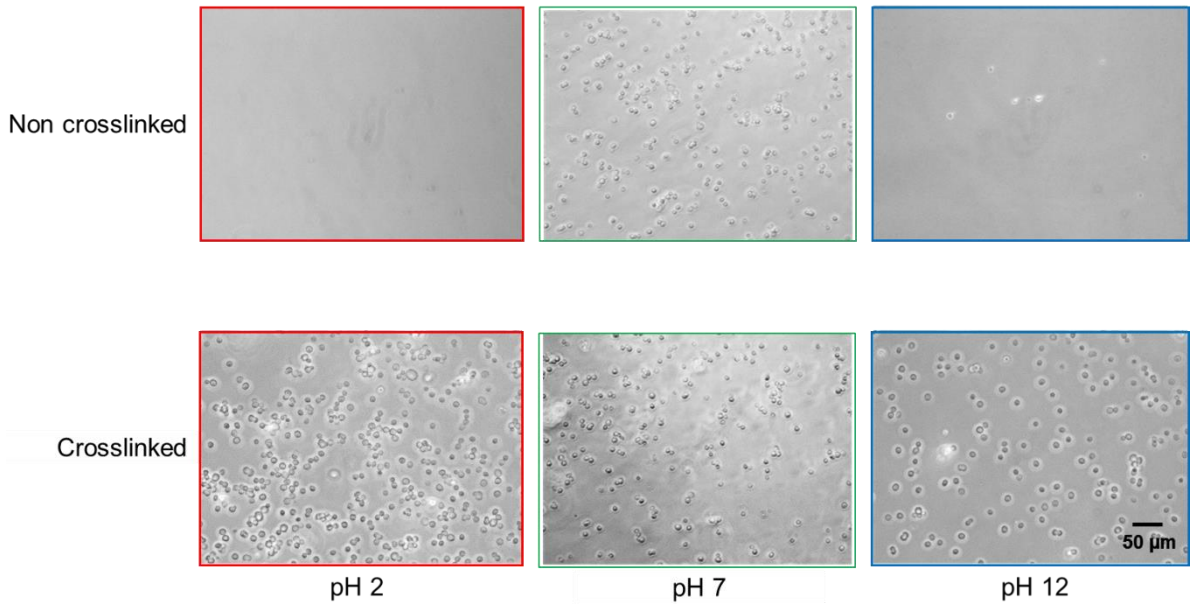

Figure 3.1: EDC crosslinking makes microcapsules resistant to extreme pH values. $(PAH/PAA)_2$ core-shell particles were prepared and crosslinked as described in 4.3.2., then the cores were dissolved with 0.2 M EDTA pH 7.2, the capsules were incubated at the indicated pH values, and then imaged in the microscope.

Following these experiments, a separate EDC crosslinking step was used in all subsequent experiments, even when the capsules were treated with EDC/sulfo-NHS anyways in the subsequent step to immobilize proteins to their surface [1–5].

3.2.2 Layer-by-layer assembly is accompanied by surface charge reversal

Layer-by-layer assembly of microcapsules works because the deposition of each layer of polyelectrolytes onto the surface of the core-shell particle leads to a charge reversal. Thus, if the particle is incubated with a positively charge polyelectrolyte, it carries a slight positive charge afterwards, which makes it possible to add the next oppositely charged layer (see 1.1).

A zeta potential measurement carried out by Tatiana Kolesnikova showed that this was indeed the case in our microcapsule production process. This experiment is shown in Figure S2 of the paper.

3.2.3 Protein A and antibodies can be immobilized on the surface of microcapsules with EDC/sulfo-NHS chemistry

We next sought to attach proteins to the surface of the core-shell particles using EDC/sulfo-NHS chemistry (see 1.7). Quantification of the proteins bound to the core-shell particle surface

is difficult in principle, since proteins are covalently bound and cannot easily be separated from the surface to perform dye binding or gel electrophoresis-based quantitative determination.

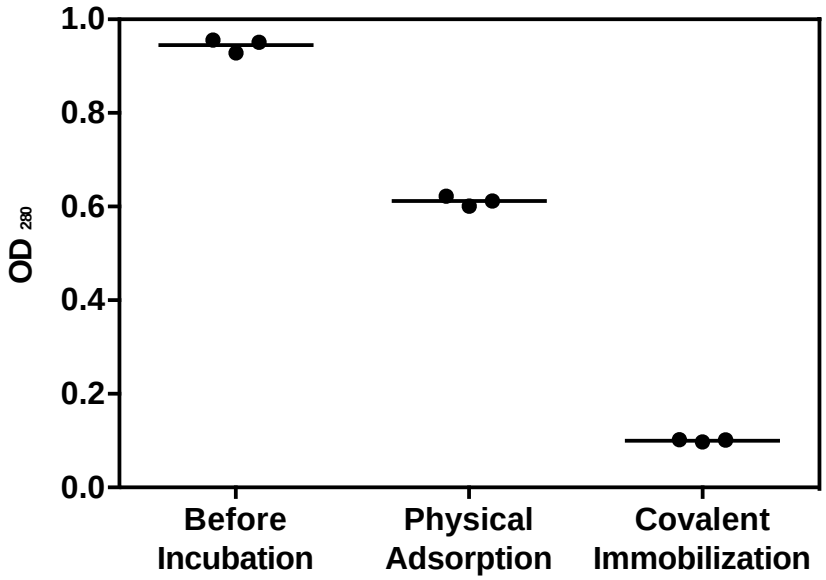

Figure 3.2: Protein A is depleted from the reaction supernatant during immobilization to the core-shell particles. To 500 µl of a 0.05 mg/ml solution of protein A, 1 x 10^7 core-shell particles (prepared as described in 4.3.2.) were added. The extinction at 280 nm (OD_{280}) was measured for the protein A solution before the addition of the capsules (left), and after overnight incubation with core-shell particles that were not activated (center) or that were activated with EDC/sulfo-NHS (right).

One way of quantifying any immobilized protein is to measure its depletion of the solution that is used for crosslinking. Such experiments are shown for protein A in **Figure 3.2**. The experiments allow a rough calculation of the amount of protein A that was bound per particle in the experiment: Based on the result of the SDS-PAGE, 2.5 µg of protein A are bound to 10^7 particles. This corresponds to 250 fg of protein A per particle, which is (250 x 10^{-15} / (42 x 10^3) [molecular weight of protein A] =) 6 x 10^{-18} mol per particle, which is (6 x 10^{-18} x 6 x 10^{23} =) 3.6 x 10^6 molecules of protein A per particle.

These experiments are also shown in the paper as Figure S3.

Another way to measure the efficiency of protein A attachment to the particles is to measure the amount of antibody that can be bound to the immobilized protein A. This can be done by eluting the bound antibody in denaturing condtions and measuring its amount by SDS-PAGE. **Figure 3.3.** shows such experiments with several antibodies. From these experiments, it appears that 10^7 protein A-modified microcapsules can bind about 1 to 1.5 µg of antibody, which corresponds to 100 fg of antibody per particle, or (100 x 10^{-15} / (150 x 10^3) [molecular weight of an antibody molecule] =) 670 x 10^{-21} mol per particle, or (670 x 10^{-21} x 6 x 10^{23} =)

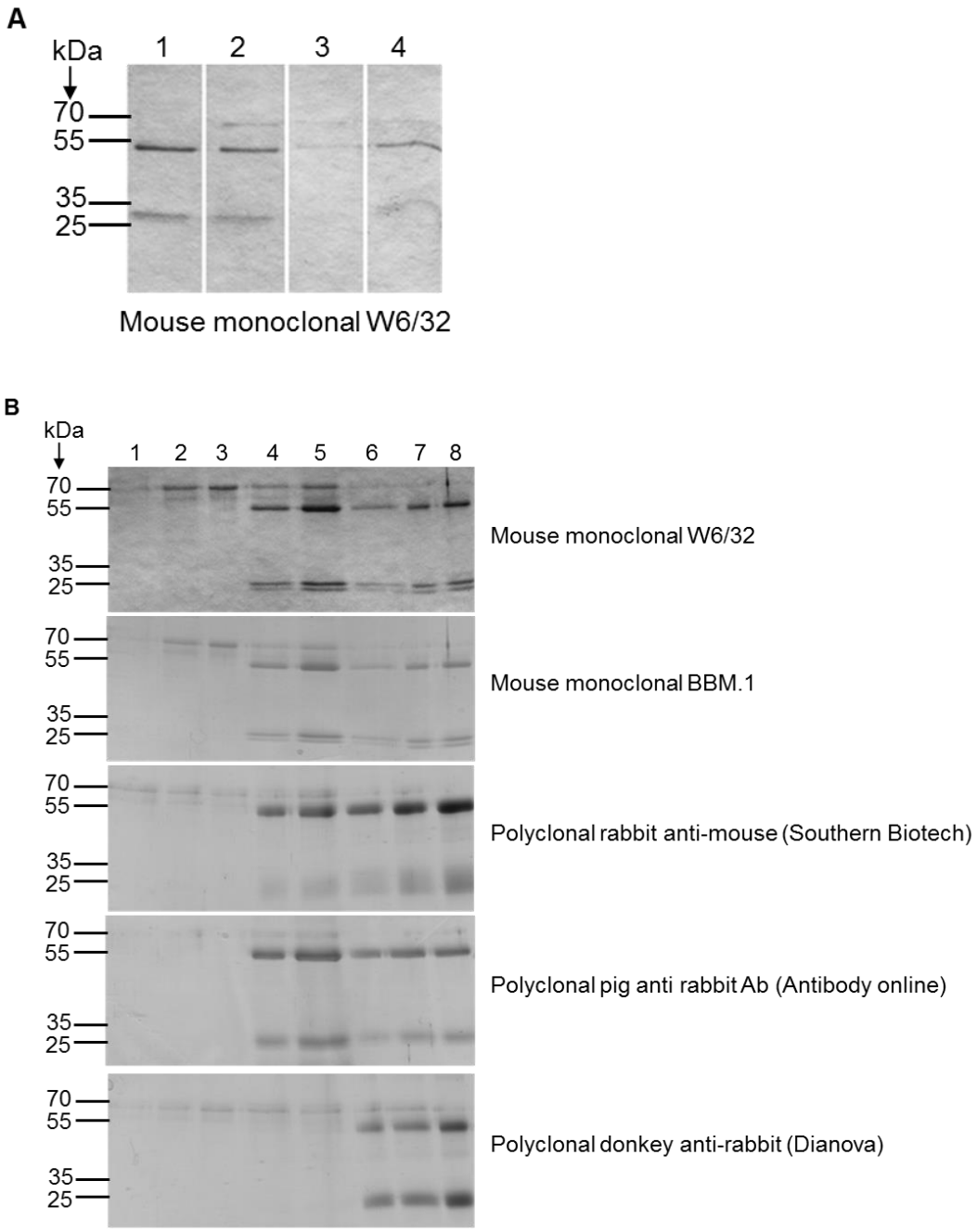

Figure 3.3: Quantification of antibody binding to protein A-coated microcapsules. A, depletion of mouse monoclonal W6/32 antibody from the supernatant of a binding reaction. To 500 µl of a 0.05 mg/ml solution of protein A, 1 x 10^7 core-shell particles (prepared as in 4.3.2.) were added, and incubation was carried out overnight, then the antibody was incubated for 2 hours, and the supernatant was analyzed by SDS-PAGE. Lanes: 1, 25 µl (containing 1 µg of antibody) before the binding reaction. 2, with non-coated and non-activated core-shell particles (= the non-specific adsorption of antibody to the core-shell particles). 3, with protein A-coated core-shell particles (for directed attachment). 4, with EDC/sulfo-NHS activated particles (leading to random orientation of the antibody). **B**, Quantification of bound antibody. Protein A-coated (or control) core-shell particles were incubated with antibodies for 120 minutes, then washed and boiled in Laemmli sample buffer (2% SDS), and the eluate loaded onto an SDS-PAGE gel. Lanes: 1, EDC-crosslinked core-shell particles without protein A or antibody; 2, core-shell particles with protein A but no antibody; 3,core-shell particles with antibody directly crosslinked via EDC/s-NHS chemistry (no protein A)4-5, 5•10^6 and 10^7 core-shell particles coated with protein A and incubated with antibody; 6-8, titration of antibody (0.5, 1, 1.5 µg). The antibodies attached are shown to the right of the gel.

400 x 10^3 antibody molecules per particle, or (only) one molecule of antibody per ten molecules of immobilized protein A.

These results suggest that the protein A crosslinked to the particles is not very active in binding the antibody, perhaps because of its random orientation, or because the EDC/sulfo-NHS reaction targets those residues on protein A that are required for its interaction with the Fc region of the antibody.

Just like protein A, of course, antibodies can also be attached directly to EDC/sulfo-NHS activated core-shell particles. **Figure 3.3.A** also compares these two kinds of attachment with the help of a supernatant depletion experiment. Indirect but directed attachment, with antibodies bound to protein A, seems to be more efficient.

Of course, due to the visual estimation of the band strengths, these numbers are very approximate, with an estimated error range of a factor of two to three in either direction.

These experiments are also shown in the paper in Figure S4.

In an independent approach, the binding of antibodies to the particles can also be measured by incubating the particles with a secondary antibody, which binds to the attached antibody, and which is modified with a fluorescent dye. If the investigated antibody is indeed attached to the capsule, then due to the subsequent binding of the secondary antibody, the particle will be fluorescent. Fluorescence of the particle can then be measured in a flow cytometer, which is essentially a microfluidic fluorimeter that can quantify the fluorescence of many thousands of micrometer-sized individual particles within a few minutes, such that statistics is easily possible.

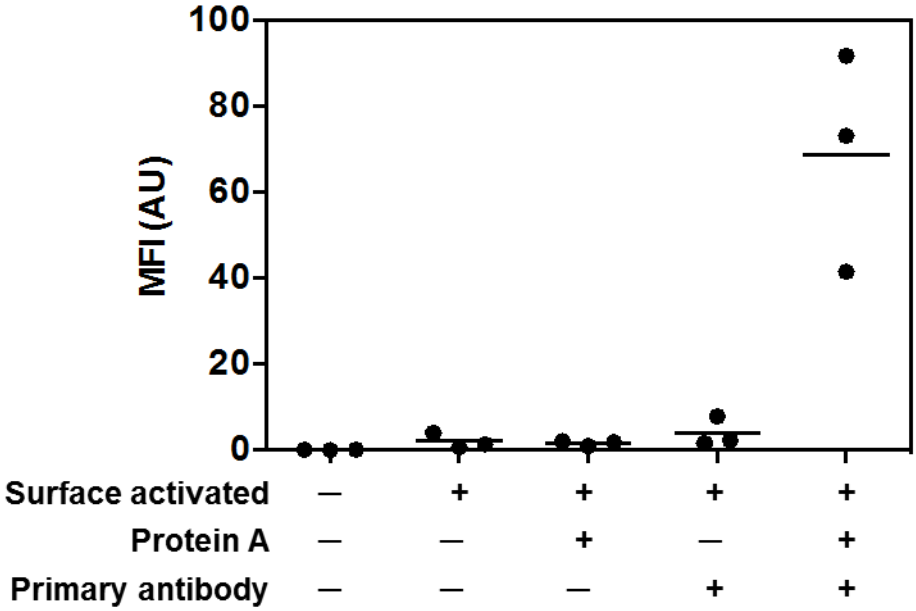

Figure 3.4: Indirect binding of antibody via protein A leads to the binding of more antibody than direct, random, immobilization. Core-shell particles were surface-activated and coated with protein A as indicated and then incubated with antibody ('primary antibody') that was subsequently detected by a 'secondary' antibody labeled with Alexa 488. Concentrations of the antibodies were as in 4.3.4. Fluorescence of the core-shell particles was detected by dissolution of the cores and flow cytometry (see 4.3.8.).

A flow cytometry plot as in Figure 2 of the paper is a histogram chart that for each fluorescence intensity level (on the x axis) displays the number of events (on the y axis). The curves shown are the enveloping curves of the histograms for each experiment. Typically, they have a Gaussian distribution on a logarithmically scaled axis; if this is the case, one usually represents the mean of the fluorescence intensity (the MFI) in a bar chart or dot plot to compare the values of different samples. In the experiment shown in Figure 2 of the paper and in **Figure 3.4**, two ways of attaching the monoclonal mouse antibody W6/32 to the particle surface are compared in this way: by direct EDC/sulfo-NHS crosslinking (in the following called 'random attachment'), and to protein A that was previously attached to the surface by EDC/sulfo-NHS crosslinking (in the following called 'indirect attachment').

The data show that the amount of W6/32 detected by the secondary goat anti-mouse antibody is at least 15 times higher in the indirect attachment sample. Even though the quantification response in flow cytometry is not necessarily linear, one can conclude that indirect attachment immobilizes substantially more antibody than random attachment. This result tells about the amount of immobilized antibody, but it does not tell of the ability of the immobilized antibody to bind its antigen.

I carried out another, semi-quantitative, comparison of random and indirect attachment by recording confocal laser scanning micrographs of the particles after treatment with the

fluorophore-conjugated secondary antibody. Some representative images are shown in **Figure S5** of the paper. They show rather strong florescence for indirect, and no to weak fluorescence for random attachment, confirming the data in **Figure 3.4.**

3.3 A microcapsule-based assay for the protein, beta-2 micro-globulin (β_2m)

3.3.1 Demonstration of the principle

We next thought to establish a microcapsule-based analytical assay for a real-world analyte. Because of the easy availability of antibodies, we chose human beta-2 microglobulin (hβ_2m). This is the light chain of a number of transmembrane protein complexes, such as major histocompatibility complex (MHC) class I proteins and CD 1 (cluster of differentiation 1). Hβ_2m is carried to the surface of the cell associated with its heavy chain binding partners and then released into the extracellular space [6–8]. It ends up dissolved in the blood (where its levels are elevated in several diseases), and it is also detected in the urine, in very low concentrations in cases of renal failure [9–13]. In hemodialysis, hβ_2m is notorious because of its ability to form amyloids in the tubing, against which the patients sometimes mount an immune response with serious consequences.

The principle of the assay described here is a fluorescence sandwich immunoassay. One hβ_2m-specific antibody (the 'capture antibody') is immobilized to the core-shell particle, and the resulting conjugate is then incubated with the analyte (hβ_2m) solution. The hβ_2m, if present, binds to the capture antibody on the core-shell particle. The particles are then washed and incubated with another hβ_2m-specific antibody (the 'detector antibody'), washed, and then treated with a fluorescence-conjugated secondary antibody, which must bind to the detector antibody but not to the capture antibody. This is most easily realized by using capture and the detector antibodies from different species and using species-specific secondary antibodies. (In principle, it is also possible to use no secondary antibody but instead to couple the detector antibody directly to a fluorophore, but the use of secondary antibody is much more convenient since only one fluorescent antibody can be used for any and all assays.) Finally, the particles are washed again, the cores dissolved, and the capsules are read in the flow cytometer.

Figure 3.5. shows such an assay after optimization. The antibodies used were BBM.1 (a murine monoclonal anti-hβ_2m) for capture, and a polyclonal rabbit anti-hβ_2m serum (here also abbreviated sometimes as Rαhβ_2m) as detector antibody. The data show that the limit of quantification for hβ_2m is less than one picogram per ml (or about 10^{-9} / (11 x 10^3) = 100 fM) in

PBS and less than one ng/ml (or about 100 pM) in fetal calf serum (as an approximation of blood serum). In the presence of large amounts of irrelevant protein, the detection of hβ_2m was not impaired.

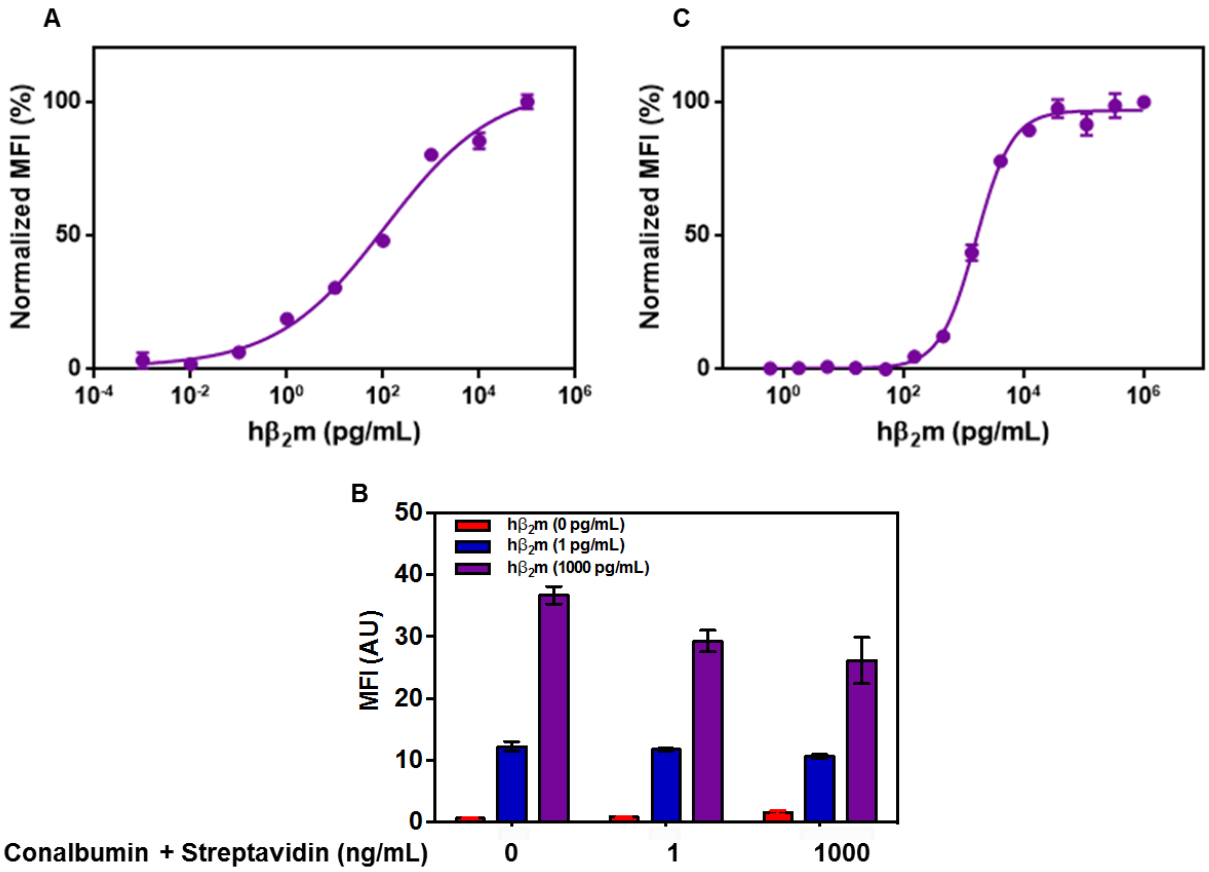

Figure 3.5: The hβ_2m fluorescence immunoassay on core-shell particles is highly sensitive and resistant to irrelevant proteins. Assays were carried out as described in the text and in 4.3.6. Capture antibody, BBM.1 (a murine monoclonal anti-hβ_2m); detector antibody, Rαhβ_2m (a polyclonal rabbit anti-hβ_2m serum). Where no error bars are visible, they are smaller than the size of the point. **A**, analyte in phosphate-buffered saline (PBS). **C**, analyte in fetal calf serum (FCS). **B**, in a three-step assay, the irrelevant proteins conalbumin and streptavidin were each added at the indicated final concentrations.

These data are also shown in the paper as Figure 3.

3.3.2 Optimization

3.3.2.1 Optimizing the blocking conditions

One important element of the optimization of the assay shown in **Figure 3.5** was the development of the right blocking technique. In many antibody-based assay systems, blocking

agents are used to saturate non-specific low-affinity binding to that can give false positive results. In plate assays, such non-specific binding usually occurs to the plastic plate itself.

In our particle-based assay, there was also some background binding of the secondary antibody to the core-shell particles, as shown in **Figure 3.6**. This was best alleviated by using 1% bovine serum albumin (BSA) as a blocking agent, which I did in all subsequent experiments. Some blocking agents such as milk and FCS clearly interfered with the assay.

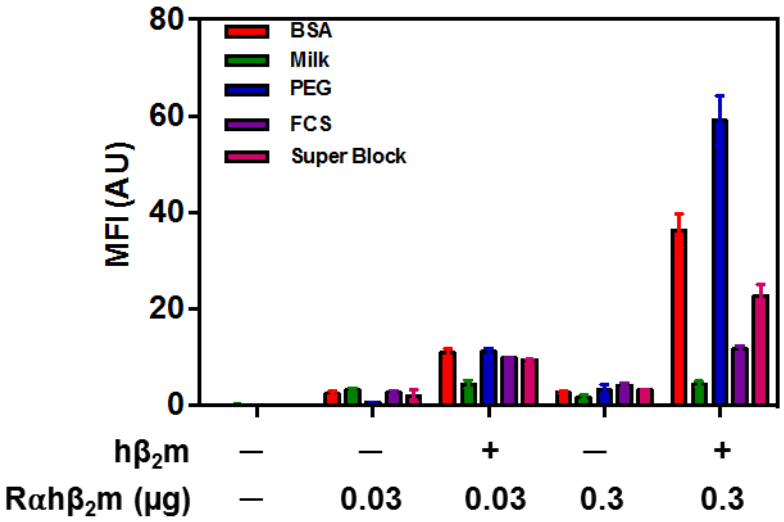

Figure 3.6: BSA and PEG work best as blocking agents for the assay. An assay for β_2m was carried out as in Figure 3.5. After incubation with the analyte, and before incubation with the detection antibody, core-shell particles were incubated with the agents indicated (1%BSA; 1% milk; 1% polyethylene glycol (PEG) 3500; 10% FCS; 5% BSA + 2% milk (superblock)) in PBS. Rαhβ_2m, rabbit anti-human β_2m antibody.

Some, but not all, of these experiments are also shown in Figure S7 of the paper, which shows also the shape of the flow cytometry curves.

3.3.2.2 The order of antibody addition plays a major role

In the experiment shown in Figure 3.5, a monoclonal antibody (BBM.1, a murine monoclonal anti-hβ_2m) was used as capture antibody, and Rαhβ_2m, a polyclonal rabbit anti-hβ_2m serum as detector antibody. The idea behind this arrangement was that the monoclonal antibody, which recognizes only one epitope on hβ_2m, should be used first such that this epitope cannot be occupied by the Rαhβ_2m (in case that the epitopes should overlap). If the opposite order was used, then capturing the hβ_2m on the particle would block the BBM.1 epitope, making it impossible for the detector antibody BBM.1 to bind to the particle and leading to a decrease in

the signal. In order to test whether indeed the order of antibody added during the detection reaction plays a major role, I performed one set of experiments where I first added the polyclonal antibody Rαhβ_2m to protein A microcapsules as capture antibody. The microcapsules were then incubated with the analyte hβ_2m, blocked with 1% BSA, and further incubated with mAb BBM.1 as a detector antibody. The samples were then incubated with goat anti-mouse antibody conjugated to Alexa Fluor 488 (GαM-AF488) and measured in flow cytometry. As seen in Error! Reference source not found.**7**, the mean fluorescence intensity (MFI) was considerably lower than in the comparable experiment shown in Figure 3.6 (BSA columns). I conclude that that the polyclonal antibody Rαhβ_2m probably blocks some of the sites for binding of the mouse mAb BBM.1, thereby reducing the overall sensitivity of the assay. Thus, in the following, the arrangement was used with BBM.1 as the capture antibody, and Rαhβ_2m as detector (see also Chapter 4).

These data are not shown in the paper.

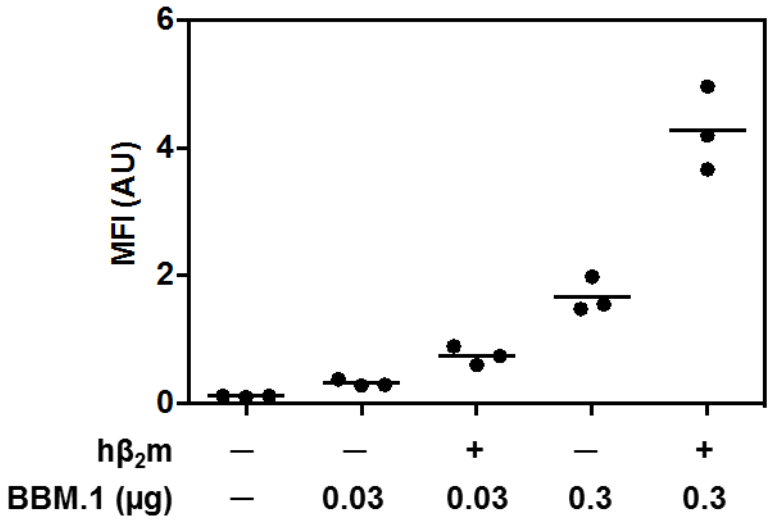

Figure 3.7: The order of antibody addition is important for the strength of the signal. In a role reversal compared to Figures 3.5 and 3.6, the polyclonal antibody Rαhβ_2m was used as capture antibody, and the monoclonal antibody BBM.1 was used as a detector antibody followed by goat anti-rabbit fluorescently labeled antibody for detection. BSA was used for blocking. Compare the numbers to the BSA columns in Figure 3.6.

3.3.3 Conclusions and outlook

The work above has demonstrated that sandwich immunoassays for specific proteins can be performed on capsules and read out by flow cytometry. In the case of β_2m shown here, the limit of detection is impressively low, but the detection results in serum are not as good as those with pure irrelevant proteins, suggesting that the assay may be inhibited by BSA or by the lipids present in the serum preparation. This is of interest when the use of the assay for detection in complex mixtures is considered.

It remains to be demonstrated that the assay is universally applicable, *i.e.*, that it will work for many proteins. In direct comparison with plate-based assays, it is important that the cores of the particles must be dissolved before they can be measured on the flow cytometer (since they otherwise settle to the bottom of the tube too rapidly), which means some additional waiting time that will ultimately be unacceptable if the assay is to be used commercially. Thus, it becomes important to try and remove the core already before the assay; but if the core is not present, separating bound from free analytes and reagents by centrifugation becomes impossible. This may necessitate some kind of filter device; or else, a protocol of fast dissolution of the cores would need to be devised. These are all promising approaches.

3.4 A microcapsule-based sequence-specific assay for oligonucleotides

The second assay that we wished to demonstrate with the microcapsules was for the sequence-speific detection of oligonucleotides. Among the many possible implementations, we chose again the sandwich principle: one oligonucleotide (the 'anchor') is attached to the particles, then the analyte nucleic acid is bound to this anchor oligonucleotide, and finally the particle-bound analyte would be detected by hybridization of a single-stranded portion to a detector oligonucleotide that is fluorescently labeled, subsequent dissolution of the core, and flow cytometry. This detection principle is schematically shown in Figure 6A of the manuscript.

Table 3.1: List of oligonucleotides.

Name	Sequence	Length (bp)	Function
Oligo1	5´-Biotin-GTAAAACGACGCCGAGT-Cy5-3´	17	Detector
Oligo2	5´-Biotin-GGGGAAGGAAAGGAAAAAGAGTAAAAGGACGCCGAGT-3´	37	Anchor
Oligo3	5´-FITC-GGGGAAGGAAAGGAAAAAGAACTCGGCGTCCTTTTAC-3´	37	Detector
Oligo4	5´-TGAGCCGCAGGAAAATGAGAAAAAGGAAAGGAAGGGG-FITC-3´	37	Detector
Oligo5	5´-CATTTTCCTGCGGCTCAACTCGGCGTCCTTTTAC-3´	34	Analyte
Oligo6	5´-CTAGCGCCGGCTTCGAAACCGGTG-3´	24	Additive
Oligo7	5´-CGATCCACCGGTTTCGAAGCCGGCG-3´	25	Additive

3.4.1 Attachment of streptavidin and oligonucleotides to capsules

Initially, I demonstrated that in a standard 1 ml binding reaction, 25 µg/ml of FITC-streptavidin was enough to saturate 10^7 activated particles (**Figure 3.8A**). When using 50 µg/ml of unlabeled streptavidin, 10 nM of 5'-biotinylated and 3'-fluorescently labeled (Cy5) oligonucleotide were sufficient to obtain a good signal in flow cytometry (**Figure 3.8B;**

Figure 3.9). The oligonucleotide used was Oligo1 (see **Table 3.1.** for all oligonucleotide sequences).

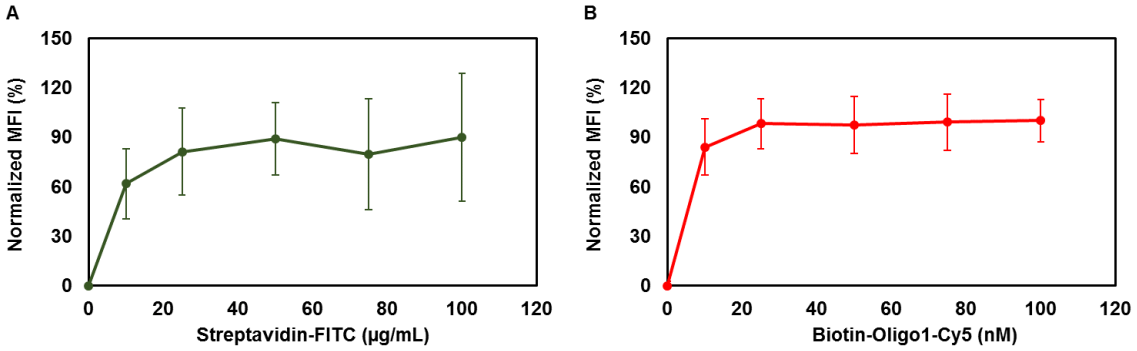

Figure 3.8: Determination of optimal concentrations of streptavidin and Oligo1. Core-shell particles were prepared and crosslinked as in 4.3.2. and modified with different concentrations of streptavidin (**A**) or with 50 µg/ml streptavidin (**B**) as in 4.3.5, then incubated with 10 nM (**A**) or different concentrations (**B**) of Oligo1 that was biotinylated at the 5' end and Cy5-fluorescently labeled at the 3' end as in 4.3.7., and then cores were dissolved, and fluorescence was read in the flow cytometer as in 4.3.8.

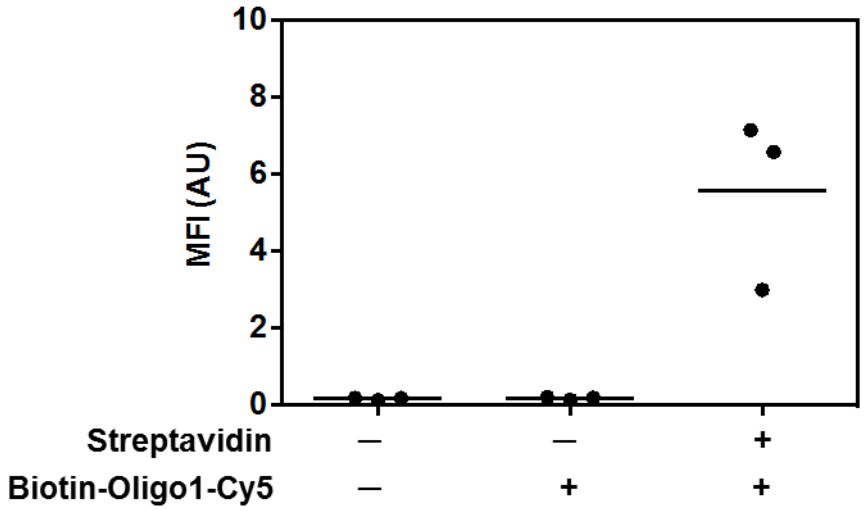

Figure 3.9: 50 µg/ml of streptavidin and 10 nM of 5'-biotinylated and 3'-fluorescently labeled oligonucleotide are sufficient for a good signal in flow cytometry. With these concentrations, an assay was carried out as in Figure 3.8.

The data of **Figure 3.8** and **Figure 3.9** are also shown in Figure S6 and Figure 4A of the paper.

3.4.2 Nucleic acid hybridization on the capsules

The next task was to determine whether one nucleic acid, bound to the particles, would be able to bind to a complementary sequence on another oligonucleotide. This is not *a priori* clear

since nucleic acids, as negatively charged polyelectrolytes, might interact with the highly-charged surface, or the walls, of the particles in some unpredicted fashion.

To investigate this, I used streptavidin-modified particles coupled with 5'-biotinylated Oligo2 as described (0) and incubated them with the partially complementary Oligo3, which was FITC-modified at the 5' end. There was significant concentration-dependent background binding of FITC-Oligo3 even to unmodified particles, but sequence-specific and Oligo2-dependent binding was significantly higher at all concentrations (**Figure 3.10**). We concluded that sequence-specific nucleic acid hybridization on the particles is in principle possible.

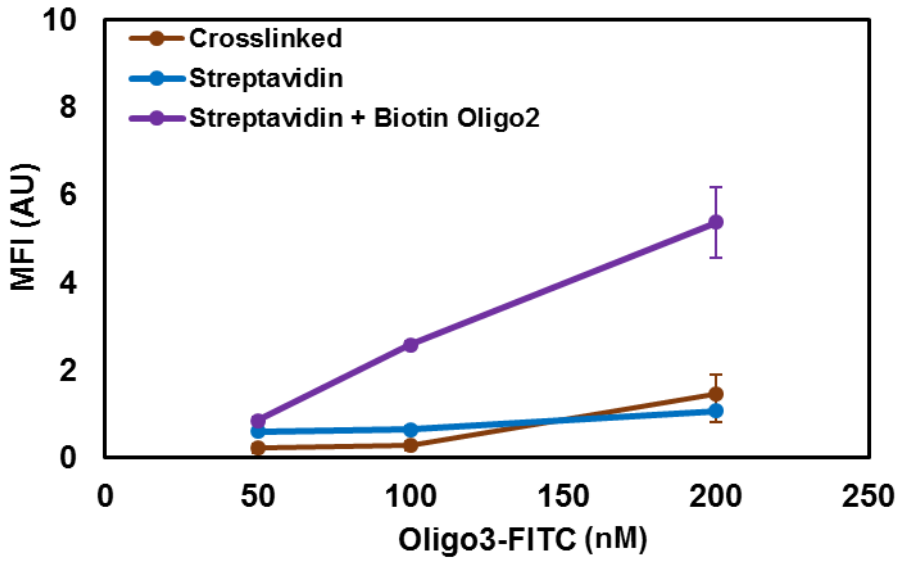

Figure 3.10: Sequence-specific hybridization of two oligonucleotides on the surface of core-shell particles. Core-shell particles were prepared, and Biotin-Oligo2 was bound to them, as in Figure 3.9. Then, Oligo3-FITC was added at the concentrations indicated, and binding evaluated by flow cytometry as in 4.3.8.

The data shown in **Figure 3.10** are also shown in Figure 5 of the paper.

3.4.3 Proof of principle of the nucleic acid assay

We next sought to implement an example sandwich assay for single-stranded nucleic acids as explained above (3.4). I used streptavidin-modified particles, attached 5'-biotinylated Oligo2 to them, incubated with different concentrations of the nucleic acid analyte (an oligonucleotide called Oligo5, which was partially complementary to Oligo2), and then detected the Oligo5 recruited to the particle surface with 5'-FITC labeled Oligo4, which was complementary to that region of the analyte oligo that could not bind to Oligo2. The cores were dissolved, and the fluorescence of Oligo4 bound to the capsules was read by flow cytometry.

Oligo5 showed sigmoidal binding kinetics in this assay (**Figure 3.11A**), with low background, a limit of detection (LoD) of 1.8 nM, and a response midpoint (inflection of the binding curve) of 10-20 nM. Remarkably, binding and detection of Oligo5 was entirely unaffected by the presence of other single-stranded oligonucleotides at 1 µM (**Figure 3.11B**).

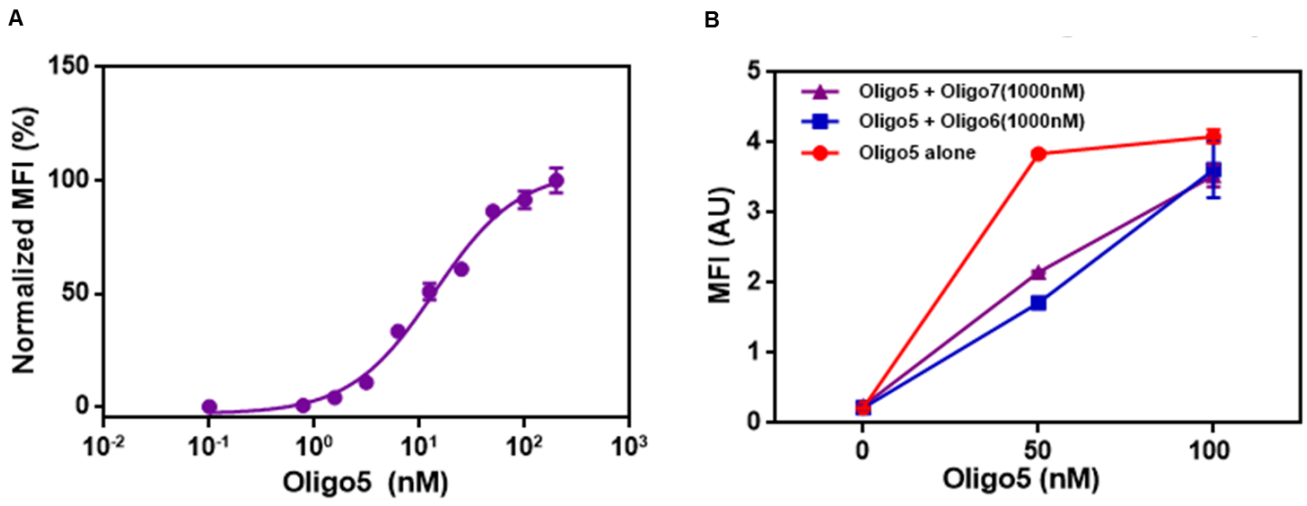

Figure 3.11: Detection of nucleic acids using streptavidin-coated microcapsules. A, Core-shell particles were prepared and modified with Oligo2 as in Figure 3.10, and a binding assay as described in the text was carried out as in 4.3.7. and read out by flow cytometry. Data analysis was as in 4.3.12. **B**, To the assay at three different concentrations, irrelevant oligonucleotides were added in excess as indicated.

We concluded that a sequence-specific assay for the detection of oligonucleotides is possible.

The data shown in **Figure 3.11** are also shown in the paper, in Figure 6. Figure 6A of the paper shows a schematic of the assay.

3.4.4 Conclusions and outlook

With the data reported above, the proof of concept for an assay for the sequence-specific detection of nucleic acids has been achieved. Work remains to be done on demonstrating that this assay is universally applicable, *i.e.*, that it will work for a wide range of sequences. We have anecdotal evidence (not shown) that some single-stranded oligonucleotides bind to the unmodified particles, and it is important to find out what the limitations of the method are.

The potential uses of a sequence-specific nucleic acid detection assay are diverse, and its main advantage over massive parallel sequencing and PCR-based methods is the speed with which detection can be completed, the simplicity, and the low cost. One might for example detect the production of mRNAs of interest in *in vitro* transcription/translation systems for

protein production, or the occurrence of extracellular DNA and (micro-)RNA molecules in the blood. For this, much further work is required.

3.5 Attachment of biotinylated proteins to streptavidin-modified particles

Attachment of proteins other than antibodies to the microcapsules or particles might be achieved through several strategies. First, one might directly crosslink the protein of interest to the particles by EDC/sulfo-NHS chemistry. As described above (3.2.3), this randomly oriented attachment can lead to a loss of activity. Second, one might fuse the protein of interest to the Fc domain of an antibody, and in this way bind it to protein A-modified particles. We did not follow up on this possibility. Third, one might use any other amino acid tag on the protein of interest that binds to a protein that can be immobilized on the particles, such as an antibody epitope tag (for example HA = influenza hemagglutinin, myc, or FLAG) that binds to an antibody, or a Strep-tag that binds to streptavidin [14].

We decided to use the fourth option, the streptavidin-biotin interaction. Proteins can be easily biotinylated *in vitro* through the action of a recombinant bacterial enzyme, *BirA*, which biotinylates the lysine in the amino acid sequence GLNDIFEAQKIEWHE (or similar, [15]). The biotinylated protein then binds through the biotin residue to streptavidin with high affinity and in a defined orientation. Biotinylated proteins are for example used in immunological diagnostics, where major histocompatibility complex (MHC) class I proteins are tetramerized after biotinylation through binding to (naturally tetrameric) streptavidin, yielding T cell-specific reagents of high avidity [16].

I obtained from Sunil Kumar Saini biotinylated recombinant MHC class I proteins, consisting of the heavy chain allotype HLA-A*02:01 bound to the fluorescent peptide, NLVPK$_{FITC}$VATV, with the FITC attached to the lysine side chain in such a manner that it did not interfere with the binding of the peptide to the class I protein, and the light chain beta-2 microglobulin. The biotinylation was close to the C terminus of the heavy chain. Incubation of the protein with streptavidin-modified microcapsules resulted in a strong and specific fluorescence signal (**Figure 3.12**) after the removal of the core.

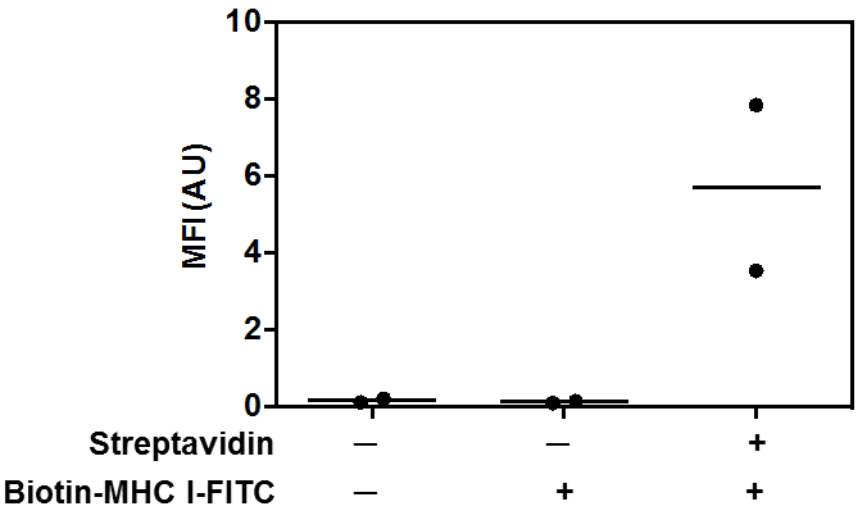

Figure 3.12: Binding of biotinylated MHC class I to microcapsules. The heavy and light chains of the MHC class I protein HLA-A*02:01 were produced in *E.coli* and purified from inclusion bodies, and the trimeric complex of heavy chain, light chain, and the peptide NLVPMVATV (in single-letter amino acid code) was folded *in vitro.* Then, the bound peptide was exchanged for the fluorescently labeled peptide NLVPK$_{FITC}$ATV in a dipeptide-catalyzed exchange reaction. Procedures to this point are described in [17] and were carried out by Sunil Kumar Saini. The MHC class I protein was then rebuffered by gel filtration. Core-shell particles were produced and surface-modified with streptavidin as in Figure 3.8., then incubated with 2 mg/ml class I protein. Core-shell particles were washed in PBS, cores were dissolved with EDTA, and capsule fluorescence was determined by flow cytometry.

This experiment was carried out together with the undergraduate, Ulla Schellhaas. The data are also shown in Figure 4B of the paper.

We concluded that it is technically feasible to immobilize a biotinylated protein on the surface of the particles. The case of MHC class I proteins is especially interesting, because the coupling of many class I proteins to the surface of the particle may give rise to higher T cell binding avidity than the MHC tetramers that are now used in diagnosis. Thus, even T cells with very weakly binding T cell receptors might be detected. Another possible application for MHC-modified capsules is to use them not just to find or to isolate but also to activate T cells, perhaps with the help of some other surface molecules that are usually found on antigen presenting cells, such as B7 [18].

3.6 Materials and Methods for this chapter

The experiments shown in this chapter are described in the figure legends. More detailed descriptions of the methodology are found in the Experimental Section of Chapter 4 (4.3) and in the Experimental Sections of the paper (both in the main body of the paper, and in the supplement).

3.7 Chapter 3 Appendix: Published Paper

3.7.1 Individual contributions to the published paper

For the following paper, the contributions of the individual researchers were as follows:

Sujit Kumar Verma: Designed, carried out, and interpreted experiments in Figures 2, 3, 4A, 5. 6, S1, S3, S4, S5, S6 and S7 and wrote the paper.

Amanda Amoah: Carried out initial experiments for oligonucleotide detection.

Ulla Schellhaas: Carried out the experiment in Figure 4B.

Mathias Winterhalter: Provided laboratory space and equipment.

Sebastian Springer: Designed, wrote, and administered the third-party grant application that provided the salaries of SKV and TK and all consumables of the project; provided laboratory space and equipment; determined the overall direction of the work; designed and interpreted some experiments.

Tatiana Kolesnikova: Designed, carried out, and interpreted experiment in Figure S2. Co-designed, discussed, and interpreted the other experiments in the paper. Wrote the paper and drew the figures and made the tables shown in the paper.

Sunil Kumar Saini: Custom-prepared the biotinylated HLA-A*02:01 proteins with fluorescently labeled peptides in Figure 4B (no coauthorship).

3.8 References

[1] Z. Grabarek, J. Gergely, Zero-length crosslinking procedure with the use of active esters, Anal. Biochem. 185 (1990) 131–135. doi:10.1016/0003-2697(90)90267-D.

[2] P. Schuetz, F. Caruso, Copper-Assisted Weak Polyelectrolyte Multilayer Formation on Microspheres and Subsequent Film Crosslinking, Adv. Funct. Mater. 13 (2003) 929–937. doi:10.1002/adfm.200304483.

[3] T. Mauser, C. Déjugnat, G.B. Sukhorukov, Reversible pH-dependent properties of multilayer microcapsules made of weak polyelectrolytes, Macromol. Rapid Commun. 25 (2004) 1781–1785. doi:10.1002/marc.200400331.

[4] W. Tong, C. Gao, Stable microcapsules assembled stepwise from weak polyelectrolytes followed by thermal crosslinking, Polym. Adv. Technol. 16 (2005) 827–833. doi:10.1002/pat.659.

[5] M. Germain, S. Grube, V. Carriere, H. Richard-Foy, M. Winterhalter, D. Fournier, Composite nanocapsules: Lipid vesicles covered with several layers of crosslinked polyelectrolytes, Adv. Mater. 18 (2006) 2868–2871. doi:10.1002/adma.200600860.

[6] R.A. Jones, J.A. Child, P.S. Master, C.S. Scott, The MHC class I associated beta 2-microglobulin (beta 2m) light chain is expressed in a molar excess over HLA-ABC and CD1 on the membrane of leukaemic B cells but not leukaemic T cells: evidence for further beta 2m-associated molecules., Scand. J. Immunol. 34 (1991) 53–61.

[7] L. Li, M. Dong, X.G. Wang, The implication and significance of beta 2 microglobulin: A conservative multifunctional regulator, Chin. Med. J. (Engl). 129 (2016) 448–455. doi:10.4103/0366-6999.176084.

[8] U.M. Abdel Motal, M.X. Zhou, A.R. Siddiqi, M. Jondal, Regulation of MHC class I membrane expression by beta 2-microglobulin., Scand. J. Immunol. 38 (1993) 395–400.

[9] H. Hagberg, A. Killander, B. Simonsson, Serum beta 2-microglobulin in malignant lymphoma., Cancer. 51 (1983) 2220–5. http://www.ncbi.nlm.nih.gov/pubmed/6189572.

[10] P.W. Johnson, J. Whelan, S. Longhurst, K. Stepniewska, J. Matthews, J. Amess, A. Norton, A.Z. Rohatiner, T.A. Lister, Beta-2 microglobulin: a prognostic factor in diffuse aggressive non-Hodgkin's lymphomas., Br. J. Cancer. 67 (1993) 792–797. http://www.ncbi.nlm.nih.gov/pmc/articles/PMC1968369/.

[11] C. Yoo, D.H. Yoon, C. Suh, Serum beta-2 microglobulin in malignant lymphomas: An old but powerful prognostic factor, Blood Res. 49 (2014) 148–153.

doi:10.5045/br.2014.49.3.148.

[12] T. Fiseha, A. Gebreweld, Urinary Markers of Tubular Injury in HIV-Infected Patients, Biochem. Res. Int. 2016 (2016). doi:10.1155/2016/1501785.

[13] P.S. Mitchell, R.K. Parkin, E.M. Kroh, B.R. Fritz, S.K. Wyman, E.L. Pogosova-Agadjanyan, A. Peterson, J. Noteboom, K.C. O'Briant, A. Allen, D.W. Lin, N. Urban, C.W. Drescher, B.S. Knudsen, D.L. Stirewalt, R. Gentleman, R.L. Vessella, P.S. Nelson, D.B. Martin, M. Tewari, Circulating microRNAs as stable blood-based markers for cancer detection., Proc. Natl. Acad. Sci. U.S.A. 105 (2008) 10513–10518. doi:10.1073/pnas.0804549105.

[14] T.G. Schmidt, A. Skerra, One-step affinity purification of bacterially produced proteins by means of the "Strep tag" and immobilized recombinant core streptavidin., J. Chromatogr. A. 676 (1994) 337–345. doi:10.1016/0021-9673(94)80434-6.

[15] P.J. Schatz, Use of peptide libraries to map the substrate specificity of a peptide-modifying enzyme: a 13 residue consensus peptide specifies biotinylation in Escherichia coli., Biotechnology. (N. Y). 11 (1993) 1138–1143.

[16] J.D. Altman, P.A. Moss, P.J. Goulder, D.H. Barouch, M.G. McHeyzer-Williams, J.I. Bell, A.J. McMichael, M.M. Davis, Phenotypic analysis of antigen-specific T lymphocytes., Science. 274 (1996) 94–96.

[17] S.K. Saini, H. Schuster, V.R. Ramnarayan, H.-G. Rammensee, S. Stevanović, S. Springer, Dipeptides catalyze rapid peptide exchange on MHC class I molecules, Proc. Natl. Acad. Sci. . 112 (2015) 202–207. doi:10.1073/pnas.1418690112.

[18] L.J. Eggermont, L.E. Paulis, J. Tel, C.G. Figdor, Towards efficient cancer immunotherapy: advances in developing artificial antigen-presenting cells., Trends Biotechnol. 32 (2014) 456–465. doi:10.1016/j.tibtech.2014.06.007.

Chapter 4

In this chapter, I report that the microcapsules are more sensitive than the commercial available beads for the detection of protein analyte, whereas for nucleic acid detection, both the microcapsules and the beads have similar sensitivity. The microcapsules also show high sensitivity in the detection of antibodies from hybridoma supernatant when compared with a standard immunoassay plate.

All the experimental work in this chapter was carried out by me, except **Figure 4.7** (microplate) **Figure 4.8** (microplate), which was performed by Anja Karin Albrecht and Verena Siebecke, our collaborators from Hochschule Bremen. The manuscript was written by Sebastian Springer and myself.

4 Chapter 4: Comprehensive and comparative validation of a microcapsule-based immunoassay for the detection of proteins and nucleic acids

4.1 Abstract

Polyelectrolyte microcapsules are versatile, robust, and highly sensitive tools for the detection of proteins and nucleic acid sequences in assays that use optical readout. Here, we compare their performance with commercially available micrometer-sized beads made of polystyrene and various other materials and with standard microplate immunoassays. The protein A-coated microcapsules detect the disease biomarker beta-2 microglobulin with a 450-fold higher sensitivity than PS beads. For sequence-specific nucleic acid detection, the sensitivity of oligonucleotide-coated microcapsules was similar to that of PS beads. The microcapsules detected the presence of a monoclonal antibody in hybridoma supernatant with the same sensitivity as a microplate assay. Our results show that microcapsule-based assays can serve as a platform for the rapid quantitative detection of analytes at very low concentrations.

Keywords: Polyelectrolyte microcapsules; Biomarker; Immunoassay; Beads; Validation; Flow cytometry.

4.2 Introduction

The rapid and sensitive detection of protein analytes, a critical technique in diagnostic science, can be achieved with the help of specific antibodies. Although enzyme-linked immunosorbent assays (ELISAs) are currently the most popular method of antibody-based assays, there are more sensitive, robust, and economical alternatives. For example, while ELISAs can detect one analyte [1], bead- or particle–based immunoassays

allow simultaneous detection of multiple analytes in a single well [2–7]. We have recently introduced the use of hollow polyelectrolyte microcapsules for such assays [8]. Their porous surface can be modified with large amounts of antibodies [9–11], and their great physico-chemical stability aids the development of assays that are fast and robust in a broad range of experimental conditions. One can also attach nucleic acids to the microcapsule surface for the sequence-specific detection of nucleic acids [8].

The polyelectrolyte microcapsules used in our assays are produced through assembly of alternating layers of polyallylamine and polyacrylic acid onto calcium carbonate cores, driven by electrostatic attraction [12,13], and subsequent covalent cross-linking with 1-ethyl-3-(3-dimethylaminopropyl) carbodiimide (EDC) [14]. Dissolution of the cores with ethylenediaminetetraacetic acid (EDTA) yields multilayered shells that are resistant to even extreme pH and salt conditions [15–18]. Onto the outermost polyacrylic acid layer, we attach proteins via their lysine side chains using EDC and N-hydroxysulfosuccinimide (sulfo-NHS) [19]. We perform all assay manipulations with the $CaCO_3$ cores in place (*i.e.*, with core-shell particles which makes it easier to perform the washes), and we remove the cores only just before reading the assay in the flow cytometer which allows it not to sediment as compared to the solid beads during the acquisition process.

This study describes the validation and application of the microcapsule-based immunoassay that we have established for the detection of proteins and nucleic acids with high sensitivity and selectivity [8]. We compare our microcapsules with commercially available polystyrene (PS) beads in the detection of a protein (the disease marker human beta-2 microglobulin, $h\beta_2m$) and a nucleic acid. We find that our microcapsule-based assay is ultra-sensitive and detects $h\beta_2m$ in the femtomolar range, whereas the detection limit of the PS beads for the same protein is in the nanomolar range. We also demonstrate the use of protein A-coated microcapsules to monitor the production of a monoclonal antibody by a hybridoma. The results show that polyelectrolyte microcapsule-based immunoassays are robust techniques for protein and nucleic acid detection.

4.3 Experimental Section

4.3.1 Materials

5-6 µm diameter calcium carbonate ($CaCO_3$) particles (Cat No. PL-CA6-10g) were purchased from PlasmaChem (Berlin, Germany). Poly(allylamine hydrochloride) (PAH) sodium salt (Cat No. 283223), N-Hydroxysulfosuccinimide sodium salt (sulfo-NHS) (Cat No. 56485), ethylenediaminetetraacetic acid (EDTA) disodium salt dehydrate (Cat No. A3553) were purchased from Sigma-Aldrich. Poly(acrylic acid) (PAA) sodium salt (Cat No. 18611) was purchased from Polysciences (Hirschberg, Germany). 1-(3-Dimethylaminopropyl)-3-ethylcarbodiimide hydrochloride (EDC) (Cat No. A10807) was purchased from Alfa Aesar (Heysham, UK). Protein A (Cat No. 21181) and FITC-labeled streptavidin (Cat No. 21224) were purchased from Thermo Scientific. Sodium chloride (Cat No. A4857), disodium hydrogen phosphate (Cat No. A3905), sodium carbonate (Cat No. A1881), sodium bicarbonate (Cat No. A1940), potassium chloride (Cat No. A2939), potassium dihydrogen phosphate (Cat No. A3095) streptavidin (Cat No. A1495), bovine serum albumin (BSA) (Cat No. A1391), sodium azide (Cat No. A1430), and 2-morpholinoethanesulfonic acid (MES) (Cat No. A1074), were purchased from AppliChem (Darmstadt, Germany). Polyclonal goat anti-mouse antibody (Cat No. A11001) and goat anti-rabbit antibody (Cat No. A11008) labeled with Alexa Fluor 488 were purchased from Invitrogen, and polyclonal rabbit anti-human β_2m (Batch 5511) was purchased from Nordic Immunology. RPMI media (Cat No. 880175) was purchased from Lonza. Tween 20 (Cat No. 9127) was purchased from Roth. 0.45 µm syringe filters (Cat No. 16555K) and spin filters of 0.8 µm pore size (Cat No.VK01P042) were purchased from Sartorius Stedim Biotech. High-binding black 96 well flat polystyrene microplates with clear bottom (Cat No. 655097) were purchased from Greiner Bio-One (Frickenhausen, Germany). Carboxylated silica (SiO_2) beads of 1.01 µm and 2.12 µm (Cat No. AR756 and AR833), poly(methylmethacrylate) (PMMA) beads of 1.02 µm and 2.08 µm (Cat No. AR830 and AR145) and polystyrene (PS) beads of 1.20 µm and 2.35 µm (Cat No. A1482 and B874) sizes were purchased from microparticles (Berlin, Germany). Murine monoclonal hybridomas BBM.1 (against hβ_{2m}) [20] and W6/32 (against human MHC class I) were from Alain Townsend (Oxford University) and Peter Cresswell (Yale University); the antibodies were purified with standard methods using protein A agarose beads. Human beta-2 microglobulin (hβ_2m) was produced in *E.coli*, folded in vitro as described [21], and then purified by size exclusion chromatography on a Superdex 200 10/30 GL column (GE Biosciences). The oligonucleotides were supplied by Eurofins Genomics (Munich, Germany; **Table 4.1**).

4.3.2 Preparation and crosslinking of core-shell particles

50 mg of $CaCO_3$ particles were suspended in 2 mL of Milli-Q water, sonicated for 5 min, and then washed three times by centrifugation (all the washes were done at 3000 rpm for 2 min with Milli-Q water). After the washes, 2 mL of PAH (2 mg mL^{-1} in 0.5 M NaCl, pH 7.0) were added and incubated for 10 min, continuously shaking at 1200 rpm. The particles were then washed three times, and 2 mL of PAA (2 mg mL^{-1} in 0.5 M NaCl, pH 7.0) were added and incubated for 10 min to adsorb the second layer of polyelectrolyte. In total, two layers of PAH and PAA each were adsorbed. The $(PAH/PAA)_2$ polymer layers were crosslinked with 10 mg mL^{-1} EDC in MES buffer (0.1 M MES in 0.5 M NaCl, pH 6.0) overnight while shaking at 1200 rpm. The resulting core-shell particles were washed three times with ice-cold Milli-Q water.

4.3.3 Functionalization of $(PAH/PAA)_2$ polymers and beads with proteins

The carboxyl groups on the $(PAH/PAA)_2$ polymers and the beads were surface-activated by incubating them with 500 µL of freshly prepared 0.4 M EDC/0.1 M sulfo-NHS mixture in phosphate buffered saline (PBS, pH 7.2), shaking at 1200 rpm at room temperature (RT) for 1 h. After surface activation, particles were washed three times with PBS (pH 7.2). The surface activated particles were then modified with adaptor proteins by incubating them either with 50 µg of protein A or streptavidin in 500 µL PBS (FITC-streptavidin was titrated to get the optimal concentration needed to coat the surface pf the beads), pH 7.2 at RT overnight, shaking at 1200 rpm. All particles were washed three times with Milli-Q water to wash away any unbound protein. Residual NHS esters were quenched by incubating the particles in 500 µL of 50 mM Tris-Cl (pH 8.8) at RT for 30 min. Before measurement in the flow cytometer, the core-shell particles were re-suspended in 0.2 M EDTA (pH 7.2) to dissolve the $CaCO_3$ core, thoroughly washed three times with Milli-Q water, and collected using spin filters at 800 rpm.

4.3.4 Proof of binding: Antibodies

Three samples of the different beads were taken, of which one sample was taken as a background control. Other two samples were surface-activated with EDC/sulfo-NHS as described in section 4.3.3, washed, and then incubated with 50 µg protein A in 500 µL PBS, pH 7.2 each at RT overnight. Out of them, one sample was incubated with 10 µg of BBM.1 antibody in 1 mL PBS (pH 8.2) for 2 h, followed by the secondary GαM-AF488 antibody (0.2 µg in 1 mL PBS, pH 7.2) for 30 min. Last sample was incubated with GαM-AF488 (0.2 µg in 1 mL PBS, pH 7.2) for 30 min (control). All the samples were washed thrice with Milli-Q water

after every step of incubation. All the particles were then measured in the flow cytometer for AF488 fluorescence.

4.3.5 Proof of binding: Oligonucleotides

Polystyrene beads were surface-activated as described in section **4.3.3**. One sample was taken for setting the background signal. The other samples were incubated with 50 µg streptavidin in 500 µL 1x PBS (pH 7.2) overnight shaking at 1200 rpm at RT. The streptavidin-coated PS beads were then incubated with different concentrations (1 nM – 1000 nM) of biotinylated and Cy5-labeled oligonucleotide Oligo1 in 1 mL PBS (pH 7.2) for 2 h. All samples were washed with Milli-Q and then measured in the flow cytometer for Cy5 fluorescence.

4.3.6 Detection of hβ_2m in PBS

Core-shell particles were prepared and cross-linked as described in section **4.3.2**. The core-shell particles and the PS beads were then surface-modified with protein A as described in section 2.3. The protein A-coated particles were incubated with 10 µg BBM.1 antibody (murine monoclonal anti-hβ_2m) in 1 mL PBS (pH 8.2) for 2 h, followed by incubation with the analyte hβ_2m at different concentrations (10^{-3}–10^{5} pg mL^{-1} for core-shell particles and 10^{-3}–10^{6} pg mL^{-1} for PS beads) in PBS (pH 7.2) for 1 h [22]. The hβ_2M-bound particles were washed thoroughly to remove all unbound hβ_2m and blocked with 1% BSA for 45 minutes in 1x PBS (pH 7.2). The samples were washed three times to remove all non-specifically bound protein, followed by incubation with 0.3 µg polyclonal rabbit anti-hβ_2m (Rαhβ_2m) in 1 mL PBS (pH 7.2) for 2 h. Finally, the particles were incubated with 0.2 µg detector antibody GαR-AF488 (polyclonal goat anti-rabbit) in 1 mL PBS (pH 7.2) for 30 min. As a negative control, BBM.1-modified particles were incubated with Rαhβ_2m and GαR-AF488 antibodies but without analyte. Particles were washed three times with Milli-Q water after every step of incubation. The core-shell particles were dissolved with 0.2 M EDTA (pH7.2). All the particles were then measured in the flow cytometer. As a background control, crosslinked particles were used.

4.3.7 Detection of nucleic acids in PBS

Core-shell particles were prepared and crosslinked as described in section **4.3.2**. The core-shell particles and the PS beads were then surface-modified with streptavidin as described in section **4.3.5**. The streptavidin-coated particles were incubated with 50 nM biotinylated Oligo2 in 1 mL PBS (pH 7.2) for 2 h shaking at 1200 rpm at RT. For the analyte dose response, the Oligo2-modified particles were incubated with different concentrations of the analyte Oligo3 (10^{-1} –10^{3} nM) in 1 mL PBS (pH 7.2) for 1 h, shaking at 1200 rpm. All the particles were then

washed three times with Milli-Q water to wash off any unbound analyte. The particles were incubated with 200 nM FITC-Oligo5 (detector) in 1 mL PBS (pH 7.2) for 30 min. As negative controls, 200 nM FITC-Oligo5 was added directly to the crosslinked or streptavidin-coated particles or to the Oligo2-modified particles in the absence of the analyte Oligo4. The core-shell particles were dissolved with 0.2M EDTA (pH7.2). All the particles were then measured in the flow cytometer. As a background control, crosslinked particles were used.

4.3.8 Flow cytometry and plate spectroscopy

Flow cytometry data were acquired on a CyFlow Space flow cytometer (Partec) using green (488 nm) and red (638 nm) lasers and analyzed using FlowJo (FlowJo Enterprise). All plates were read on an Infinite M1000 plate reader (TECAN) with the excitation wavelength at 488 nm and the emission wavelength at 519 nm.

4.3.9 Detection of BBM.1 antibody

Core-shell particles were prepared, crosslinked, and surface-modified with protein A as described in section **4.3.2** and **4.3.3**. High-binding 96-well black well plates were coated with 100 µg mL^{-1} protein A in carbonate buffer (pH 9.6) overnight at 4^0C and then blocked with 1% BSA (w/v) overnight. The protein A-coated core-shell particles were incubated in 1 mL with purified murine monoclonal BBM.1 either at a concentration of 2×10^{-3} – 3×10^{1} µg mL^{-1} in 1x PBS (pH 7.2) or at a concentration of 1×10^{-3} – 3×10^{1} µg mL^{-1} in complete RPMI media for 2 h shaking at 1200 rpm. The 96-well plates were also incubated in 100 µL with purified murine monoclonal BBM.1 at a concentration of 1.9×10^{-2} – 1×10^{1} µg mL^{-1} either in 1x PBS (pH 8.2) or at a concentration of 5×10^{-4} – 10^{1} µg mL^{-1} in complete RPMI media for 2 h shaking at 400 rpm. All samples were then incubated with the detector antibody GαM-AF488 (0.2 µg in 1 mL PBS, pH 7.2) for 30 min shaking at RT. All samples were triply washed either with Milli-Q (for core-shell particles) or with PBST (PBS with 0.01% Tween 20, for 96-well plates) after every steps of incubation. Samples incubated with detector antibody GαM-AF488 alone serve as negative controls. The cores of the core-shell particles were dissolved with 0.2 M EDTA (pH 7.2), and the microcapsules were then measured in the flow cytometer. The 96-well plates were read in the TECAN Infinite reader.

4.3.10 Sample collection during BBM.1 hybridoma culture

BBM1 hybridoma was grown in RPMI media (10% fetal calf serum with glutamine), and eight different fractions of the hybridoma were collected at eight different days (day 2, 5, 9, 12, 16, 19, 23, and 26). All samples were centrifuged at 2000 g for 10 minutes, and the collected

supernatants were filtered through a 0.45 µm syringe filter. The samples were then stored at 4 ^{0}C with 0.01% sodium azide.

4.3.11 Monitoring the growth of BBM.1 antibody in the hybridoma supernatant

Microcapsules and 96 well plates were functionalized with protein A as described in section 4.3.3. Murine monoclonal BBM.1 hybridoma cells were grown in a T-225 flask. The media was not replaced, and samples were collected at different days of culture and the cells counted (**Table 4.4**). The collected fractions were centrifuged, filtered through a 0.45 µm syringe filter, and stored at 4 ^{0}C with 0.01% NaN_3. 1 µL and 2 µL of the different hybridoma fractions collected during different days of culture were added to both the core-shell particles (in a total volume of 2 mL) or to the 96-well plates (in a total volume of 100 µL/well) and incubated for 2h at RT. All the samples were then washed and incubated with detector antibody GαM-AF488 (0.2 µg in 1 mL PBS, pH 7.2) for 30 min shaking at RT. All samples were washed thrice either with Milli-Q (for core-shell particles) or with PBST (PBS with 0.01% Tween 20, for 96-well plates) after every step of incubation. Samples with detector antibody GαM-AF488 alone serve as negative controls. The core-shell particles were dissolved with 0.2M EDTA (pH 7.2) and then measured.

4.3.12 Data analysis

Dose-response curves were fitted using a four-parameter logistic curve obtained with a nonlinear regression fitting procedure in the GraphPad Prism 7.0 analytical software (GraphPad, La Jolla, CA). The LoB, LoD, and LoQ values for each analyte were calculated using the following equations: LoB = mean blank + 1.645 x (SD of blank); LoD = LoB + 3 x (SD of a low-concentrated sample); LoQ = LoB + 10 x (SD of an accurately quantified sample). The calculated values were interpolated from the corresponding calibration curves using GraphPad Prism.

4.4 Results and Discussion

4.4.1 Preparation and characterization of microcapsules and beads

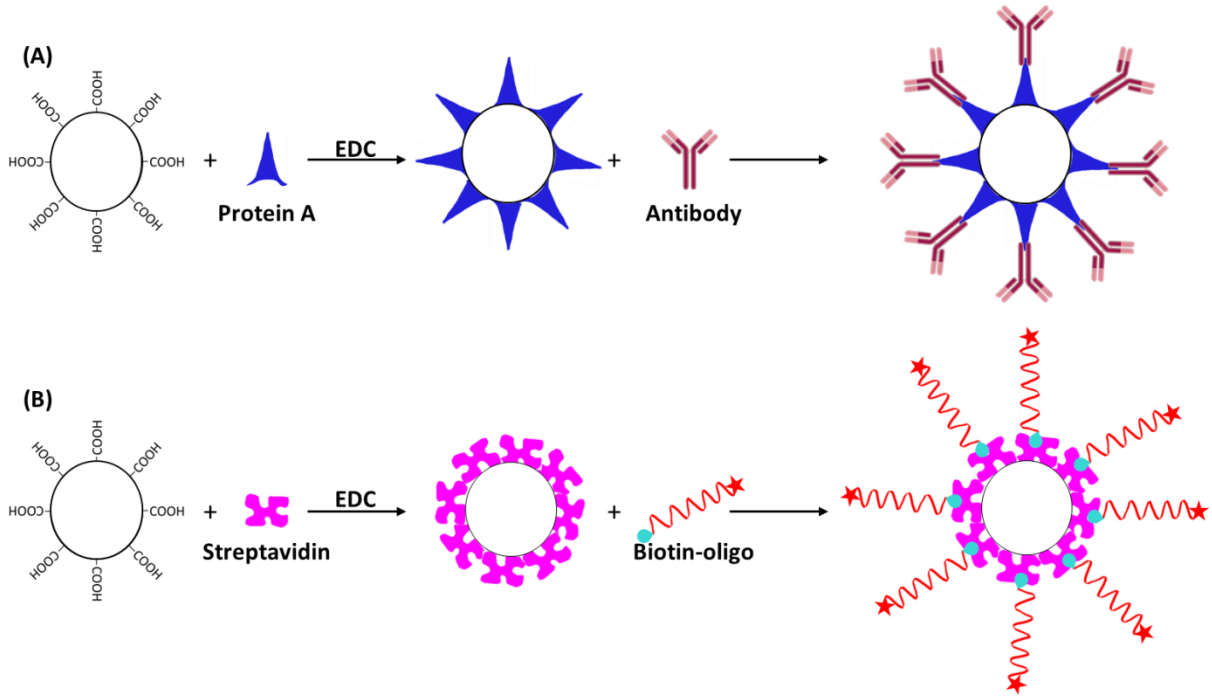

Figure 4.1: Coating of microcapsules and beads with proteins or nucleic acids. The carboxylic acid groups in the outmost layer of the microcapsules were surface-activated by EDC/sulfo-NHS. Then, either protein A was attached onto the activated surface for oriented binding of antibodies (**A**), or streptavidin was immobilized for the binding of biotinylated oligonucleotides (**B**). The coating of the commercially available beads was performed in the same way. Drawings are not to scale.

Commercial beads made of polystyrene (PS), silica (SiO_2), or poly(methylmethacrylate) (PMMA) are currently used for detection of analytes and for multiplexing studies that are read out by flow cytometry [1,23]. Since our microcapsule assay detects proteins and nucleic acids (analytes) at very low concentrations [8], we wanted to directly compare microcapsules with these beads with respect to their binding capacity for antibodies and their sensitivity for protein and nucleic acid analytes.

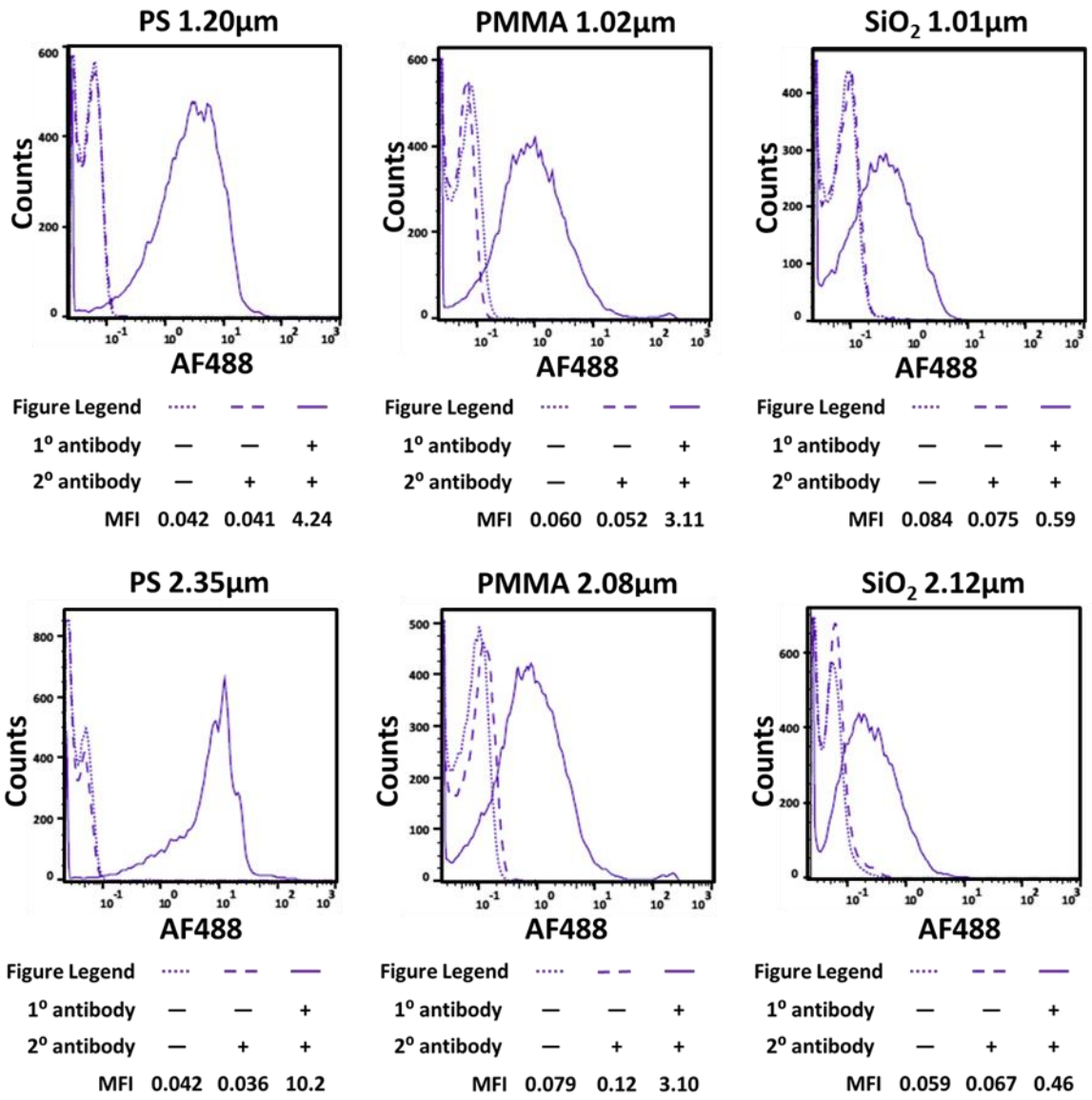

Figure 4.2: Determination of antibody immobilization efficiency of commercially available carboxylated beads. Murine monoclonal BBM.1 antibody (1° antibody) was added to protein A-coated PS, PMMA, and SiO_2 beads. The BBM.1 antibody was then detected by goat anti-mouse secondary antibody coupled to Alexa Fluor 488. Fluorescence of the beads was measured by flow cytometry.

First, we tested which of the commercially available beads are most suitable for binding antibodies. Solid beads used for these assays must be in the size range between one and 2.5 µm to remain in suspension during flow cytometry. Beads made of SiO_2, (1.01 and 2.12 µm), PMMA (1.02 and 2.08 µm), and PS (1.2 and 2.35 µm), all of which had carboxylic acid groups at their surface, were surface–activated by EDC/sulfo-NHS and then coated with *Staphylococcus aureus* protein A. The coated beads were then incubated with the murine monoclonal antibody BBM.1 (**Figure 4.1A**). To study antibody binding to the beads, they were treated with a fluorescence–labeled secondary antibody and then measured by flow cytometry. Among all the beads tested, the 2.35 µm PS beads bound the largest amount of the BBM.1

antibody per bead (**Figure 4.2**). We therefore used these beads for comparison to the polyelectrolyte microcapsules.

4.4.2 Microcapsules are better tools for the detection of protein analytes

We next produced 6 µm microcapsules and confirmed their correct assembly with zeta potential measurements (**Figure 4.3**). We then compared them to the 2.35 µm PS beads in the BBM.1 antibody binding assay, and we found that they bound two to three times more antibody than the PS beads (**Figure 4.4A, Figure 4.4B**).

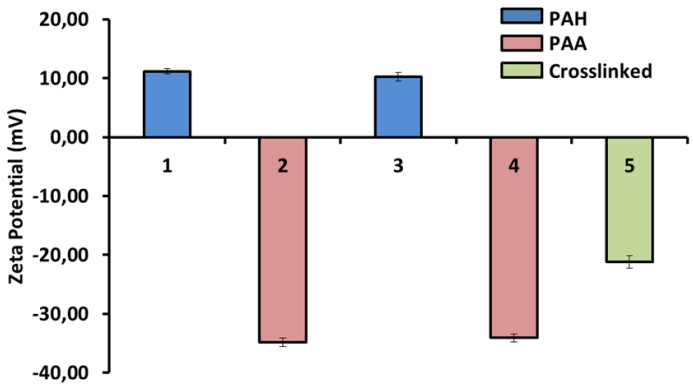

Step	Layer	Zeta Potential (mV)
1	PAH	+11.17 ± 0.45
2	PAA	-34.80 ± 0.75
3	PAH	+10.26 ± 0.68
4	PAA	-34.07 ± 0.68
5	Crosslinking	-21.23 ± 1.06

Figure 4.3: Monitoring of the production of the polyelectrolyte microcapsules by zeta potential measurement after each adsorption step. Microcapsules were layered onto 6 µm $CaCO_3$ particles. Error bars indicate the SD (n=3).

We then tested both microcapsules and PS beads in an antibody sandwich assay [8] for a protein analyte, human beta-2 microglobulin (hβ_2m). In this assay, BBM.1 on microcapsules or beads binds hβ_2m, which is then detected with polyclonal rabbit anti-hβ_2m antibody, followed by fluorescently labeled anti-rabbit secondary antibody (**Figure 4.4C**). The concentration of hβ_2m is measured in the plasma to detect cancer, and in the urine to detect renal failure [24] in a variety of diseases.

Abbreviation	Sequence	N_{nt}	Function
Oligo1	5′-Biotin-GTAAAACGACGCCGAGT-Cy5-3′	17	Anchor + Detector
Oligo2	5′-Biotin-GGGGAAGGAAAGGAAAAAGAGTAAAAGGACGCCGAGT-3′	37	Anchor
Oligo3	5′-CATTTTCCTGCGGCTCAACTCGGCGTCCTTTTAC-3′	34	Analyte
Oligo4	5′-TGAGCCGCAGGAAAATGAGAAAAAGGAAAGGAAGGGG-FITC-3′	37	Detector

Table 4.1: Overview of oligonucleotides including abbreviation, sequence, length of the sequence and its function.

Compared to PS beads, the microcapsules detected hβ_2m with much higher sensitivity (**Figure 4.4D**), and they showed a better signal-to-noise ratio (**Figure 4.4E**). The effective

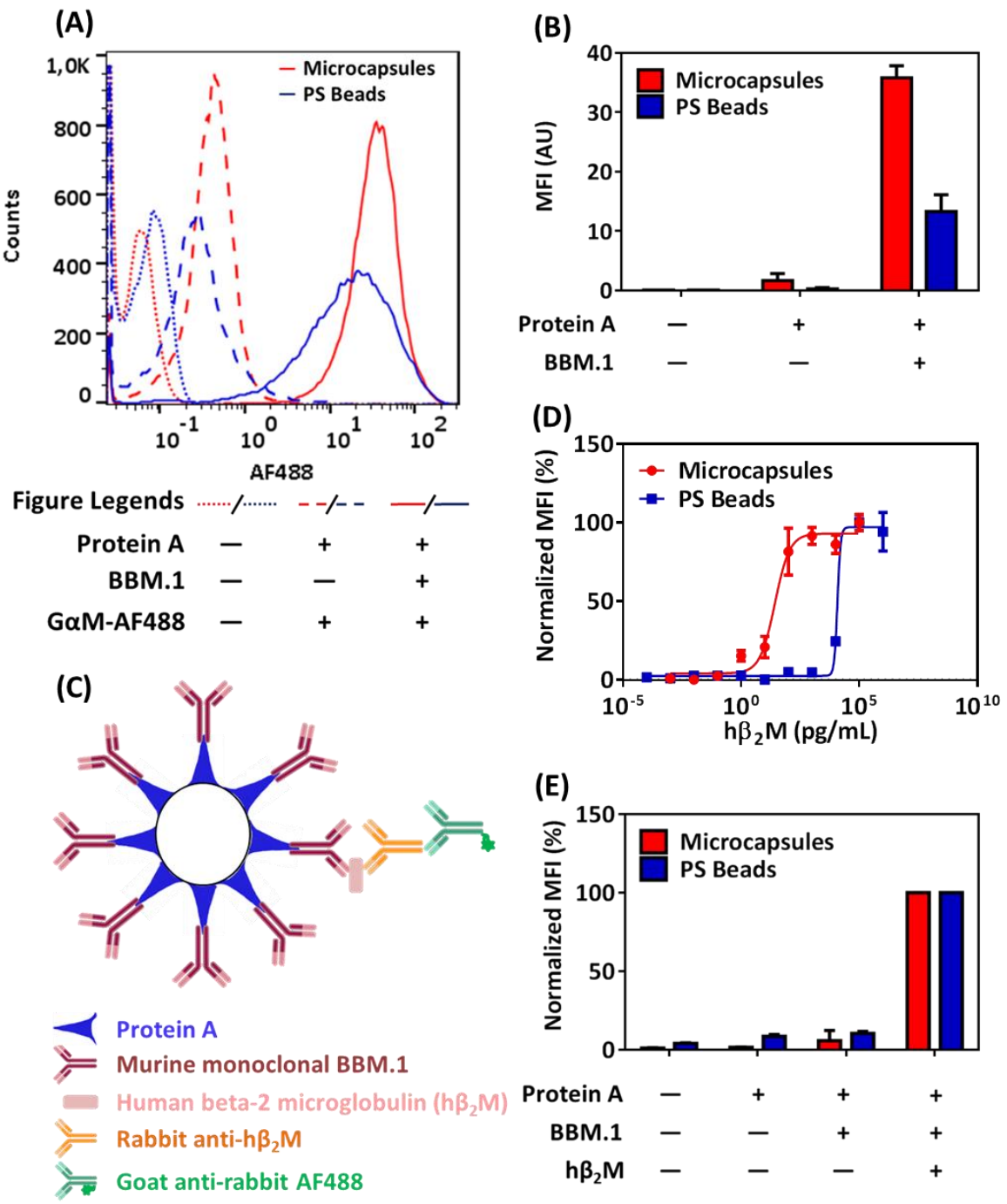

Figure 4.4: Comparison of 6 µm microcapsules and 2.35 µm PS beads for binding of antibody and for the detection of a protein analyte. (**A+B**) Detection of the capture antibody, BBM.1, on microcapsules and beads with fluorescently labeled goat anti-mouse antibody (GαM-AF488) by flow cytometry. (**A**) shows a representative experiment, (**B**) the average of two experiments with standard deviations (SD). (**C**) Schematics for the detection of human beta-2 microglobulin (hβ2M). The capture antibody, BBM.1, is immobilized on the protein A-coated microcapsules/PS beads. BBM.1 antibody binds specifically to hβ2m, which is sandwiched by the polyclonal rabbit anti-hβ2M (RαhβM) antibody. The sandwich is then detected by adding AF488 labeled goat anti-rabbit (GαR-AF488) antibody. (**D**) Detection of hβ2m in PBS. Dose-response curves for assay as in (**C**) with microcapsules or PS beads. MFI values are normalized to the maximum values. Error bars are SD (n=3). Invisible error bars are smaller than the size of the marker. (**E**) Control samples of hβ2m plotted as histograms. Experiments were performed as in (**C**). Samples with analyte (10^5 pg mL^{-1} for microcapsules and 10^6 pg mL^{-1} for PS beads) were used as positive control and for normalization. Error bars are SD (n=3).

concentration at half-maximal response (EC_{50}) was 26.9 pg mL^{-1} for the microcapsules, whereas that of the PS beads was 12 ng mL^{-1} (**Table 4.1**); thus, the microcapsules had a 450-fold better sensitivity. The limit of detection (LoD; definition see section 4.3.12) were 99 fg mL^{-1} for the microcapsules and 5.02 ng mL^{-1} for the PS beads. The much higher sensitivity of the microcapsule assay for $h\beta_2m$ may be crucial for detection in the urine (see section **4.5**).

4.4.3 Microcapsules exhibit similar sensitivity to PS beads for the detection of nucleic acids

In the next set of experiments, we compared microcapsules and PS beads for the detection of nucleic acids. In this assay [8], biotinylated anchor oligonucleotides are attached to streptavidin-coated microcapsules or beads (**Figure 4.1B**). The nucleic acid analyte, for example a single-stranded plasmid, an RNA transcript, or an oligonucleotide, is then bound to the microcapsule or bead through specific base pairing with the anchor oligonucleotide. A detection oligonucleotide, which is complementary to a free sequence in the analyte and labeled with a fluorescent dye, is then hybridized, and detection is again carried out by flow cytometry (**Figure 4.6A**).

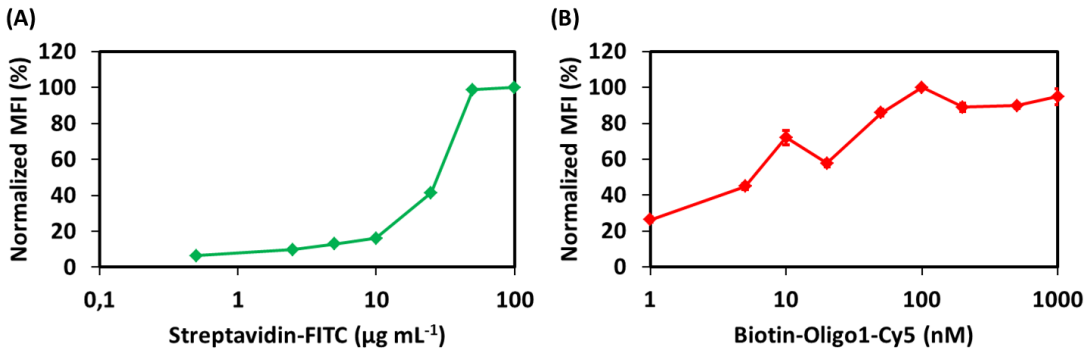

Figure 4.5: Determination of streptavidin and oligonucleotide optimal concentrations. (**A**) Titration of streptavidin. Different concentrations of FITC-streptavidin were immobilized on the PS bead surface via EDC/sulfo-NHS chemistry. MFI values were normalized by the maximum value. (**B**) Titration of anchor oligonucleotide: Biotinylated Cy5-labeled oligo1 was immobilized to the streptavidin functionalized PS beads at different concentrations. MFI values are normalized by maximum value; error bars indicate the (SD; n=3).

We first determined the optimal concentrations of streptavidin and anchor oligonucleotide (**Figure 4.5A**). The covalently immobilized streptavidin on the PS beads was functional since it bound fluorescently labelled biotinylated oligonucleotides with a three to five-fold increase in the signal over the background (**Figure 4.5B**). For microcapsules, we have previously reported a tenfold increase in the same situation [8].

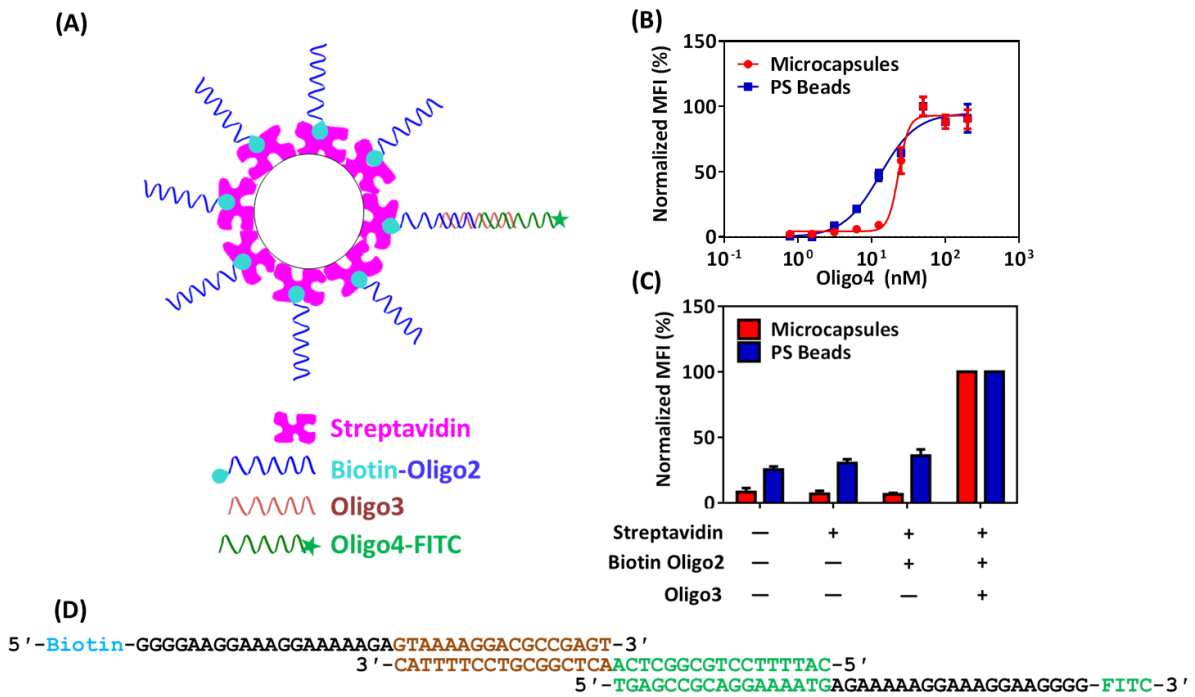

Figure 4.6: Comparison of microcapsules and PS beads for the detection of nucleic acids. (**A**) **Schematics.** The anchor, Biotin-Oligo2, is attached to streptavidin-coated microcapsules or PS beads. Biotin-Oligo2 hybridizes specifically to its complementary sequence on the analyte Oligo3, which in turn hybridizes to its complementary sequence on the detector, Oligo4-FITC. (**B**) **Analyte dose-response** of the assay in (**A**) for streptavidin-coated microcapsules and PS beads measured by flow cytometry. MFI values were normalized by the maximum value. The error bars are SD (n=3). Invisible error bars are smaller than the size of the marker. (**C**) **Background controls** for the assay in (**B**). MFI values were normalized to the maximum value. The error bars indicate the SD (n=3). (**D**) **Hybridization scheme of the three oligonucleotides used in the current assay.** Biotin-Oligo2 hybridizes to the 17 complementary nucleotide bases (brown) of analyte Oligo3, and the remaining free 17 bases of the analyte hybridize to the detector Oligo4-FITC (green).

We then compared the sensitivity of microcapsules and PS beads for the detection of an oligonucleotide analyte, Oligo3, which is recruited to the beads/microcapsules by the anchor Biotin-Oligo2 and detected by the detector Oligo4-FITC (**Figure 4.6B** and **Figure 4.6C**). Here, the microcapsules and the PS beads showed similar sensitivity with EC_{50} values of 23.2 nM and 12.9 nM, respectively.

We conclude that polyelectrolyte microcapsules are suitable for highly sensitive protein and nucleic acid assays, and that for protein assays, they outperform the commercially available solid beads. **Table 4.2** contains the complete validation data for both the protein and the nucleic acid assays [25,26].

	hβ$_2$m in PBS		Oligo3 in PBS	
	Microcapsules	PS beads	Microcapsules	PS beads
Bottom	4.01	2.38	4.14	-0.24
Top	92.98	97.06	92.91	94.81
Hill Slope	1.38	6.44	6.23	1.75
EC_{50}	26.9 pg mL^{-1}	12 ng mL^{-1}	23.2 X 10^{-9} M	12.9 X 10^{-9} M
R^2	0.9696	0.9891	0.9824	0.9695
LoB	32.2 fg mL^{-1}	3.8 ng mL^{-1}	7.5 X 10^{-9} M	4.8 X 10^{-9} M
LoD	99 fg mL^{-1}	5.02 ng mL^{-1}	9.9 X 10^{-9} M	5.9 X 10^{-9} M
LoQ	2.1 pg mL^{-1}	8.7 ng mL^{-1}	12.4 X 10^{-9} M	16.5 X 10^{-9} M
Linear Range (EC_{20}-EC_{80})	9.9 to 73.5 pg mL^{-1}	9.7 to 14.9 ng mL^{-1}	18.5 to 28.9 X 10^{-9} M	5.9 to 28.6 X 10^{-9} M
Concentration tested	10^{-3} to 10^{5} pg mL^{-1}	10^{-4} to 10^{6} pg mL^{-1}	10^{-10} to 10^{-6} M	10^{-10} to 10^{-6} M

Table 4.2: Analytical performance of hβ$_2$m and oligonucleotide detection using microcapsule and PS beads. Best fit values were obtained with a four-parameter fit equation. Limit of blank (**LoB**), limit of detection (**LoD**) and limit of quantification (**LoQ**) were determined as described in the section **4.3.12**.

4.4.4 Monitoring antibody production during hybridoma culture

We next wished to test the microcapsule assay in a practical application, namely to monitor antibody production from a hybridoma supernatant, and we wanted to compare its performance with that of a standard 96-well plate sandwich immunoassay that followed the same principle: the microcapsules or plates were coated with protein A, which then binds the analyte antibody, which is then detected with fluorescently labeled anti-mouse antibody and flow cytometry (for the microcapsules) or in a plate reader. For both assays, we first recorded a dose-response curve with purified antibody in PBS and in complete RPMI medium (with 10% fetal calf serum (FCS), to replicate the hybridoma growth conditions). While in PBS, the plate-based assay was more sensitive than the microcapsules (**Figure 4.7A**), the assays were very similar in the realistic RPMI/FCS medium (**Figure 4.7B**).

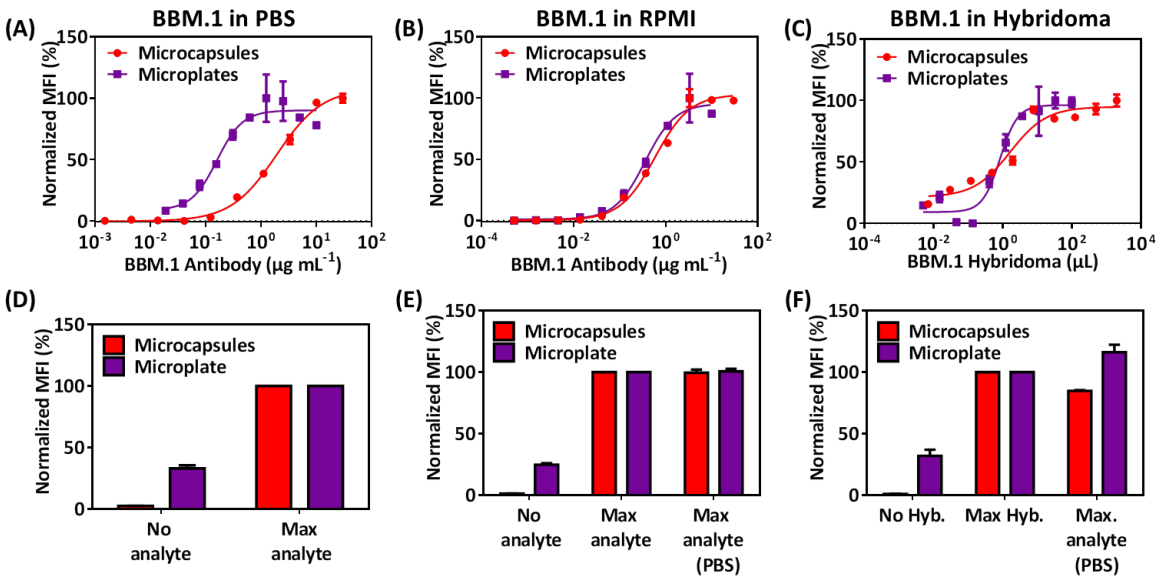

Figure 4.7: Comparison of microcapsule and microplate assays in the detection of BBM.1 antibody in hybridoma supernatant. (**A-C**), analyte dose-response curves for BBM.1 antibody in PBS (**A**), RPMI (**B**), and dilutions of hybridoma supernatant (**C**). Microcapsules or plates were coated with protein A. After binding of the analyte, samples were incubated with detector antibody GαM-AF488 and measured either by flow cytometry (microcapsules) or in a plate reader (microplates). LoDs are: in (**A**) 26 ng mL^{-1} for microcapsules and 24 ng mL^{-1} for plates; in (**B**), 7 ng mL^{-1} for microcapsules and 54 ng mL^{-1} for plates. See Table 2 for complete data. (**D-F**), background controls and comparisons for the curves above. For (**D**) and (**E**), 'Max analyte' is the larges amount of analyte used in the assay above (20 µg mL^{-1} for microcapsules and 10 µg mL^{-1} for microplate). For (**F**), 'Max Hyb.' is the largest volume of hybridoma used in the assay above (2000 µL for microcapsules and 100 µL for microplate). For (**E**) and (**F**), 'Max. analyte (PBS)' is 20 µg µL^{-1} in PBS. MFI values were normalized by the highest value (**A-C**), the 'Max analyte' value (**D-E**), and the 'Max Hyb.' value (**F**). Error bars are the SD (n=3). Invisible error bars are smaller than the size of the marker.

To measure the antibody concentration in the hybridoma supernatant, we then titrated the supernatant either onto the protein A-coated microcapsules or into the protein A-coated 96-

	BBM.1 in PBS		BBM.1 in RPMI		BBM.1 in Hybridoma	
	Microcapsules	Microplates	Microcapsules	Microplates	Microcapsules	Microplates
Bottom	0.41	8.67	0.13	0.91	21.42	9.28
Top	108	90.02	103	95.55	94.9	96.25
Hill Slope	1.05	1.88	1.15	1.33	0.83	1.71
EC50 (mL^{-1})	1.91 µg	0.16 µg	0.59 µg	0.36 µg	1.66 µL	0.84 µL
R^2	0.9947	0.9217	0.9893	0.9704	0.9464	0.9455
LoB (mL^{-1})	21 ng	13 ng	5 ng	21 ng	0.9 nL	124 nL
LoD (mL^{-1})	26 ng	24 ng	7 ng	54 ng	2.8 nL	158 nL
LoQ (mL^{-1})	69 ng	125 ng	38 ng	118 ng	13.6 nL	882 nL
Linear Range (EC20-EC80) (mL^{-1})	0.5 to 7.2 µg	0.07 to 0.3 µg	0.2 to 1.9 µg	0.1 to 1.02 µg	0.3 to 8.8 µL	0.4 to 1.9 µL
Concentration tested	2x10^{-3} to 3x10^{1} µg mL^{-1}	1.9x10^{-2} to 1x10^{1} µg mL^{-1}	1x10^{-3} to 3x10^{1} pg mL^{-1}	5x10^{-4} to 1x10^{1} pg mL^{-1}	7x10^{-3} to 2x10^{3} µL	1x10^{-2} to 1x10^{2} µL

Table 4.3: Analytical performance of BBM.1 detection using microcapsule and microplate for BBM.1 hybridoma. Best fit values were obtained with a four-parameter fit equation. Limit of blank (**LoB**), limit of detection (**LoD**) and limit of quantification (**LoQ**) were determined as described in the section **4.3.12**.

well plates, followed by washing and incubation with fluorescently labeled secondary antibody (**Figure 4.7C**). Both assays measured the same antibody concentration, ca. 330 µg mL^{-1}, in the hybridoma supernatant sample, with the microcapsule assay showing a much better signal-to-noise ratio (**Figure 4.7D-F**). The validation data for both assays are in **Table 4.3**.

Finally, we used our microcapsule-based assay to monitor the production of BBM.1 antibody during the course of hybridoma culture, again compared with the plate assay. Supernatant samples were collected at different days of culture (**Table 4.4**) and measured in either assay as above (**Figure 4.8**). Both assays monitored equally well the production of antibody, which reached a plateau already at day 5.

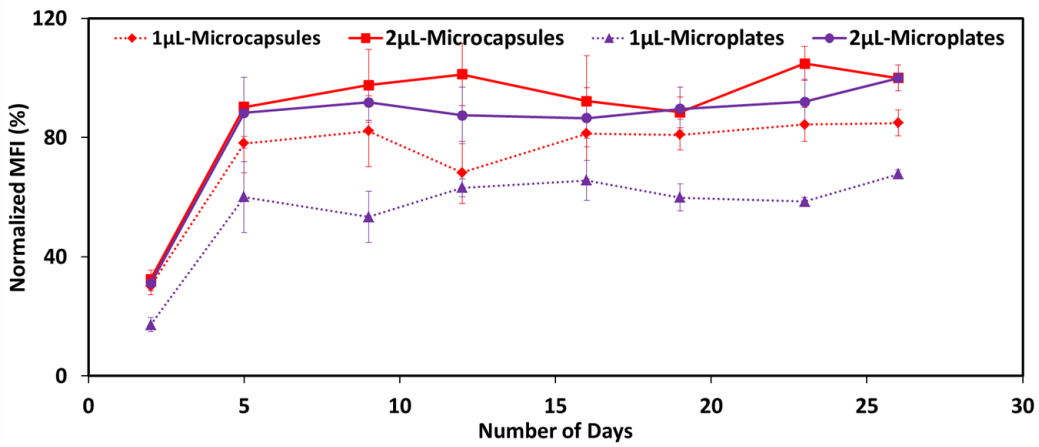

Figure 4.8: Monitoring the production of BBM.1 antibody in hybridoma supernatant. Protein A-coated microcapsules and microplates were incubated with 1 µL and 2 µL hybridoma supernatants that were collected from different days of culture. Binding of the BBM.1 antibody was measured through binding of the detector antibody GαM-AF488. MFI values were normalized for each assay by the final value of the 2 µl curve. The error bars indicate the SD (n=3). Invisible error bars are smaller than the size of the marker.

4.5 Conclusion and Outlook

We have shown here that our polyelectrolyte microcapsule-based assays [8] are sensitive and powerful tools for the detection of proteins and nucleic acids; especially, in the detection of protein analytes, microcapsules are 450-fold more sensitive than a similar assay based on PS beads (**Figure 4.4D**).

The microcapsule-based assays presented in this study have several advantages over the plate or bead assays that are currently used. First, with respect to the immobilization of the first layer of protein (such as protein A for antibodies or streptavidin for biotinylated oligonucleotides), microcapsules and beads have the common advantage over plates that proteins can be covalently attached through EDC/sulfo-NHS chemistry, which prevents the

leaching of protein into the assay solution. But for the covalent attachment of proteins, microcapsules are more efficient: they bind at least twice as much functional protein A than PS beads (**Figure 4.4A**), probably because the high porosity of the microcapsules offers a larger surface area. Second, our microcapsules have the advantage over filled beads that they contain $CaCO_3$ cores that can be dissolved. The cores make them heavy, i.e., easy to handle at every step of the assay, since they can be sedimented in a microcentrifuge (3000 rpm for 2 minutes). But after the cores are dissolved at the end of the assay, the hollow microcapsules, which now have approximately the same density as the buffer, can be read conveniently and reproducibly in the flow cytometer, whereas PS, SiO_2 or PMMA beads, in our experience, tend to settle at the bottom of the tubes, which makes aspiration and acquisition difficult and error-prone. This is especially important if the assay is performed in a high-throughput format, where individual samples may wait some time to be read. The synthesis of the $CaCO_3$ microparticles that we use as cores can be performed in any analytical laboratory from sodium carbonate and calcium nitrate solutions [27,28]; they are also commercially available. Third, like other particle-based assays, the microcapsule assay can be used for multiplexing with different antibodies attached to different sets of microcapsules. Such capsule sets can have different sizes or fluorescent colors, which are either attached to the capsule walls or contained inside (e.g., coupled to dextran), and the sets can easily be distinguished in the flow cytometer by gating on size or fluorescence. Fourth, and perhaps most importantly, our microcapsule assay is simple and robust and shows a higher sensitivity for proteins, with an LoD in the fg mL^{-1} range, while commercially available bead-based assays detect protein biomarkers in the pg ml^{-1} concentrations [2–5,29,30], and traditional ELISA assays for proteins have LoD values in the ng ml^{-1} range [31].

No. of days	Live Cells	Dead Cells	Live/Dead Cells	(10^6)Live Cells/mL
2	78	7	11.1	0.39
5	124	89	1.39	0.62
9	46	72	0.64	0.23
12	33	113	0.29	0.17
16	50	174	0.29	0.25
19	22	212	0.10	0.11
23	10	161	0.06	0.05
26	0	173	0.00	0.00

Table 4.4: Cell counts for BBM.1 hybridoma during culture. Aliquots of cell culture supernatant were collected and counted on the respective days.

The increased sensitivity of the microcapsules in the detection of hβ_2m has an important practical application. Beta-2 microglobulin serves as a prognosis marker for several cancer types such as multiple myeloma and lymphoma [32–34], with its concentration increased in the blood when disease occurs. The concentrations of hβ_2m in the blood (1.4-2.5 µg mL^{-1}) [35] do not require an ultra-sensitive assay, but the currently available rapid bioassays cannot detect hβ_2m in the urine, where its normal level is only 30 ng mL^{-1} [24]. Thus, a microcapsule-based assay might be crucial for the rapid early detection of renal failure, which accompanies a variety of diseases [36]. For other protein markers of disease, similar assays are achievable.

For the sequence-specific detection of nucleic acids, microcapsules showed similar sensitivity to the commercially available PS beads, and so they can be used to detect single-stranded nucleic acids such as microRNAs, which are blood-based markers of cancer [37], or antibiotic resistance genes from denatured samples for the rapid identification of multidrug-resistant bacteria. For that application, it is important to develop test kits that do not require a PCR reaction that consumes time and complicates the analysis. It is likely that a microcapsule-based assay may allow the direct detection of the pathogen nucleic acids; this is an exciting direction for future research.

4.6 Acknowledgements

The authors thank Mohamed Aboelmagd for providing purified hβ_2m and Ursula Wellbrock for technical support. The authors gratefully acknowledge the financial support of the German Ministry for Education and Research (BMBF; Kooperationsprojekt 031A153A-B 'Prozessüberwachung in vivo und in vitro mit Polyelektrolyt-Nanokapseln').

4.7 References

[1] S. Hansenova Manaskova, F.J. Bikker, E.C.I. Veerman, A. van Belkum, W.J.B. van Wamel, Rapid detection and semi-quantification of IgG-accessible Staphylococcus aureus surface-associated antigens using a multiplex competitive Luminex assay, J. Immunol. Methods. 397 (2013) 18–27. doi:10.1016/j.jim.2013.07.016.

[2] L.P. Rodríguez, N. Vilariño, M.C. Louzao, T.J. Dickerson, K.C. Nicolaou, M.O. Frederick, L.M. Botana, Microsphere-based immunoassay for the detection of azaspiracids, Anal. Biochem. 447 (2014) 58–63. doi:10.1016/j.ab.2013.10.035.

[3] M. Fraga, N. Vilariño, M.C. Louzao, L.P. Rodríguez, A. Alfonso, K. Campbell, C.T. Elliott, P. Taylor, V. Ramos, V. Vasconcelos, L.M. Botana, Multi-detection method for five common microalgal toxins based on the use of microspheres coupled to a flow-cytometry system, Anal. Chim. Acta. 850 (2014) 57–64. doi:10.1016/j.aca.2014.08.030.

[4] Y.K. Hahn, J.B. Chang, Z. Jin, H.S. Kim, J.K. Park, Magnetophoretic position detection for multiplexed immunoassay using colored microspheres in a microchannel, Biosens. Bioelectron. 24 (2009) 1870–1876. doi:10.1016/j.bios.2008.09.016.

[5] A. de la Escosura-Muñiz, Z. Plichta, D. Horák, A. Merkoçi, Alzheimer's disease biomarkers detection in human samples by efficient capturing through porous magnetic microspheres and labelling with electrocatalytic gold nanoparticles, Biosens. Bioelectron. 67 (2015) 162–169. doi:10.1016/j.bios.2014.07.086.

[6] B.A. Wood, K.P. O'Halloran, S. VandeWoude, Development and validation of a multiplex microsphere-based assay for detection of domestic cat (Felis catus) cytokines, Clin. Vaccine Immunol. 18 (2011) 387–392. doi:10.1128/CVI.00289-10.

[7] R.M. Lequin, Enzyme immunoassay (EIA)/enzyme-linked immunosorbent assay (ELISA), Clin. Chem. 51 (2005) 2415–2418. doi:10.1373/clinchem.2005.051532.

[8] S.K. Verma, A. Amoah, U. Schellhaas, M. Winterhalter, S. Springer, T.A. Kolesnikova, ???To Catch or Not to Catch???: Microcapsule-Based Sandwich Assay for Detection of Proteins and Nucleic Acids, Adv. Funct. Mater. 26 (2016) 6015–6024. doi:10.1002/adfm.201601328.

[9] A.P.R. Johnston, C. Cortez, A.S. Angelatos, F. Caruso, Layer-by-layer engineered capsules and their applications, Curr. Opin. Colloid Interface Sci. 11 (2006) 203–209. doi:10.1016/j.cocis.2006.05.001.

[10] G.B. Sukhorukov, H. Möhwald, Multifunctional cargo systems for biotechnology, Trends Biotechnol. 25 (2007) 93–98. doi:10.1016/j.tibtech.2006.12.007.

[11] B.G. De Geest, A.G. Skirtach, G.B. Sukhorukov, J. Demeester, S.C. De Smedt, W.E. Hennink, Stimuli-responsive polyelectrolyte microcapsules for biomedical applications, Am. Chem. Soc. Polym. Prepr. Div. Polym. Chem. 49 (2008) 1074–1075. doi:10.1039/b808262f.

[12] E. Donath, G.B. Sukhorukov, F. Caruso, S. a Davis, H. Möhwald, Novel Hollow Polymer Shells by Colloid Templated Assembly of Polyelectrolytes, Angew Chem Int Ed Engl. 37 (1998) 2201–2205. doi:10.1002/(SICI)1521-3773(19980904)37:16<2201::AID-ANIE2201>3.0.CO;2-E.

[13] G.B. Sukhorukov, E. Donath, S. Davis, H. Lichtenfeld, F. Caruso, V.I. Popov, H. Möhwald, Stepwise polyelectrolyte assembly on particle surfaces: a novel approach to colloid design, Polym. Adv. Technol. 767 (1998) 759–767. doi:10.1002/(sici)1099-1581(1998100)9:10/11<759::aid-pat846>3.0.co;2-q.

[14] Z. Grabarek, J. Gergely, Zero-length crosslinking procedure with the use of active

esters, Anal. Biochem. 185 (1990) 131–135. doi:10.1016/0003-2697(90)90267-D.

[15] P. Schuetz, F. Caruso, Copper-Assisted Weak Polyelectrolyte Multilayer Formation on Microspheres and Subsequent Film Crosslinking, Adv. Funct. Mater. 13 (2003) 929–937. doi:10.1002/adfm.200304483.

[16] T. Mauser, C. Déjugnat, G.B. Sukhorukov, Reversible pH-dependent properties of multilayer microcapsules made of weak polyelectrolytes, Macromol. Rapid Commun. 25 (2004) 1781–1785. doi:10.1002/marc.200400331.

[17] W. Tong, C. Gao, Stable microcapsules assembled stepwise from weak polyelectrolytes followed by thermal crosslinking, Polym. Adv. Technol. 16 (2005) 827–833. doi:10.1002/pat.659.

[18] M. Germain, S. Grube, V. Carriere, H. Richard-Foy, M. Winterhalter, D. Fournier, Composite nanocapsules: Lipid vesicles covered with several layers of crosslinked polyelectrolytes, Adv. Mater. 18 (2006) 2868–2871. doi:10.1002/adma.200600860.

[19] J. V. Staros, R.W. Wright, D.M. Swingle, Enhancement by N-hydroxysulfosuccinimide of water-soluble carbodiimide-mediated coupling reactions, Anal. Biochem. 156 (1986) 220–222. doi:10.1016/0003-2697(86)90176-4.

[20] J. Du, H. Yang, B. Peng, J. Ding, Structural modeling and biochemical studies reveal insights into the molecular basis of the recognition of beta-2-microglobulin by antibody BBM.1., J. Mol. Recognit. 22 (2009) 465–73. doi:10.1002/jmr.964.

[21] S.K. Saini, E.T. Abualrous, A.S. Tigan, K. Covella, U. Wellbrock, S. Springer, Not all empty MHC class I molecules are molten globules: Tryptophan fluorescence reveals a two-step mechanism of thermal denaturation, Mol. Immunol. 54 (2013) 386–396. doi:10.1016/j.molimm.2013.01.004.

[22] F.M. Brodsky, W.F. Bodmer, P. Parham, Characterization of a monoclonal anti?????2???microglobulin antibody and its use in the genetic and biochemical analysis of major histocompatibility antigens, Eur. J. Immunol. 9 (1979) 536–545. doi:10.1002/eji.1830090709.

[23] T. Kojima, T. Mizoguchi, E. Ota, J. Hata, K. Homma, B. Zhu, K. Hitomi, H. Nakano, Immobilization of proteins onto microbeads using a DNA binding tag for enzymatic assays, J. Biosci. Bioeng. 121 (2016) 147–153. doi:10.1016/j.jbiosc.2015.06.003.

[24] D.A. Brott, S.T. Furlong, S.H. Adler, J.W. Hainer, R.B. Arani, M. Pinches, P. Rossing, N. Chaturvedi, Characterization of renal biomarkers for use in clinical trials: Effect of preanalytical processing and qualification using samples from subjects with diabetes, Drug Des. Devel. Ther. 9 (2015) 3191–3198. doi:10.2147/DDDT.S78792.

[25] D.A. Armbruster, T. Pry, Limit of blank, limit of detection and limit of quantitation., Clin. Biochem. Rev. 29 Suppl 1 (2008) S49-52. doi:citeulike-article-id:3416410.

[26] A. Shrivastava, V. Gupta, R. Article, Methods for the determination of limit of detection and limit of quantitation of the analytical methods, Chronicles Young Sci. 2 (2011) 21–25. doi:10.4103/2229-5186.79345.

[27] G.B. Sukhorukov, D. V. Volodkin, A.M. Gunther, A.I. Petrov, D.B. Shenoy, H. Mohwald, Porous calcium carbonate microparticles as templates for encapsulation of bioactive compounds, J. Mater. Chem. 14 (2004) 2073. doi:10.1039/b402617a.

[28] A.A. Antipov, D. Shchukin, Y. Fedutik, A.I. Petrov, G.B. Sukhorukov, H. Möhwald, Carbonate microparticles for hollow polyelectrolyte capsules fabrication, Colloids Surfaces A Physicochem. Eng. Asp. 224 (2003) 175–183. doi:10.1016/S0927-7757(03)00195-X.

[29] M. Sun, J. Manolopoulou, A. Spyroglou, F. Beuschlein, C. Hantel, Z. Wu, M. Bielohuby, A. Hoeflich, C. Liu, M. Bidlingmaier, A microsphere-based duplex competitive

immunoassay for the simultaneous measurements of aldosterone and testosterone in small sample volumes: Validation in human and mouse plasma, Steroids. 75 (2010) 1089–1096. doi:10.1016/j.steroids.2010.07.005.

[30] H.C. Tekin, M. a M. Gijs, Ultrasensitive protein detection: a case for microfluidic magnetic bead-based assays., Lab Chip. 13 (2013) 4711–39. doi:10.1039/c3lc50477h.

[31] A. Qureshi, Y. Gurbuz, J.H. Niazi, Biosensors for cardiac biomarkers detection: A review, Sensors Actuators, B Chem. 171–172 (2012) 62–76. doi:10.1016/j.snb.2012.05.077.

[32] H. Hagberg, A. Killander, B. Simonsson, Serum beta 2-microglobulin in malignant lymphoma., Cancer. 51 (1983) 2220–5. http://www.ncbi.nlm.nih.gov/pubmed/6189572.

[33] P.W. Johnson, J. Whelan, S. Longhurst, K. Stepniewska, J. Matthews, J. Amess, A. Norton, A.Z. Rohatiner, T.A. Lister, Beta-2 microglobulin: a prognostic factor in diffuse aggressive non-Hodgkin's lymphomas., Br. J. Cancer. 67 (1993) 792–797. http://www.ncbi.nlm.nih.gov/pmc/articles/PMC1968369/.

[34] C. Yoo, D.H. Yoon, C. Suh, Serum beta-2 microglobulin in malignant lymphomas: An old but powerful prognostic factor, Blood Res. 49 (2014) 148–153. doi:10.5045/br.2014.49.3.148.

[35] D.R. Norfolk, M.A. Forbes, E.H. Cooper, J.A. Child, Changes in plasma beta 2 microglobulin concentrations after allogeneic bone marrow transplantation., J. Clin. Pathol. 40 (1987) 657–62. doi:10.1136/jcp.40.6.657.

[36] T. Fiseha, A. Gebreweld, Urinary Markers of Tubular Injury in HIV-Infected Patients, Biochem. Res. Int. 2016 (2016). doi:10.1155/2016/1501785.

[37] P.S. Mitchell, R.K. Parkin, E.M. Kroh, B.R. Fritz, S.K. Wyman, E.L. Pogosova-Agadjanyan, A. Peterson, J. Noteboom, K.C. O'Briant, A. Allen, D.W. Lin, N. Urban, C.W. Drescher, B.S. Knudsen, D.L. Stirewalt, R. Gentleman, R.L. Vessella, P.S. Nelson, D.B. Martin, M. Tewari, Circulating microRNAs as stable blood-based markers for cancer detection., Proc. Natl. Acad. Sci. U.S.A. 105 (2008) 10513–10518. doi:10.1073/pnas.0804549105.

Chapter 5

In this section, I report on the proximity studies between two or more microcapsules that are surface-coated with antibodies and/or oligonucleotides, using flow cytometry for detection. I modified the surface of the microcapsules with either protein A or streptavidin to attach antibodies or biotinylated oligonucleotides to be used to induce proximity between two or more microcapsules. At first, I performed a biophysical proof-of-principle experiment, wherein two or more microcapsules are brought to close proximity by means of complimentary interaction, followed by analyte-induced proximity.

The chapter is divided into two parts. **Chapter 5.6.1** describes the antibody-mediated proximity induction of microcapsules, whereas **chapter 5.6.2** focuses on the induction of proximity between two or more microcapsules based on complementary oligonucleotides. All experimental work in this chapter was carried out by myself, except for Figure 5.23 and Figure 5.24 which was performed by Ulla Schellhaas, our undergraduate rotation student and figures Figure 5.25, Figure 5.27, Figure 5.28, Figure 5.29 and Figure 5.30 which was performed by Amanda Amoah, our Master's rotation student. This chapter was written by Sebastian Springer and myself.

5 Chapter 5: Polyelectrolyte Microcapsules: Induced proximity as a versatile tool for monitoring biotechnological processes

5.1 Abstract

Polyelectrolyte microcapsules produced through layer-by-layer assembly can serve as a platform for multiple sensing tasks because their surface chemistry can be broadly adapted to detect various biomolecules. This chapter focuses on the work for the development of a new modular assay that is based on the novel principle of analyte-induced proximity of polyelectrolyte microcapsules with optical readout. That assay, when its development is complete, will be marker-free and non-invasive in nature, and it will have the potential to monitor, with high temporal and spatial resolution, diverse components of biotechnological production processes such as nucleic acids, proteins, or small molecule metabolites. The measurement principle can be applied to cell culture media, in cell free production systems, and also inside cells.

5.2 Introduction

Detecting analytes or biomarkers at low concentrations, primarily at the initial stages of disease, is of utmost importance, especially in the field of biomedical sciences, and can have a variety of scientific applications. For the development of an assay system that is sensitive, selective, and robust, it is essential to develop a detection method that can detect analytes at low concentrations. This can be achieved with adaptor proteins such as protein A and streptavidin for the attachment of biomolecules such as antibodies and biotinylated molecules (oligonucleotides, proteins etc...) to achieve optimized oriented attachment of biomolecules on the surfaces of polyelectrolyte microcapsules.

Based on the preliminary work with the microcapsules as sensors [1–7], the work described here features the development of a novel detection system that can be used to sense a variety of small molecules such as plasmids, transcripts, proteins, and low molecular weight molecules in realistic environments and that can be of biotechnological and commercial importance. Here, I introduce modified microcapsules with functional protein A and streptavidin. The detection of analytes through protein A and streptavidin-modified microcapsules as a platform with an optical readout is shown in this chapter.

5.3 General Measurement Principle

The detection of analytes with microcapsules has been attempted before, but only for simple measurement techniques such as pH sensing [1], ion sensing [4], or ratiometric pH measurements [3], and as biosensors for glucose [7] and urea [5]. These conventional techniques have very limited applications, since only analytes that bind directly to a dye or can be measured by enzymatic assays may be determined in this way. The induction of proximity of two or more microcapsules by the analyte makes an innovative leap and allows, in principle, much more sophisticated measurements (**Figure 5.1**). The measuring principle is as follows: Due to the proximity of the microcapsules to each other, which is caused by the analyte, an optical signal is generated that can be read without contact. Optical fluorescence-based measurement methods have the advantage that they are non-invasive and in principle also do not affect the sterility of the culture as long as the signal is detected from the outside. Due to the large number of binding sites for the analyte on the surface of the microcapsules, it can principally be expected that the analyte will be detectable over a wide concentration range. Induced proximity may also lead to an accumulation of many microcapsules, resulting in signal amplification. The relatively large size of the microcapsule compared to nanometer-sized microcapsules should in principle lead to a strong signal, because large quantities of fluorophore that are embedded inside the walls of the microcapsules or coupled to the microcapsule surface are brought into proximity to each other. The measuring principle should theoretically allow the detection of any protein, nucleic acid or metabolite that can be bound by two independent antibodies or similar binding proteins.

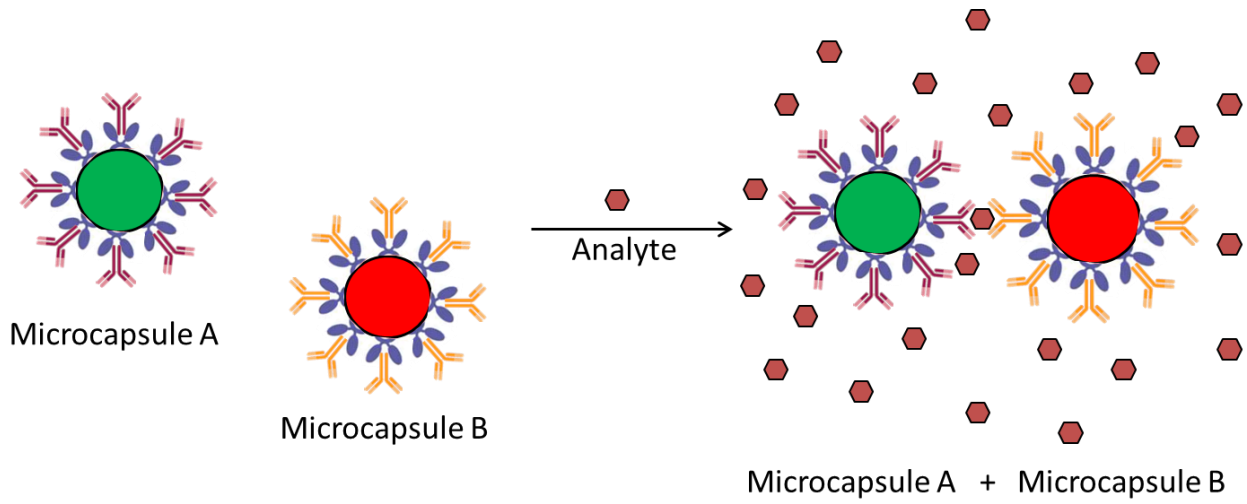

Figure 5.1: Schematics for analyte-induced proximity. Two or more microcapsules filled with red and green dye and carrying different antibodies on their surfaces recognize two different epitopes of the same analyte. Thus, in the presence of the analyte, two or more microcapsules are brought together in proximity.

5.3.1 Proximity induction in the literature

Proximity assays with optical readout have scientific and commercial applications already. A proximity assay called AlphaScreen is used for the measurement of protein-protein interactions[12]. In this assay, the donor beads (polystyrene with a phthalocyanine dye) transfer singlet oxygen to the acceptor thioxene beads upon laser activation.

In the literature, some preliminary observations on the induced proximity of microcapsules have been reported already. Microcapsules made with weak polyelectrolytes on their outer surfaces can be used as pH sensors. Such microcapsules lower their charge density when the pH of the surrounding medium becomes close to the pK_a of one or both polyelectrolytes. This decreases the electrostatic interaction between the layers, resulting in swelling and decomposition of the microcapsules. It was also demonstrated that these microcapsules (made from PDADMAC (polydiallyldimethyl ammonium chloride) and fluorescently labeled MRho-PSS (methacroyloxyethylthiocarbamoyl rhodamine B-PSS) on SiO_2 templates) came in close proximity [8]. They showed that with increasing salt concentration, microcapsules lost their mutual repulsion due to a decrease in the electrostatic forces and fused together. Based on this work, Pechenkin et al., found that changes in pH also induced proximity between microcapsules of opposite charge, which came in close proximity only after a considerable time period, but then they exchanged polymers and eventually fused together [9].

5.3.2 Proximity readout

In an ideal assay system, surface modification and analyte-induced proximity of two or more microcapsules will lead to a change in the optical properties of at least one of the microcapsules, thus generating an optical signal. This optical signal, which is either active (luminescence) or reactive (fluorescence), can in principle be detected in a cuvette spectrometer, by microscopy, or by flow cytometry. The use of a confocal laser scanning microscope to measure proximity of microcapsules in cultured cells provides a high spatial resolution, where each cell can be monitored for changes in optical readout. The use of flow cytometry as a readout system offers an advantage of high throughput, since many events can be read in a short period of time. Flow cytometry also gives a measurement of the heterogeneity of the sample.

[12] AlphaScreen is distributed by PerkinElmer, see http://www.perkinelmer.com/CMSResources/Images/APP_AlphaScreen_Principles.pdf.

5.4 General aim of the work

The major aim of the work was to establish a new assay method that will be able to measure the production of proteins and metabolites during biotechnological processes. The new assay should be able to detect various biotechnologically important substances (plasmids, transcripts, proteins and protein complexes, low molecular weight metabolites, as well as enzyme activity), and it should be marker free and non-invasive in nature. Two different detectors, coupled to two individual microcapsules, will lead to the proximity of the two microcapsules when binding to the analyte at the same time, enabling the detection.

The assay should be applicable to any biomolecule for which there are specific binding partners such as antibodies that can be coupled to a surface. The measuring principle is based on the induced proximity of two different microcapsules by the analyte (**see section 5.3**).

My work was initially planned to be focused on fluorescence resonance energy transfer (FRET) between two different microcapsules but this was not successful primarily due to the large sizes of the microcapsules (6 µm) that made it difficult for the microcapsules to come within the Förster radius (1-10 nm).

Instead, the two microcapsule populations were modified with two different fluorescent dyes, red and green. It was assumed that binding of the analyte by both kinds of microcapsules would lead to the formation of a cluster of both red and green microcapsules. This was measured in a flow cytometer.

5.5 Fabrication and functionalization of microcapsules by surface modification

The surface of the microcapsules must be modified such that different adaptor proteins such as streptavidin (for attaching oligonucleotides) and protein A (for attaching antibodies) can be attached through EDC/sulfo-NHS chemistry (**Figure 1.1**). Some factors that probably influence the performance of the assay are the size of microcapsules, the density of the surface modification for the attachment of detectors (antibodies and streptavidin), the surface porosity, and the efficiency of the conjugation of the microcapsules with fluorescent dyes. To create an assay with consistent performance, I anticipated that it would be important to control these details in a reproducible manner:

Microcapsules were produced by the LbL [10,11] technique, in which the amine groups (from PAH) and the carboxyl groups (from PAA) bind to each other due to electrostatic forces and are then chemically crosslinked with EDC to form a stable covalent amide bond, increasing the mechanical stability of microcapsules [12,13]. The size of the microcapsules was studied by light scattering with the help of flow cytometry, which also gives a detailed analysis of the size

distribution and homogeneity of the population. The exact size of the microcapsules can be measured by light microscopy.

For coupling the detecting antibodies, I chemically modified the surfaces of the microcapsules. I used PAA as the final polymer layer and activated the carboxyl groups with EDC/sulfo-NHS [14]. The microcapsules are then coupled with protein A. To the microcapsules containing protein A, antibodies were then bound.

Similarly, to attach biotin-labeled nucleic acids to microcapsules, I activated the carboxyl groups with EDC/sulfo-NHS in order to subsequently bind streptavidin.

The interior of the microcapsules was then filled with fluorescent dyes by incubating the cores with dye-labeled proteins or dextran prior to LbL assembly of the microcapsules. The dyes were coupled to large molecules to prevent them from leaking from the finished microcapsules.

5.6 Results

5.6.1 Proximity induction using antibodies as detector molecules

5.6.1.1 Fluorescent dyes can be absorbed into the cores of $(PAH/PAA)_2$ microcapsules

For the induced proximity experiments, it is necessary that the microcapsules coupled with different antibodies have different colors. Modification of the surface of the microcapsules with dyes might lead to artefacts given the hydrophobic character of the fluorescent dyes. Therefore, I tested whether fluorescent dyes could be included into the core of the capsule. I decided to allow the fluorescent dyes to diffuse into the $CaCO_3$ cores before assembly of the microcapsules. The dyes were first coupled to dextran to prevent them from leaving the finished microcapsules by diffusion through the capsule wall. The $CaCO_3$ cores were then incubated with Atto-488 for 30 minutes (RT, shaking at 2000 rpm). Flow cytometry measurements of microcapsules showed 100-fold greater fluorescence intensity compared to control microcapsules not incubated with the dye (**Figure 5.2**). I conclude that the method is suitable to produce microcapsules that are fluorescently labeled on the inside.

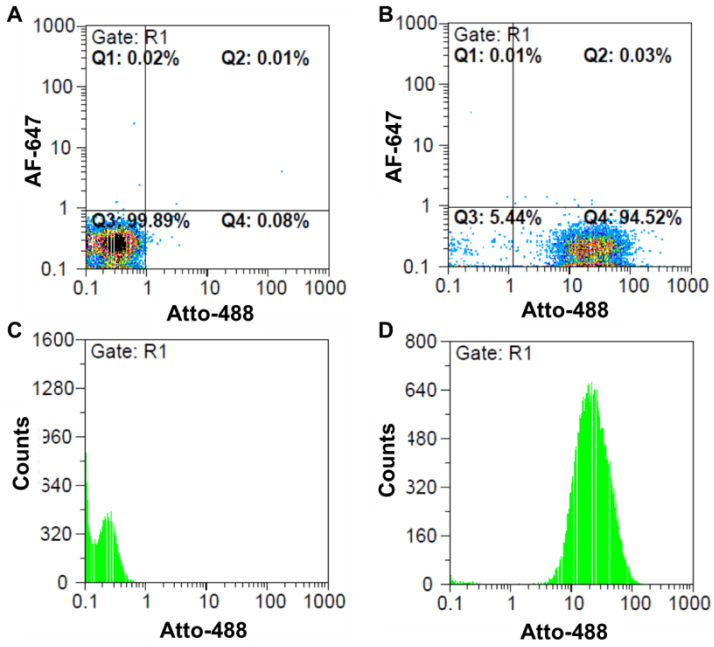

Figure 5.2: Microcapsules are rendered fluorescent by inclusion of Atto-488. Flow cytometry dot plots (**A and B**) and histogram (**C and D**) analysis of fluorescence intensity for control (**A and C**) and fluorescently labeled microcapsules (**B and D**).

5.6.1.2 Protein A-mediated optimized orientation leads to the binding of more antibody to microcapsules than random orientation

It has been shown previously that optimized orientation of antibody serves as better sensors than randomly oriented antibody on planar surfaces [15–18]. Hence, I thought that for a microcapsule to be used as a sensor, it is necessary that the antibody immobilized on its surface is in optimized orientation so that the analyte binding region is free for the analyte to bind. This makes antibody based sensors more sensitive for the detection of analytes. Therefore, I tested whether antibodies can be attached in an optimized orientation (through protein A) and compared the results to those without protein A (random orientation). For the antibody modification experiment, microcapsules were made on $CaCO_3$ templates using the LbL technique with PAH and PAA polyelectrolytes. The microcapsules were crosslinked using EDC (MES buffer, pH 6.0) followed by activation of the surface carboxyl groups of PAA by EDC/Sulfo-NHS chemistry. Protein A was then added (PBS, pH 7.2) on the $(PAH/PAA)_2$ microcapsule, and the unreacted groups were quenched (Tris-Cl, pH 8.8). To the microcapsules with protein A, primary antibody (W6/32) was added and incubated for 2 hours at room temperature with constant shaking. Finally, secondary antibody (goat anti-mouse IgG-AF488) was added, which recognized the primary antibody and emitted green fluorescence. The cores were dissolved with 0.2 M EDTA, pH 7.2. The microcapsules were then taken for characterization by confocal laser scanning microscopy (**Figure 5.3**) and flow cytometry (**Figure 5.4**).

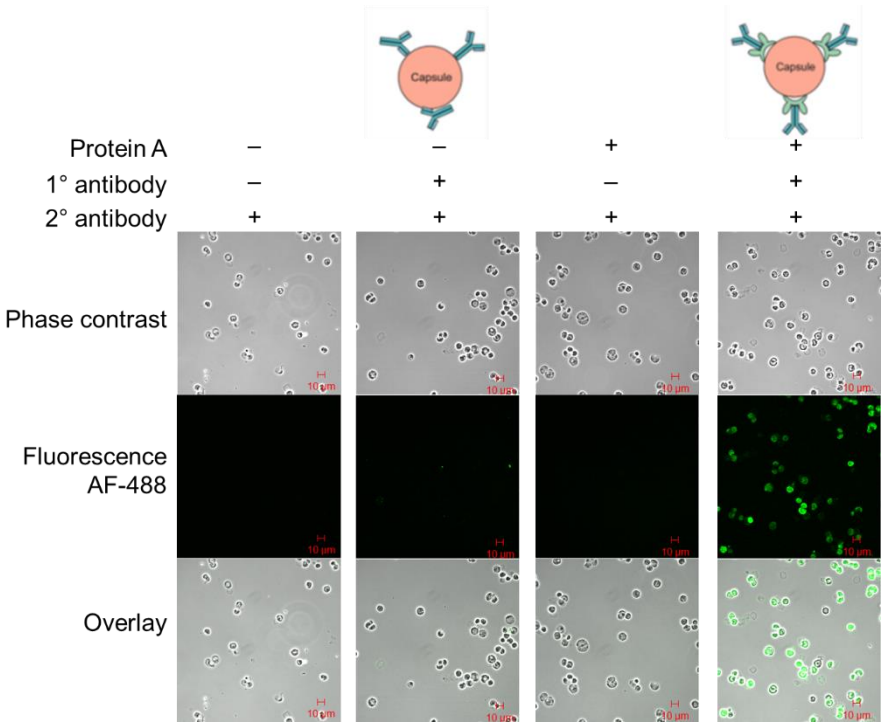

Figure 5.3: Microscopic (CLSM) study of microcapsules. $(PAH/PAA)_2$ microcapsules were prepared with and without protein A and observed for AF488 fluorescence (present in the secondary antibody) by confocal laser scanning microscopy. Four sets of microcapsules were prepared as described in the text, then functionalized with protein A and primary antibody as indicated, and finally incubated with secondary antibody. The microcapsules with protein A gave a brighter fluorescence than microcapsule without protein A, which is due to the greater availability of functional antibodies. The secondary antibody alone does not give any fluorescence, which shows that there is not any non-specific binding of the antibodies on the microcapsule surface.

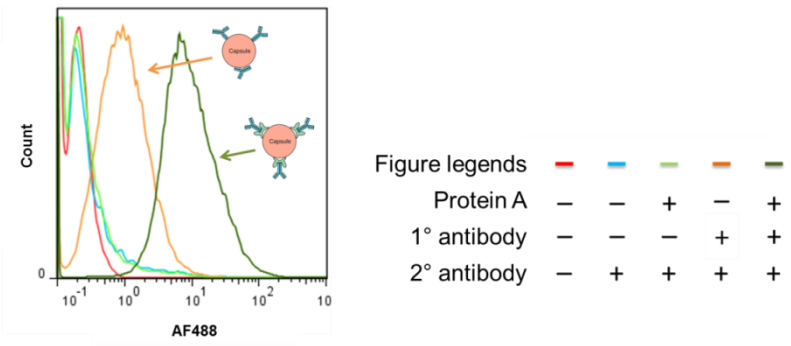

Figure 5.4: Flow cytometry readout of $(PAH/PAA)_2$ microcapsules with and without protein A. Five sets of microcapsules were prepared on $CaCO_3$ cores by LbL assembly of PAH and PAA polyelectrolytes. All microcapsules were then cross-linked with EDC, and one set was taken as a negative control. It can be seen that the dark green curve (microcapsules with protein A) gives more fluorescence than the brown curve (microcapsules without protein A), which may be due to the tail-on orientation of the antibodies on the capsule. All secondary antibody controls (light green with protein A and blue without protein A) show the same intensity as the no antibody control (red), which suggests that there is no unspecific binding of the antibodies; n=3.

It can be seen from both figures that microcapsules with protein A gave more fluorescence than the microcapsules without protein A. Thus, protein A modification allows the microcapsules to bind more antibody.

5.6.1.3 Proximity induction without analyte

The main aim of my work was to develop robust methods of proximity induction and readout between two or more microcapsules for detecting biotechnologically important substrates such as plasmids, transcripts, proteins, and low molecular weight molecules. This was done by optimizing the physical properties of the microcapsules. In a simple way, to begin with, I induced proximity between two microcapsules by attaching two different antibodies to the surfaces of the microcapsules. Proximity was achieved by direct interaction between the two antibodies when the antibody on one microcapsule recognized and bound the antibody on the surface of the other microcapsule. The microcapsule with one antibody on the outer surface

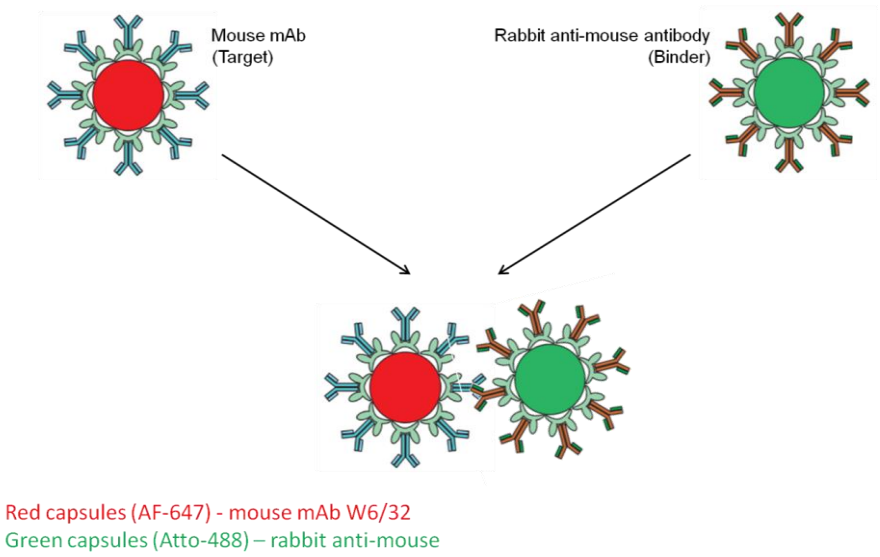

Figure 5.5: Schematic representation of induced proximity between two microcapsules. Two sets of microcapsules with covalently attached protein A have W6/32 and rabbit anti-mouse AF488 antibodies on their surface. The microcapsule with anti-mouse AF488 antibody (Binder) recognizes the microcapsule with W6/32 antibody (Target), and both microcapsules are brought to close proximity, which is detected because the resulting cluster shows both red and green fluorescence.

contained AF-647 inside, and the other microcapsule with the other antibody on the outer surface contained Atto-488. When two different microcapsule populations with two different set of antibodies come in close proximity, a cluster of two or more microcapsules is generated that fluoresces both red and green and can therefore be detected in the flow cytometer (**Figure 5.5**).

For a proximity induction experiment without analyte, the $CaCO_3$ cores were first incubated with green and red dyes[13] separately. One aliquot of the $CaCO_3$ cores was incubated with Atto-488 (green), while the other aliquot of the cores was incubated with AF-647 (red). The microcapsules with Atto-488 were functionalized with anti-mouse IgG antibody (Binder). The microcapsules with AF-647 inside were functionalized with the mouse monoclonal W6/32 antibody at room temperature. After incubation, the microcapsules were washed three times with water to remove non-specific and unbound antibodies, followed by the dissolution of the cores with 0.2 M EDTA, pH 7.2. Both types of microcapsules were then incubated together for different lengths of time, up to 30 minutes. Then, all samples were read in the flow cytometer to check for proximity.

The flow cytometry plot shows the control unlabeled microcapsules in the lower left quadrant, which is negative for both green (Atto-488) and red (AF-647), green microcapsules in the lower right quadrant, red microcapsules in the upper left quadrant, and double-positive microcapsules (i.e. clusters of microcapsules of both types that have come in close proximity) in the upper right quadrant. The percentage of double-positive microcapsules was calculated as the percentage of the total red microcapsules that was bound to the green microcapsules using the formula

$$\frac{Q2}{Q1 + Q2} \text{ X } 100$$

with

Q1 = percentage value from flow cytometry of red-only microcapsules

Q2 = percentage value from flow cytometry of double-positive microcapsules

For example, for the first panel of Figure 6B, the percentage of double-positive microcapsules calculates as

Q2/(Q1+Q2) x100 = 4.63/(56.04+4.63)x100 = 8%

The percentages of the double-positive percentages are written in the Q2 quadrant in red.

For the experiment, the microcapsules were mixed at different ratios of 1:1 (1.5×10^5: 1.5×10^5), 1:5 (6×10^4: 2.4×10^5) and 1:10 (3×10^4: 2.7×10^5) to find the optimal ratio required to get the maximum effect and a minimum background signal (**Figure 5.6**). The maximum double-positive population was observed when the microcapsules were mixed in 1:10 ratio,

[13] Atto-488 and AF-647 were coupled to BSA using “Click-chemistry” before inucbating with the cores

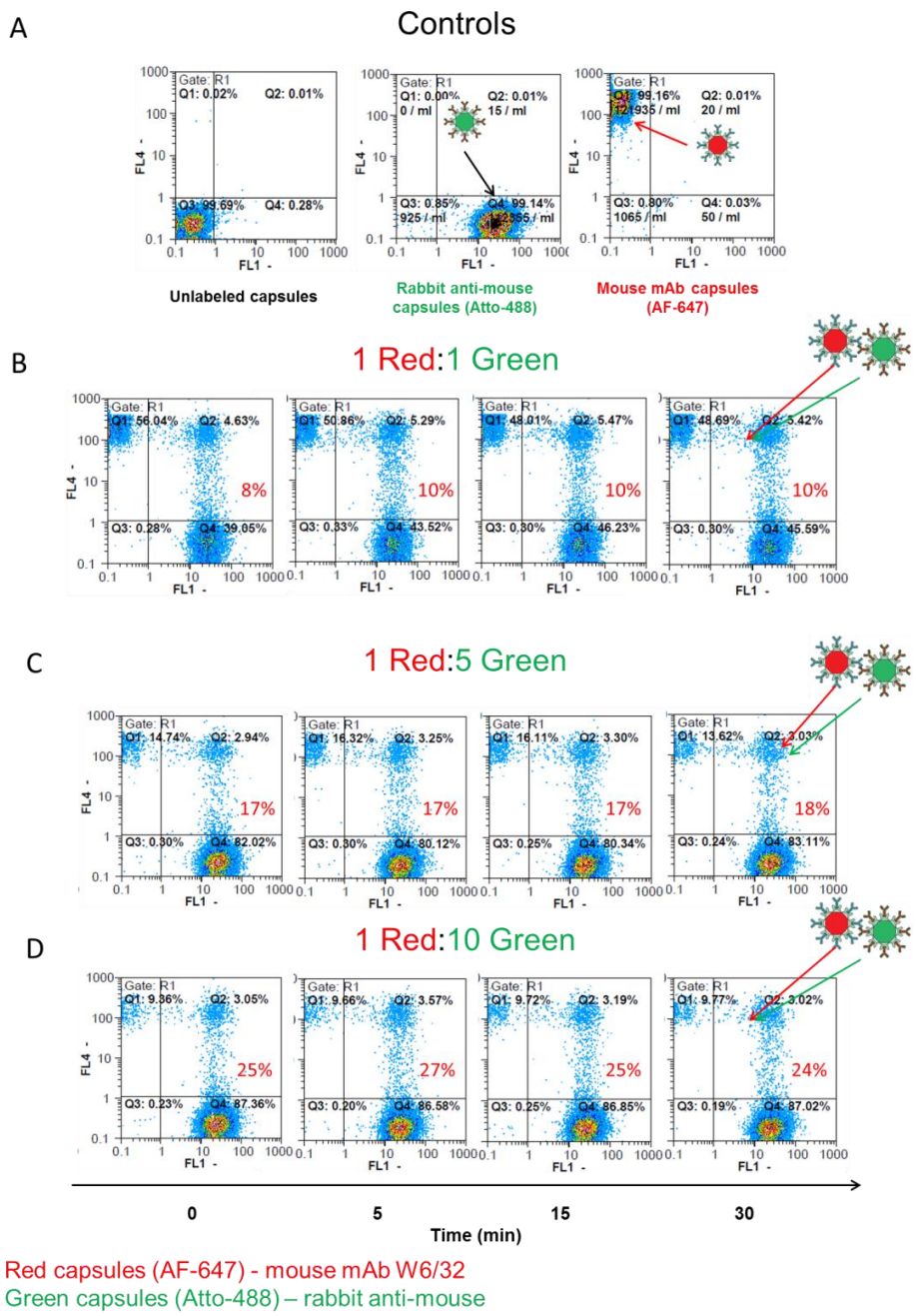

Figure 5.6: Biophysical proof-of-principle studies. Red microcapsules (filled with AF-647) surface-functionalized with mouse mAb W6/32 and incubated together with green microcapsules (filled with Atto-488) surface-functionalized with rabbit anti-mouse in 1 mL PBS for 0, 5, 15, and 30 minutes. The red and green microcapsules were incubated together at different ratio of 1:1 (**B**), 1:5 (**C**) and 1:10 (**D**). The red and green microcapsules alone and the control crosslinked microcapsules were also run on flow cytometry for background signal (**A**). Total beads per sample were 3 x 10^5; n=3.

but to make sure that there are enough red microcapsules present during the experiment for the green microcapsules to bind, I decided to do all the further experiments at a ratio of 1:5, which also showed high double-positive populations.

5.6.1.4 Biophysical proof-of-principle studies with controls

My next aim was to investigate specific interactions between the red and green microcapsules to get a high signal and a low background (non-specific interactions). For the experiment, red microcapsules were functionalized with mouse monoclonal W6/32 and incubated with green microcapsules that were functionalized with rabbit anti-mouse (specific interaction) or with pig anti-rabbit (non-specific interaction) antibodies. The red W6/32 microcapsules were also incubated with green crosslinked, surface-activated, or protein A microcapsules as control samples. The red and green microcapsules were mixed at a ratio of 1:5 with a total of 3×10^5 microcapsules per reaction in 1 mL of PBS. All samples were read in flow cytometry for red (AF-647) and green (Atto-488) fluorescence (**Figure 5.7**). A two- to threefold increase was observed in the specific interaction of the microcapsules over the non-specific interactions. To see whether increasing the total number of microcapsules per reaction had any effect on the outcome, I increased the total number of microcapsules per reaction to 5×10^5 (an increase of 2×10^5 microcapsules per reaction). As seen in the result (**Figure 5.8**), there was an two-to threefold increase in the positive signal when W6/32-functionalized microcapsules were incubated with rabbit anti-mouse, but it also lead to an increase in the non-specific interactions as seen with other green microcapsules. So it was concluded that for all future reactions concerning the proximity studies of red and green microcapsules, a total number of 3×10^5 microcapsules would be used per reaction with a ratio of 1:5.

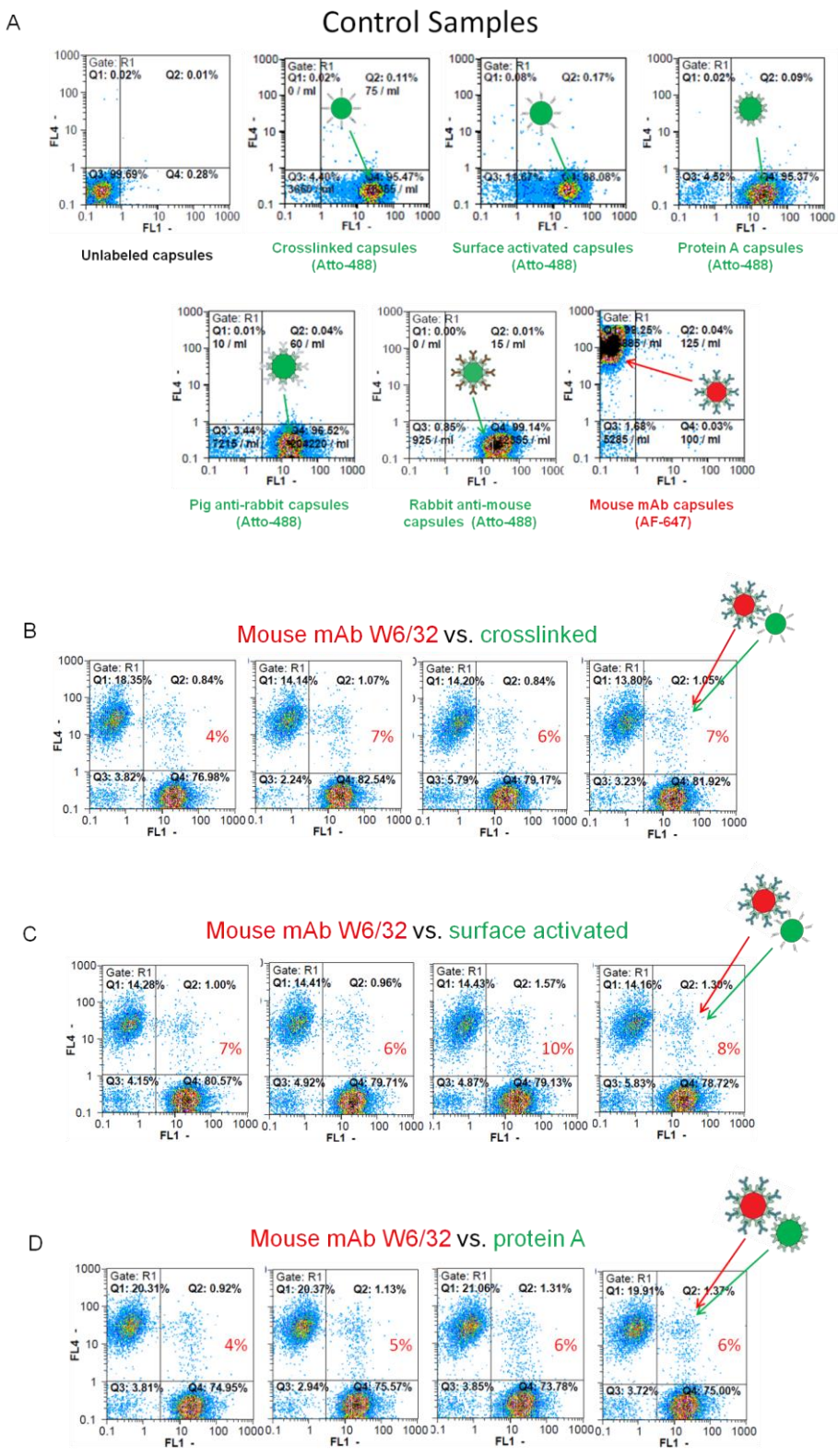

*Figure continued to page 89

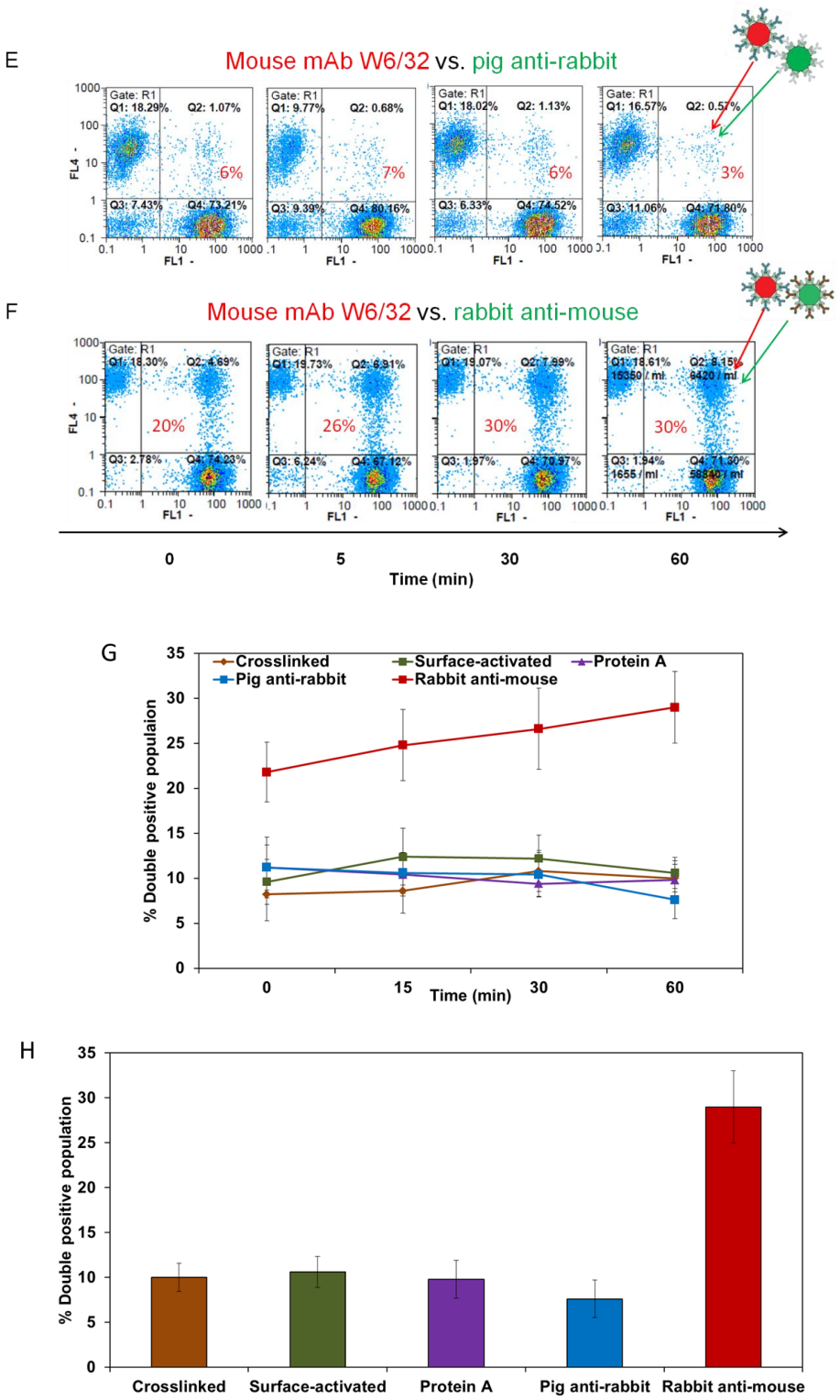

Figure 5.7: Biophysical proof of principle studies with controls and 3 x 10^5 samples per reaction. Red microcapsules (filled with AF-647) surface-functionalized with mouse monoclonal W6/32 were incubated together in a 1:5 ratio with green microcapsules (filled with Atto-488), which are either cross-linked (**B**), surface-functionalized (**C**), protein A-coated (**D**), pig anti-rabbit (**E**) or rabbit anti-mouse (**F**) in 1 mL PBS for 0, 15, 30, and 60 minutes. The red and green microcapsules alone and the control crosslinked microcapsules were also run on flow cytometry for background signal (**A**). Summarized data of five different experiments with time on x axis and percentage of double positive population of red and green microcapsules on the y axis (**G**) and bar diagram showing the double positive population at 60 minutes on y axis and different sample type on x axis (**H**). Total beads per sample was 3 x 10^5; (n=5).

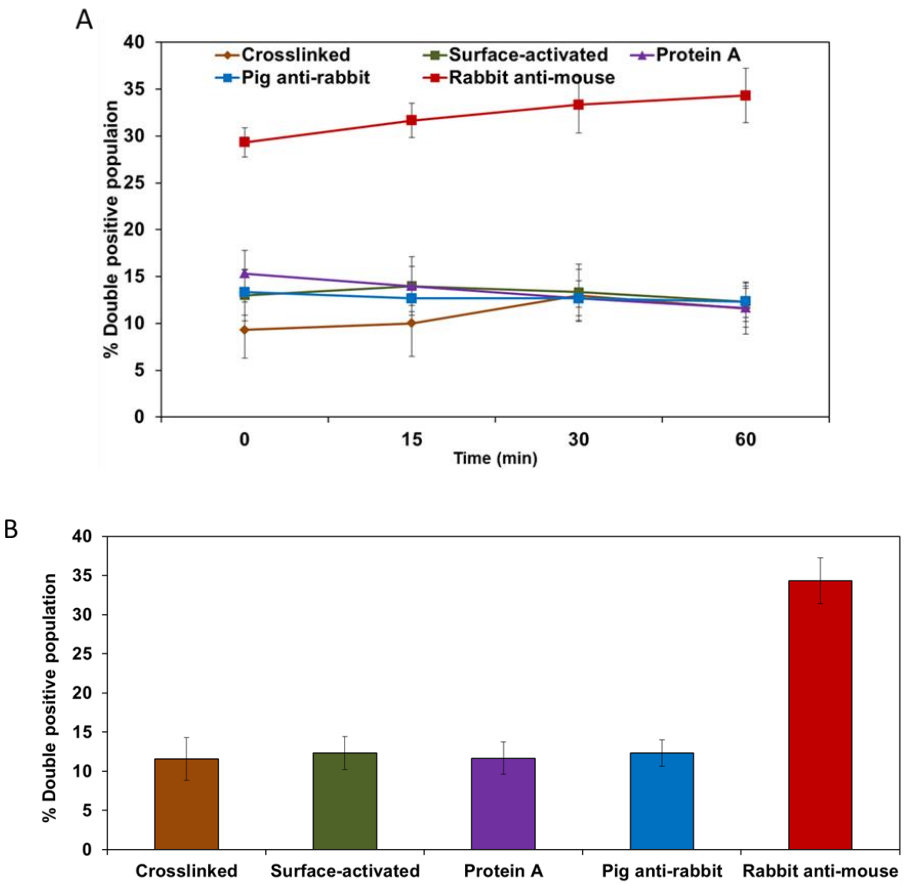

Figure 5.8: Biophysical proof of principle studies with controls and 5 x 10^5 samples per reaction. Line diagram (A) and bar diagram (B) summarizing the interaction of the red (AF-647) microcapsules surface-functionalized with W6/32 and green (Atto-488) microcapsules surface-functionalized with rabbit anti-mouse (specific interaction) or pig anti-rabbit, protein A, surface activated and crosslinked (non-specific interactions). Total beads per sample was 5 x 10^5 in 1:5 ratio; (n=3). For raw data refer **Figure 5.31** of appendix.

5.6.1.5 Assay optimization

5.6.1.5.1 Microcapsule ratio and amounts

For the induced proximity between two or more microcapsules with different detector molecules, the concentration of microcapsules needed for specific interaction was optimized. A larger number of microcapsules in the assay lead to a stronger signal, but also, a significant increase in the background signal was observed.

5.6.1.5.1.1 Varying ratio of red and green microcapsules

As a first step, to determine the optimal concentration of microcapsules for the reaction to obtain a high specific signal and a low background, different ratios of red and green

microcapsules (1:1, 1:5, 1:10, and 1:25) were tried. The red microcapsules were surface-functionalized with the mouse monoclonal W6/32 antibody, whereas the green microcapsules were surface-functionalized either with pig anti-rabbit (non-specific interaction) or with rabbit anti-mouse antibody (specific interaction). A 1.5-fold difference was observed between the specific and the background signals of the double-positive population when the samples were mixed in a 1:25 ratio with 5 x 10^5 samples. No major difference was observed in the other samples (**Figure 5.9**). Form the study, it can be concluded that changing the microcapsule ratio and amount did not help in increasing the signal to noise ratio.

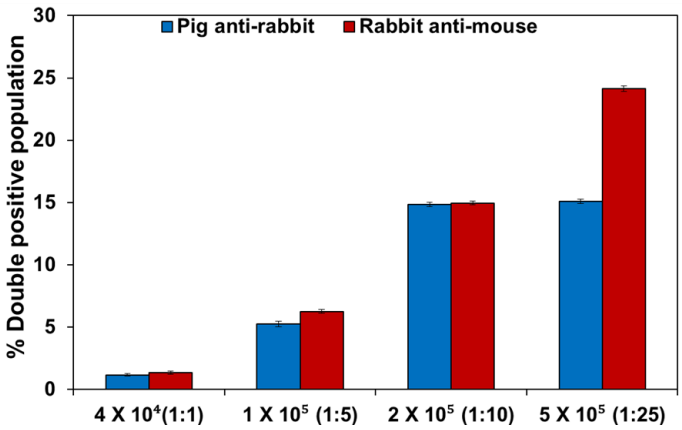

Figure 5.9: Microcapsule amount and ratio. Summarized data for red microcapsules (filled with AF-647) surface-functionalized with mouse mAb W6/32 were incubated with green microcapsules (filled with Atto-488) surface-functionalized with pig anti-rabbit (non-specific) and rabbit anti-mouse (specific) in 1 mL PBS for 60 minutes. The total number of microcapsules used in the reaction with the ratio of red and green microcapsules are on the x-axis and the percentage of double positive population on the y-axis; (n=3). For raw data refer to **Figure 5.32** of the appendix.

5.6.1.5.1.2 Ratiometric study (1:10)

In the next experiment, the ratio of the red and green microcapsules was kept constant at 1:10, but the total number of microcapsules per reaction was changed accordingly to see if there are any changes in the interaction when increasing the number of samples per reaction. As seen in the data, no significant differences were observed in the double-positive population between the non-specific and the specific interaction populations (**Figure 5.10**).

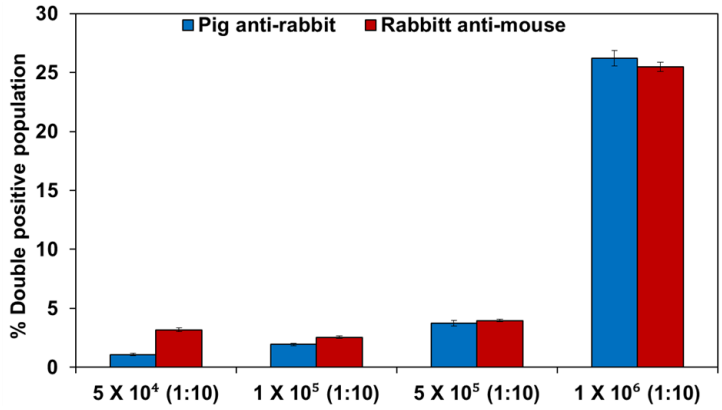

Figure 5.10: Fixed microcapsule amount in 1:10 ratio. Summarized data of W6/32 surface-functionalized microcapsules (red microcapsules filled with AF-647) interaction with rabbit anti-mouse and pig anti-rabbit surface-functionalized microcapsules (green microcapsules with Atto-488) with total number of events per sample along with the ratio on the x axis and percentage double positive population at 60 minutes on the y axis. The samples were incubated together in 1 mL PBS for 60 minutes in 1:10 ratio; (n=2). For raw data refer **Figure 5.33** of appendix.

5.6.1.5.1.3 Ratiometric study (1:25)

In a different approach, I took a constant ratio (1:25) of red and green microcapsules but changed the total number of microcapsules per reaction accordingly. Even changing different ratios and/or total number of events did not increase the specific signal of the proximity interaction, and a high background signal (non-specific interaction) was observed (**Figure 5.11**).

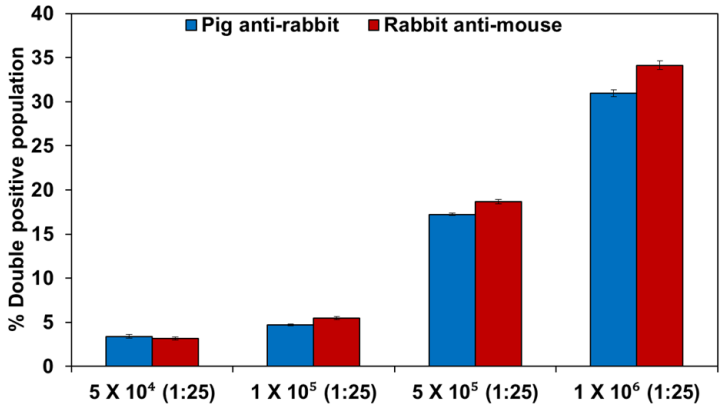

Figure 5.11: Fixed microcapsule amount in 1:25 ratio. Summarized data for red microcapsules (filled with AF-647) surface-functionalized with mouse mAb W6/32 were incubated with green microcapsules (filled with Atto-488) surface-functionalized with pig anti-rabbit (non-specific) and rabbit anti-mouse (specific) in 1 mL PBS for 60 minutes. The total number of microcapsules used in the reaction with the ratio of 1:25 are on the x axis and the percentage of double positive population at 60 minutes on the y axis; (n=2). For raw data refer **Figure 5.34** of appendix.

From the above data (**Figure 5.10**, **Figure 5.11**), it can be concluded that a ratio of 1:10 or 1:25 does not give the desired signal to background ratio, and even a 1:5 ratio with 1 x 10^5 samples (**Figure 5.9**) did not allow me to distinguish significantly between the specific (mAb W6/32 vs rabbit anti-mouse) and the non-specific (mAb W6/32 vs pig anti-rabbit) interactions. So, it can be confirmed that a ratio of 1:5 with 3 x 10^5 samples gives the best signal to background ratio of two-to threefold (**Figure 5.7**).

5.6.1.5.1.4 Varying the reaction volume

To study whether the volume of the medium in which the incubation of the red and green microcapsules is carried out has an effect on the outcome of the assay, I varied the reaction volume between 0.5 mL, 1.0 mL, and 2.0 mL. The reactions were kept shaking with the exception of one 1 mL sample that was kept rotating during the reaction incubation. The study was carried out with all controls by incubating the red microcapsules surface-functionalized with mouse monoclonal W6/32 either with green crosslinked, surface-activated, protein A, pig anti-rabbit (non-specific interactions) or with rabbit anti-mouse (specific interaction). It can be observed that the smaller the reaction volume, the higher the percentage of the double-positive population observed in both the specific and the non-specific interaction. However, a two- to threefold increase in the specific signal can be seen when the mouse monoclonal W6/32 microcapsules were incubated with the rabbit anti-mouse microcapsules as compared to the other controls, be it in 0.5 ml, 1 mL, or 2 mL reaction volume. Moreover, a slight increase in the specific signal can also be seen when the samples were left rotating during the incubation. In summary, it can be concluded that 1 mL reaction volume either with rotating or shaking seemed to the best option for obtaining a specific signal with a low background (**Figure 5.12**).

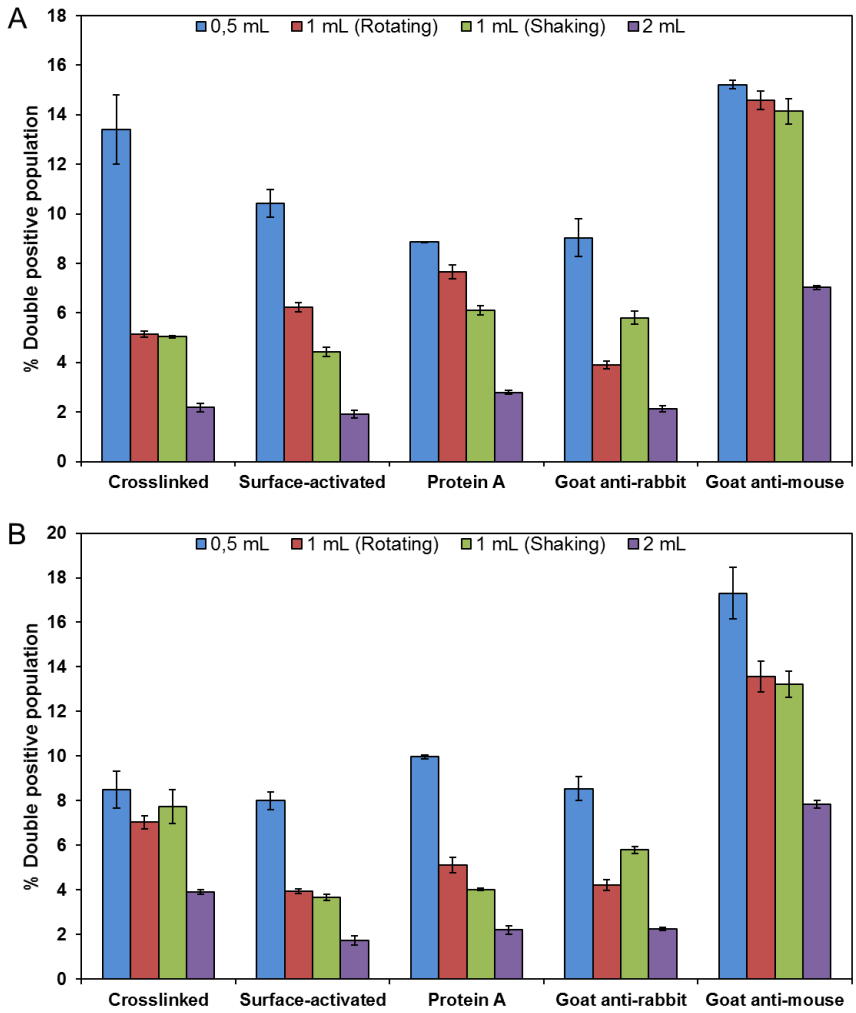

Figure 5.12: Reaction volume. Red microcapsules (filled with AF-647) and surface-functionalized with mouse mAb W6/32 were incubated with green microcapsules (filled with Atto-488) surface-functionalized with rabbit anti-mouse (specific) and pig anti-rabbit, protein A, surface-activated and crosslinked (non-specific) for their interactions in 0.5, 1 and 2 mL (shaking) and 1 mL (rotating) PBS for 0 minute (A) and 60 minutes (B) in 1:5 ratio. The results obtained were plotted for bar-diagram with the sample types on the x axis and percentage of double positive population on the y axis. Total samples per reaction was 3 x 10^5; (n=2). For raw data refer **Figure 5.35** of appendix.

5.6.1.5.2 Speed Test

For the standardization of the assay and to check if the speed at which the flow cytometry reads the microcapsules will have any effect on the readout of the proximity studies of the microcapsules, I varied the acquisition speed of the flow cytometry (viz. 0.1, 0.2, 0.5, 1, 2, 5, 10, and 15 µL/second). The experiment was carried out with red microcapsules that were surface-functionalized with mouse mAb W6/32 and green microcapsules surface-functionalized either with pig anti-rabbit (non-specific interaction) and rabbit anti-mouse (specific interaction). Increased acquisition speed led to an increase in the specific interaction

between the microcapsules, but at higher speeds, higher non-specific interaction was also observed, increasing the background signal. This might be due to the fact that by increasing the speed of acquisition, the flow channel is widened in order to acquire more samples, which ultimately also leads to various and many non-specific acquisitions being read-out in the flow cytometer. Examining carefully the experimental data, we concluded that an acquisition speed of 5 µL/second was suitable for the optimal signal to noise ratio (**Figure 5.13**).

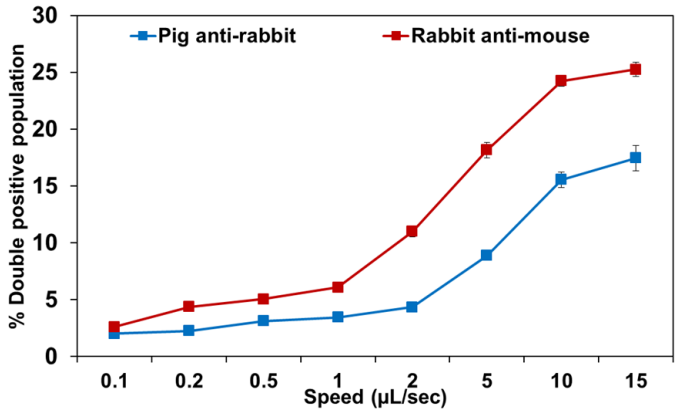

Figure 5.13: Speed test. Red microcapsules (filled with AF-647) and surface-functionalized with mouse mAb W6/32 were incubated with green microcapsules (filled with Atto-488) surface-functionalized with rabbit anti-mouse (specific) and pig anti-rabbit (non-specific) in 1 mL PBS (1:5 ratio) for 60 minutes and their affinity to interact with each other was checked via flow cytometry. The samples measured with flow cytometry with different speeds of acquisition ranging from 0.1 µL to 15 µL per second. The data obtained are plotted as a line diagram with the speed of acquisition on the x axis and the percentage double positive population on the y axis. Total samples per reaction was 3 x 10^5;(n=2). For raw data refer **Figure 5.36** of appendix.

5.6.1.5.3 PEGylation studies

The major problem of our measurement principle was high non-specific interaction, and so, to minimize the background signal, I tried to block any non-specific binding sites on the microcapsules with polyethylene glycol (PEG) after crosslinking. At the same time, the idea was to attach antibodies on the carboxyl surface of the microcapsules; keeping in mind that blocking the microcapsules with PEG might hinder the binding of the antibodies, I used NH_2-PEG-COOH which has dual functionality, blocking as well as having carboxyl groups at their ends, onto which antibodies can be crosslinked. Two different PEGs with molecular weights of 3.5 and 20 KDa were used in comparison. The PEGylated microcapsules were used at a ratio of 1:5 with a total of 3 x 10^5 beads per sample with incubation time of 0 and 60 minutes. As seen in the figure, a one- to twofold increase was observed in the signal to noise ratio (**Figure 5.14**), compared to non-PEGylated microcapsules.

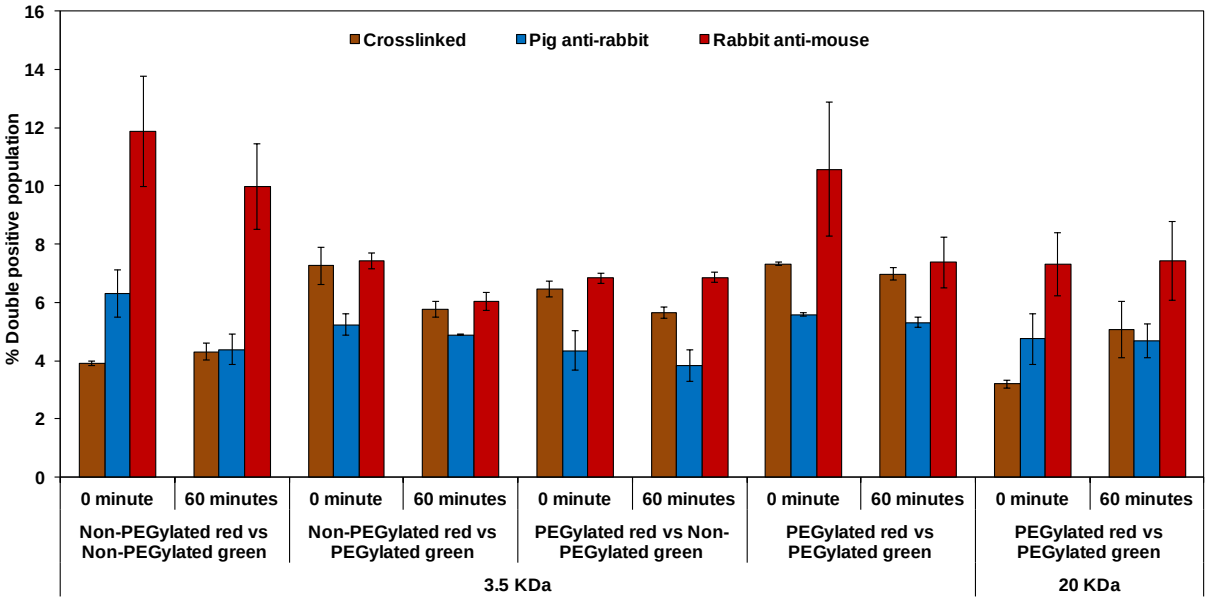

Figure 5.14: PEGylation studies. Red microcapsules (filled with AF-647) surface-functionalized with mouse mAb W6/32 were incubated with green microcapsules (filled with Atto-488) surface-functionalized with rabbit anti-mouse (specific interaction) and pig anti-rabbit or crosslinked alone (non-specific interactions) in 1 mL PBS either for 0 minute or 60 minutes. The microcapsules were either PEGylated (3.5 KDa and 20 KDa) or non-PEGylated and were looked for specific and non-specific interactions by measuring them in flow cytometry. The data were plotted for the level of interaction with different sample type on the x axis and percentage double positive population on the y axis. Total samples per reaction was 3 x 10^5; (n=2). For raw data refer **Figure 5.37** of appendix.

5.6.1.5.4 Microcapsule sizes

The microcapsule sizes were varied for maximum effectiveness of induced proximity. Microcapsules with 6 µm and 3 µm sizes were mixed together for induced proximity as I hypothesized that the smaller microcapsules might be able to bind around the larger microcapsules. Red microcapsules of 6 µm were surface-functionalized with mouse monoclonal W6/32 (target) and incubated together with 3 µm green microcapsules surface-functionalized with rabbit anti-mouse (binder). There was no negative control in this experiment. The data show that mixing many small microcapsules and a few large microcapsules gave a high double-positive population (**Figure 5.15**). From the result, it can be seen that there was a very high binding of the red and the green microcapsules (up to 70% even at time 0 min, which is concurrent with data obtained before as the reaction happens very fast), but further studies with controls need to be performed to demonstrate specificity between the microcapsules.

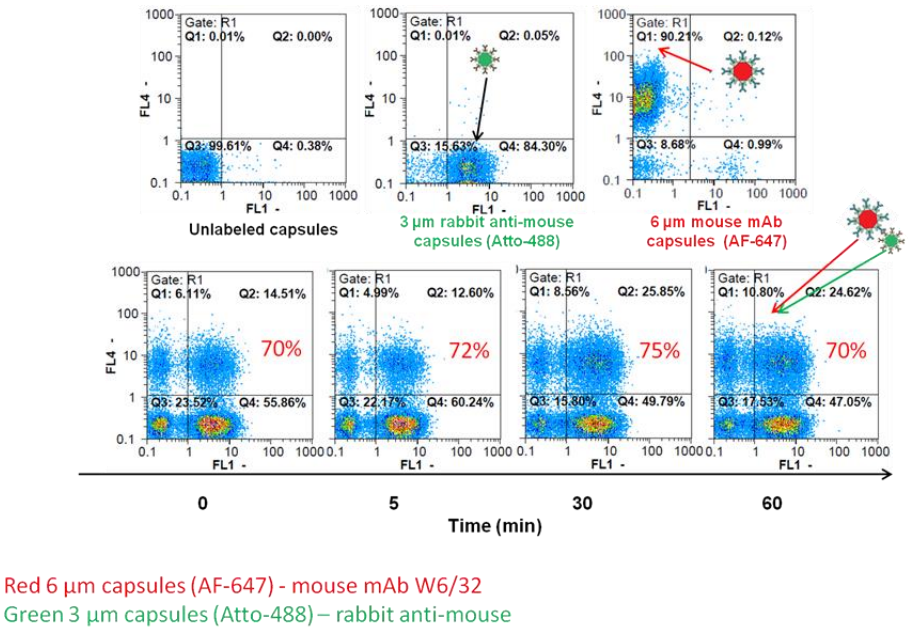

Figure 5.15: 6 µM big vs 3 µm small microcapsules. 6 µm red microcapsules (filled with AF-647) surface-functionalized with mouse monoclonal W6/32 were incubated together with 3 µm green microcapsules (filled with Atto-488) surface-functionalized with rabbit anti-mouse in 1 mL PBS for 0, 15, 30, and 60 minutes at a ratio of 1:5. Total number of beads per sample was 3 x 10^5; (n=3).

5.6.1.6 Proximity induction with analyte

To induce proximity with an analyte, which was the primary initial aim of the work, an antigen-antibody reaction was used. In such a case, one population of microcapsules with red AF-647 dye inside it, recognizing one epitope of an antigen (for example human beta-2 microglobulin,

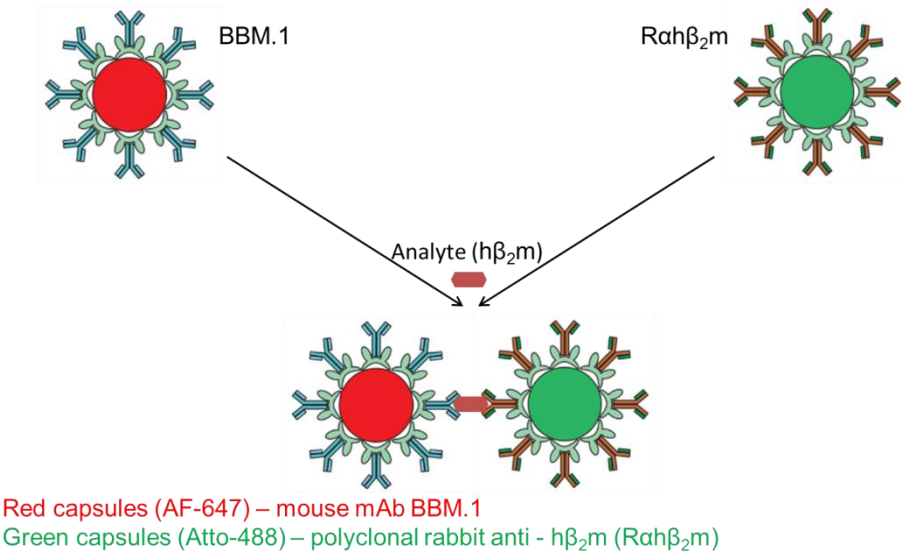

Figure 5.16: Analyte-induced proximity (antibody-based). Schematic representation of analyte-induced proximity between two microcapsules. Two sets of microcapsules with protein A on their surface mediated by EDC/sulfo-NHS chemistry was modified with two different antibodies recognizing two different epitopes of the same antigen. When the antigen was added, both antibodies recognized their respective epitopes of the antigen, which led to analyte-induced proximity between the microcapsules. This generates a signal that was detected.

hβ_2m), and the other microcapsule population with Atto-488 dye inside it, recognizing another epitope of the same antigen, were used for analyte-induced proximity (**Figure 5.16**).

As a step forward, I tried to induce proximity between two or more microcapsules in the presence of analyte. For the experiment, hβ_2m was chosen as an analyte, since it provides binding sites for two different antibodies. The red microcapsules were surface-functionalized with the mouse mAb BBM.1, which recognizes a single epitope on hβ_2m, and the green microcapsules were surface-functionalized with the polyclonal rabbit anti-hβ_2m serum, which presumably is able to detect a number of epitopes on hβ_2m. The BBM.1-modified microcapsules were first incubated with hβ_2m to allow BBM.1 to bind to the analyte at its specific site, then the microcapsules were washed, and then they were incubated with the green microcapsules such that the polyclonal rabbit anti hβ_2m could bind to the hβ_2m, inducing proximity. The analyte was added at eight different concentrations of 1 pg to 10 µg, with a tenfold increase between samples. As a control, red and green microcapsules were incubated together in the absence of the analyte. All experiments were done in a ratio of 1:1 of red and green microcapsules with a total count of 3 x 10^5 microcapsules per sample. As seen in the result, a threefold signal increase can be seen in the presence of analyte, but no substantial increase in the signal was seen even if the analyte concentration was increased tenfold. This may be due to the saturation of all binding sites present on the surface of the microcapsule even at a very low concentration of the analyte (**Figure 5.17**). The signal-to-background ratio was suboptimal (about 3-4 fold).

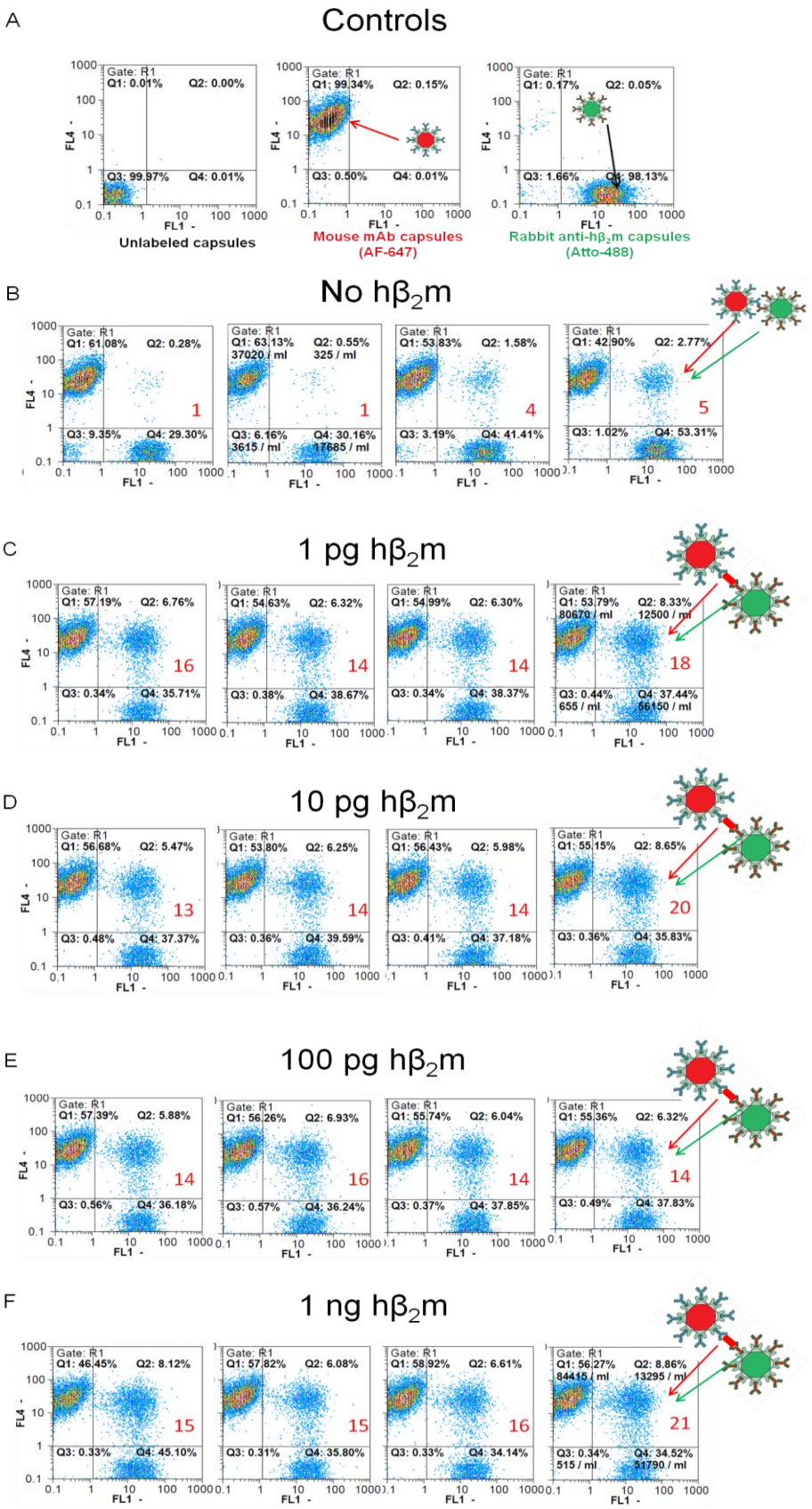

*Figure continued to page 100

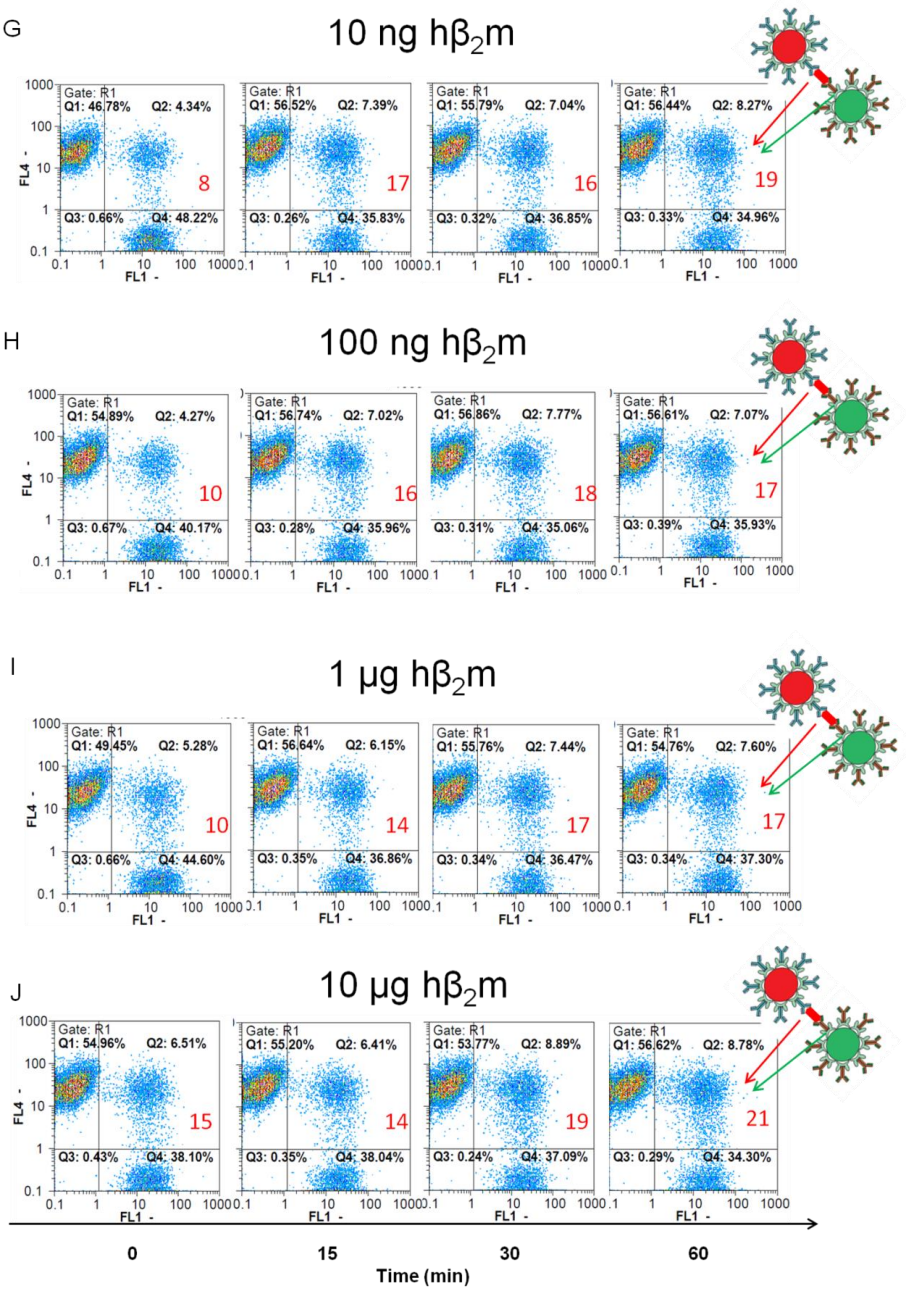

Red capsules (AF-647) - mouse mAb BBM.1
Green capsules (Atto-488) –rabbit polyclonal anti-human β_2m

*Figure continued to page 101

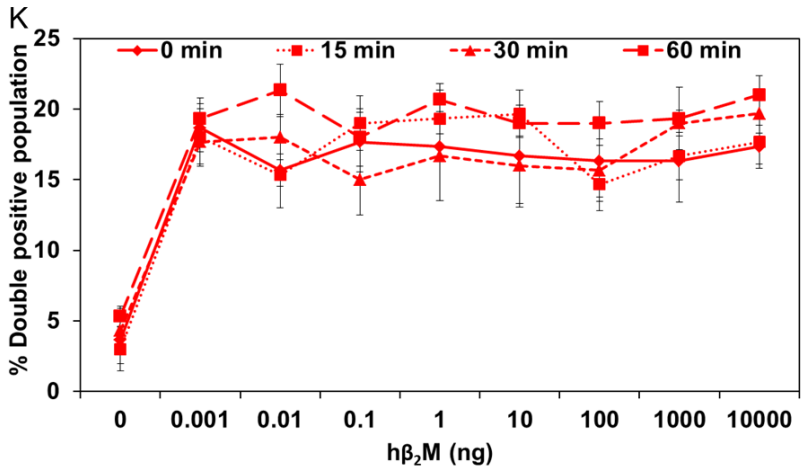

Figure 5.17: Analyte-induced proximity using hβ2m. Red microcapsules (filled with AF-647) surface-functionalized with mouse monoclonal BBM.1 were incubated together in 1:1 ratio with green microcapsules (filled with Atto-488) and surface-functionalized with polyclonal rabbit anti hβ2m either in the absence of analyte (**B**) as a control or in the presence of different amounts of analytes as indicated (**C-J**). The red and green microcapsules alone and the control crosslinked microcapsules were also run on flow cytometry for background signal (**A**). Summarized data of analyte induced proximity using hβ2m is plotted with the analyte concentration on the x axis and the percentage of double positive population on the y axis (K). Total number of beads per sample was 3 x 10^5 (n=5).

5.6.1.6.1 Standardization of analyte-induced proximity studies

To standardize the analyte-induced proximity studies using antibody, I tried varying the reaction volume in which the samples were incubated, and also incubating the samples either rotating or shaking. To study the effect of reaction volumes on the outcome of the assay, the reaction volumes were varied to 0.5 mL, 1 mL, and 2 mL. As seen in the figure below, there was a high percentage of double-positive population of red and green microcapsules at low reaction volume of 0.5 mL, but as the reaction volume increased, the samples got diluted, and the interaction between the microcapsules decreased considerably. However, a two-fold difference was observed between the interaction of the microcapsules in the presence and the absence of the analyte hβ2m (**Figure 5.18**).

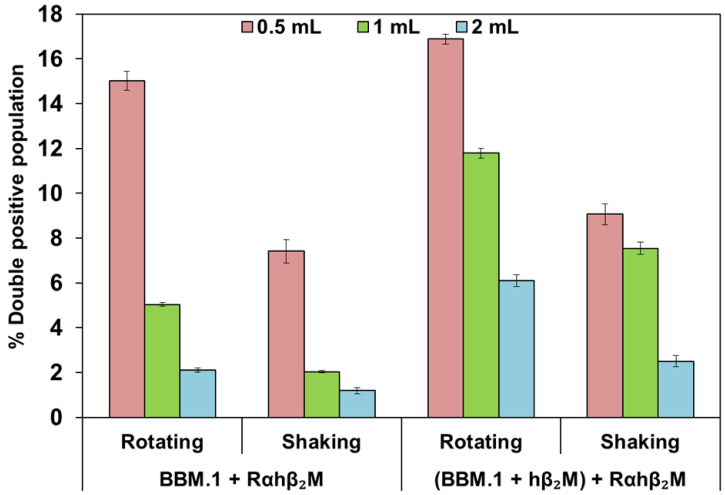

Figure 5.18: Standardization of analyte-induced proximity studies with controls. BBM.1 modified red microcapsules (filled with AF-647) were incubated together in 1:1 ratio with rabbit polyclonal anti $h\beta_2m$ green microcapsules (filled with Ato-488) for 60 minutes at room temperature, shaking at 1200 rpm either in the absence (left) or in the presence (right) of the analyte $h\beta_2m$. All the samples were incubated in 0.5 mL, 1 mL and 2 mL of PBS and measured in flow cytometry for red and green microcapsules. Total number of beads per sample was 3×10^5 (n=2). For raw data refer **Figure 5.38** of appendix.

5.6.1.6.2 Analyte-induced proximity with controls

For a proper negative control, I tried incubating both the red BBM.1 microcapsule and the green rabbit anti-$h\beta_2m$ microcapsule separately with the analyte $h\beta_2m$ before mixing them together. So, if both antibodies on the different microcapsules have already analyte bound to them, there should be no interaction between the red and green microcapsules, which should in principle serve as a negative control. There was a two-fold increase in the double-positive population of the red and green microcapsules in the presence of the analyte $h\beta_2m$ as compared to the sample without any analyte or to the negative control where the binding sites are pre-saturated with analyte. No significant difference was seen in the double-positive population whether the samples were kept shaking or rotating (**Figure 5.19**). A background signal was seen in the double-positive population which was similar to the samples without any analyte. The data suggest the surprising conclusion that after separate incubation of the microcapsules with the analyte, the surface-coupled antibodies are not saturated, and that specific proximity, though weak, is still induced. This has not been investigated further.

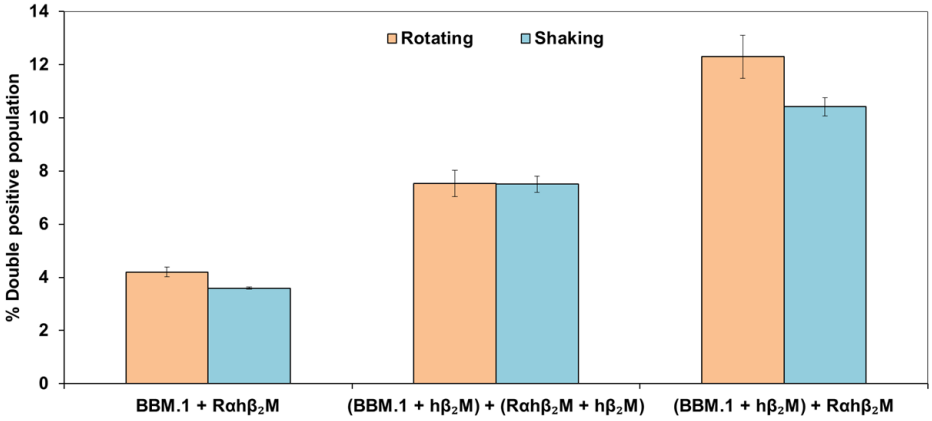

Figure 5.19: Analyte-induced proximity with controls. Summarized data of red microcapsules (filled with AF-647) and surface-functionalized with mouse mAb BBM.1 and green microcapsules (filled with Atto-488) surface-functionalized with rabbit polyclonal anti-hβ_2m incubated together either in the presence of analyte hβ_2m or in the absence of hβ_2m. As a specificity control, both the BBM.1 microcapsule and the Rαhβ_2m microcapsules were pre-incubated with hβ_2m and then incubated together. Different sample types are on the x axis and the percentage double positive population at 60 minutes of incubation are on the y axis. All the samples were incubated at a ratio of 1:1 with a total of 3 x 10^5 samples per reaction in 1 mL of PBS; (n=2). For raw data refer **Figure 5.39** of appendix.

5.6.1.6.3 Buffer and Charge Experiments

Initially, the assay was read only in PBS, but once the assay was established and optimized, the assay was also read out in distilled water, Milli-Q water, flow cytometry buffer (sheath fluid), and 10 mM phosphate buffer. Experiments in all these buffers gave similar readings, which suggests that the assay buffer had no effect on the results. In the same experiment, microcapsules of different surface charges were added to see whether charges have any role to play in bringing the microcapsules in close proximity. For the experiment, four layers of PAH (positively charged) and PSS (negatively charged) microcapsules were prepared either as $(PAH/PSS)_4$ microcapsules, with negative charges in the surface layer, or as $(PSS/PAH)_4$ microcapsules, with positive charges in the surface layer. Then, either red and green $(PAH/PSS)_4$ microcapsules or red $(PAH/PSS)_4$ and green $(PSS/PAH)_4$ microcapsules were incubated together. As seen in the result, charges play a minor role, as a 2-fold increase was observed in the double-positive population in case of oppositely charged microcapsules vs. same charge microcapsules (**Figure 5.20**). There were no major differences in the data across different buffers, and hence it was decided to use PBS for all future experiments.

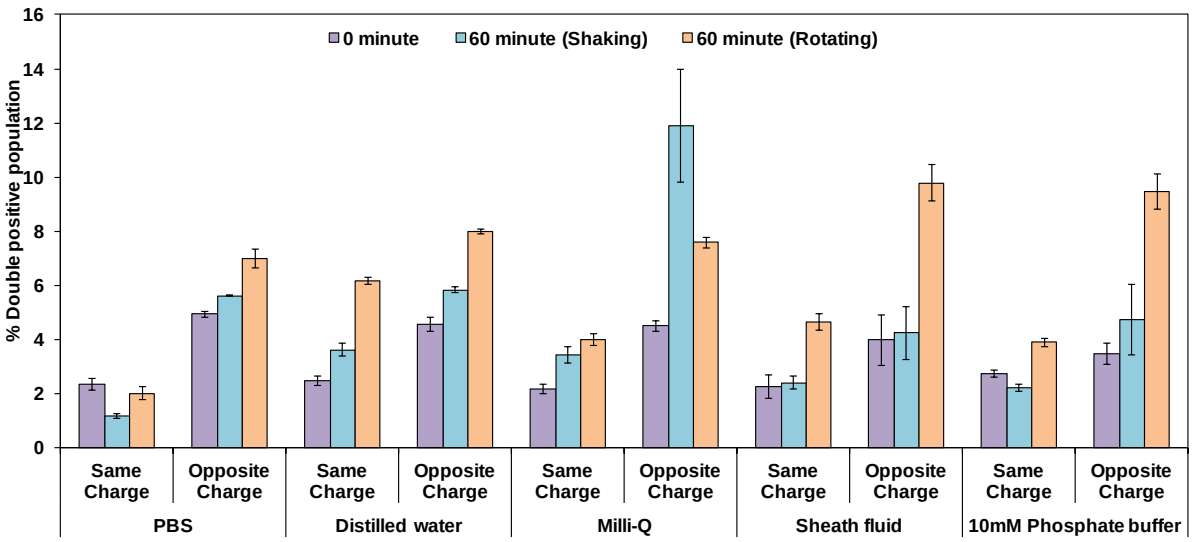

Figure 5.20: Buffer and charge experiments with controls. Positively charged red $(PAH/PSS)_4$ microcapsules (filled with AF-647) were incubated together with positively and negatively charged $(PSS/PAH)_4$ and green $(PAH/PSS)_4$ microcapsules (filled with Atto-488) in a ratio of 1:1 in 1 mL of PBS, distilled water, milli-Q, sheath fluid and 10 mM phosphate buffer for 60 minutes and then measured in flow cytometry. The results obtained are summarized in the bar diagram with the charges and buffer on the x axis and the percentage double positive population at 0 minute and 60 minutes on the y axis. Total samples per reaction mixture was 3 x 10^5; (n=2). For raw data refer **Figure 5.40** of appendix.

5.6.2 Proximity induction using oligonucleotides as detector molecules

5.6.2.1 Coating the microcapsule surface with streptavidin and oligonucleotides

In the second approach of proximity induction between microcapsules using oligonucleotides, microcapsules were surface-modified by EDC/sulfo-NHS crosslinking chemistry. The first step was to confirm that the streptavidin binds to the surface-activated microcapsules. Streptavidin coupled to FITC was used in two different conditions: first, crosslinked microcapsules were incubated with streptavidin-FITC (to check for physical adsorption as a measurement for non-specific binding): and second, crosslinked microcapsules were first surface-activated with EDC/sulfo-NHS chemistry and then incubated with streptavidin-FITC (to check for covalent immobilization as a measurement for specific binding). The samples were incubated overnight and then quantified with flow cytometry, which revealed higher efficiency of the covalent immobilization approach (**Figure 5.21B**).

The next approach was to make sure that the biotinylated oligonucleotides (**Table 5.1**) bind specifically to the streptavidin-coated microcapsules. As a control to check for non-specific biotin-independent binding, crosslinked microcapsules were incubated with biotinylated Cy5-labeled oligo1.

Abbreviation	Sequence	N_{nt}	Function
oligo1	5′-Biotin-GTAAAACGACGCCGAGT-Cy5-3′	17	Anchor + Detector
oligo2	5′-Biotin-GGGGAAGGAAAGGAAAAAGAGTAAAAGGACGCCGAGT-3′	37	Anchor
oligo3	5′-Biotin-GGGGAAGGAAAGGAAAAAGAACTCGGCGTCCTTTTAC-3′	37	Anchor
oligo4	5′-TGAGCCGCAGGAAAATGAGAAAAAGGAAAGGAAGGGG-Biotin-3′	37	Anchor
oligo5	5′-CATTTTCCTGCGGCTCAACTCGGCGTCCTTTTAC-3′	34	Analyte
oligo6	5′-GGGAAAAAGAGTAAAAGGACGCCGAGT-3′	27	Anchor
oligo7	5′-GGGAAAAAAAAAAAAAAAAAAAAAAAAAGAAGGAAAGGAAAA AGAGTAAAAGGACGCCGAGT-3′	62	Anchor
oligo8	5′-TGAGCCGCAGGAAAATGAGAAAAAGGAAAGGAAGGGG-FITC-3′	37	Detector

Table 5.1: List of oligonucleotides used in the experiment with sequences, nucleotide length (N_{nt}) and function.

Another set of microcapsules were surface-activated via EDC/sulfo-NHS chemistry, incubated with streptavidin, and then oligo1 was added (specific binding)[14]. As expected, specific binding of the oligonucleotides occurred due to the biotin-streptavidin interaction (**Figure 5.21C**).

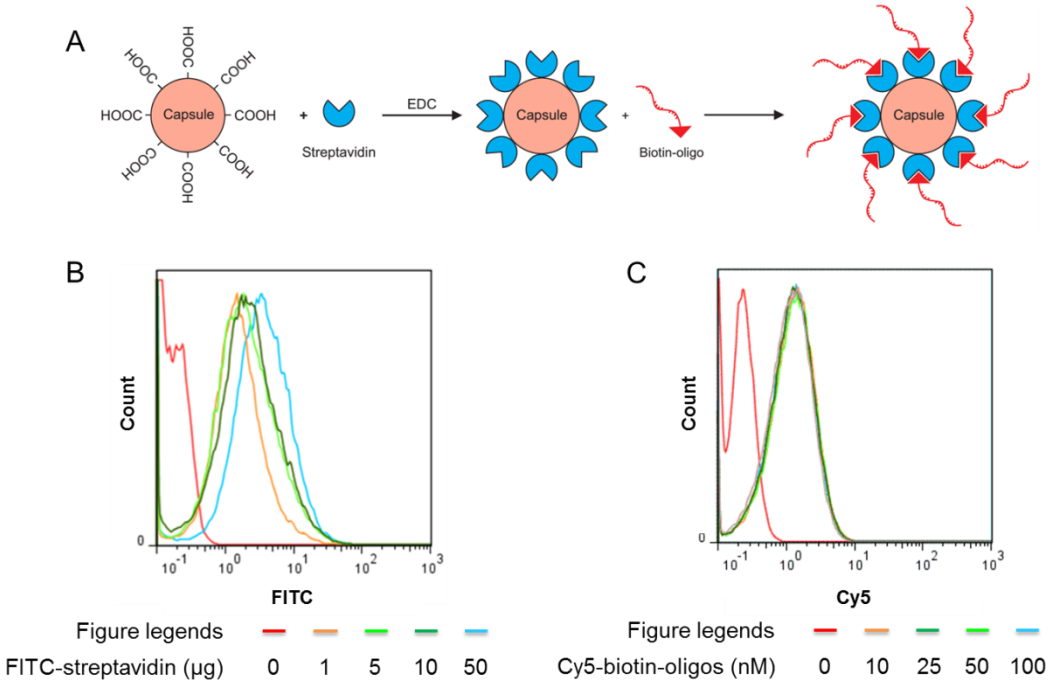

Figure 5.21: Schematic representation of attachment of biotinylated oligonucleotide on the microcapsule surface via streptavidin (**A**). Different concentrations of streptavidin-FITC (0, 1, 5, 10, and 50 µg/ml) were immobilized on the microcapsule surface by EDC/sulfo-NHS chemistry (**B**). Different concentrations of biotinylated Cy5-labeled oligo1 (0, 10, 25, 50 and 100 nM) were incubated with streptavidin-coated microcapsules (**C**). All samples were measured with flow cytometry (n=5).

[14] Streptavidin-biotin interactions are one of the strongest non-covalent biological interaction with a dissociation constant (Kd) of 4 x 10^{-14} M[35]

5.6.2.2 Proximity induction without analyte

I next used the base pairing of complementary oligonucleotides to induce proximity. To two different microcapsules containing red and green dye and coated with streptavidin, I attached different complementary biotinylated oligonucleotides. When the microcapsules were mixed together, the complementary bases will pair, bringing the microcapsules into close proximity (**Figure 5.22**).

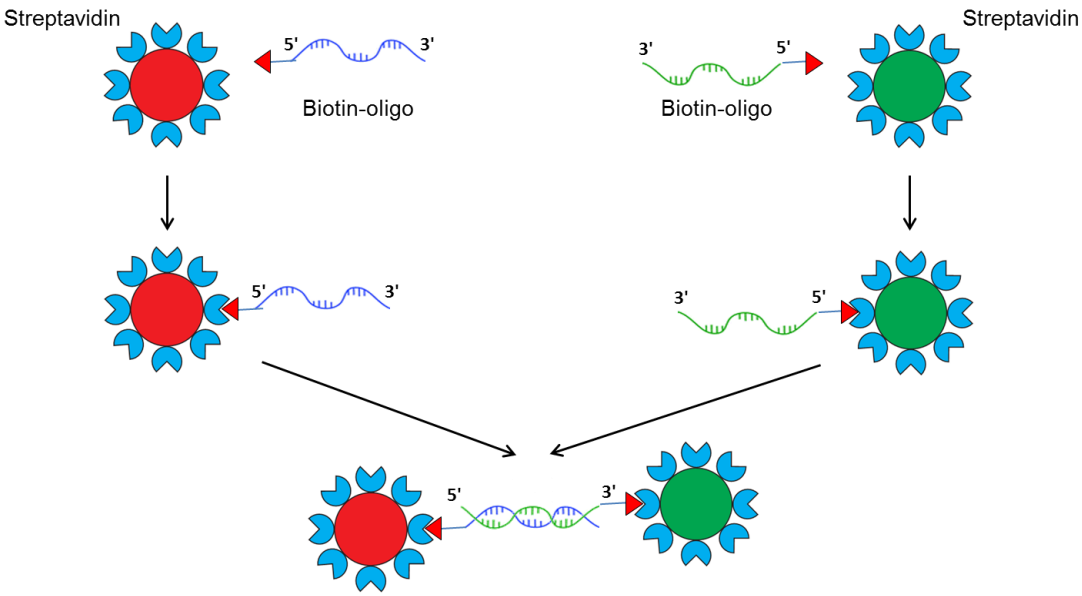

Figure 5.22: Schematic representation of the principle of oligonucleotide-based induced proximity between two microcapsules. Two sets of microcapsules coated with streptavidin on EDC/sulfo-NHS activated surface with red and green dyes inside are incubated with biotinylated complementary oligonucleotides. One oligonucleotide is added to the red microcapsules, while the complementary oligonucleotide is added to the green microcapsules. When both microcapsules are mixed together, the complementary bases pair, bringing the microcapsules into close proximity.

5.6.2.2.1 Biophysical proof of principle

The red and green microcapsules were prepared, crosslinked, and surface-activated as described before (see section **5.5**). Both types of microcapsule were incubated with streptavidin, and then the red streptavidin-coated microcapsule was incubated with oligo2, whereas the green streptavidin-coated microcapsule was incubated with oligo3. After the incubation, the microcapsules were washed three times to remove any unbound oligonucleotides, followed by the dissolution of the cores with 0.2 M EDTA, pH 7.2. Both microcapsules were then incubated together for different lengths of time, up to 120 minutes. The samples were then measured with flow cytometry and checked for proximity of the red

and green microcapsules occurring as a result of complementary base pairing of the oligonucleotides (**Figure 5.23**).

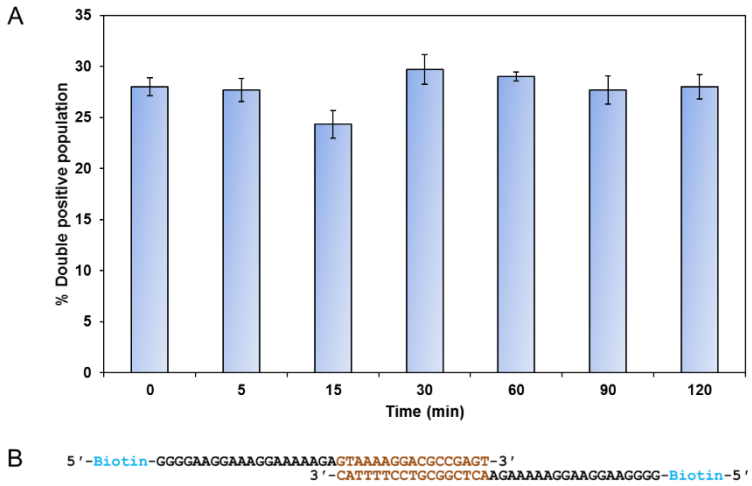

Figure 5.23: Biophysical proof of principle studies. Summarized data of 2 oligo proximity assay where red microcapsules (filled with AF-647) surface-functionalized with oligo2 are incubated together with green microcapsules (filled with Atto-488) surface-functionalized with oligo3 in 1mL PBS for the times indicated. The percentage double positive population is on the y axis (**A**). Hybridization scheme of the two oligonucleotide used in the current assay (**B**). Total counts per reaction, 3 x 10^5; n=3. Experiment performed by Ulla Schellhaas. For raw data refer **Figure 5.41** of appendix.

5.6.2.2.2 Biophysical proof of principle with controls

To check for non-specific proximity of microcapsules, red and green microcapsules were prepared as described before, as individual crosslinked, surface-activated, streptavidin bound, and oligo2 or oligo3-functionalized samples. All different combinations were mixed together and incubated for different lengths of time. As seen in **Figure 5.24**, the 1.5-2 fold increase in the signal over background that was observed was due to the complementary base pairing of the oligonucleotides bound to the red and green microcapsules. To check for the specificity, red microcapsules bound with oligo2 were pre-incubated with free oligo2 and then incubated with green microcapsules bound to oligo3.

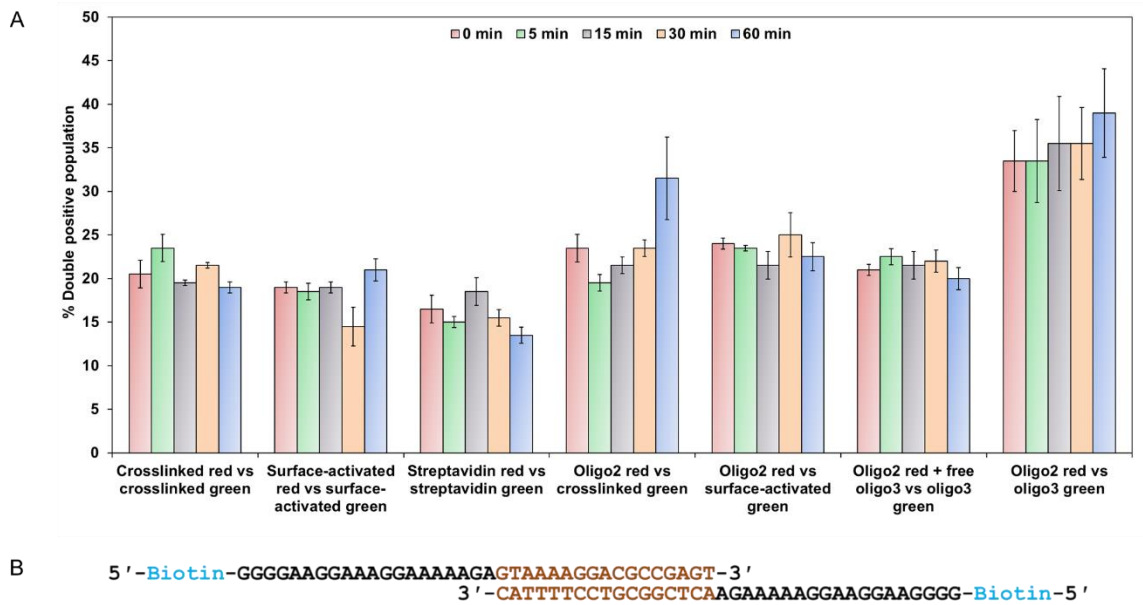

Figure 5.24: Biophysical proof of principle studies with controls. Red microcapsules (filled with AF-647) either crosslinked, surface-activated, streptavidin bound or with oligo2 and green microcapsules (filled with Atto-488) either crosslinked, surface-activated, streptavidin-bound or with oligo3 were incubated together in 1mL PBS at 1:1 ratio for the times indicated. Summarized data showing the percentage double positive population on the y axis and the different sample types incubated together is shown on the x axis (**A**). Hybridization scheme of the two oligonucleotides used in the current assay (**B**). Total counts per reaction, 3 x 10^5; n=2. Experiment performed by Ulla Schellhaas. For raw data refer **Figure 5.42** of appendix.

5.6.2.3 Assay Optimization

5.6.2.3.1 Buffers and ionic concentrations

The constituents of the assay solution, such as buffers, ions, and EDTA, usually play an important role in the outcome of an assay, and hence, an important aspect in the development of the assay was to optimize the assay solution and find which ones function best for the proximity studies of the microcapsules using oligonucleotides. As a test, different assay solutions such as potassium acetate (pH 7.5), 5 mM Mg, 0.5 M Tris phosphate (pH 7.5), 1 M Tris (pH 7.5), 0.2 M EDTA (pH 7.2), 0.5 M EDTA (pH 8.0) and Milli-Q water were tried for different lengths of time, 0, 60 and 120 minutes. This experiment was carried out to check the assay solutions' suitability and also to see if increasing the ionic concentrations helps in increasing the specific interaction between the microcapsules. As seen in Figure 5.25, no significant differences were observed between the assay solutions except for 0.5 M EDTA and Milli-Q. On carefully observing the data we found that Milli-Q gives the best signal (**Figure 5.25**) to noise ratio (**Figure 5.43 A**) and less variability between the samples (low error bars as compared to 0.5 M EDTA) and hence, all the future experiments were carried out in Milli-Q water.

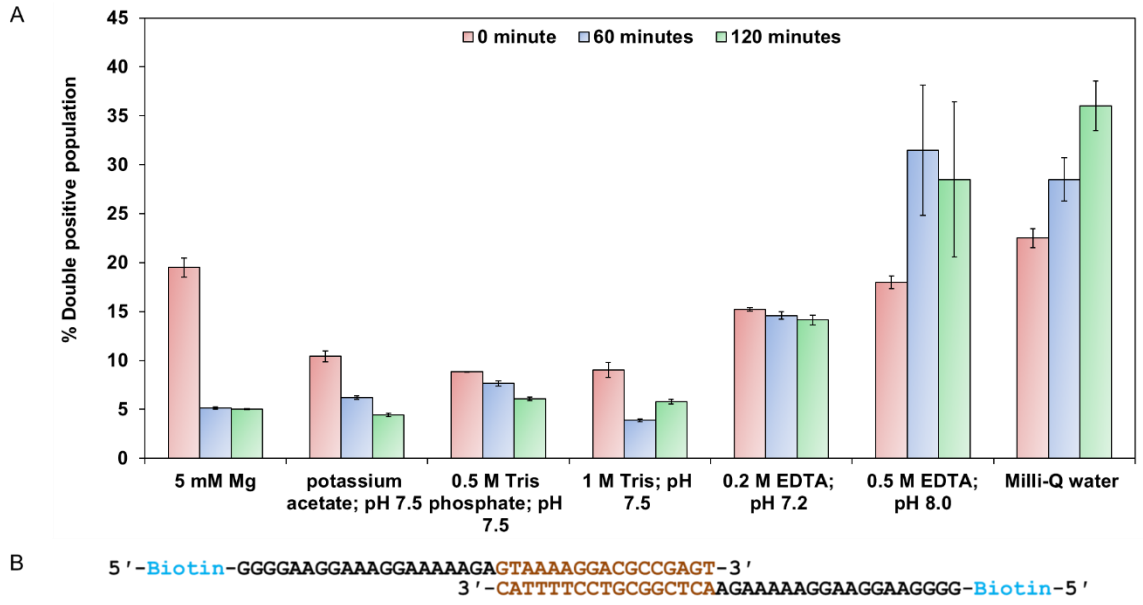

Figure 5.25: Two-dimensional plots of direct proximity in a two-bead assay using oligonucleotide-coated microcapsules to determine the ideal reaction buffer. Red microcapsules (filled with AF-647) and green microcapsules (filled with Atto-488) were either crosslinked or attached with oligo2 and oligo3 and incubated in different assay solutions with different buffering strength and ionic concentrations for different times (**A**). Hybridization scheme of the two oligonucleotides used in the current assay (**B**). Total counts per reaction, 3 x 10^5; n=2. The red and green crosslinked microcapsules incubated together for 2 hours in Milli-Q water served as a negative control and other crosslinked microcapsules were also run on flow cytometry for background signal (see **Figure 5.43A** of appendix). Experiment performed by Amanda Amoah. For raw data refer **Figure 5.43** of appendix.

5.6.2.4 Analyte induced proximity using oligonucleotides

To generate analyte-induced proximity with the help of oligonucleotides, biotinylated oligonucleotides are attached to two different streptavidin-modified microcapsule samples. These microcapsules with two different colors inside (red and green) are then brought into close proximity by the use of a third complementary oligonucleotide (the analyte), which binds to the complementary base pairs on the oligonucleotides attached to the microcapsules (**Figure 5.26**).

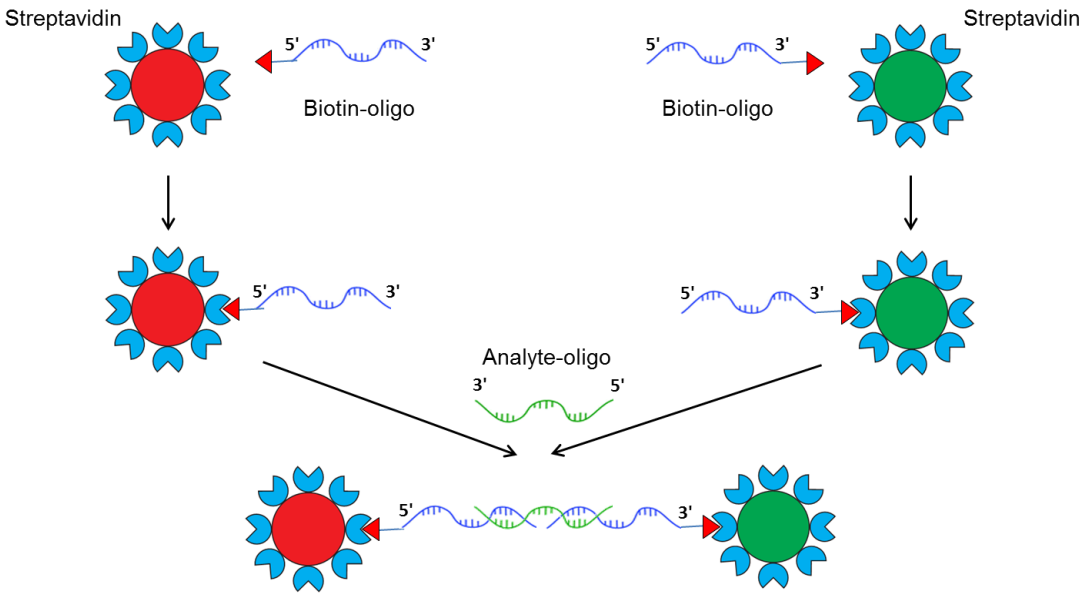

Figure 5.26: Principle of analyte-induced proximity between two microcapsules through oligonucleotides. Two sets of microcapsules with streptavidin attached on their surface by EDC/sulfo-NHS chemistry with red and green dye inside are prepared. The microcapsules are then mixed with biotinylated oligonucleotide, which binds to the surface of microcapsules because of their strong affinity towards streptavidin. To this sample, a third complementary oligonucleotide (analyte) is added, the complementary bases pair, and the microcapsules are brought into close proximity.

5.6.2.4.1 Analyte-induced proximity

Red and green microcapsules were prepared and surface-modified with streptavidin as described (see section **5.5**). Red streptavidin-coated microcapsules were further modified with biotinylated oligo2, and the green streptavidin-coated microcapsule with biotinylated oligo4. The red oligo2 microcapsules were incubated for 1 hour with the analyte oligo5[15]. Finally, both the red and the green microcapsules were incubated for core dissolution in 0.2 M EDTA, pH 7.2. The green oligo4-coated microcapsules were collected and incubated with the red oligo2-oligo5-hybridized microcapsules rotating for 0, 5, 15, 30, 60, 90 and 120 minutes, and the assay was subsequently analyzed in the flow cytometer. The red and the green microcapsules incubated together without any analyte served as control for this experiment. As seen in the result (**Figure 5.27**), no difference was observed in the presence or the absence of the analyte oligo5, which might be due to the non-specific interactions between the oligonucleotide microcapsules.

[15] The analyte oligo5 was one half the sequence complementary to oligo2 and the other half complementary to oligo4, allowing for hybridization to both microcapsule mounted oligonucleotides (oligo2 and oligo4).

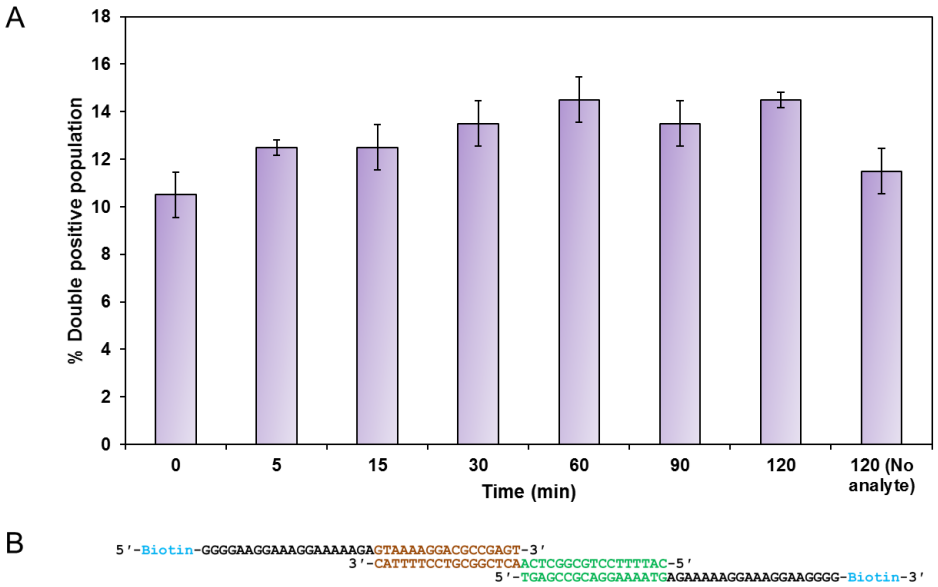

Figure 5.27: Analyte-induced proximity between two microcapsules. Summarized results of the analyte induced proximity using oligonucleotides with red and green microcapsules. The red and the green microcapsules were attached with oligo2 and oligo4 and then incubated with oligo5 (analyte) at different points of 0, 5, 15, 30, 60, 90 and 120 minutes in a ratio of 1:1. The percentage double positive population is on the y axis and the different time points of incubation on the x axis (**A**). Hybridization scheme of the three-oligonucleotide used in the current assay (**B**). Total counts per reaction, 3 x 10^5; n=2. Experiment performed by Amanda Amoah. For raw data refer **Figure 5.44** of appendix.

5.6.3 Conclusion: analyte-induced proximity with oligonucleotides

Due to high non-specific interaction among the oligonucleotide-coated microcapsules, only a very small specific signal was observed (**Figure 5.27**). This led to further optimization experiments considering the length of the anchor residues (number of base pairs) used for binding the analyte oligo and to try and reduce non-specific interactions by blocking the microcapsules with different blocking buffers which might lead to increase specificity thereby increasing the signal to noise ratio.

5.6.3.1 Blocking assay

To minimize the non-specific attachment of free oligonucleotides to crosslinked microcapsules, we tried blocking all the microcapsules prior to the incubation with oligo8-FITC. For the experiment, crosslinked microcapsules were blocked with 5% milk, 5% BSA, 1% milk, and 1% BSA for 1 hour and incubated with the detector oligo8-FITC for 30 minutes. The samples were then measured in flow cytometry to check for green fluorescence (= nonspecific binding of the detector). As seen in the data, a decrease in the FITC fluorescence of all microcapsules can

be seen that were blocked prior to use. The results of this experiment (**Figure 5.28**) confirm that blocking minimizes attachment of free oligonucleotides to microcapsule surfaces. The best blocking reagent is 1% milk.

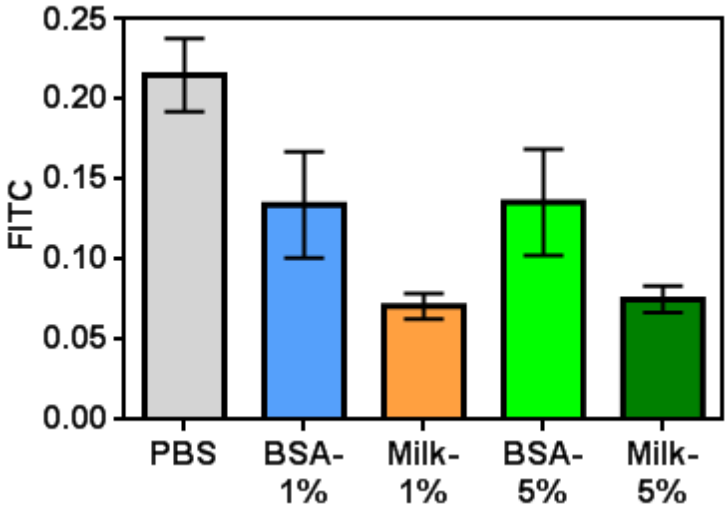

Figure 5.28: Blocking with BSA and milk minimizes non-specific attachment of oligo8-FITC to crosslinked microcapsules. Crosslinked microcapsules blocked overnight in 1% BSA, 5% BSA, 1% milk and 5% milk show a decrease in the non-specific attachment. The grey curve represents unblocked microcapsules which served as the control for the experiment. Summarized data with the mean fluorescence intensity (MFI) values obtained on the y axis and the different blocking buffers used on the x axis. The best blocking reagent was 1% milk, which resulted in a 70% decrease in non-specific attachment of oligo8-FITC (the orange bar). Total counts per reaction, 3 x 10^5; n=2. Experiment performed by Amanda Amoah.

In an another attempt to minimize the non-specific binding of oligo8-FITC to the crosslinked microcapsules, the samples were blocked with 0, 100, 500, 1000, and 1500 μg/mL of herring sperm DNA either for 1 hour, 2 hours, or overnight shaking at 1200 rpm at room temperature followed by the addition of oligo8-FITC. The samples were measured in flow cytometry after the dissolution of the cores with 0.2 M EDTA, pH 7.2. As seen in the data below (**Figure 5.29**), herring sperm DNA was able to reduce the non-specifc binding of the free oligonucleotide oligo8-FITC partially even at higher concentrations of 1500 μg/mL. Carefully looking at the data from **Figure 5.28** and **Figure 5.29** it looked like 1% milk is the best blocking agent to reduce the non-specific attachment of the oligonucleotide to the microcapsules surface. However, the blocking experiment needs to be repeated and then if the data is reproduced, can be used further for proximity experiments using oligonucleotides.

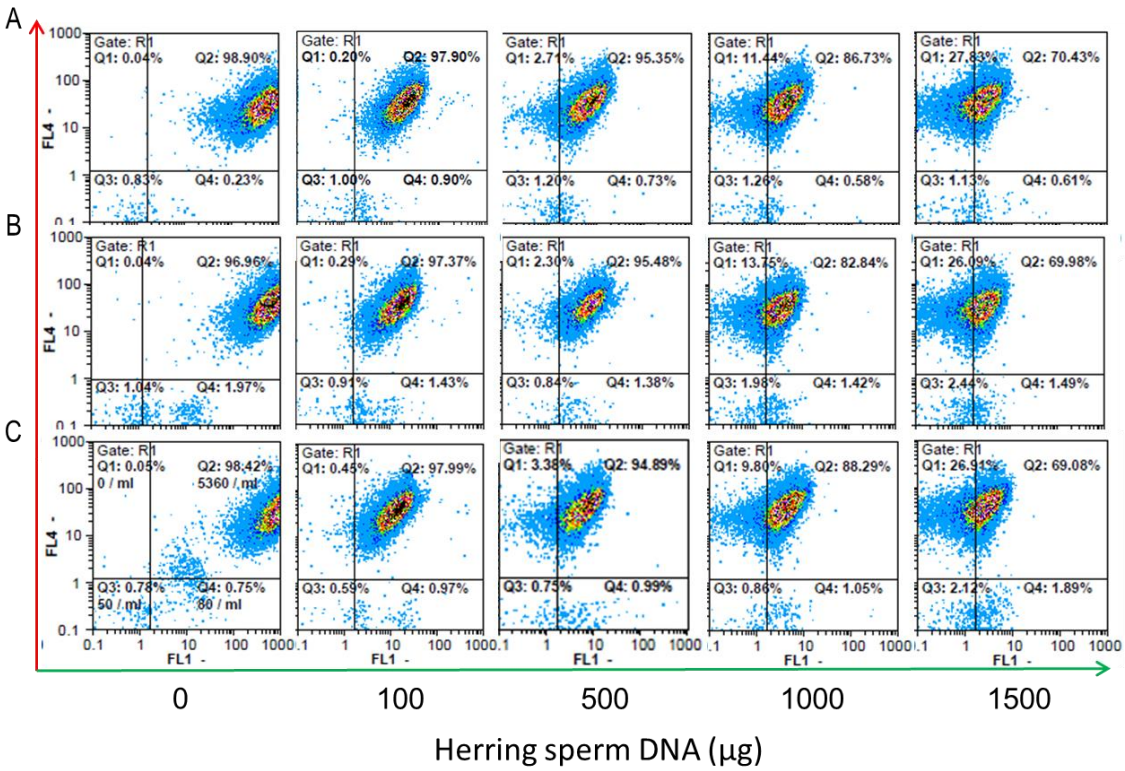

Figure 5.29: Attempts to block binding of oligo8-FITC to microcapsules by prior incubation with herring sperm DNA. The microcapsules (filled with AF-647) were blocked either for 1 hour (A), 2 hours (B) or overnight (C) with different amounts of herring sperm DNA (as shown on the x axis). Total counts per reaction, 3 x 10^5; n=2. Experiment performed by Amanda Amoah.

5.6.3.2 Investigating the binding efficiency with respect to oligonucleotide length

To find out whether the length of the anchor oligonucleotide (length of the spacer between the microcapsule and the analyte) has an effect on binding of the analyte, we tried to assess the binding efficiency of the oligo5 analyte using anchor oligonucleotides of three different lengths. This might be important as it will tell us if due to smaller anchor oligonucleotides there is a stearic hindrance (form the microcapsule surface as well as analyte oligo) in the binding of the analyte oligo.

Red microcapsules (filled with AF-647) that were surface-modified with anchor oligos of three different lengths namely oligo6 (27mer), oligo2 (37mer) and oligo7 (62mer) and blocked with 1% milk were incubated with the analyte oligo5 for 1 hour in Milli-Q water shaking at 1200 rpm at room temperature. All microcapsules were then washed three times with Milli-Q water and incubated with the detector oligo8-FITC for 30 minutes shaking at 1200 rpm at room temperature. All microcapsules were finally washed, incubated in 2 mL of 0.2 M EDTA for core dissolution, and measured in flow cytometry to check for green fluorescence. An increase in

green fluorescence was observed with the 27 and 37 nucleotide long anchor oligos (**Figure 5.30 A** and **Figure 5.30 B**) but not with the 62 nucleotide long oligo (**Figure 5.30 C**). This might be due to formation of hairpin loop structures (tertiary structure formation) of the long anchor oligonucleotides although careful consideration was given when designing the oligonucleotide sequence such that there is no tertiary structure formation. From this study, it can be concluded that length of the oligonucleotide plays a major role in the binding efficiency of the analyte and that all our anchor oligos are within the good binding efficiency length of 37 base pairs.

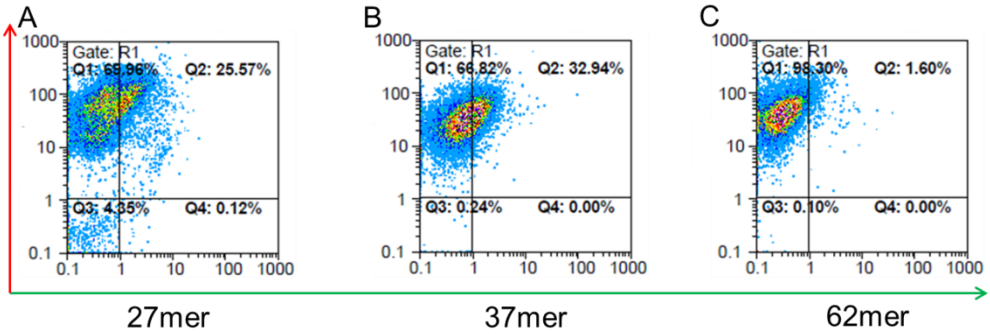

Figure 5.30: Binding of oligo5 to anchor oligos of different lengths. An increase in oligonucleotide length from 27 to 37 (**A and B**) shows a corresponding increase in the green fluorescence in the top right quadrant of the plots. Increasing the oligonucleotide length further to 62 (**C**) leads to loss of the double-positive population. Total counts per reaction, 3 x 10^5; n=2. Experiment performed by Amanda Amoah.

5.6.3.3 Future steps

In the next steps, it would be important to investigate if after blocking with 1 % milk, biotinylated oligonucleotides can still bind to the surfaces of microcapsules since milk contains biotin. By using oligo1, an estimate of the amount bound to microcapsule can be determined. It would also be interesting to see whether binding of oligo8-FITC to oligonucleotide-coated microcapsules via oligo5 can be enhanced after blocking. Blocked microcapsules have not yet been used in the two-bead proximity assay, and this might reduce the random clustering of microcapsules in the assay and increase the specificity. Trying different blocking buffers such as milk, triton, polyethylene glycol, etc. might be necessary to reduce non-specific aggregation of the microcapsules [19].

The use of blocking reagents such as milk or BSA in the actual binding reaction, for both the direct proximity and analyte induced proximity, are also yet to be tested. Following the establishment of the basic reaction conditions, the sensitivity of the assay by determining the lowest concentration of analyte required for binding should be investigated, and the ratio of analyte to binder should also be considered. Investigating the specificity of the assay in the presence of other irrelevant oligonucleotides would improve the fidelity of the assay system.

In regular systems such as in cell lysates, oligonucleotides of interest would most likely be in a mixture with others and the ability of microcapsules to detect the relevant oligonucleotide would tell about the specificity and the superiority of the assay system.

5.6.4 Proximity readout

Readout of the proximity induction and the measuring process was of utmost importance. The flow cytometer is a laser based instrument employed in cell counting, cell sorting, biomarker detection and protein engineering. It is designed to simultaneously measure multiple parameters, such as the physical and chemical characteristics of a cell, in seconds. Particles pass through a stream of fluid and are detected and displayed on a computer screen.

Flow cytometry analysis offers the advantage that the size and fluorescence intensity of a single cluster can be determined very accurately, and that the analysis of many clusters is possible. Modern flow cytometers can analyze thousands of particles per sample, separating and isolating them according to their specific properties such as color, size, granularity, etc., based on light scattering and fluorescent characteristics. The flow cytometer has become a widely-used instrument with cells and particles as it provides objective and quantitative results of fluorescent signals of interest.

5.6.5 Outlook (see also Chapter 6)

Microcapsules are a promising new platform for biomedical applications [20] because they can be filled with molecules such as peptides [21], plasmids [22], and drugs [23] once their cores have been chemically dissolved [24]. The surfaces of microcapsules can also be further modified with light emitting polymers [25], DNA [26], proteins [27], and inorganic substances [28,29] making them suitable in principle for tissue engineering [29], targeted drug delivery [30], and for use as biosensors [1,31,32].

Protein A binds to the crystallizable fragment of the antibodies [33,34]. I have shown that it is possible to attach functional protein A to the surface of $(PAH/PAA)_2$ microcapsules with EDC/sulfo-NHS chemistry. The attached protein A is functional and can bind to antibodies that can be detected with fluorescently labelled antibodies Such protein A-modified microcapsules are a powerful tool, since any IgG antibody of interest can now be added to the microcapsules and rapidly bind to the protein A in an oriented fashion. These antibodies can be used in further experiments to target microcapsules to their ligands (in the case of immobilized or surface-bound ligands) or to concentrate the ligands on the microcapsule surface.

With a view on validation, I performed a study on the non-specific background interactions between the microcapsule populations, *i.e.,* between the red microcapsules surface-functionalized with one of the detector molecule and green microcapsules either crosslinked, surface-activated with EDC/sulfo-NHS, protein A, and streptavidin or with a different non-specific detector molecules. The stability of the microcapsules in different buffers and storage conditions was also studied, and it was found that the microcapsules and the core-shelled particles were stable for a period of 3 and 6 months, respectively, when kept in PBS at 4°C without loss of activity.

5.7 References

[1] O. Kreft, A.M. Javier, G.B. Sukhorukov, W.J. Parak, Polymer microcapsules as mobile local pH-sensors, J. Mater. Chem. 17 (2007) 4471. doi:10.1039/b705419j.

[2] L.I. Kazakova, L.I. Shabarchina, S. Anastasova, A.M. Pavlov, P. Vadgama, A.G. Skirtach, G.B. Sukhorukov, Chemosensors and biosensors based on polyelectrolyte microcapsules containing fluorescent dyes and enzymes, Anal. Bioanal. Chem. 405 (2013) 1559–1568. doi:10.1007/s00216-012-6381-0.

[3] L. Kastl, D. Sasse, V. Wulf, R. Hartmann, J. Mircheski, C. Ranke, A. Martı, R. Ferna, S. Carregal-romero, Multiple Internalization Pathways of Polyelectrolyte Multilayer Capsules into Mammalian Cells, (2013) 6605–6618.

[4] L.L. Del Mercato, A.Z. Abbasi, M. Ochs, W.J. Parak, Multiplexed sensing of ions with barcoded polyelectrolyte capsules, ACS Nano. 5 (2011) 9668–9674. doi:10.1021/nn203344w.

[5] L.I. Kazakova, L.I. Shabarchina, G.B. Sukhorukov, Co-encapsulation of enzyme and sensitive dye as a tool for fabrication of microcapsule based sensor for urea measuring, Phys. Chem. Chem. Phys. 13 (2011) 11110–11117. doi:Doi 10.1039/C1cp20354a.

[6] M. McShane, D. Ritter, Microcapsules as optical biosensors, J. Mater. Chem. 20 (2010) 8189. doi:10.1039/c0jm01251c.

[7] S. Chinnayelka, M.J. McShane, Microcapsule biosensors using competitive binding resonance energy transfer assays based on apoenzymes, Anal. Chem. 77 (2005) 5501–5511. doi:10.1021/ac050755u.

[8] R. Zhang, K. Köhler, O. Kreft, A. Skirtach, H. Möhwald, G. Sukhorukov, Salt-induced fusion of microcapsules of polyelectrolytes, Soft Matter. 6 (2010) 4742. doi:10.1039/c0sm00218f.

[9] M.A. Pechenkin, H. Möhwald, D. V. Volodkin, pH- and salt-mediated response of layer-by-layer assembled PSS/PAH microcapsules: fusion and polymer exchange, Soft Matter. 8 (2012) 8659. doi:10.1039/c2sm25971k.

[10] E. Donath, G.B. Sukhorukov, F. Caruso, S. a Davis, H. Möhwald, Novel Hollow Polymer Shells by Colloid Templated Assembly of Polyelectrolytes, Angew Chem Int Ed Engl. 37 (1998) 2201–2205. doi:10.1002/(SICI)1521-3773(19980904)37:16<2201::AID-ANIE2201>3.0.CO;2-E.

[11] G.B. Sukhorukov, E. Donath, S. Davis, H. Lichtenfeld, F. Caruso, V.I. Popov, H. Möhwald, Stepwise polyelectrolyte assembly on particle surfaces: a novel approach to colloid design, Polym. Adv. Technol. 767 (1998) 759–767. doi:10.1002/(sici)1099-1581(1998100)9:10/11<759::aid-pat846>3.0.co;2-q.

[12] P. Schuetz, F. Caruso, Copper-Assisted Weak Polyelectrolyte Multilayer Formation on Microspheres and Subsequent Film Crosslinking, Adv. Funct. Mater. 13 (2003) 929–937. doi:10.1002/adfm.200304483.

[13] J.H. Dai, Z.Y. Bao, L. Sun, G.L. Baker, M.L. Bruening, Use of porous membranes modified with polyelectrolyte multilayers and brush polymers as substrates for highly sensitive protein arrays, Abstr. Pap. Am. Chem. Soc. 231 (2006) 135–140. papers2://publication/uuid/3620BB45-E331-4A6A-A23A-0573358FF2B3.

[14] C.G. dos Remedios, M. Miki, J.A. Barden, Fluorescence resonance energy transfer measurements of distances in actin and myosin. A critical evaluation, J. Muscle Res. Cell Motil. 8 (1987) 97–117. doi:10.1007/BF01753986.

[15] A.P. Le Brun, S.A. Holt, D.S.H. Shah, C.F. Majkrzak, J.H. Lakey, The structural

orientation of antibody layers bound to engineered biosensor surfaces, Biomaterials. 32 (2011) 3303–3311. doi:10.1016/j.biomaterials.2011.01.026.

[16] B. Feng, S. Huang, F. Ge, Y. Luo, D. Jia, Y. Dai, 3D antibody immobilization on a planar matrix surface, Biosens. Bioelectron. 28 (2011) 91–96. doi:10.1016/j.bios.2011.07.003.

[17] N. Tajima, M. Takai, K. Ishihara, Significance of antibody orientation unraveled: Well-oriented antibodies recorded high binding affinity, Anal. Chem. 83 (2011) 1969–1976. doi:10.1021/ac1026786.

[18] R. Danczyk, B. Krieder, A. North, T. Webster, H. HogenEsch, A. Rundell, Comparison of antibody functionality using different immobilization methods, Biotechnol. Bioeng. 84 (2003) 215–223. doi:10.1002/bit.10760.

[19] H. Hirayama, J. Tamaoka, K. Horikoshi, Improved immobilization of DNA to microwell plates for DNA-DNA hybridization, Nucleic Acids Res. 24 (1996) 4098–4099. doi:10.1093/nar/24.20.4098.

[20] M. Wilchek, E.A. Bayer, The avidin-biotin complex in bioanalytical applications, Anal. Biochem. 171 (1988) 1–32. doi:10.1016/0003-2697(88)90120-0.

[21] R. Palankar, A.G. Skirtach, O. Kreft, M. Bédard, M. Garstka, K. Gould, H. Möhwald, G.B. Sukhorukov, M. Winterhalter, S. Springer, Controlled intracellular release of peptides from microcapsules enhances antigen presentation on MHC class I molecules, Small. 5 (2009) 2168–2176. doi:10.1002/smll.200900809.

[22] J.L. Santos, A. Nouri, T. Fernandes, J. Rodrigues, H. Tomás, Gene delivery using biodegradable polyelectrolyte microcapsules prepared through the layer-by-layer technique, Biotechnol. Prog. 28 (2012) 1088–1094. doi:10.1002/btpr.1576.

[23] B.M. Wohl, J.F.J. Engbersen, Responsive layer-by-layer materials for drug delivery, J. Control. Release. 158 (2012) 2–14. doi:10.1016/j.jconrel.2011.08.035.

[24] W. Tong, C. Gao, Stable microcapsules assembled stepwise from weak polyelectrolytes followed by thermal crosslinking, Polym. Adv. Technol. 16 (2005) 827–833. doi:10.1002/pat.659.

[25] K. Ariga, Y. Lvov, T. Kunitake, Assembling alternate dye-polyion molecular films by electrostatic layer-by-layer adsorption, J. Am. Chem. Soc. 119 (1997) 2224–2231. doi:10.1021/ja963442c.

[26] K.C. Wood, J.Q. Boedicker, D.M. Lynn, P.T. Hammond, Tunable drug release from hydrolytically degradable layer-by-layer thin films, Langmuir. 21 (2005) 1603–1609. doi:10.1021/la0476480.

[27] S.Y. Wong, Q. Li, J. Veselinovic, B.S. Kim, A.M. Klibanov, P.T. Hammond, Bactericidal and virucidal ultrathin films assembled layer by layer from polycationic N-alkylated polyethylenimines and polyanions, Biomaterials. 31 (2010) 4079–4087. doi:10.1016/j.biomaterials.2010.01.119.

[28] B.S.L. Clark, E.S. Handy, M.F. Rubner, P.T. Hammond, 4-1999-Luminiscent Layer-by-layer.pdf, (1999) 1031–1035.

[29] Y. Lvov, G. Decher, G. Sukhorukov, Assembly of Thin Films by Means of Successive Deposition ofAlternate Layers of DNA and Poly(allylamine), Macromolecules. 26 (1993) 5396–5399. doi:10.1021/ma00072a016.

[30] Y. Lvov, K. Ariga, I. Ichinose, T. Kunitake, Assembly of Multicomponent Protein Films by Means of Electrostatic Layer-by-Layer Adsorption, J. Am. Chem. Soc. 117 (1995) 6117–6123. doi:10.1021/ja00127a026.

[31] S. Yabuki, Polyelectrolyte Complex Membranes for Immobilizing Biomolecules , and Their Applications to Bio-analysis, Anal. Sci. 27 (2011) 695–702. doi:10.2116/analsci.27.695.

[32] S.K. Verma, A. Amoah, U. Schellhaas, M. Winterhalter, S. Springer, T.A. Kolesnikova, ???To Catch or Not to Catch???: Microcapsule-Based Sandwich Assay for Detection of Proteins and Nucleic Acids, Adv. Funct. Mater. 26 (2016) 6015–6024. doi:10.1002/adfm.201601328.

[33] H.Y. Song, X. Zhou, J. Hobley, X. Su, Comparative study of random and oriented antibody immobilization as measured by dual polarization interferometry and surface plasmon resonance spectroscopy, Langmuir. 28 (2012) 997–1004. doi:10.1021/la202734f.

[34] A.A. Karyakin, G. V. Presnova, M.Y. Rubtsova, A.M. Egorov, Oriented immobilization of antibodies onto the gold surfaces via their native thiol groups, Anal. Chem. 72 (2000) 3805–3811. doi:10.1021/ac9907890.

[35] N.M. Green, Avidin and streptavidin, Methods Enzymol. 184 (1990) 51–67. doi:10.1016/0076-6879(90)84259-J.

5.8 Appendix

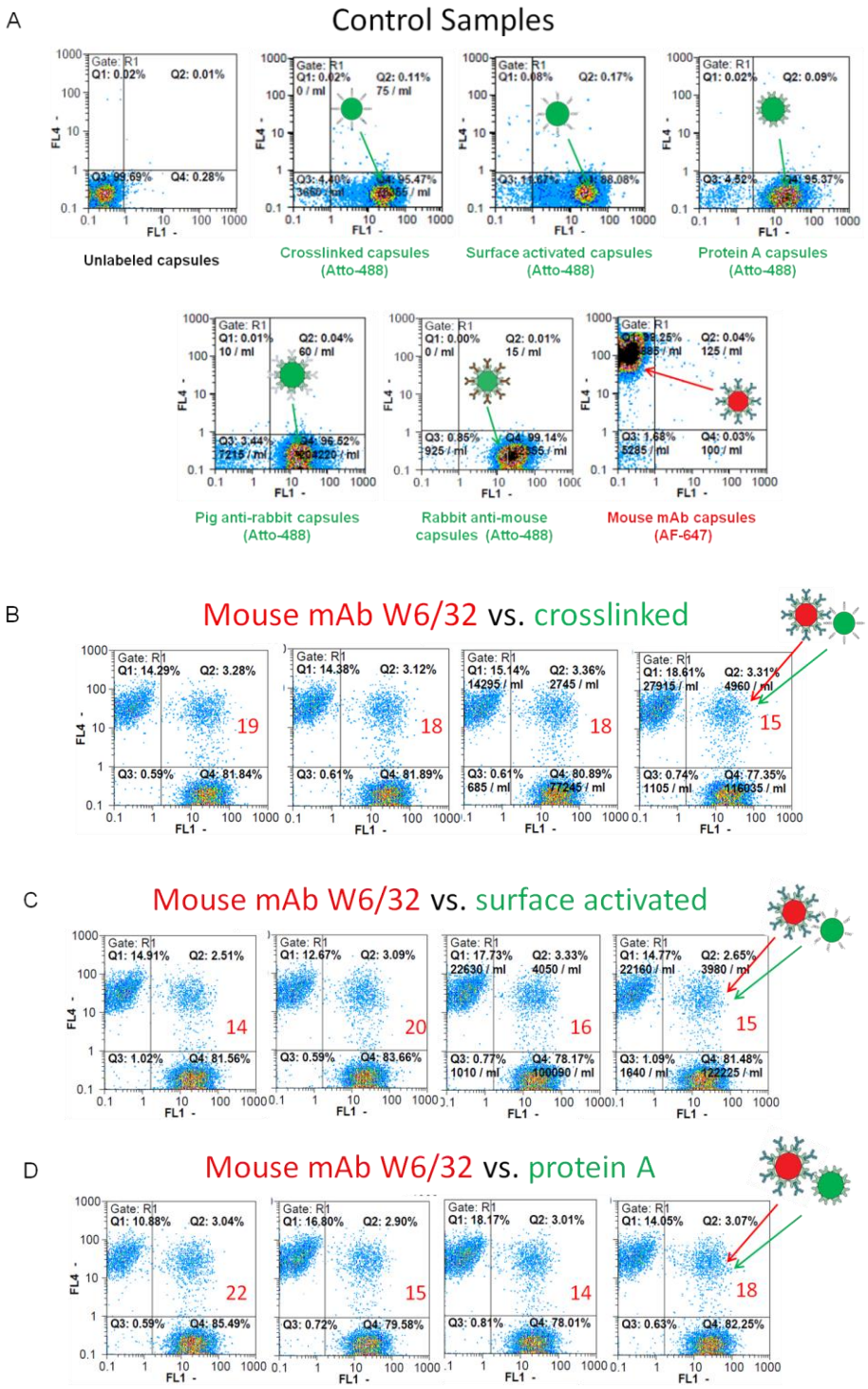

*Figure continued to page 121

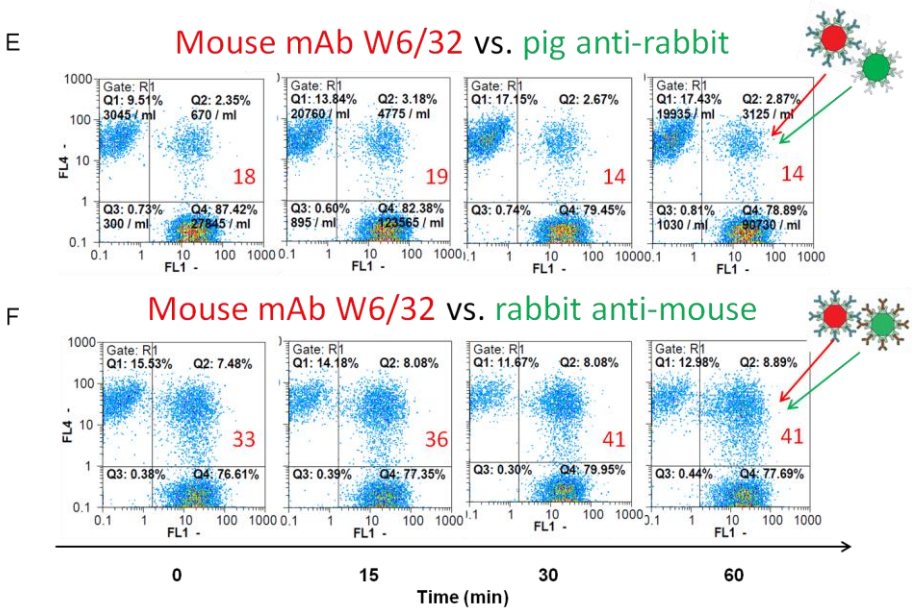

Figure 5.31: Biophysical proof of principle studies with controls and 5 x 10^5 samples per reaction. Red microcapsules (filled with AF-647) surface-functionalized with mouse monoclonal W6/32 were incubated together in a 1:5 ratio of green microcapsules (filled with Atto-488) which are either cross-linked (**B**), surface-functionalized (**C**), protein A (**D**), pig anti-rabbit (**E**) and rabbit anti-mouse (**F**) in 1 mL PBS for 0, 15, 30 and 60 minutes at a ratio of 1:5. The red and green microcapsules alone and the control crosslinked microcapsules were also run on flow cytometry for the background signal (**A**). Total beads per sample was 5 x 10^5; (n=3).

A

Control Samples

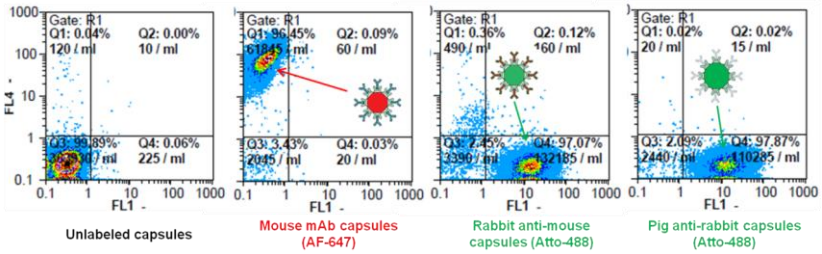

B

4 X 10^4 capsules in 1:1 ratio of mouse mAb W6/32 vs

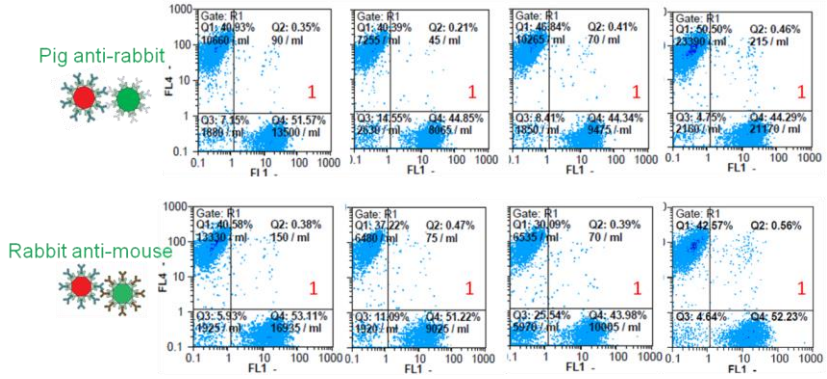

C

1 x 10^5 capsules in 1:5 ratio of mouse mAb W6/32 vs

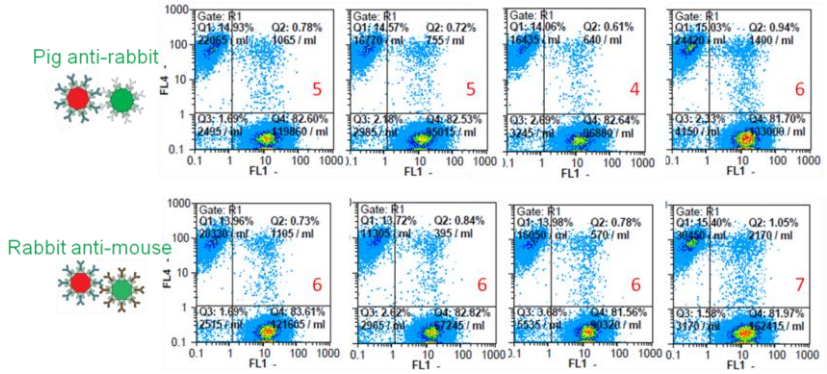

D

2 X 10^5 capsules in 1:10 ratio of mouse mAb W6/32 vs

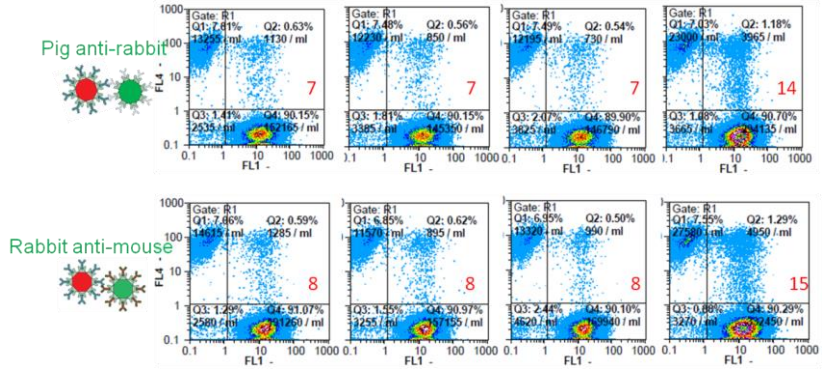

*Figure continued to page 123

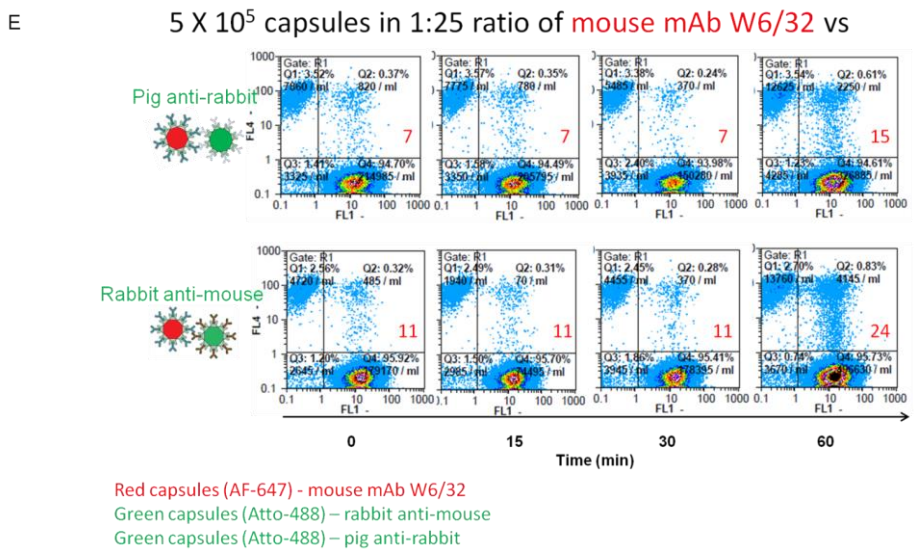

Figure 5.32: Microcapsule amount and ratio. Red microcapsules (filled with AF-647) surface-functionalized with mouse monoclonal W6/32 are incubated with green microcapsules (filled with Atto-488) surface-functionalized with pig anti-rabbit (non-specific) and rabbit anti-mouse (specific) in 1 mL PBS for 0, 15, 30, and 60 minutes. The red and green microcapsules were incubated together at ratios of 1:1 (**B**), 1:5 (**C**), 1:10 (**D**), and 1:25 (**E**). The red and green microcapsules alone and the crosslinked control microcapsules were also run on flow cytometry for background signal (**A**); (n=3).

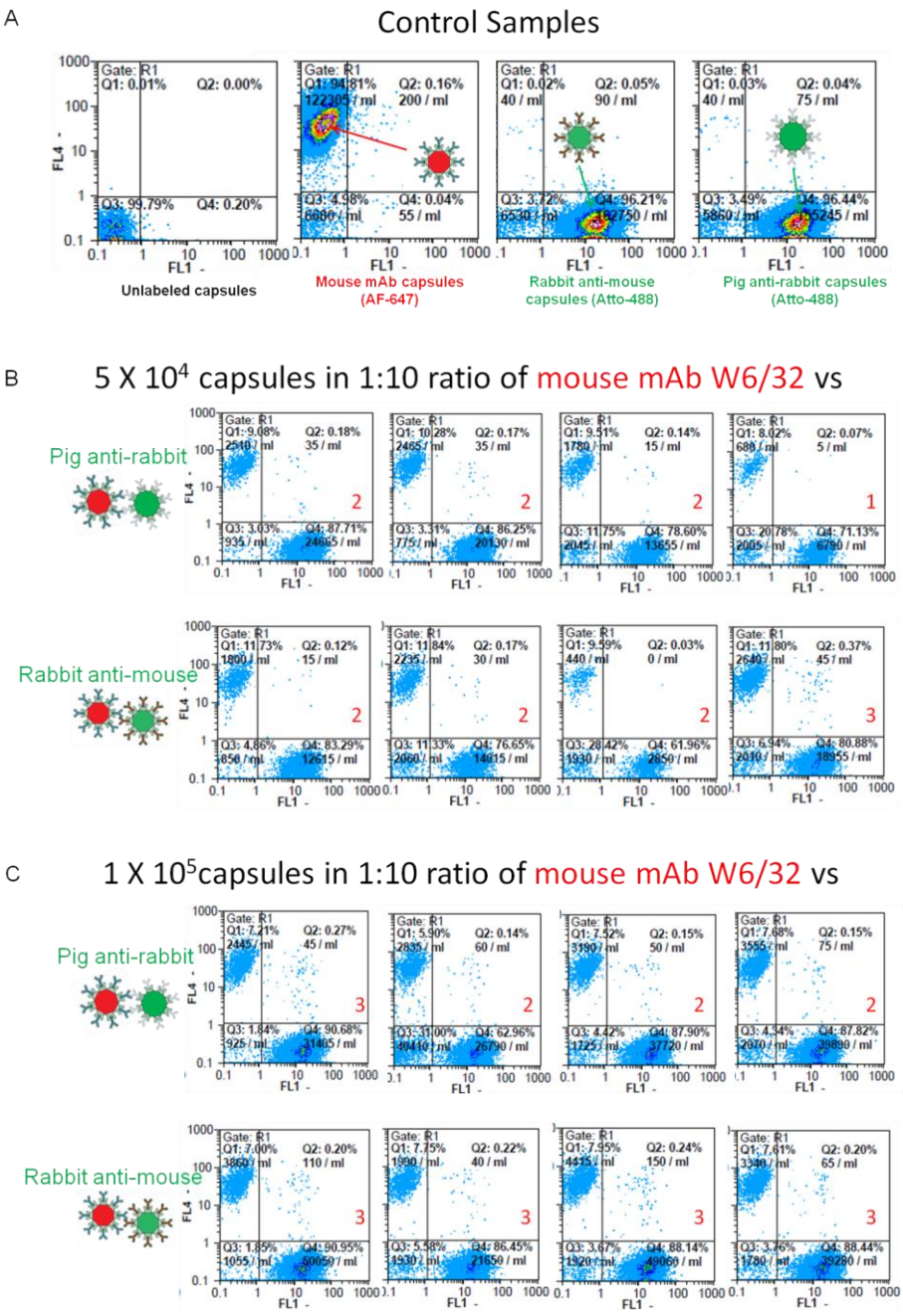

*Figure continued to page 125

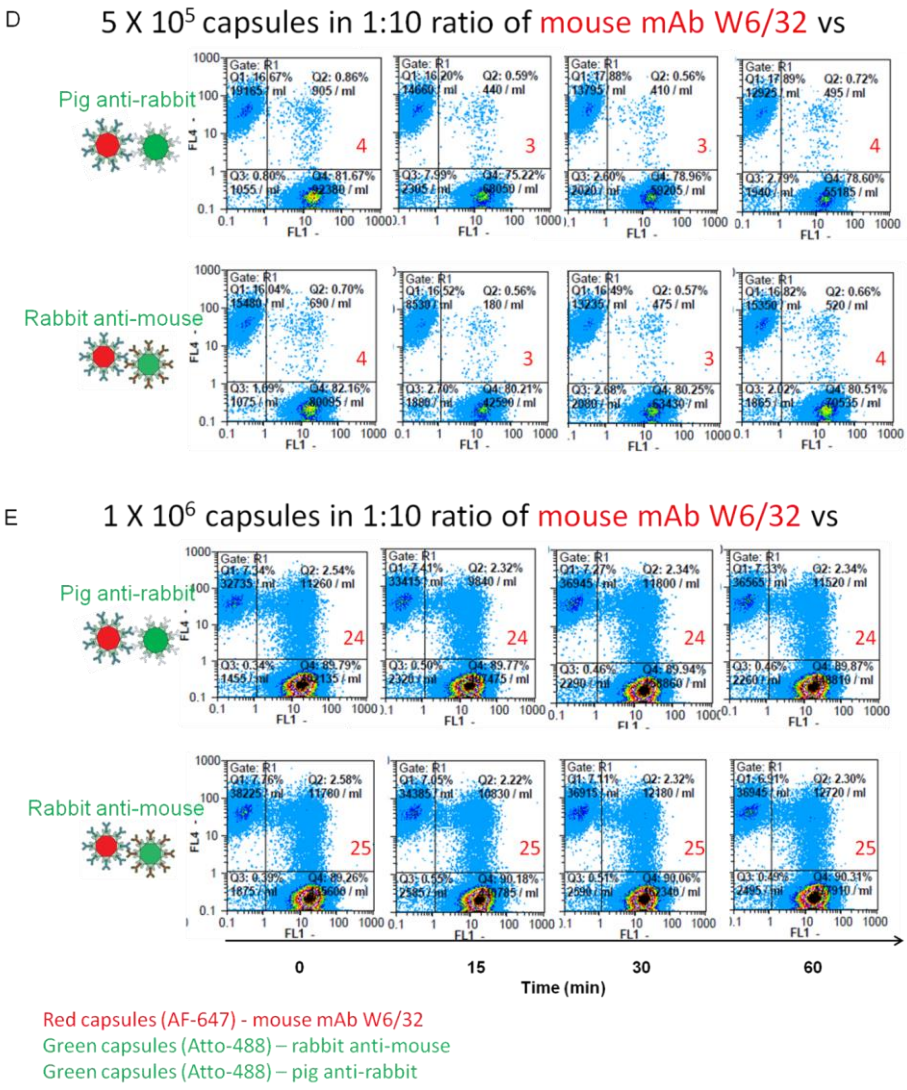

Figure 5.33: Fixed microcapsule amount in 1:10 ratio. Red microcapsules (filled with AF-647) surface-functionalized with mouse monoclonal W6/32 were incubated together with green microcapsules (filled with Atto-488) surface-functionalized with pig anti-rabbit (non-specific) and rabbit anti-mouse (specific) in 1 mL PBS for 0, 15, 30 and 60 minutes at a ratio of 1:10. Total events per sample was 5 x 10^4 (**B**), 1 x 10^5 (**C**), 5 x 10^5 (**D**) and 1 x 10^6 (**E**). The red and green microcapsules alone and the control crosslinked microcapsules were also run on flow cytometry for background signal (**A**) (n=3).

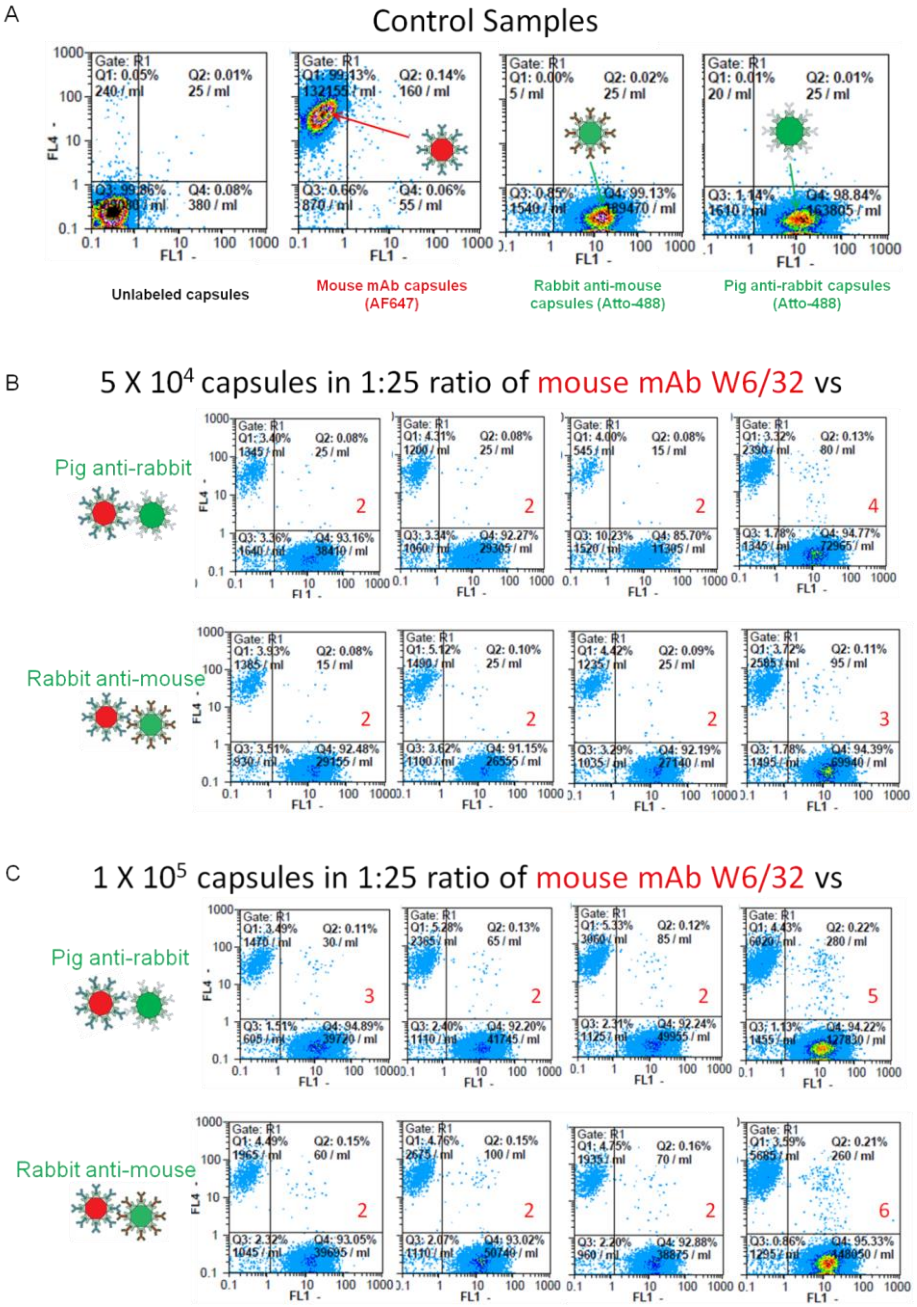

*Figure continued to page 127

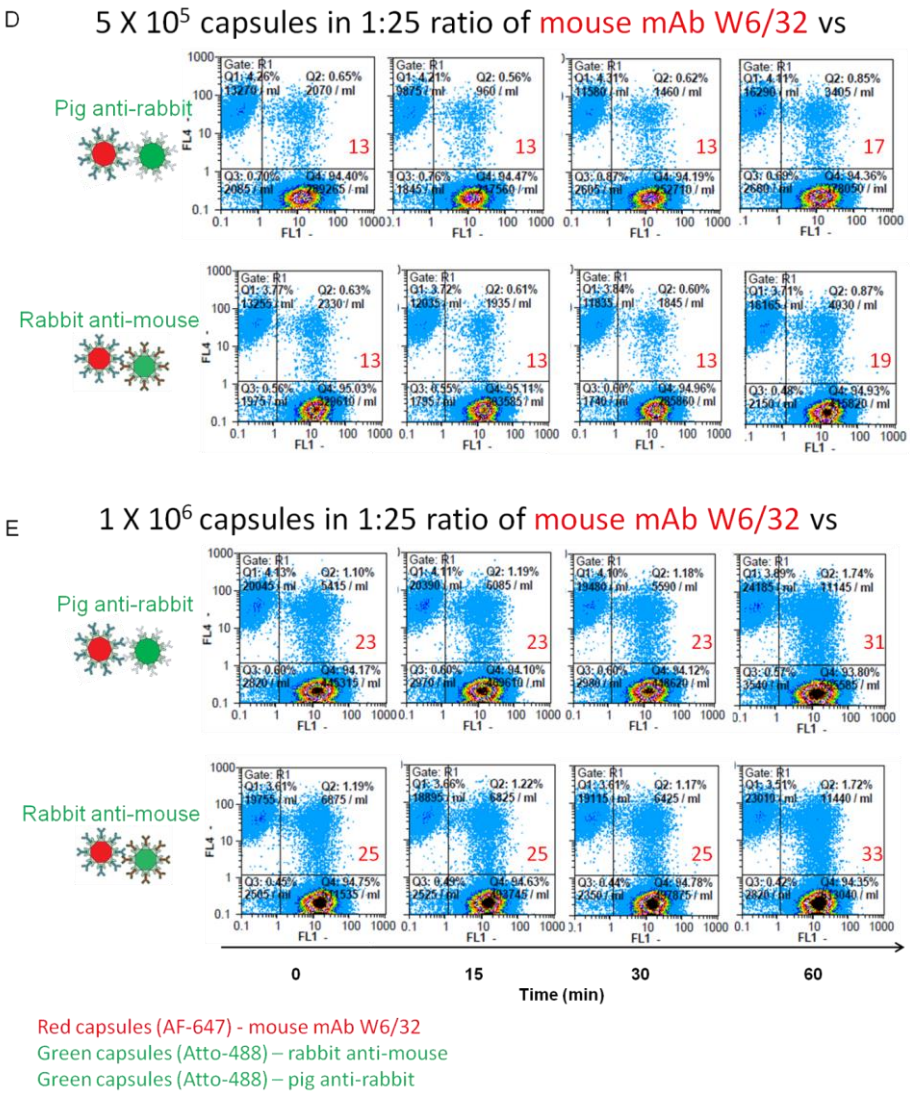

Figure 5.34: Fixed microcapsule amount in 1:25 ratio. Red microcapsules (filled with AF-647) surface-functionalized with mouse monoclonal W6/32 were incubated together with green microcapsules (filled with Atto-488) surface-functionalized with pig anti-rabbit (non-specific) and rabbit anti-mouse (specific) in 1 mL PBS for 0, 15, 30, and 60 minutes at a ratio of 1:25. Total events per sample were 5 x 10^4 (**B**), 1 x 10^5 (**C**), 5 x 10^5 (**D**) and 1 x 10^6 (**E**). The red and green microcapsules alone and the control crosslinked microcapsules were also run on flow cytometry for background signal (**A**): (n=2).

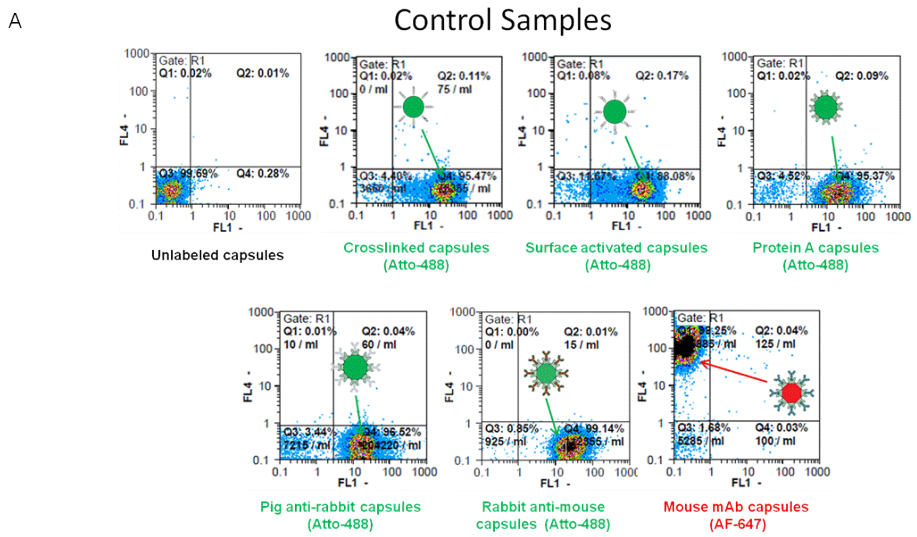

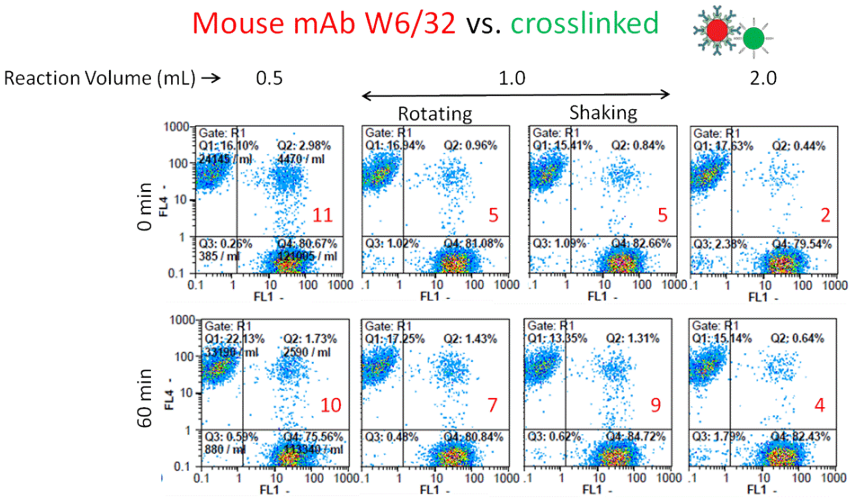

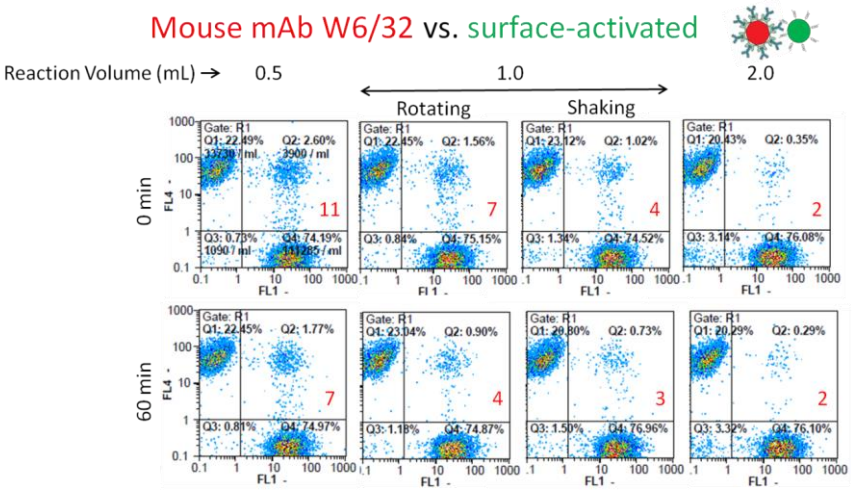

*Figure continued to page 129

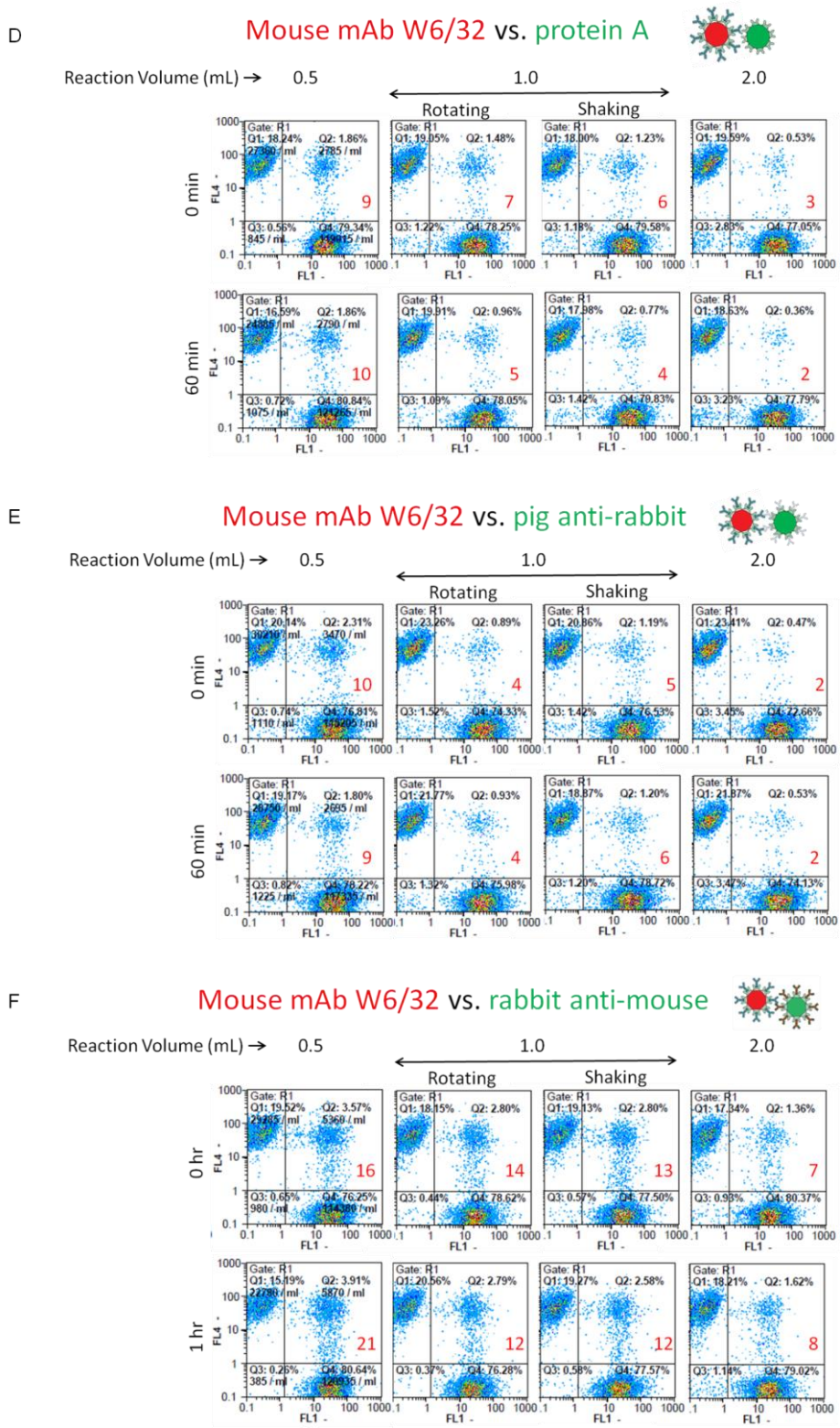

Figure 5.35: Reaction volume. Red microcapsules (filled with AF-647) surface-functionalized with mouse monoclonal W6/32 is incubated together with green microcapsules (filled with Atto-488) which are either cross-linked (**B**), surface-activated (**C**), protein A (**D**), pig anti-rabbit (**E**) and rabbit anti-mouse (**F**) in 1 mL PBS for 0 min or 1 hour at a ratio of 1:5. All the incubation were carried out in 0.5 mL (shaking), 1.0 mL (rotating and shaking) and 2 mL (shaking). The red and green microcapsules alone and the control crosslinked microcapsules were also run on flow cytometry for background signal (**A**). Total number of beads per sample was 3 x 10^5; (n=2).

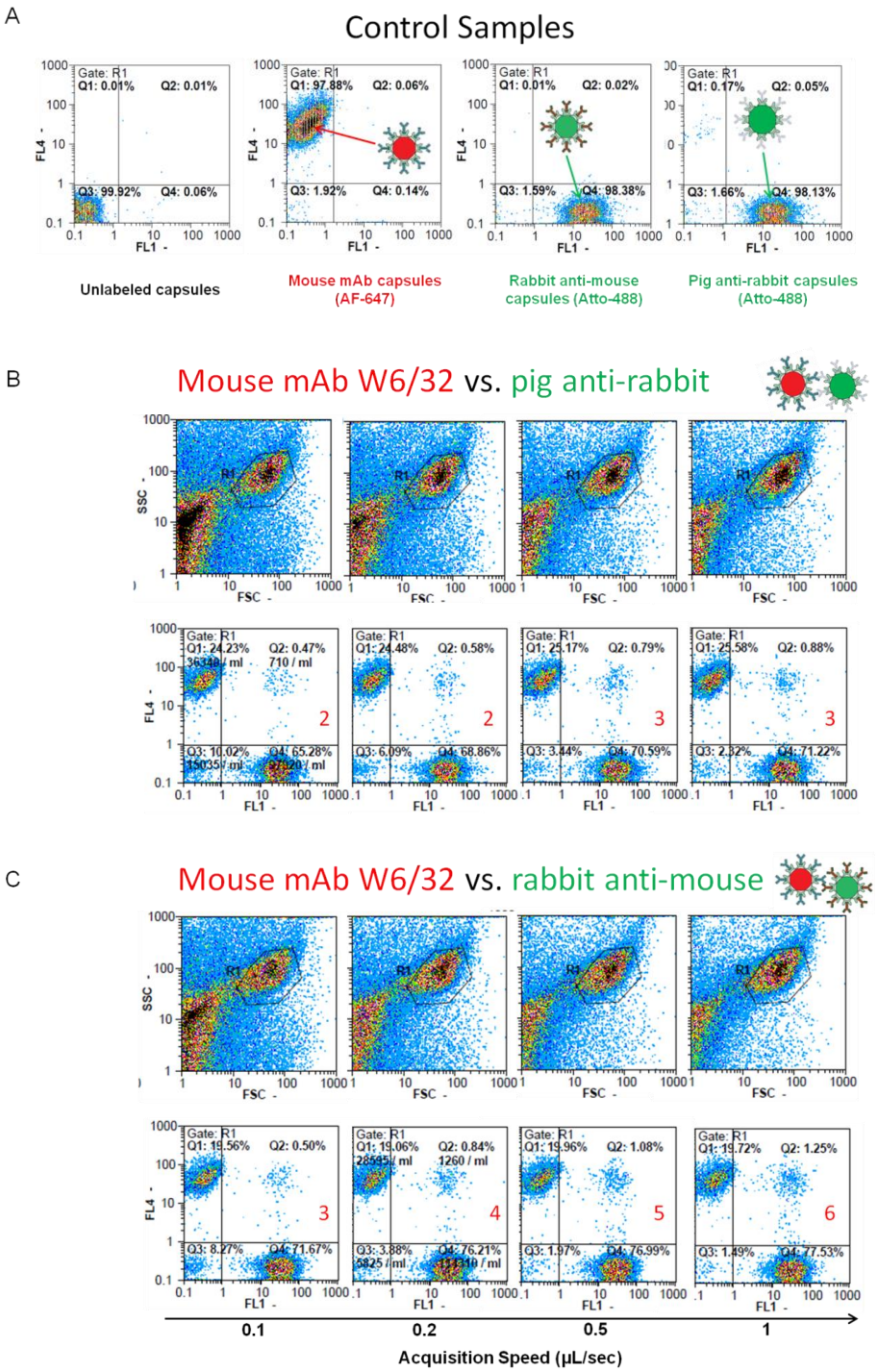

*Figure continued to page 131

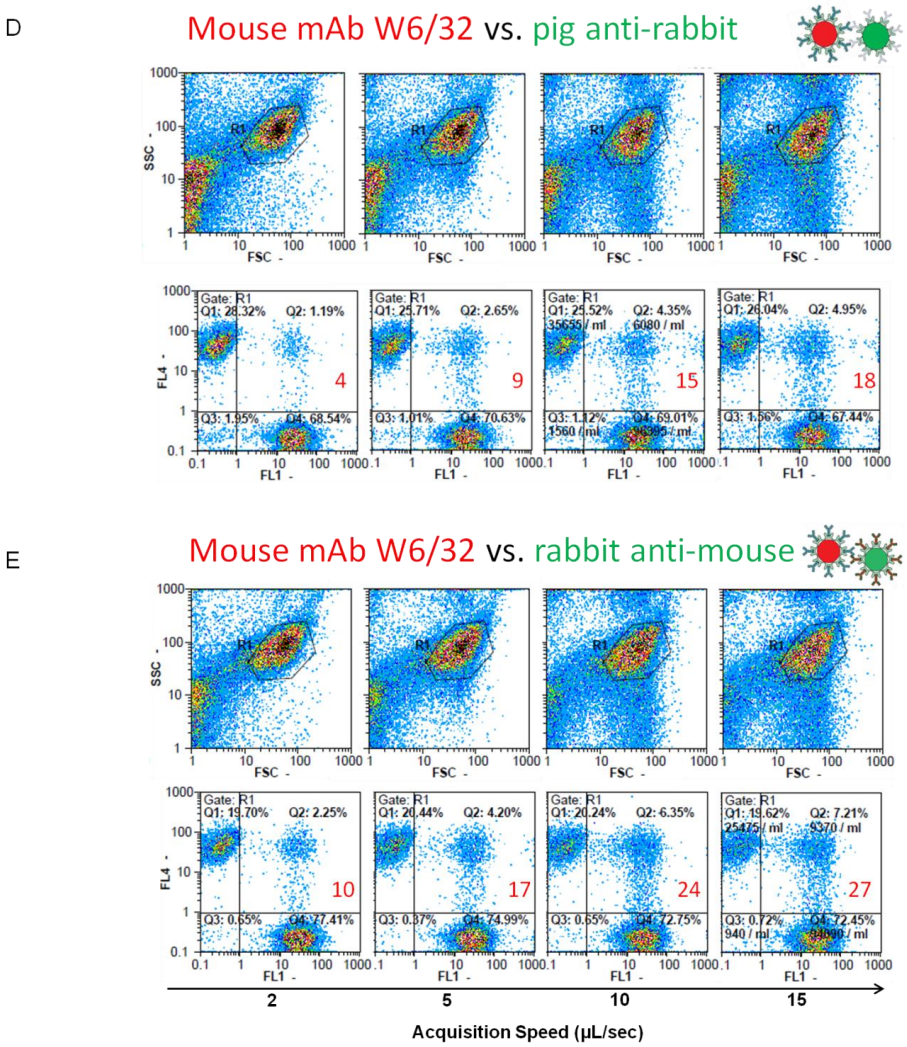

Figure 5.36: Speed test. Red microcapsules (filled with AF-647) surface-functionalized with mouse monoclonal W6/32 were incubated together with green microcapsules (filled with Atto-488) surface-functionalized with pig anti-rabbit (non-specific) and rabbit anti-mouse (specific) in 1 mL PBS for 30 minutes at a ratio of 1:5. The acquisition speed in the flow cytometry was varied from 0.1, 0.2, 0.5, 1, 2, 5, 10, and 15 µL/second (**B-E**). The red and green microcapsules alone and the control crosslinked microcapsules were also run on flow cytometry for background signal (**A**). Total number of bead per sample was 3 x 10^5; (n=2).

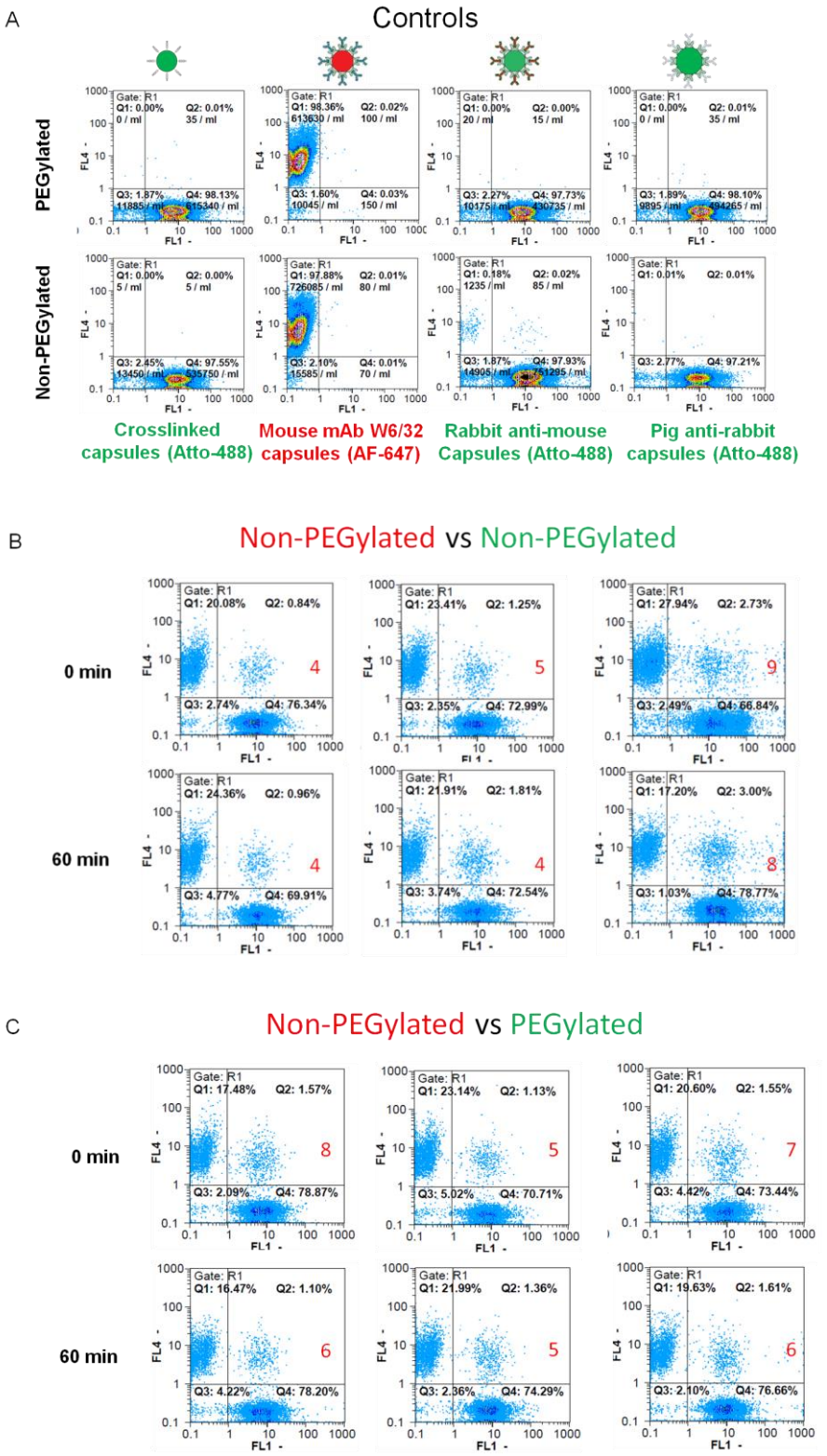

*Figure continued to page 133

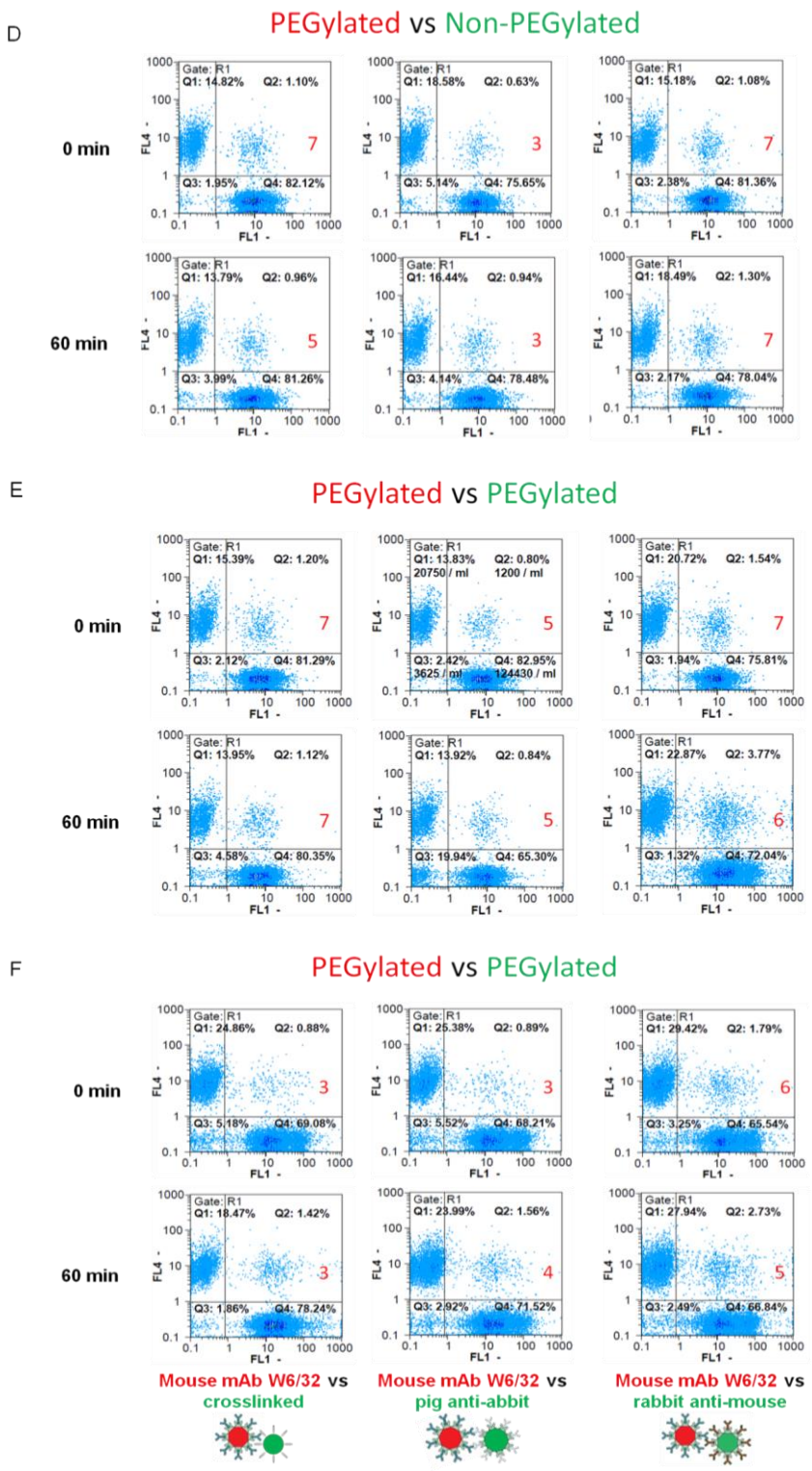

Figure 5.37: PEGylation studies. Red microcapsules (filled with AF-647) surface-functionalized with mouse monoclonal W6/32 is incubated together with green microcapsules (filled with Atto-488) which are either cross-linked, pig anti-rabbit and rabbit anti-mouse in 1 mL PBS for 0 and 60 minutes at a ratio of 1:5. Non-PEGylated red microcapsules were incubated together with non-PEGylated green (**B**), PEGylated green (**C**) or the PEGylated red microcapsules were incubated with non-PEGylated green (**D**), PEGylated green (**E**). The PEG used for this studies was 3.5 KDa NH_2-PEG-COOH. As a control to PEGylated red microcapsules were incubated with PEGylated green microcapsules (**F**) with 20 kDa NH_2-PEG-COOH. The red and green microcapsules alone and the control crosslinked microcapsules (both PEGylated and non-PEGylated) were also measured for background signal (**A**). Total number of beads per sample was 3 x 10^5 (n=2).

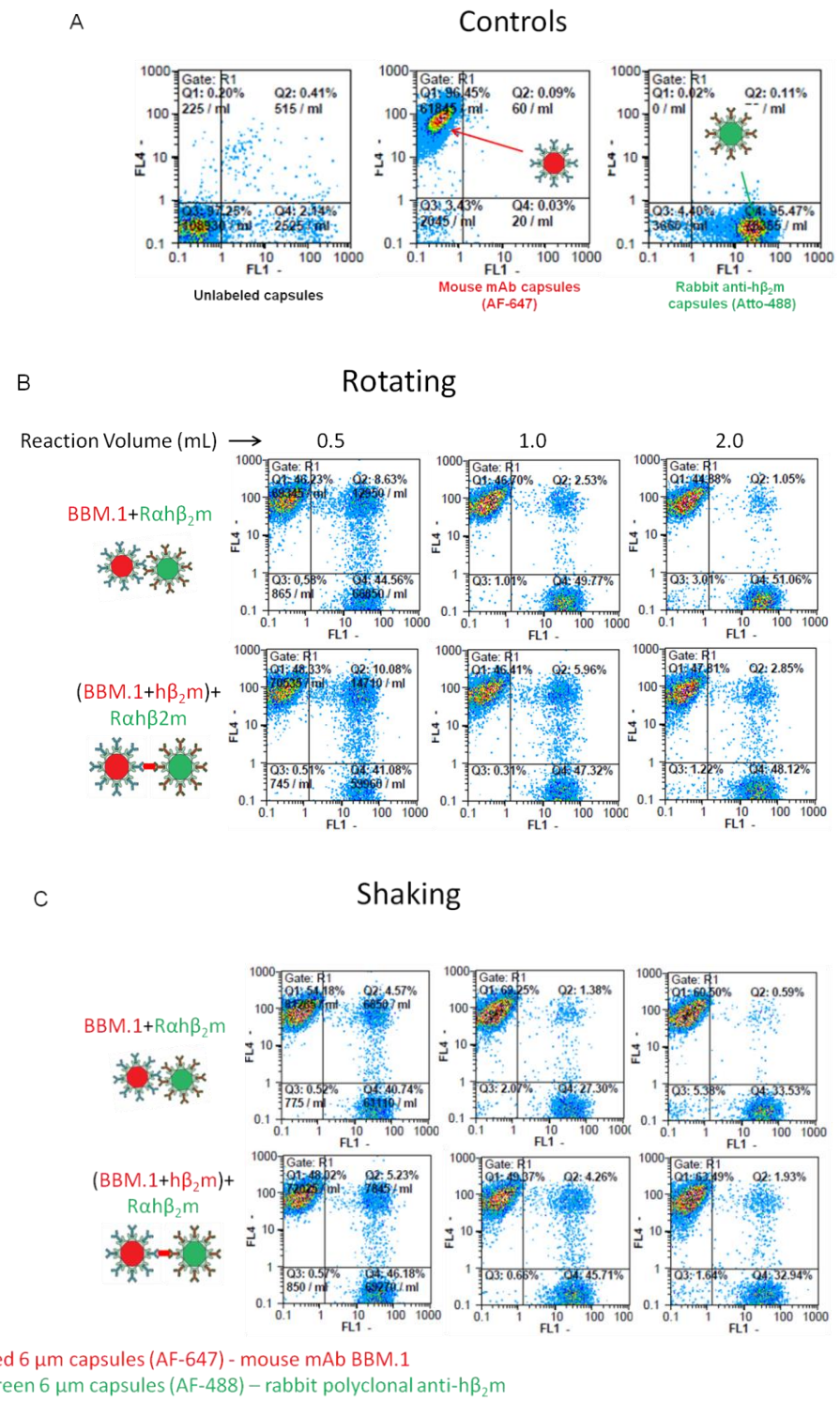

Figure 5.38: Standardization of analyte-induced proximity studies with controls. Red microcapsules (filled with AF-647) surface-functionalized with mouse monoclonal BBM.1 were incubated together with green microcapsules (filled with Atto-488) and surface-functionalized with polyclonal rabbit anti $h\beta_2M$ either in the absence of analyte (top lane) as a control or in the presence of 1 ng analyte $h\beta_2M$ (bottom lane). The reaction was carried out either rotating (**A**) or shaking (**B**) in different reaction volumes of 0.5 mL (left lane), 1 mL (middle lane) and 2 mL (right lane). Total number of beads per sample was 3 x 10^5 (n=2).

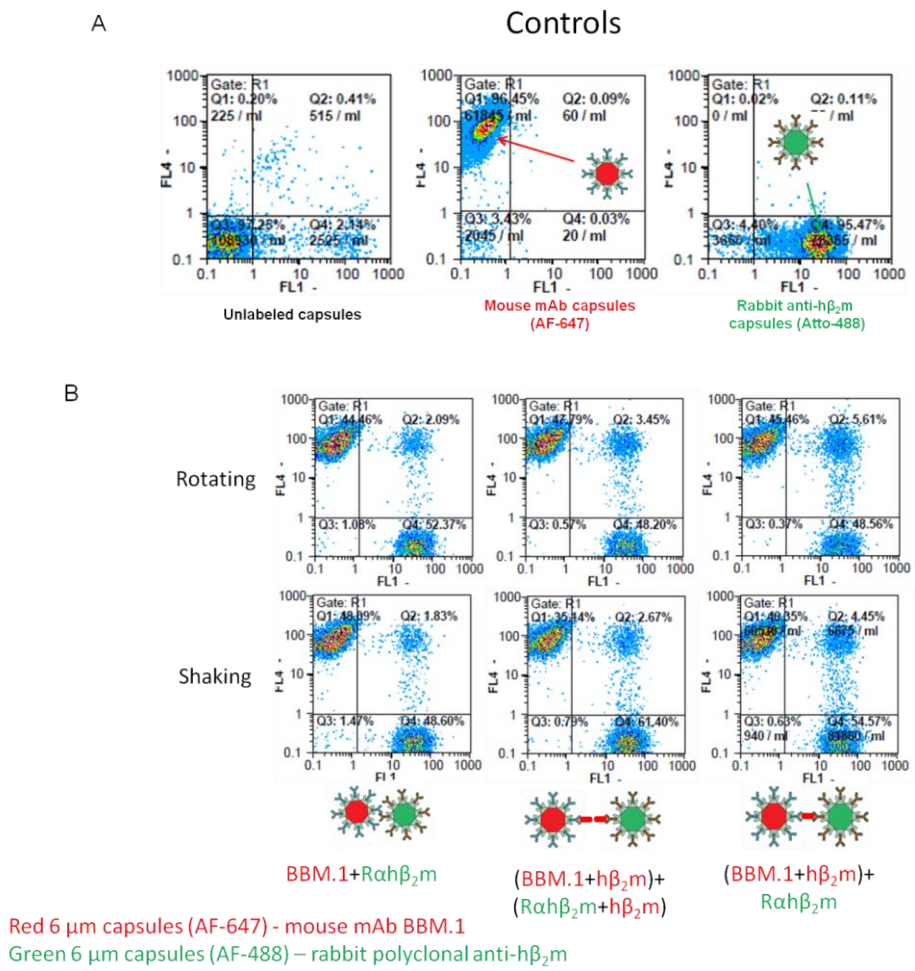

Figure 5.39: Analyte-induced proximity with controls. Red microcapsules (filled with AF-647) surface-functionalized with mouse monoclonal BBM.1 were incubated together with green microcapsules (filled with Atto-488) and surface-functionalized with polyclonal rabbit anti-hβ_2M either in the absence of analyte (left lane) as a control or in the presence of 1 ng analyte hβ_2M (right lane). As a negative control (middle lane), both the red and the green microcapsules were incubated with the analyte hβ_2M separately. Total number of beads per sample, 3 x 10^5; (n=2).

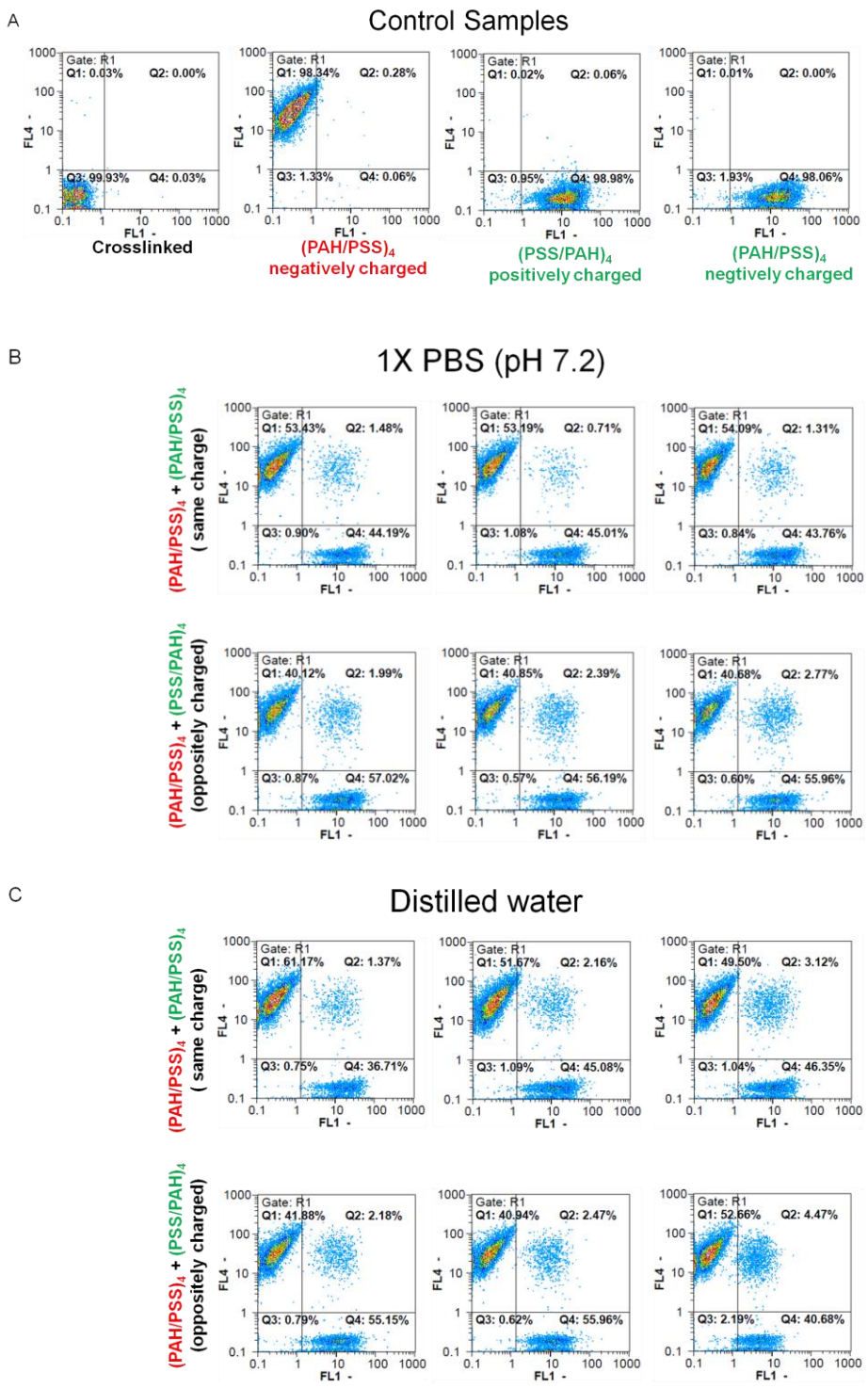

*Figure continued to page 137

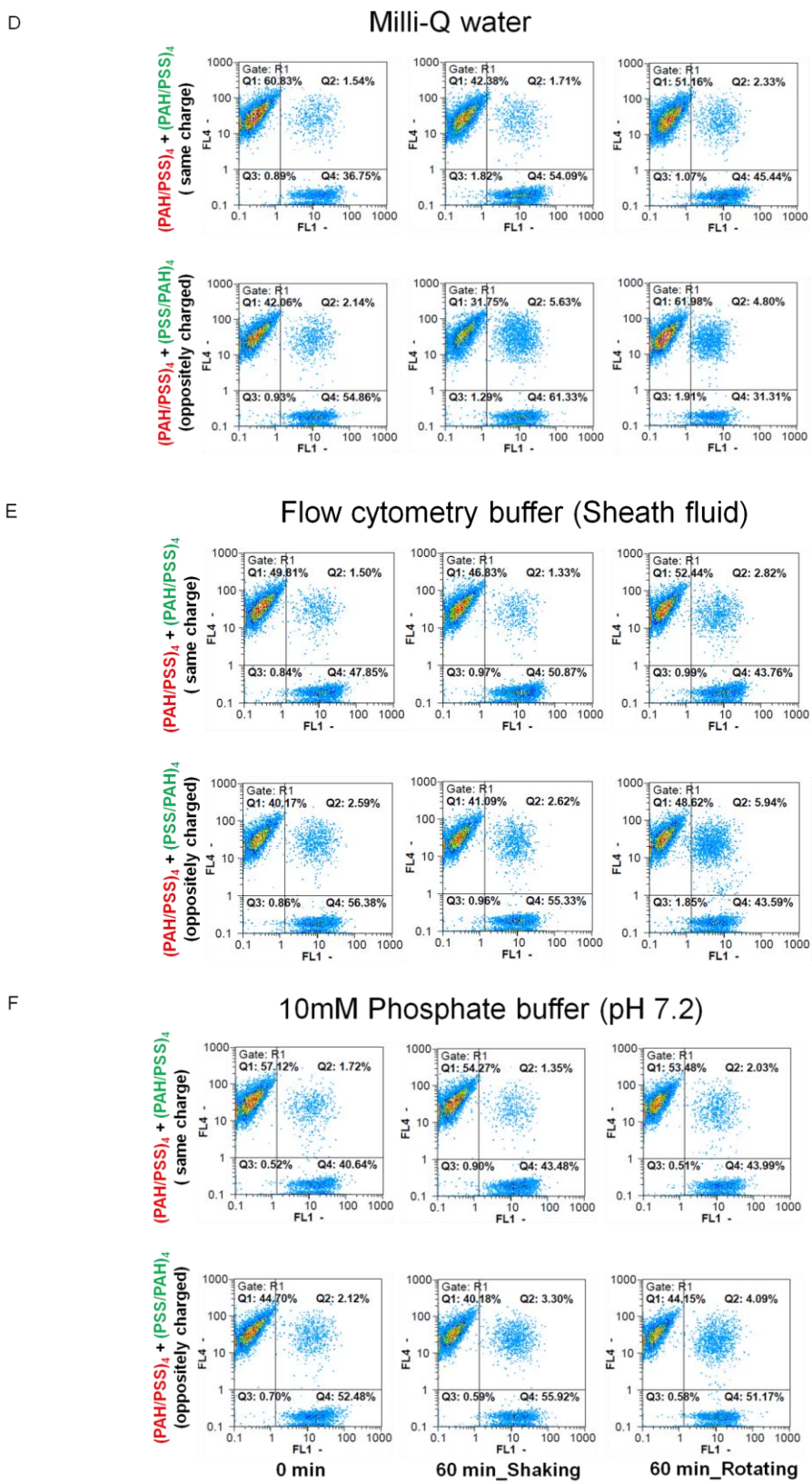

Figure 5.40: Buffer and charge experiments with controls. A total of 3 x 10^5 microcapsules were incubated together in a 1:1 ratio of red and green microcapsules either having similar charges on the outermost layer or having opposite charges. There was no major difference in the double-positive population of red (negatively charged microcapsules) and green microcapsules (positively or negatively charged microcapsules) between the different buffers as shown (**B-F**). Crosslinked microcapsules, red negatively charged microcapsules and green positively and negatively charged microcapsules are shown in controls (**A**); (n=2).

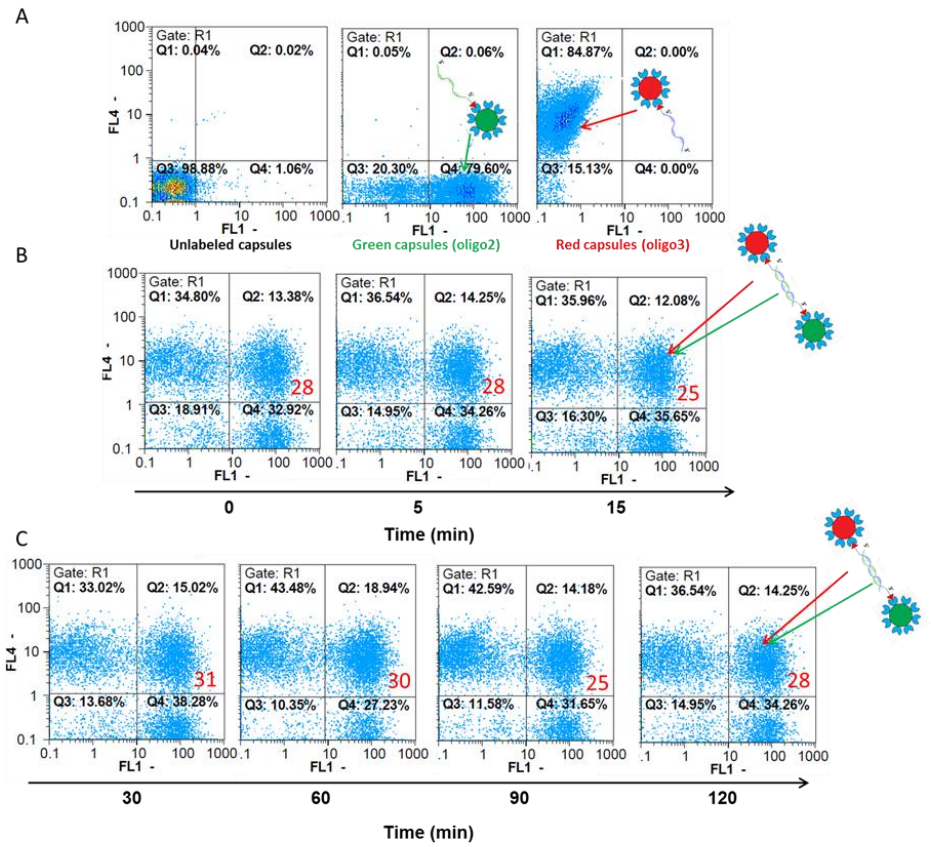

D

5′-Biotin-GGGGAAGGAAAGGAAAAAGAGTAAAAGGACGCCGAGT-3′
3′-CATTTTCCTGCGGCTCAAGAAAAAGGAAGGAAGGGG-Biotin-5′

Figure 5.41: Biophysical proof of principle studies. Red microcapsules (filled with AF-647) surface-functionalized with oligo2 are incubated together with green microcapsules (filled with Atto-488) surface-functionalized with oligo3 in 1mL PBS for 0, 5, 15, 30, 60, 90, and 120 minutes. The red and green microcapsules were incubated together at a ratio of 1:1 (**B, C**). The red and green microcapsules with their respective oligonucleotides alone and the control cross-linked microcapsules were also run on flow cytometry for background signal (**A**). Hybridization scheme of the two oligonucleotides used for the current assay (**D**). Total samples per reaction was 3 x 10^5; (n=2).

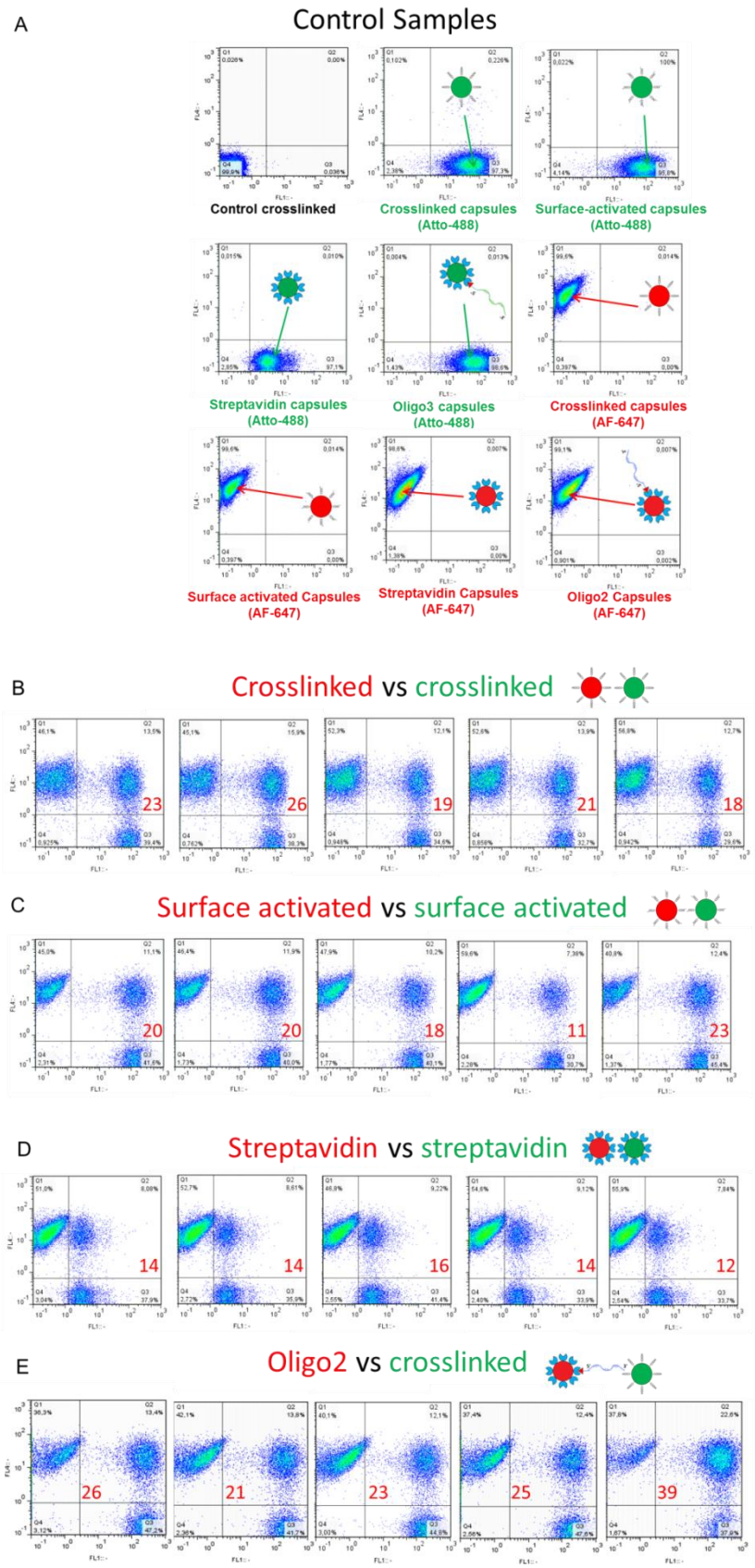

* Figure continued to page 140

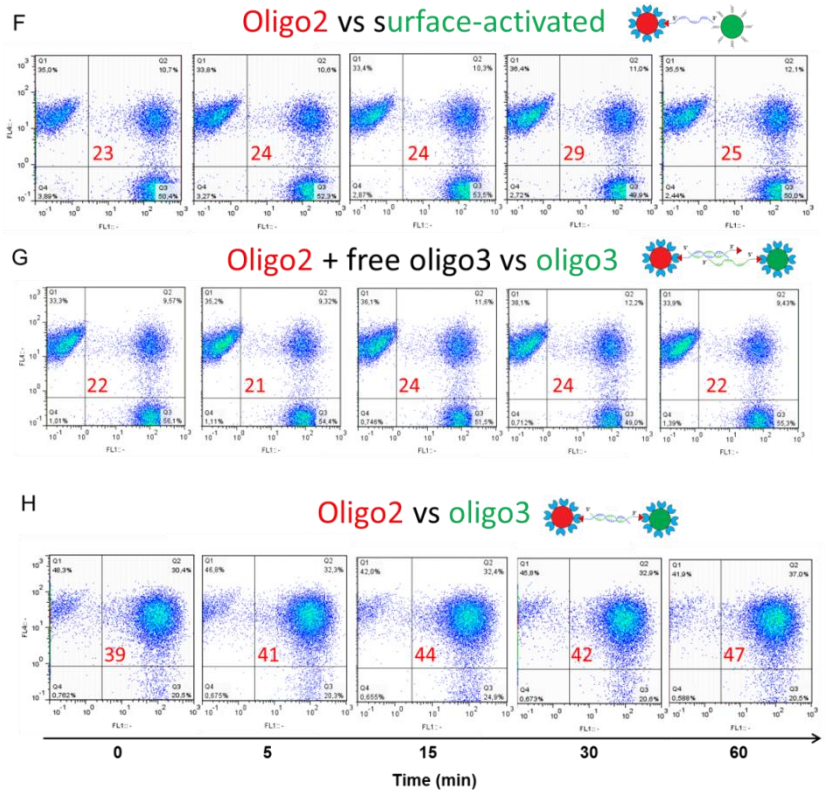

I

5'-Biotin-GGGGAAGGAAAGGAAAAAGAGTAAAAGGACGCCGAGT-3'
3'-CATTTTCCTGCGGCTCAAGAAAAAGGAAGGAAGGGG-Biotin-5'

Figure 5.42: Biophysical proof of principle studies with controls. Red microcapsules (filled with AF-647) and green microcapsules (filled with Atto-488) either crosslinked (**B**), surface-activated (**C**), streptavidin-bound (**D**) or red oligo2 and green crosslinked (**E**), green surface-activated (**F**), free oligo3 and then green oligo3 (**G**) (non-specific controls) or red and green with oligo2 and oligo3 (**H**) (specific binding) were incubated together in 1mL PBS for 0, 5, 15, 30, and 60 minutes. The red and green microcapsules were incubated together at a ratio of 1:1 (**B, C**). The red and green microcapsules with their respective oligonucleotides alone and the control cross-linked microcapsules were also run on flow cytometry for background signal (**A**). Hybridization scheme of the two oligonucleotides used for the current assay (**I**). Total samples per reaction was 3 x 10^5; (n=2). Experiment performed by Ulla Schellhaas.

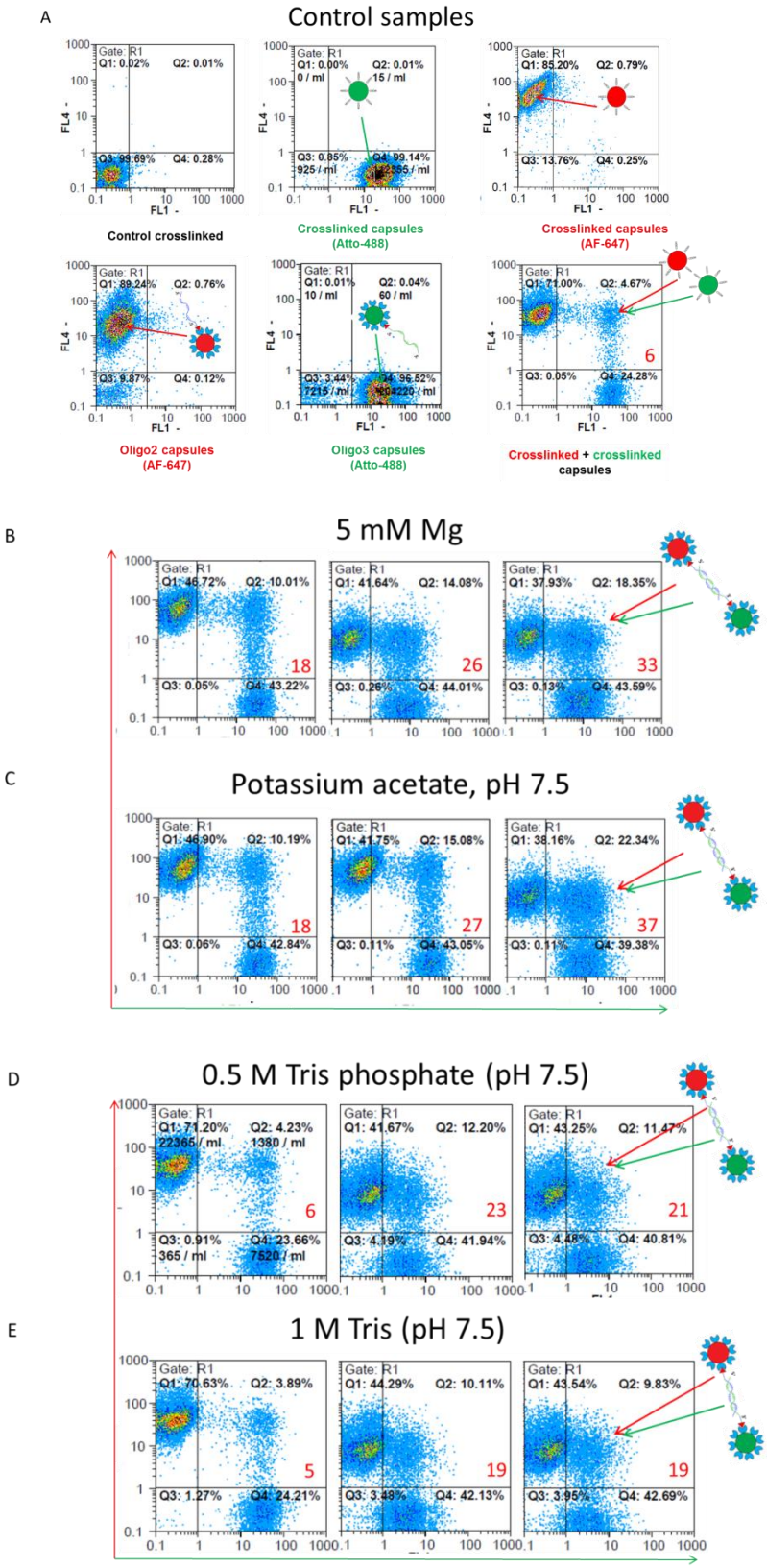

* Figure continued to page 142

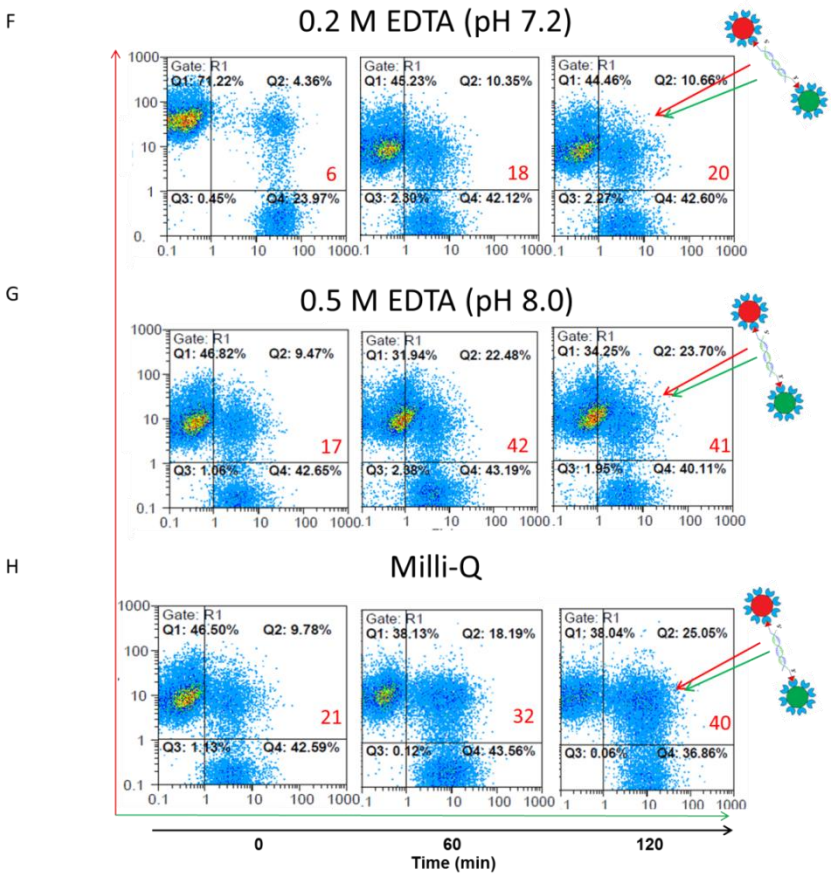

I

5′-Biotin-GGGGAAGGAAAGGAAAAAGAGTAAAAGGACGCCGAGT-3′
3′-CATTTTCCTGCGGCTCAAGAAAAAGGAAGGAAGGGG-Biotin-5′

Figure 5.43: Two-dimensional plots of direct proximity in a two-bead assay using oligonucleotide-coated microcapsules to determine the ideal reaction buffer. Red microcapsules (filled with AF-647) and green microcapsules (filled with Atto-488) were either crosslinked or attached with oligo2 and oligo3 and incubated in different buffers. Red microcapsule with oligo2 and green microcapsule with oligo3 were incubated either in 5 mM Mg (**B**), potassium acetate; pH 7.5 (**C**), 0.5 M Tris phosphate; pH 7.5 (**D**), 1 M Tris; pH 7.5 (**E**), 0.2 M EDTA; pH 7.2 (**F**) 0.5 M EDTA; pH 8.0 (**G**) or Milli-Q water (**H**) at different time points of 0, 60 and 120 minutes to see if buffer has any role in inducing proximity of microcapsules. The red and green microcapsules with their respective oligonucleotides alone and the control cross-linked microcapsules were also run on flow cytometry for background signal (**A**). Hybridization scheme of the two oligonucleotides used for the current assay (**I**). Total samples per reaction was 3 x 10^5; (n=2). Experiment performed by Amanda Amoah.

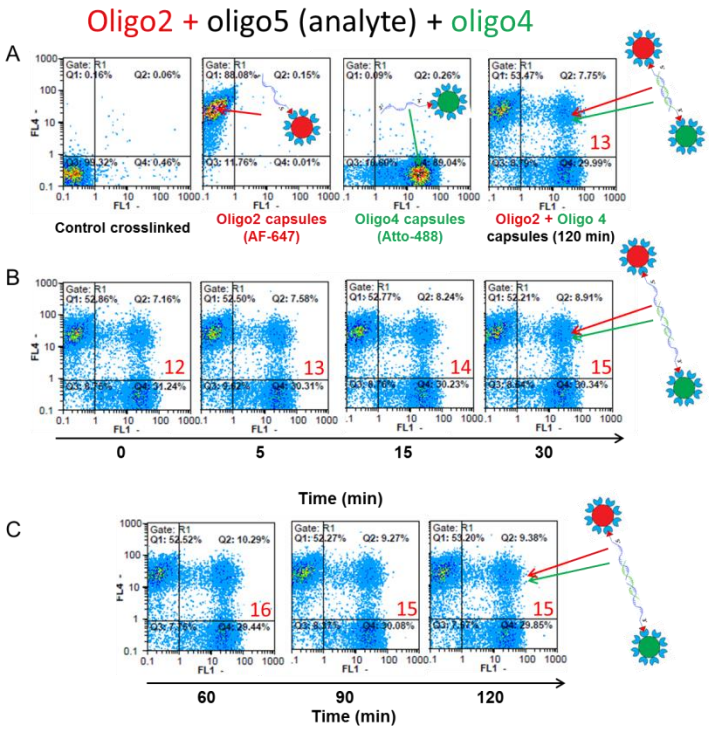

D

5′-Biotin-GGGGAAGGAAAGGAAAAAGAGTAAAAGGACGCCGAGT-3′
3′-CATTTTCCTGCGGCTCAACTCGGCGTCCTTTTAC-5′
5′-TGAGCCGCAGGAAAATGAGAAAAAGGAAAGGAAGGGG-Biotin-3′

Figure 5.44: Analyte induced proximity between two microcapsules. Results of the analyte induced proximity using oligonucleotides with red and green microcapsules. The red and the green microcapsules were attached with oligo2 and oligo4 and then incubated with oligo5 (analyte) at different points of 0, 5, 15, 30, 60, 90 and 120 minutes (**B, C**) in a ratio of 1:1. The red and green microcapsules with their respective oligonucleotides alone and the control set of microcapsules with no analyte (incubated for 120 minutes) were also run on flow cytometry for background signal (**A**). Total samples per reaction was 3 x 10^5; (n=3). Experiment performed by Amanda Amoah.

6 Chapter 6: Outlook

6.1 Microcapsules for detection

Over the last two decades, the field of medical science has improved in the treatment of diseases with increases efficacy of drugs and reduced side effects. The drugs available in the market today are more potent and are directed towards working on the diseased cells with increased sensitivity and selectivity. However, with the emergence of new diseases and the onset of diseases at early ages of life, more challenges have arisen.

One important problem is that some diseases are diagnosed late, since the biomarkers[16] are initially present only at very low levels that cannot be detected with the available assay systems. Many of the available assay systems detect biomarkers only in the nanomolar range [1,2], and hence, development of a new assay system that can detect biomarkers at ultra-low concentrations, picomolar or femtomolar, is of utmost importance. Early detection of clinically relevant biomarkers, ideally right at the onset of disease, will help in early diagnosis, eventually leading to an early treatment and thus helping in the eradication of the disease.

6.1.1 Developing a novel commercial assay technology

The primary objective of my PhD work was to develop a novel, modular assay with an optical readout capable of detecting biological analytes with high sensitivity and selectivity and with high temporal and spatial resolution. The biological analytes might include proteins, peptides, nucleic acids, plasmids, transcripts, and biological process intermediates. To be a viable alternative to existing methods, any novel assay has to be commercially competent (*i.e.*, superior to existing systems) in terms of sensitivity, selectivity, robustness and overall assay timing, and it must be easy to perform.

6.1.1.1 State of the work

My work has shown that functional protein A and streptavidin can be attached covalently to the surface of microcapsules and detected by flow cytometry. The attached protein A bound to the F_c region of antibodies, resulting in oriented immobilization of the antibodies (**see section** Error! Reference source not found.**3**), whereas the streptavidin-functionalized microcapsules w

[16] Biomarkers are indicators for either the stage of a disorder or its clinical manifestation.

ere able to bind biotinylated biomolecules (oligonucleotides and MHC class I proteins) on the surface (**see section** Error! Reference source not found.**1** and Error! Reference source not fo und.**2**). Both types of microcapsules were able to detect the presence of their respective analyte with high sensitivity and selectivity (**see section** Error! Reference source not found. a nd Error! Reference source not found.**3**).

6.1.1.2 Proof of principle of measurement

As a proof of principle that the microcapsule based assay can be used for measurement *via* flow cytometry, an initial study was performed to detect the binding of antibody in the presence and absence of protein A on the microcapsule assay. It was observed that oriented immobilization of antibody (mediated through protein A) gives a higher signal in flow cytometry compared to the microcapsules that have randomly immobilized antibody, detected by incubating the samples with a secondary antibody conjugated to a fluorophore (**see section 3.3.2.22.2**). The microcapsule preparation was very homogeneous, and the antibody was bound to the microcapsule surface as observed in flow cytometry. (**see section** Error! R eference source not found.**3**).

6.1.1.3 Standardizing the assay protocol

The microcapsule based assay showed very high variability between the replicates and so, as a first step in developing and standardizing the assay protocol, I tried to validate each step of the protocol and hence designed an experiment to study at which step does the variability starts. For the experiment, I started with the with microcapsule preparation (LbL assembly) and during each further step (crosslinking, surface-activation, protein A, anchor Ab, analyte, binder Ab, detector Ab), the microcapsules were divided into three and then processed further for measuring in the flow cytometry. As seen in the **Figure 6.1**, high variability between the samples was observed during the crosslinking step, after which the sample variability is reduced and the replicates give similar fluorescence when compared to each other. So as a future step, we decided to mix together all the crosslinked microcapsules together and then take out the required microcapsule amount from the mixed sample (mix and match), to reduce the variability between the replicates. The entire work presented with the single bead assay in **chapter 3** and **chapter 5** is processed the same way.

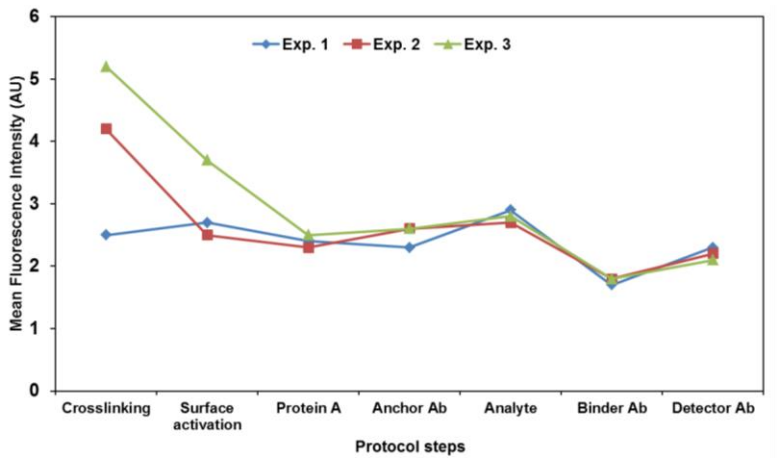

Figure 6.1. Standardizing the assay protocol: Microcapsules were prepared by LbL assembly onto $CaCO_3$ cores and then divided into three aliquots after the steps described in the x axis of the figure. After the final step of detector Ab addition, all the microcapsules were processed for $CaCO_3$ core dissolution in 0.2M EDTA (pH 7.2) and measured in flow cytometry. X-axis is the mean fluorescence intensity (MFI) as observed with Flow Jo (n=3).

6.2 Conclusion

The microcapsule-based single bead assay presented here in the thesis is particularly more sensitive for the detection of proteins. The assay is simple, robust and is able to detect the prognosis marker human beta-2 microglobulin (hβ_2m) in fg/mL, whereas the detection limit for proteins using bead based assays is in pg/mL [3–7]. Beta-2 microglobulin is an important biomarker in the clinical field as it serves as an marker for multiple myeloma and lymphoma [8–10] as well as for renal failure [11]. The detection limit of hβ_2m as per the available kit[17] is less than 0.2 µg/mL, which makes the detection of hβ_2m in urine samples in case of renal failures difficult where the normal levels are 30 ng/mL [11]. This makes the application of microcapsule based assay for the detection of hβ_2m as a clinically important diagnostic tool.

[17] http://www.bio-rad.com/en-us/product/bio-plex-pro-rbm-human-kidney-toxicity-assays. 20.02.2017

6.3 References

[1] R.L. Davis, C. Liang, C.M. Sue, A comparison of current serum biomarkers as diagnostic indicators of mitochondrial diseases, Neurology. 86 (2016) 2010–2015. doi:10.1212/WNL.0000000000002705.

[2] P. Beirne, P. Pantelidis, P. Charles, A.U. Wells, D.J. Abraham, C.P. Denton, K.I. Welsh, P.L. Shah, R.M. Du Boise, P. Kelleher, Multiplex immune serum biomarker profiling in sarcoidosis and systemic sclerosis, Eur. Respir. J. 34 (2009) 1376–1382. doi:10.1183/09031936.00028209.

[3] A. de la Escosura-Muñiz, Z. Plichta, D. Horák, A. Merkoçi, Alzheimer's disease biomarkers detection in human samples by efficient capturing through porous magnetic microspheres and labelling with electrocatalytic gold nanoparticles, Biosens. Bioelectron. 67 (2015) 162–169. doi:10.1016/j.bios.2014.07.086.

[4] M. Fraga, N. Vilariño, M.C. Louzao, L.P. Rodríguez, A. Alfonso, K. Campbell, C.T. Elliott, P. Taylor, V. Ramos, V. Vasconcelos, L.M. Botana, Multi-detection method for five common microalgal toxins based on the use of microspheres coupled to a flow-cytometry system, Anal. Chim. Acta. 850 (2014) 57–64. doi:10.1016/j.aca.2014.08.030.

[5] L.P. Rodríguez, N. Vilariño, M.C. Louzao, T.J. Dickerson, K.C. Nicolaou, M.O. Frederick, L.M. Botana, Microsphere-based immunoassay for the detection of azaspiracids, Anal. Biochem. 447 (2014) 58–63. doi:10.1016/j.ab.2013.10.035.

[6] M. Sun, J. Manolopoulou, A. Spyroglou, F. Beuschlein, C. Hantel, Z. Wu, M. Bielohuby, A. Hoeflich, C. Liu, M. Bidlingmaier, A microsphere-based duplex competitive immunoassay for the simultaneous measurements of aldosterone and testosterone in small sample volumes: Validation in human and mouse plasma, Steroids. 75 (2010) 1089–1096. doi:10.1016/j.steroids.2010.07.005.

[7] H.C. Tekin, M. a M. Gijs, Ultrasensitive protein detection: a case for microfluidic magnetic bead-based assays., Lab Chip. 13 (2013) 4711–39. doi:10.1039/c3lc50477h.

[8] H. Hagberg, A. Killander, B. Simonsson, Serum beta 2-microglobulin in malignant lymphoma., Cancer. 51 (1983) 2220–5. http://www.ncbi.nlm.nih.gov/pubmed/6189572.

[9] P.W. Johnson, J. Whelan, S. Longhurst, K. Stepniewska, J. Matthews, J. Amess, A. Norton, A.Z. Rohatiner, T.A. Lister, Beta-2 microglobulin: a prognostic factor in diffuse aggressive non-Hodgkin's lymphomas., Br. J. Cancer. 67 (1993) 792–797. http://www.ncbi.nlm.nih.gov/pmc/articles/PMC1968369/.

[10] C. Yoo, D.H. Yoon, C. Suh, Serum beta-2 microglobulin in malignant lymphomas: An old but powerful prognostic factor, Blood Res. 49 (2014) 148–153. doi:10.5045/br.2014.49.3.148.

[11] D.A. Brott, S.T. Furlong, S.H. Adler, J.W. Hainer, R.B. Arani, M. Pinches, P. Rossing, N. Chaturvedi, Characterization of renal biomarkers for use in clinical trials: Effect of preanalytical processing and qualification using samples from subjects with diabetes, Drug Des. Devel. Ther. 9 (2015) 3191–3198. doi:10.2147/DDDT.S78792.